SWZ Clausthal – Göttingen
Simulationswissenschaftliches Zentrum

Bericht 2017–2018

Bericht 2017–2018

Simulationswissenschaftliches Zentrum Clausthal-Göttingen

Vorwort

Der vorliegende Berichtsband beschreibt die Forschungsaktivitäten des Simulationswissenschaftlichen Zentrums Clausthal-Göttingen (SWZ) in den Jahren 2017 und 2018. Es handelt sich dabei bereits um den dritten Zweijahresbericht des SWZ. Das SWZ wurde am 1.1.2013 von der Technischen Universität Clausthal und Georg-August-Universität Göttingen als Partnern gegründet. In unserem Bericht stellen wir die aktuellen Forschungsthemen des SWZ vor.

Um das SWZ in Lehre und Forschung an beiden Standorten längerfristig zu etablieren, wurde beschlossen, sowohl in Clausthal als auch in Göttingen eine SWZ-Juniorprofessur einzurichten. An der Universität Göttingen trat Herr Dr. Marcus Baum bereits Ende 2015 diese SWZ-Juniorprofessur im Bereich der Informatik an. An der TU Clausthal wurde zu Anfang September 2017 Frau Dr. Nina Gunkelmann als SWZ-Juniorprofessorin für das Thema **Computational Material Sciences** ernannt, siehe auch Beitrag „Druckinduzierte Festkörperphasenübergänge und plastische Verformung in Eisen-Kohlenstoff-Legierungen“ ab Seite 86.

Ein Highlight ist die im Mai 2017 durch das SWZ ausgerichtete zweitägige Konferenz **„Clausthal-Göttingen International Workshop on Simulation Science“** mit knapp 100 Teilnehmern und einem in der „Communications in Computer and Information Science“-Reihe bei Springer erschienenen Post-Proceedings-Band[1] (siehe auch Seite 231). Im Bereich der Forschung ist durch die Einwerbung der DFG-Forschergruppe **„Integrierte Planung im öffentlichen Verkehr“** durch Frau Prof. Dr. Anita Schöbel ein wesentlicher Beitrag zur Weiterführung der Arbeiten im SWZ Projektbereich **„Optimierung von Netzen“** erreicht worden. Im SWZ Projektbereich **„Materialsimulation“** konnte ein neues Projekt bei der DFG eingeworben werden. Darin untersuchen Wissenschaftler aus Clausthal (AG Prof. Brenner, Institut für Technische Mechanik) und Göttingen (AG Dr. Mettin, Drittes Physikaliches Institut) in den kommenden drei Jahren Kavitation und dessen erosive Wirkung. Im Bereich des **Transfers von Forschungsergebnissen** in praktische Anwendungen hat das SWZ 2017 ein Forschungsvorhaben mit der AG der Dillinger Hüttenwerke zur Simulation und Optimierung der Logistikprozesse im Walzwerk[2] gestartet und hat im August 2018 einen Rahmenvertrag mit der Avista Oil AG, bei der Herr Bernd Althusmann, niedersächsischer Minister für Wirtschaft, Arbeit, Verkehr und Digitalisierung, die Schirmherrschaft übernommen hat[3], geschlossen.

Das Vorlesungsangebot mit Simulationsbezug konnte durch die Übertragung der in Clausthal entwickelten Veranstaltung „Simulationsmethoden in den Ingenieurwissenschaften“ nach Göttingen erweitert werden. Neben dem Angebot in der SWZ-Ringvorlesung (siehe Seite 209) beteiligt sich das SWZ auch intensiv an der Doktorandenausbildung durch die Unterstützung des Anfang 2019 gestarteten Leitprojektes HerMes (Heterogene Mensch-Maschine-Teams) der TU Clausthal. Das Projekt soll den Nukleus einer Graduiertenschule

im Forschungsfeld der **Offenen Cyberphysischen Systeme und Simulation (OCSS)** etablieren. Vier Doktoranden/innen forschen dort in den Räumlichkeiten des SWZ an querschnittlichen Themen der Entwicklung, Absicherung und Optimierung der Zusammenarbeit zwischen Mensch und Maschine und nutzen dabei die Infrastruktur des SWZ. Die dort entwickelte Forschungsplattform und die Qualifikationsangebote der Graduiertenschule werden für alle interessierten Mitglieder des Forschungsfeldes OCSS nutzbar gemacht.

Nach dem großen Erfolg des ersten Clausthal-Göttingen International Workshop on Simulation Science im Mai 2017 in Göttingen liegt für die im Mai 2019 in Clausthal stattfindende zweite Auflage des Workshops[4] bereits eine höhere Anzahl an Einreichungen vor, so dass auch die Zukunft spannend bleiben wird.

Unser Jahrbuch ist in **Deutsch und Englisch** verfasst: Die deutschen Beschreibungen geben einen Überblick über die jeweiligen Projekte und nennen die grundsätzlichen Ideen, Ansätze und Ergebnisse. Die sich anschließenden englischen Beschreibungen sind wissenschaftliche Texte, die detaillierter auf Herleitungen und Methoden eingehen. Wir hoffen, dass die Beschreibungen für Sie interessant sind und wünschen Ihnen: **Viel Spaß beim Blättern und Lesen!**

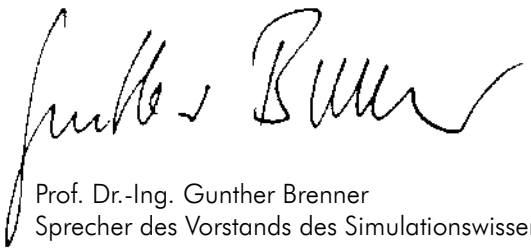

Prof. Dr.-Ing. Gunther Brenner
Sprecher des Vorstands des Simulationswissenschaftlichen Zentrums Clausthal-Göttingen

---

1 https://www.springer.com/series/7899
2 https://www.tu-clausthal.de/presse/nachrichten/details/2433/
3 https://www.tu-clausthal.de/presse/nachrichten/details/2422/
4 https://www.simscience2019.tu-clausthal.de/

Introduction

This report presents the research activities of the Simulation Science Center Clausthal-Göttingen (SWZ) in the years 2017 and 2018. The center was founded in 2013 by the two partners Clausthal University of Technology and Georg-August-University Göttingen. In our report, we describe the SWZ research projects we are currently working on.

In order to establish the SWZ in teaching and research at both locations in the longer term, it was decided to establish a SWZ Junior Professorship in both Clausthal and Göttingen. At the University of Göttingen, Dr. Marcus Baum took up this SWZ Junior Professorship in Computer Science at the end of 2015. At the beginning of September 2017, Dr. Nina Gunkelmann was appointed Junior Professor for **Computational Material Sciences** at the TU Clausthal, see also article " Pressure-induced phase transformations in Fe-C alloys: Molecular dynamics simulations" on page 129.

A highlight was the two-day conference **"Clausthal-Göttingen International Workshop on Simulation Science"**, hosted by SWZ in May 2017, with nearly 100 participants and a post-proceedings volume published by Springer in the "Communications in Computer and Information Science" series (see also page 231). In the area of research, Prof. Dr. Anita Schöbel's acquisition of the DFG research group **"Integrated Planning for Public Transportation"** has made a significant contribution to the continuation of work in the SWZ project area "Optimization of Networks". In the SWZ project area "Material Simulation", a new project was acquired from the DFG. In this project, scientists from Clausthal (Research group Prof. Brenner, Institute of Applied Mechanics) and Göttingen (Research group Dr. Mettin, Third Institute of Physics) will investigate cavitation and its erosive effect over the next three years.

In the area of **transferring research results** into practical applications, SWZ has started a research project with the Dillinger Hüttenwerke AG for simulating and optimizing the logistic processes in rolling mills[1] in 2017. In August 2018, a framework agreement with Avista Oil AG, under the patronage of Bernd Althusmann, Lower Saxony's Minister for Economic Affairs, Labor, Transport and Digitization, was signed[2].

The number of offered lectures in the area of simulation could be extended by the transfer of the course "Simulation Methods in the Engineering Sciences", which was developed in Clausthal, to Göttingen. In addition to the talks in the SWZ lecture series "Simulation Sciences" (see page 210), the SWZ is also intensively involved in doctoral training by supporting the lead project HerMes (Heterogeneous Human-Machine Teams) at Clausthal University of Technology, which was launched at the beginning of 2019. The project

aims to establish the nucleus of a graduate school in the research field of **Open Cyber-physical Systems and Simulation (OCSS)**. Four PhD students are researching cross-sectional topics of the development, safeguarding and optimization of the cooperation between man and machine using the infrastructure of the SWZ. The research platform developed there and the qualification offers of the graduate school will be made available to all interested members of the research field OCSS.

After the great success of the first Clausthal-Göttingen International Workshop on Simulation Science in May 2017 in Göttingen, the second edition of the workshop[3], which will take place in Clausthal in May 2019, already has a higher number of submissions, so that the future will remain exciting.

This report is written in **English and in German**. The German texts are short overviews on the projects sketching their basic ideas, approaches, and main results. The English sections contain the more scientific part in which models, results, and methodologies are described in detail. We hope that the descriptions are interesting for you and that you **enjoy reading it**.

Prof. Dr.-Ing. Gunther Brenner
President of the board of directors of the Simulation Science Center Clausthal-Göttingen

1 https://www.tu-clausthal.de/presse/nachrichten/details/2433/
2 https://www.tu-clausthal.de/presse/nachrichten/details/2422/
3 https://www.simscience2019.tu-clausthal.de/

Inhalt

Vorwort **4**

Simulation und Optimierung von Netzen **9**

Dekomposition von Mehrprodukt-Warteschlangennetzen mit „Batch-Processing“ 10

Simulation unsicherer Optimierungsprobleme mit Anwendung in der Fahrplangestaltung und der Maschinenbelegung 13

ASimOV: Agentenbasierte Simulation des Passagierverhaltens zur Optimierung des Verspätungsmanagements im Bahnverkehr 17

Anforderungsrobuste Anordnung von Betriebseinheiten und Maschinen durch Kombination von Optimierung und Simulation 21

Simulation von Materialien **76**

Kopplung multi-physikalischer Prozesse zur Simulation von Gasbohrungen 78

Verteilte Multiskalensimulation zur Optimierung der Herstellung von Faserverbundwerkstoffen für den Flugzeugbau 81

Das Virtuelle Mikroskop – Visualisierung und Inspektion der Geometrie von Partikelschüttungen 83

Druckinduzierte Festkörperphasenübergänge und plastische Verformung in Eisen-Kohlenstoff-Legierungen 86

Verteilte Simulation **143**

Multi-Level-Simulation using Dynamic Cloud Environments 144

Cloud-Efficient Modelling and Simulation of Magnetic Nano Materials 146

Numerisch intensive Simulation auf einer integrierten Recheninfrastruktur 148

Überwachung von Softwarequalität mithilfe von Agenten-basierter Simulation 150

Ringvorlesung „Simulationswissenschaften“ **209**

Übersicht über die bisherigen Vorträge **211**

Lehrangebote an den beiden Partneruniversitäten zum Thema Simulation **225**

International Simulation Science Semester **228**

Clausthal-Göttingen International Workshop on Simulation Science 2017 ..... **231**

Weitere Erfolge **240**

Mitglieder **248**

Veröffentlichungen **252**

Table of contents

Introduction **4**

Simulation and Optimization of Networks **25**

Decomposition of multi-class queueing networks with batch processing 26

Solving Robust Optimization Problems by Iterative Approaches 33

ASimOV: Studying the impact of passenger behavior on train delays using agent-based simulation 48

Demand robust arrangement of operating units and equipment by combining optimization and simulation 64

Simulation of Materials **89**

Coupling of multi-physical processes for the simulation of gas wells 91

Distributed multiscale simulation to optimize the production of fiber composites for aircraft construction 106

The Virtual Microscope: Interactive Visualization of Gaps and Overlaps for Large and Dynamic Sphere Packings 119

Pressure-induced phase transformations in Fe-C alloys: Molecular dynamics simulations 129

Distributed Simulation **154**

Multi-Level-Simulation using Dynamic Cloud Environments 155

Cloud-Efficient Modelling and Simulation of Magnetic Nano Materials 166

Numerically Intensive Simulations on an Integrated Compute Infrastructure 182

Monitoring Software Quality Using Agent-based Simulation Models 194

Lecture series „Simulation Sciences“ **210**

International Simulation Science Semester **228**

Clausthal-Göttingen International Workshop on Simulation Science 2017 ..... **231**

More Achievements **240**

Members **248**

Publications **252**

Simulation und Optimierung von Netzen

9

Die Simulation ist eine der wichtigsten und manchmal sogar die einzige praktikable Technik zur Analyse und Optimierung großer Netze. Telekommunikationsnetze, Verkehrsnetze, Logistiknetze und das „Internet of Things“ haben vieles gemeinsam. Die Komplexität der Netze mit oft Tausenden von Knoten, die sich gegenseitig beeinflussen können, ist schwer überschaubar und daher oft mit anderen Techniken als Simulation nicht beherrschbar.

Der Aufbau, der Betrieb, die Modifikation und die Optimierung großer Netze stellen in der Regel eine Infrastrukturaufgabe dar, die mit erheblichen Kosten verbunden ist. Um Fehlentwicklungen zu vermeiden, wird vor einer physischen Installation die Simulation als wichtiges Hilfsmittel eingesetzt. Mittels Simulation lassen sich Eigenschaften eines Netzes vorab zu ermitteln, z.B. bei der Organisation von Warteschlangen. Häufig werden auch Störszenarien simuliert, um die Stabilitäts- und Robustheitseigenschaften zu verstehen und so z.B. Fahrpläne zu berechnen, die nur wenig verspätungsanfällig sind.

10

Dekomposition von Mehrprodukt-Warteschlangennetzen mit „Batch-Processing“

Wiebke Klünder, Thomas Hanschke

Netze beziehungsweise Netzwerke begegnen uns oft im Alltag und wir sind abhängig von ihnen. Beispiele sind Kommunikations-, Computer-, Verkehrs-, und Produktionsnetze. Generell besteht das Interesse, dass solche Netze nicht nur funktionieren sondern auch leistungsfähig sind. Um die Leistungsfähigkeit feststellen zu können bei beispielsweise veränderten Umgebungsbedingungen werden Leistungsanalysen herangezogen. Leistungsanalysen haben die Aufgabe den optimalen Betriebspunkt von Netzen bezüglich Durchsatz, Warteplatz- und Bedienerkapazität zu bestimmen. Als Werkzeuge bieten sich beispielsweise die Monte Carlo Simulation an sowie die analytische Methode der Warteschlangentheorie. Für beide Ansätze wird der zu untersuchende Sachverhalt modelliert und eine Leistungsanalyse vorgenommen. Beispielsweise kann die Frage beantwortet werden wie sich die Erweiterung eines Maschinenparks eines Produktionssystems auf die Gesamtproduktion auswirkt.

Ein approximatives Verfahren zur Leistungsanalyse von offenen Warteschlangennetzen ist die Dekompositionsmethode.

Es ist ein Netz gegeben, das aus 1,…,N Knoten besteht. Die Knoten werden als stabile Mehrbediener-Warteschlangensysteme modelliert und sind durch gerichtete Kanten mit Übergangswahrscheinlichkeiten miteinander verbunden.

Ein Mehrbediener-Warteschlangensystem besteht aus einem unbeschränkten Warteraum und mehreren Bedienern. Die betrachteten Warteschlangensysteme berücksichtigen unterschiedliche Auftragsklassen. Die Aufträge einer Auftragsklasse treten zu zufälligen Zeitpunkten in zufällig großen Gruppen in das Warteschlangensystem ein und werden in sortenreine Batche umsortiert. Ist ein Bediener inaktiv, kann ein Batch bearbeitet werden. Für den Bedienprozess wird wie für den Ankunftsprozess eine allgemeine Verteilungsannahme genutzt, die durch das erste und zweite Moment beschrieben wird. Sind alle Bediener aktiv, reihen sich die erzeugten Batche in die Warteschlange ein. Dies gilt auch für Aufträge, deren Anzahl nicht zur Erzeugung eines Batches ausreicht. Wurde ein Batch vollständig bedient, verlässt es das Warteschlangensystem. Es wird die Annahme getroffen, dass die Vorgänge der Ankünfte und Bedienungen voneinander unabhängig sind und dass die korrespondierenden Vorgänge der Auftragsklassen voneinander unabhängig sind. Das bedeutet, dass beispielsweise die Ankunftszeitpunkte einer Gruppe bestehend aus Aufträgen der Auftragsklasse A nicht von den Ankunftszeitpunkten von Gruppen der Auftragsklasse B abhängen.

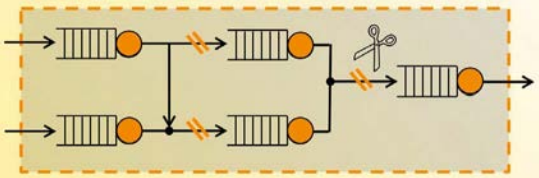

Die Dekompositionsmethode zerlegt das Netz, so dass es möglich ist, die einzelnen Knoten zu untersuchen. Die Schwierigkeit besteht darin, dass die Ströme zwischen den Knoten unbekannt sind. Mit Hilfe der Dekompositionsmethode, Grenzwertsätzen und der Theorie der Erneuerungsprozesse werden die unbekannten Parameter der Ströme bestimmt. Erst dann ist eine Leistungsanalyse der einzelnen Warteschlangensysteme durch die Zusammensetzung der ermittelten Parameter möglich. Die Leistungsanalyse für das gesamte Netz ergibt sich dann aus den Einzelanalysen der Netzkomponenten.

Wird die Dekompositionsmethode angewendet, müssen zwei Gruppen von linearen Gleichungssystemen gelöst werden. Die erste Gruppe

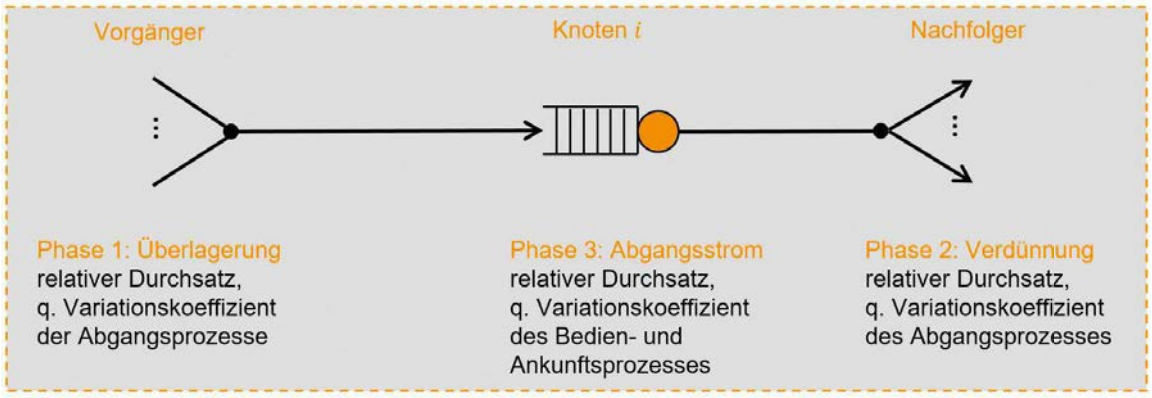

bestimmt mit Hilfe von „traffic equations" den ersten Parameter der zu beschreibenden Ströme (Erneuerungsprozesse) zwischen den Warteschlangensystemen.

$$\tau_i^k = p_{0i}^k \frac{b_0^k}{b_i^k} + \sum_{j=1}^{N} p_{ji}^k \tau_j^k \frac{b_j^k}{b_i^k}, \quad \begin{matrix} \tau_0^k := 1, \\ i,j = 1,\dots,N \\ k = 1,\dots,K \end{matrix}$$

Wird für jede Auftragsklasse k das korrespondierende Gleichungssystem aufgestellt und gelöst und der relative Durchsatz τ_i^k anschließend mit der Eingangsintensität λ_0^k multipliziert, resultiert die exakte Intensität λ_i^k als erster Parameter zur Beschreibung der unbekannten Ströme zwischen den Warteschlangensystemen. Der relative Durchsatz gibt an, wie viele Batche im Mittel das Warteschlangensystem pro Zeiteinheit verlassen und hängt von den Übergangswahrscheinlichkeiten p_{ji}^k und den Batchbediengrößen b_i^k ab.

Um den zweiten Parameter zu erhalten, der für die Beschreibung der unbekannten Ströme notwendig ist, wird eine zweite Gruppe von linearen Gleichungssystemen aufgestellt und gelöst. Der zweite Parameter bestimmt die stochastische Variabilität der unbekannten Ströme zwischen den Warteschlangensystemen in einem betrachteten Netz.

Das Gleichungssystem setzt sich aus drei Phasen zusammen.

Phase 1: $$SCV[I_i^k] = \frac{1}{\lambda_0^k \tau_i^k} \sum_{j=0}^{N} p_{ji}^k \lambda_0^k \tau_j^k SCV[A_{ji}^k]$$

Phase 2: $$SCV[A_{ji}^k] = 1 + p_{ji}^k (SCV[D_j] - 1)$$

Phase 3: $$SCV[D_j] = (\rho_j^\Sigma)^2 SCV[S_j^\Sigma] + (1-\rho_j^\Sigma) SCV[I_j^\Sigma] + (1-\rho_j^\Sigma)\rho_j^\Sigma$$

Im Gegensatz zur Bestimmung des ersten Parameters muss in jeder Phase auf Approximationen zurückgegriffen werden. Die Überlagerung mehrerer Ankunftsprozesse in Phase 1 zu einem Prozess ergibt in der Regel keinen Erneuerungsprozess. Die Verdünnung eines Abgangsprozesses in Phase 2, der selbst nur durch eine Approximation bestimmt wird (Phase 3), ergibt zwar Erneuerungsprozesse, diese sind aber abhängig voneinander. Wie zuvor beim relativen Durchsatz wird für jede Auftragsklasse k ein lineares Gleichungssystem aufgestellt und gelöst.

Durch die Lösungen der Gleichungssysteme sind die Ströme zwischen den Warteschlangensystemen im betrachteten offenen Warteschlangennetz vollständig beschrieben und durch Anwendung

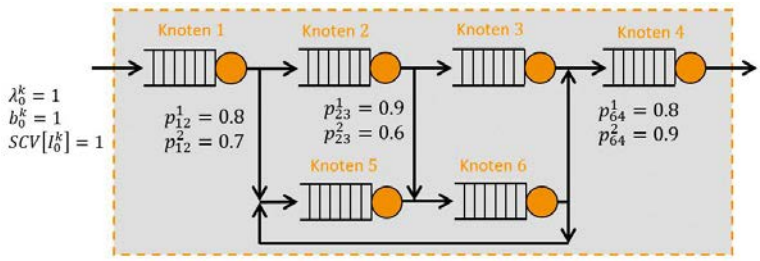

$SCV[S_i^k] = 0.5$

Knoten 1	$c_1 = 1, b_1^k = 5, \rho_1^\Sigma = 0.8$
Knoten 2	$c_2 = 3, b_2^k = 3, \rho_2^\Sigma = 0.9$
Knoten 3	$c_3 = 1, b_3^k = 4, \rho_3^\Sigma = 0.6$
Knoten 4	$c_4 = 5, b_4^k = 1, \rho_4^\Sigma = 0.8$
Knoten 5	$c_5 = 1, b_5^k = 3, \rho_5^\Sigma = 0.5$
Knoten 6	$c_6 = 2, b_6^k = 10, \rho_6^\Sigma = 0.7$

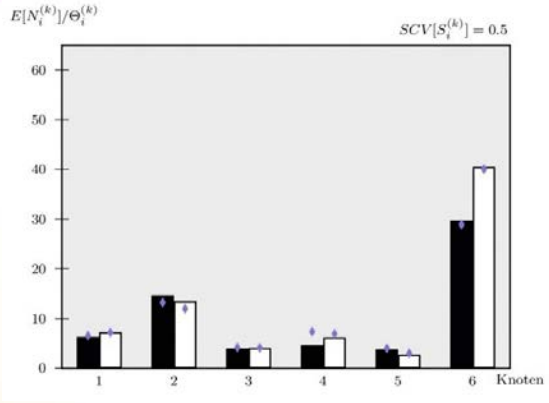

der Allen und Cunneen Approximationsformel und des Satzes von Little resultieren die Leistungsgrößen der einzelnen Warteschlangensysteme des Netzes. Durch entsprechende Aufsummierung lassen sich anschließend die Leistungsgrößen für das gesamte Netz bestimmen.

Im Rahmen der Arbeit wurden 500 Konfigurationen gerechnet, die sich auf zwei Referenzmodelle verteilen. Die berechneten Approximationen wurden mit den Ergebnissen der simulierten Konfigurationen verglichen. Die weiterentwickelte Dekompositionsmethode liefert gute Approximationen, wenn die Voraussetzungen nicht verletzt werden. Werden Voraussetzungen verletzt, wie es beispielsweise der Fall ist, wenn die mittleren Eingangsgruppengrößen um ein Vielfaches größer sind als die Batchbediengrößen, sind Abweichungen der Approximationen gegeben. Abweichungen zwischen Simulations- und Approximationsergebnisse sind auch dann gegeben, wenn ein betrachteter Knoten mehrere Vorgänger beziehungsweise Nachfolger besitzt. Trotz der Verletzung der Annahme von Erneuerungsprozessen, erzielt die Dekompositionsmethode gute Ergebnisse wie der untere Fall zeigt.

Projektdaten

Das Projekt wird seit April 2014 vom SWZ mit insgesamt 0,5 TV-L E13 Stellen an dem Standort Clausthal gefördert. Beteiligte Wissenschaftler sind:

Prof. Dr. Thomas Hanschke
Arbeitsgruppe Stochastische Modelle in den Ingenieurwissenschaften
Institut für Angewandte Stochastik und Operations Research
Technische Universität Clausthal

Dr. Wiebke Klünder
Arbeitsgruppe Stochastische Modelle in den Ingenieurwissenschaften
Institut für Angewandte Stochastik und Operations Research,
Technische Universität Clausthal

Simulation unsicherer Optimierungsprobleme mit Anwendung in der Fahrplangestaltung und der Maschinenbelegung

Stephan Westphal, Anita Schöbel, Julius Pätzold

Unsicherheiten in Optimierungsproblemen sind ein in der Praxis häufig auftretendes Problem. Oft sind die für die Planung notwendigen Informationen zu Beginn des Optimierungsprozesses nicht vollständig oder noch nicht ausreichend bekannt und werden erst im Anschluss an die ersten Planungsentscheidungen aufgedeckt. Beispiele dafür lassen sich unter anderem in der Fahrplangestaltung finden, wo durch Verspätungen oder verpasste Anschlüsse geplante Verbindungen nicht eingehalten werden können. Auch in der Maschinenbelegung beruhen Planungsentscheidungen in der Regel auf Vergangenheitsdaten und Schätzungen, sodass unerwartete Schwankungen in der Auftragslage oder Ausfälle von Maschinen zu Wartezeiten führen, die dafür sorgen, dass ein Produktionsplan nicht eingehalten werden kann. Da diese Ereignisse nicht nur ein Ärgerniss für die wartenden Fahrgäste darstellen, sondern in der Industrie regelmäßig Kosten in Millionenhöhe verursachen, ist das Ziel des Projektes, diese Unsicherheiten mit Hilfe von Simulation bereits während des Planungsprozesses einzubeziehen und in einem iterativen Prozess mit der Optimierung und der daraus resultierenden Entscheidungen zu verbinden.

Im Rahmen dieses Projektes werden zwei verschiedene Konzepte von Unsicherheiten betrachtet. In der klassischen robusten Optimierung wird nach einer Lösung gesucht, die für jedes mögliche eintretende Szenario zulässig ist und dabei das Szenario mit den höchsten Kosten in der Zielfunktion minimiert. Man bezeichnet diese Absicherung im schlechtesten Fall allgemein auch als konservative worst-case Analyse. Auf diese Art und Weise können Optimierungsprobleme, wie zum Beispiel die Produktionsprogrammplanung, in einer robusten Version formuliert werden, bei der Modellparameter - wie die Nachfrage oder die Produktionszeiten - unsicher sind. In diesem Fall muss eine Lösung entwickelt werden, die nach der Realisierung eines Szenarios möglichst gute Ergebnisse liefert.

In der Online-Optimierung werden die Unsicherheiten durch Anfragesequenzen modelliert und nicht gleichzeitig, sondern nacheinander aufgedeckt. Nach jeder neuen Anfrage muss der Online-Algorithmus eine Entscheidung treffen. Zum Beispiel ein Taxifahrer, der sich gerade für die Weiterfahrt entschieden hat, als ein neuer Fahrgast an seinem vorherigen Standort aufkreuzt. Die Realisierung eines Szenarios entspricht dabei einer vollständig aufgedeckten Eingabesequenz. Die Online-Optimierung zählt zu den konservativen Konzepten, bei denen immer nur der worst-case, also die Eingabesequenz mit den für einen bestimmte Algorithmus höchsten Kosten betrachtet wird. Die große Herausforderung in der konservativen worst-case Analyse entsteht durch die Vielzahl an Strategien und Szenarien, die für ein endgültiges Resultat untersucht werden müssen. In der Regel ändert sich das worst-case Szenario für ein Problem durch die Wahl einer anderen Strategie bzw. eines anderen Algorithmus. Dadurch werden anspruchsvolle praktische Optimierungsprobleme, wie Produktionsnetzwerke mit mehreren tausend Varianten und Produktionen am Tag schnell zu komplex, um sie allein mit theoretischen Mitteln zu analysieren. In diesem Projekte wird daher ein integrativer Simulations- und Optimierungsansatz vorgestellt und untersucht, der die fortschrittlichen theoretischen Entwicklungen der mathematischen Optimierung mit den praxisorientierten Analysemethoden und Techniken der Simulation verbindet.

Das grundlegende Konzept eines simulationsbasierten Optimierungsansatzes liegt in einem

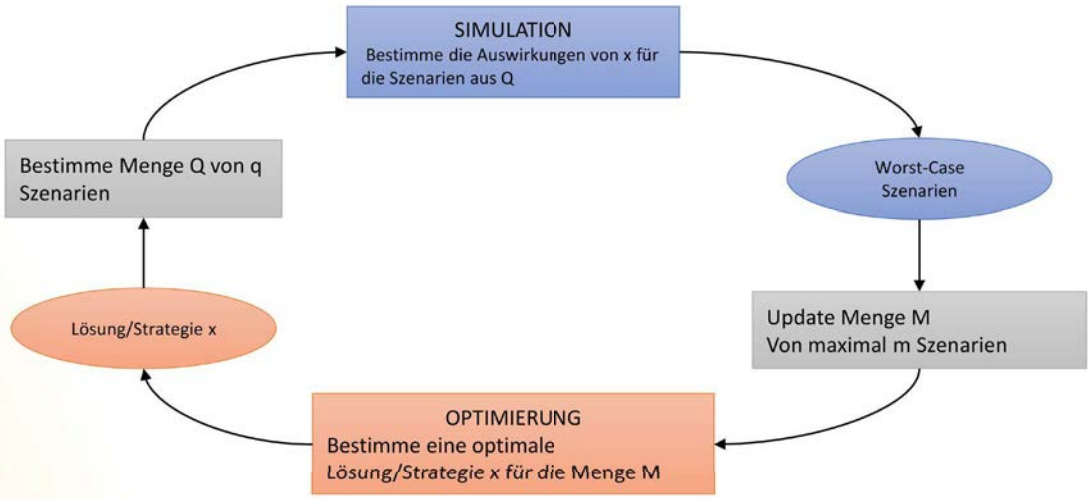

Abbildung1: Der simulationsbasierte Optimierungsyzklus

Wechselspiel zwischen einem Optimierungsprozess und einer Simulation. Dabei sollen die Ergebnisse der Optimierung als Input für die Simulation dienen und umgekehrt. Im Fokus steht dabei der iterative simulationsbasierte Optimierungszyklus aus Abbildung 1. Abwechselnd wird eine geeignete Strategie auf Basis von Inputdaten entwickelt (Optimierung) und anschließend im Rahmen einer Simulation getestet, bzw. bewertet. Hierbei wird versucht die Szenarien zu finden, für die die Strategie sehr schlecht geeignet ist (Simulation), um anschließend eine Verbesserung vornehmen zu können. Dieser iterative Prozess ermöglicht, dass nicht von Beginn an alle denkbaren Szenarien in der Optimierung oder der Simulation berücksichtigt werden müssen, sondern nur ausgewählte Szenarien in den Zyklus aufgenommen werden.

Eine der meist erforschten Fragestellungen des Operations Research ist das sogenannte Scheduling. Dabei beschäftigt man sich mit der Frage, wie eine Menge von Aufträgen auf eine gegebene Menge von Maschinen verteilt und wann deren Bearbeitung jeweils beginnen soll, so dass eine Reihe von Nebenbedingungen eingehalten werden. Dabei können sowohl die Aufträge als auch die Maschinen unterschiedliche Eigenschaften haben. Die Maschinen haben dabei z.B. unterschiedliche Geschwindigkeiten, es gibt Reihenfolgebeziehungen zwischen den Aufträgen, Zeitfenster in denen die Aufträge bearbeitet werden müssen oder Einschränkungen bzgl. der Zuweisungsmöglichkeiten der Aufträge zu den Maschinen. Im untersuchten Fall kommt hier die Online-Charakteristik zum Tragen, bei der die Aufträge nacheinander eintreffen und bei jedem Eintreffen sofort entschieden werden muss, auf welcher Maschine der jeweilige Auftrag bearbeitet werden soll. Häufig ist hier nicht nur die Wahl einer geeigneten Planungsstrategie von Relevanz, sondern auch die Frage nach besonders ungünstigen Eingabesequenzen. Mit Hilfe des simulationsbasierten Optimierungsansatzes wurden verschiedene Schedulingprobleme analysiert und insbesondere auf ihre worst-case Instanzen untersucht. Dabei wurde ein sogenannter Instanzgenerator entwickelt, der mit Hilfe von mathematischen Evolutionsverfahren besonders bösartige Eigenschaften von Eingabesequenzen bestimmt und darauf aufbauend neue Sequenzen generiert. Auf diese Art und Weise können konkrete Online-Algorithmen

auf ihr Verhalten im worst-case analysiert werden oder sogar noch unbekannte Sequenzen aufgedeckt werden. Unter anderem konnten hier neue Erkenntnisse über das Online-Intervalscheduling gewonnen werden.

Bei der robusten Optimierung werden die optimalen Lösungen und auch die worst-case Szenarien mit Hilfe mathematischer Optimierungverfahren eindeutig bestimmt, um am Ende die optimale Lösung für den gesamten Instanzraum zu erhalten. Häufig sind die zu Grunde liegenden Optimierungsprobleme allerdings schwer zu lösen und würden bei dem Einsatz konservativer Lösungsverfahren zu sehr langen Iterationszeiten innerhalb des Simulationszyklus führen. Hierzu wurden spezielle Schnittebenenverfahren entwickelt, um das Konvergenzverhalten zu beschleunigen und die Lösungen zu approximieren. Mit Hilfe dieser Schnittebenen konnte gezeigt werden, dass in den meisten Fällen bereits wenige Iterationen des Zyklus ausreichen, um das Robuste Optimierungsproblem approximativ zu lösen. Außerdem ließen sich so allgemeine obere Schranken für generelle Robuste Optimierungsprobleme beweisen.

Es hat sich gezeigt, dass das vorgestellte Konzept zur Simulation eine Bereicherung der klassischen worst-case Analyse ist. Mit Hilfe der Simulationstechniken konnten Optimierungsprobleme mit zu Grunde liegenden Unsicherheiten optimal gelöst werden, wobei die Laufzeit im Vergleich zu klassischen Lösungsverfahren teilweise deutlich reduziert werden konnte. Darüber hinaus ist der Zyklus geeignet, um worst-case Instanzen zu generieren, mit deren Hilfe die Güte von Optimierungsalgorithmen getestet werden kann. Insbesondere in der praktischen Anwendung lassen sich so extreme Störungen, die durch die Unsicherheiten auftreten können, mit einer geigneten Planungsstrategie vermeiden.

Projektdaten

Das Projekt wird seit August 2015 vom SWZ mit insgesamt einer TV-L E13 Stelle an den Standorten Clausthal und Göttingen gefördert. Beteiligte Wissenschaftler sind:

Prof. Dr. Anita Schöbel
Arbeitsgruppe Optimierung
Institut für Numerische und Angewandte Mathematik
Universität Göttingen

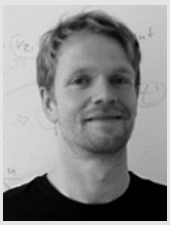

Martin Dahmen, M.Sc.
Arbeitsgruppe Diskrete Optimierung, Institut für Angewandte Stochastik und Operations Research
Technische Universität Clausthal

Prof. Dr. Stephan Westphal
Arbeitsgruppe Diskrete Optimierung, Institut für Angewandte Stochastik und Operations Research
Technische Universität Clausthal

Julius Pätzold, M.Sc.
Arbeitsgruppe Optimierung
Institut für Numerische und Angewandte Mathematik
Universität Göttingen

ASimOV: Agentenbasierte Simulation des Passagierverhaltens zur Optimierung des Verspätungsmanagements im Bahnverkehr

Sebastian Albert, Philipp Kraus, Awad Mukbil, Julius Pätzold, Jörg P. Müller, Anita Schöbel

Die häufigen Störungen und die daraus resultierenden Verspätungen im Bahnverkehr machen das Verspätungsmanagement zu einem praxisrelevanten Thema. Um bei Verspätungen einen Dispositionsfahrplan zu erstellen, ist festzulegen, welcher Zug bei einem Belegungskonflikt zuerst fahren darf, und welche Züge auf verspätete Zubringer warten sollen (Anschlusssicherung). In der betrieblichen Praxis werden dazu meist feste Wartezeitregeln verwendet, die z.B. vorgeben, dass ein ICE auf einen anderen verspäteten ICE drei Minuten wartet.

Seit mehr als zehn Jahren wird das Problem der Anschlusssicherung als Gesamtproblem aufgefasst und die Bestimmung optimierter Dispositionsstrategien auch theoretisch untersucht [DHSS2018]. Dazu sind allerdings Vereinfachungen nötig. Diese betreffen eine grobe Darstellung der Infrastruktur und vereinfachte Annahmen über das Passagierverhalten. Während Simulationsverfahren zu einer gleisgenauen Belegung auch im Rahmen der Anschlusssicherung bereits existieren (siehe DisKon [BGJ+05]) ist die Auswirkung des Passagierverhaltens kaum untersucht. Wechselwirkungen zwischen Passagierverhalten und Zugverspätungen werden vor allem am Bahnhof sichtlich: Ist ein Anschluss knapp, steigen Passagiere schneller aus und rennen auf das geplante Abfahrtsgleis. Wird ein Anschluss nicht erreicht, versuchen manche Passagiere, weitere Informationen an der Anzeigentafel oder am Schalter zu bekommen, andere bummeln durch die Geschäfte oder trinken einen Kaffee.

In den letzten Jahren ist ein Paradigmenwechsel bei der Modellierung und Simulation komplexer Netze und Systeme zu beobachten. Makroskopische Ansätze, die Flüsse mittels Differentialgleichungen und Unsicherheiten mittels stochastischer Modelle modellieren, werden zunehmend ergänzt (teilweise auch ersetzt) durch mikroskopische Ansätze. Agentenbasierte Modellierung und Simulation (ABMS) [BK2013] ist ein mikroskopisches Paradigma, das in den letzten Jahren auch im Bereich der Mobilitätssimulation – insbesondere für die Modellierung der Verkehrsnachfrage [Bal+2009] – erfolgreich Anwendung gefunden hat. Dabei nutzen die bislang verfügbaren Modelle und Plattformen weitgehend einfache Agentenmodelle, mit denen komplexeres kognitives und interaktives Verhalten nur eingeschränkt dargestellt werden kann. Auch die beschränkte Performanz und Skalierbarkeit agentenbasierter Plattformen, die effiziente Abbildung auf parallele Ausführungsarchitekturen und die Kopplung unterschiedlicher Teilmodelle sind aktuelle Herausforderungen für die Forschung.

Ziel des Projektes ist die Entwicklung einer agentenbasierten Simulation (ABS) für das Problem der Anschlusssicherung im Zugverkehr und darauf basierend die Entwicklung optimaler Dispositionsstrategien. In dieser Simulation wird jeder Passagier als Agent mit individuellen Fähigkeiten, Zielen und Verhalten beim Auftreten von Verspätungen modelliert. Die Wege der Agenten durch den Bahnhof werden anhand der Bahnhofsgeometrie simulativ abgebildet und sind damit abhängig von Anzahl und Eigenschaften der sich im Bahnhof bewegenden Fahrgäste. Lokale Dispositionsentscheidungen des Zugs am Bahnsteig (z.B. Türen schließen) werden ebenfalls agentenbasiert kontextspezifisch abgebildet. Dabei sind zwei heterogene Systeme zu koppeln: Die makroskopische Simulation der Züge auf dem Streckennetz und die mikroskopische Simulation der Passagiere im Bahnhof.

Zur Optimierung von Dispositionsmaßnahmen erlauben Rückschlüsse aus der Simulation eine

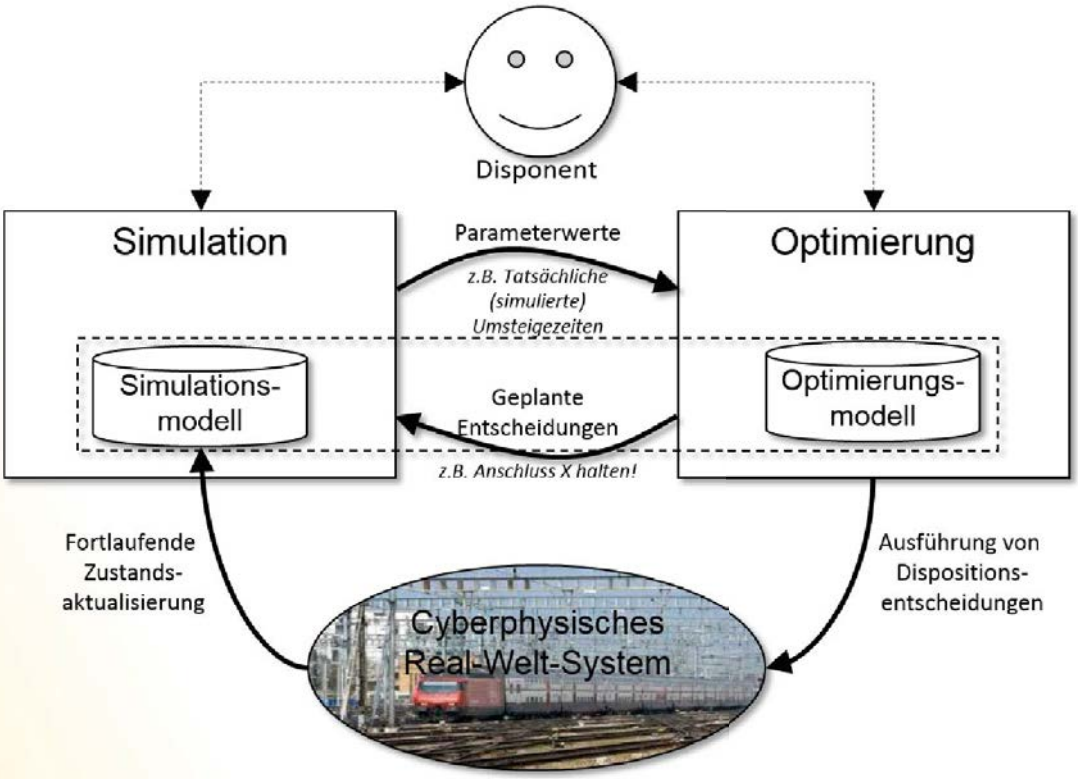

Abbildung 1: Hybride Kopplung von Simulation und Optimierung in Cyberphysischen Systemen

Verbesserung des Optimierungsmodells erlauben und werden zu neuen hybriden Algorithmen führen. Dabei werden ausgehend von der betrachteten Anwendung auch methodische Erkenntnisse bezüglich zukünftiger hybrider Verfahren zur Simulation und Optimierung cyberphysischer Systeme angestrebt, in denen der Zustand der Realwelt, ihre simulative Abbildung und die dadurch informierten Optimierungsmodelle und -methoden zu einem dynamischen Regelkreis verschmelzen (s. Abb. 1).

Die Simulation wird zunächst dazu verwendet, Eingabeparameter der Optimierung genauer zu bestimmen und damit Optimierungsmodelle zu verbessern. Letztere werden dann wieder in die Simulation zurückgespielt und validiert. Dabei müssen Simulation und Optimierung auf Änderungen in der Umgebung reagieren können, die teilweise auch die Folge von Dispositionsentscheidungen sind.

Längerfristig ist dabei eine Annäherung und Verschmelzung der heute weitgehend disjunkten Modelle für Simulation einerseits und Optimierung andererseits zu erwarten.

In der ersten Projektphase von Asimov erfolgte die Modellierung der beiden interagierenden Teilsysteme der Simulation (Netzwerk und Bahnhof), sowie die Durchführung initialer Experimente zur Auswirkung realistischerer Modelle auf Einflussfaktoren des Verspätungsmanagements.

Zur Modellierung des Netzwerks wurden Ereignis-Aktivitätsnetze zur Repräsentation der Umsteigebeziehungen verwendet (Abb. 2 zeigt ein Beispiel eines solchen Netzes für drei Züge). Weiterhin wurde ein Simulationsmodell für die Ein- und Aussteigeaktionen der Passagiere sowie die Bewegungen der Züge (und damit der Passagiere) durch das Zugnetz beschreibt. Parallel dazu wurde dabei zunächst ein initiales mesoskopisches probabilis-

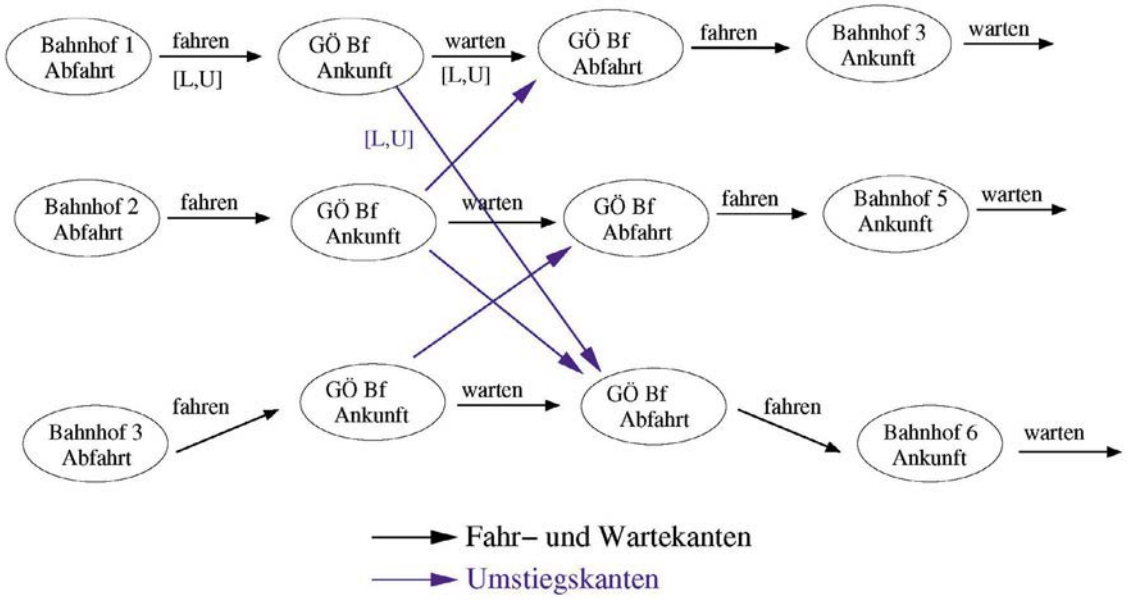

Abbildung 2: Darstellung von Wartebeziehungen in einem Ereignis-Aktivitätsnetz

tisches Modell für Passagierbewegungen (Umsteigezeiten) in einer Bahnhofsumgebung entworfen. Als Plattform für beide Modellteile diente LightJason [AKM2016], eine skalierbar nebenläufige und agentenbasierte Simulationsplattform für sozio-technische Systeme.

Auf der Basis dieses Modells wurde in [AKMS2018] anhand eines einfachen Umsteigeszenarios untersucht, wie Abfahrtsverspätungen von Zügen durch Eingangsverspätungen und die Anzahl und Heterogenität der Passagiere beeinflusst werden. Die Ergebnisse bekräftigen die Hypothese, dass Passagierverhalten in der Tat einen signifikanten Effekt auf Abfahrtsverspätungen haben kann. Insbesondere konnten wir in unseren Experimenten den bisher in der Literatur des Verspätungs-managements noch nicht betrachteten Effekt nachweisen, dass auch die Abfahrtszeit eines Zuges vom Passagierverhalten abhängig ist: der Zug kann erst losfahren, wenn keiner mehr einsteigt – das Eintreffen eines ganzen Passagierstromes nach und nach kann also eine Abfahrtzeit weiter und weiter verzögern. Basierend auf dem initialen Modell wurde im nächsten Schritt ein agentenbasiertes Passagiermodell entwickelt, das eine mikroskopische taktische Wegeplanung und regelbasierte Entscheidungsmodelle in Verbindung mit einem Social-Force-basierten Ansatz [HM1995] zur Bewegungssimulation kombiniert [JKM2017]. Der experimentelle Vergleich dieses Modells mit dem initialen Modell wird bis zum Ende der ersten Projektphase durchgeführt werden.

Zusammenfassend ist in der ersten Phase von ASimOV ein wichtiger erster Schritt zur Entwicklung eines hybriden Ansatzes zur mikroskopischen Simulation von Bahnsystemen unter Berücksichtigung von Forschungsfragen des Verspätungsmanagements und der Anschlusssicherung gelungen. Auf Basis der bislang erzielten Ergebnisse sollen in der zweiten Projektphase insbesondere reichere Passagiermodelle (Gepäck, Menschen mit Behinderungen, Nutzung von Serviceangeboten am Bahnhof, Nutzung von Smartphones zur Einholung aktueller Informationen), Bahnhofstopologien (Treppen, Aufzüge, Durchgangsverkehre) untersucht und die zur Zeit noch offline realisierte hybride Kopplung zwischen Optimierungsverfahren und Simulation in Richtung auf dynamische Übergabe von Ergebnissen und Parametern verbessert werden.

Literatur

Albert, S., Kraus, P., Müller, J., Schöbel, A. (2018). Passenger-induced delay propagation: Agent-based simulation of passengers in rail networks. In: Simulation Science. SimScience 2017: Communications in Computer and Information Science (CCIS), vol 889. pp. 3-23. Springer, Cham.

Aschermann, M., Kraus, P., Müller, J.P. (2018). LightJason: A BDI Framework inspired by Jason. In: Multi-Agent Systems and Agreement Technologies: 14th Europ. Conf., EUMAS 2016, and 4rd Int. Conf., AT 2016, Valencia, Spain, 2016. Lecture Notes in Computer Science, vol. 10207, pp. 58-66. Springer International Publishing (2017). https://lightjason.org

M. Balmer, M. Rieser, K. Meister, D. Charypar, N. Lefebre, and Nagel K. (2009). Towards truly agent-based traffic and mobility simulations. In A. L. C. Bazzan and F. Klügl, editors, Multi-agent Systems for Traffic and Transport Engineering, pages 57-78. IGI Global.

Bazzan, A.L.C., Klügl, F. (2013). Agent-based Modeling and Simulation. AI Magazine 33(3), 29-40.

Bissantz, N., Güttler, S., Jacobs, J., Kurby, S., Schaer, T., Schöbel, A., Scholl, S. (2005). DisKon - Laborversion eines flexiblen, modularen und automatischen Dispositionsassistenzsystems. Eisenbahntechnische Rundschau (ETR), 45(12):809-821.

Dollevoet, T., Huisman, D., Schmidt, M., Schöbel, A. (2018). Delay propagation and delay management in transportation networks. In: et al., C.M. (ed.) Handbook of Optimization in the Railway Industry, pp. 285-317. Springer International Publishing.

Helbing, D., Molnar, P. (1995). Social force model for pedestrian dynamics. Physical review E 51(5), 42-82.

Johora, F.T., Kraus, P., Müller, J.P. (2017): Dynamic path planning and movement control in pedestrian simulation, Preproceedings of 2nd International Workshop on Agent-based modelling of urban systems (ABMUS 2017). Sao Paulo, Brazil. http://arxiv.org/abs/1709.08235

Projektdaten

Das Projekt wird seit Juni 2016 vom SWZ mit insgesamt 1,5 TV-L E13 Stellen an den Standorten Clausthal und Göttingen gefördert. Beteiligte Wissenschaftler sind:

Prof. Dr. Jörg Müller
Arbeitsgruppe
Wirtschaftsinformatik
Institut für Informatik
Technische Universität Clausthal

Julius Pätzold, M.Sc.
Arbeitsgruppe Optimierung
Institut für Numerische und
Angewandte Mathematik
Universität Göttingen

Prof. Dr. Anita Schöbel
Arbeitsgruppe Optimierung
Institut für Numerische und
Angewandte Mathematik
Universität Göttingen

Anforderungsrobuste Anordnung von Betriebseinheiten und Maschinen durch Kombination von Optimierung und Simulation

Uwe Bracht, Anja Fischer, Thomas Krüger, Mirko Dahlbeck, Marc Schlegel

Die steigende Globalisierung und der damit verbundene Anstieg der Marktdynamik stellen Unternehmen vor neue Herausforderungen. Immer kürzer werdende Produktzyklen sowie wachsende Kundenanforderungen bezüglich Qualität und Liefertreue erfordern immer häufiger Produkt- und Programmänderungen und damit eine Anpassung der Fabrik- und Produktionsstrukturen [1].

Dies erfordert den Einsatz von Methoden der Fabrikplanung sowie den Werkzeugen der Digitalen Fabrik, um durch innovative Ansätze die Leistungsfähigkeit zu steigern und dabei den Kostendruck zu verringern [2]. Ein wichtiger Aspekt ist hierbei die Anordnung der Maschinen innerhalb der Fabrik, da diese die Abläufe und die Effizienz des Produktionsbetriebs beeinflusst und somit signifikante Auswirkungen auf die Produktionskosten hat [3, 4].

Diese sogenannten Anordnungsprobleme können mit unterschiedlichen Verfahren gelöst werden. In der Regel werden in der Fabrikplanung heuristische Verfahren verwendet [5, 6]. Diese erzeugen schnell zulässige Lösungen, aber es können keine Aussagen über die Qualität der Lösungen getroffen werden. Zur Berechnung einer optimalen Lösung werden in der Literatur eine Vielzahl von Vereinfachungen getroffen, wie zum Beispiel bezüglich der Wegstruktur [7, 8]. Beim Double-Row Facility Layout Problem (DRFLP) ist eine Menge von Maschinen mit paarweisen Transportbeziehungen zwischen den Maschinen gegeben, die die Anzahl der notwendigen Transporte zwischen den Maschinen beschreibt. Das Ziel ist es, die Maschinen entlang beider Seiten eines Weges überlappungsfrei anzuordnen, sodass die Summe der gewichteten Distanzen zwischen den Maschinen minimiert wird. Die Distanzen werden in der Literatur jeweils von den Mitten der Maschinen ausgehend gemessen. Ein Beispiel für ein double-row layout ist in Abbildung 1 illustriert.

Das DRFLP ist NP-schwer [7, 9–11]. Der zurzeit beste Lösungsansatz für das DRFLP enumeriert über alle möglichen Reihenzuweisungen der Maschinen und löst das DRFLP jeweils mit fixierter Reihenzuweisung. Damit können DRFLP Instanzen mit bis zu 16 Maschinen innerhalb von 12 Stunden exakt gelöst werden.

Die Lösung des DRFLP stellt eine Basis für weitere Fabrikplanungsschritte dar und hat somit Einfluss auf die Qualität der Planungsergebnisse und den

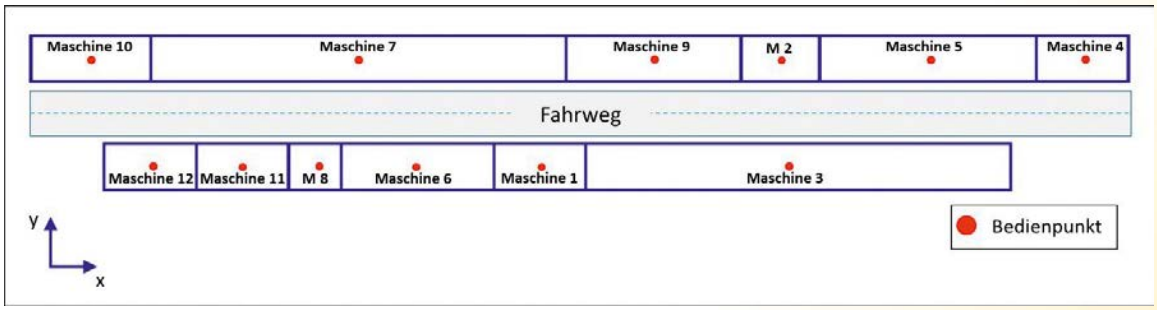

Abbildung 1: Beispiellösung einer DRFLP Anordnung

weiteren Planungsaufwand. Ein Hauptziel unseres Projekts war und ist deshalb die Verbesserung exakter Lösungsansätze für das DRFLP. In diesem Projekt benutzen wir einen Ansatz, der Optimierung und Simulation kombiniert. Zunächst berechnen wir eine optimale Lösung für das DRFLP. Diese wird dann mit Hilfe der Simulation anhand zahlreicher Kennzahlen, wie z.B. Durchlaufzeiten, Bestände oder Auslastungen ausgewertet. Diese Werte werden während eines Simulationslaufes dynamisch ermittelt. Sollte es zu Engpässen oder Problemen kommen, so wird anschießend nach möglichen Verbesserungsansätzen für die Anordnung gesucht. Es werden dann zusätzliche Nebenbedingungen in das DRFLP Modell integriert und dieses wird erneut gelöst. Dieser iterative Vorgang ist in Abbildung 2 skizziert.

Ein weiteres Ziel in diesem Projekt war die Erweiterung bestehender DRFLP-Modelle um praxisrelevante Aspekte. So gibt es etwa in realitätsnahen double-row Instanzen häufig identische Maschinen, d.h. Maschinen mit gleicher Länge und gleichem Transportaufkommen zu den anderen Maschinen. Wir betrachteten eine realistische Instanz [12] mit 21 Maschinen, in der zwei Maschinen viermal und drei Maschinen doppelt vorkommen. Wir konnten unter dieser Annahme die Anzahl der unterscheidbaren Reihenzuweisungen signifikant reduzieren und somit mit dem Ansatz aus [8] diese Instanz in weniger als 14 Stunden lösen.

Weiterhin haben wir das DRFLP Modell [8] um realistische Aspekte erweitert, wie zum Beispiel

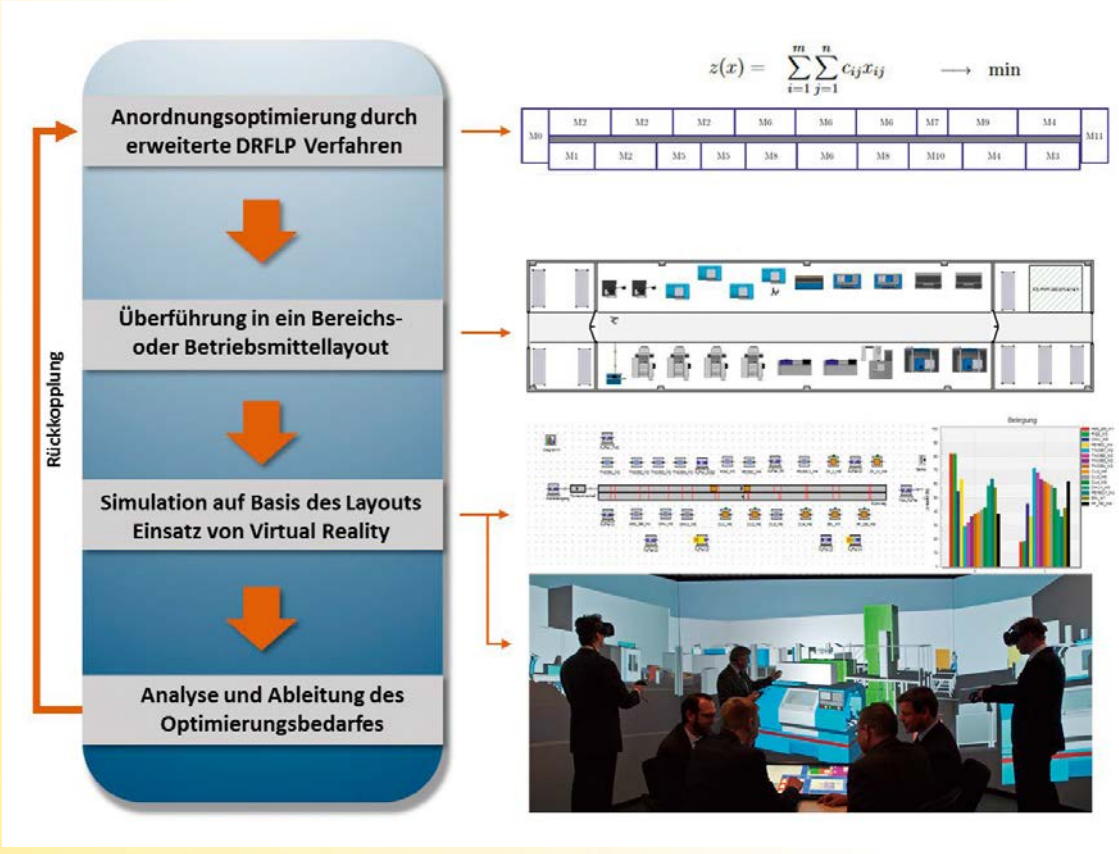

Abbildung 2: Vorgehensweise zur Erweiterung und Validierung der Anordnungsoptimierung

asymmetrische Sicherheitsabstände zwischen (benachbarten) Maschinen. Diese sind beispielsweise erforderlich, um erforderliche Durchgangsbreiten oder Wartungsbereiche einzuhalten. Außerdem haben wir die Fläche, auf der die Maschinen angeordnet werden, beschränkt und vertikale Distanzen zum Modell hinzugefügt, d.h. der Abstand zwischen zwei Maschinen in zwei unterschiedlichen Reihen entspricht dann mindestens der Breite des Weges.

Häufig werden bei der Layoutplanung die Lagerflächen (beispielsweise für den Wareneingang und den Warenausgang) am linken und rechten Rand fixiert, um einen möglichst transparenten Materialfluss mit einer Haupttransportrichtung zu erhalten. Auch diese Variante lässt sich mit den entwickelten Optimierungsmodellen behandeln.

Im Hinblick auf Industrie 4.0 und flexible Fertigungssysteme mit selbststeuernden Regelkreisen, die komplexe und ungerichtete Materiaflussstrukturen beherrschbar machen, berechnen wir auch optimale Lösungen, in denen die Lagerflächen auf beliebigen Positionen angeordnet werden dürfen. Dabei werden die Lagerflächen wie normale Maschinen behandelt.

Zur Erweiterung der Verfahren und der Absicherung der Lösungsqualität des DRFLP kommen Methoden und Werkzeuge der Digitalen Fabrik, wie die Materialflusssimulation und Virtual Reality, zum Einsatz (siehe Abbildung 2).

Im ereignisdiskreten Materialflusssimulator „Plant Simulation“ werden die dynamischen Produktionsabläufe nachgebildet und in Verbindung mit dem double-row layout simuliert.

Zusätzlich kommen zur Absicherung der räumlichen Anordnung Methoden der Virtual Reality (VR) zum Einsatz. Mit dieser dynamischen Visualisierung kann die Anwenderin oder der Anwender in die virtuelle dreidimensionale Produktionsumgebung „eintauchen“. Dabei lassen sich z.B. die Größenverhältnisse sowie erforderliche Bedien- und Wartungsabstände überprüfen oder die kollisionsfreie Platzierung der Maschinen absichern. Der bei der Simulation und in der VR-Umgebung eventuell auftretende Verbesserungsbedarf wird wieder in der Anordnungsoptimierung berücksichtigt.

Mit dem kombinierten Einsatz von Optimierung und Simulation wurde unter anderem eine realistische Instanz mit 21 Maschinen näher untersucht. Dafür wurde zunächst eine in der Fabrikplanung häufig verwendete Heuristik [5, 13] eingesetzt und diese von Hand zu einer zweireihigen Anordnung mit zentralem Transportweg angepasst und verbessert. Zusätzlich wurde jeweils eine optimale Lösung mittels DRFLP für die Variante mit fixierten Wareneinen- und -ausgängen am Rand sowie bei freier Positionierung dieser Lagerflächen erstellt. Die drei verschiedenen Layouts wurden mittels Simulation ausgewertet. In dieser Instanz werden insgesamt acht Einzelteile gefertigt und in einer Maschine zu einem Endprodukt verarbeitet. In einem Simulationslauf wird die Jahresproduktion von 36.000 Endprodukten abgebildet. Die optimierte Variante mit fixierten Lagerpositionen erlaubt es, die insgesamt zurückgelegten Distanzen aller Produkte um 4% im Vergleich zur heuristisch bestimmten Lösung zu verbessern. Bei freier Anordnung ist im Vergleich zu den beiden anderen Varianten eine Reduktion der Summe der Transportdistanzen um 34,4% bzw. um 31,4% möglich.

Diese Ergebnisse zeigen, dass durch eine Kombination von Optimierung und Simulation ein hohes Potential zur Senkung der Produktionskosten aufgedeckt werden kann.

Projektdaten

Das Projekt wird seit April 2016 vom SWZ mit insgesamt 1,5 TV-L E13 Stellen an den Standorten Clausthal und Göttingen gefördert. Beteiligte Wissenschaftler sind:

Prof. Dr.-Ing. Uwe Bracht
Arbeitsgruppe Anlagen-projektierung und Material-flusslogistik, Institut für Maschinelle Anlagentechnik und Betriebsfestigkeit
Technische Universität Clausthal

Dipl.-Wirtschaftsing. Thomas Krüger
Arbeitsgruppe Anlagenprojektierung und Materialflusslogistik
Institut für Maschinelle Anlagentechnik und Betriebsfestigkeit
Technische Universität Clausthal

Jun.-Prof. Dr. Anja Fischer
Arbeitsgruppe Management Science, Fakultät Wirtschaftswissenschaften
Technische Universität Dortmund

Marc Schlegel, M.Sc.
Arbeitsgruppe Anlagenprojektierung und Materialflusslogistik
Institut für Maschinelle Anlagentechnik und Betriebsfestigkeit
Technische Universität Clausthal

Mirko Dahlbeck, M.Sc.
Arbeitsgruppe Management Science, Fakultät Wirtschaftswissenschaften
Technische Universität Dortmund

Simulation and Optimization of Networks

Simulation is one of the most important and sometimes even the only possible technique for analyzing and optimizing large networks. Telecommunication networks, transport networks, logistic networks and the Internet of Things have much in common. The complexity of a network with many thousands of nodes, which can interfere with each other is so high that simulation techniques are often the only tools for its analysis. The design, operation, modification and optimization of the infrastructure of a large network is a task that comes with considerable costs. To avoid wrong decisions, simulation is used to determine the properties of a network before it is built. An example is the organization of queueing networks. Often, also disturbed scenarios are simulated in order to evaluate stability and robustness properties. This is done, e.g., to construct timetables which are more resistant against delays.

Decomposition of multi-class queueing networks with batch processing

Thomas Hanschke, Wiebke Klünder

Introduction

We often use networks in our everyday life and we depend on them; examples include computer, communication, traffic and production systems. Generally there is an need for those networks to provide stability and high performance. This means for example that a production process should not stagnate. Another example is a traffic network: In a traffic network a gridlock occurrence should be avoided. The performance of networks under changing environmental conditions is determined by performance analysis.

The purpose of the performance analysis shall be to calculate the optimal working point of a network or system in regard to throughput and the capacity of queues and servers. Possible tools are the Monte Carlo simulation and the analytical method of queueing theory. For both approaches the situation being investigated is modeled and a performance analysis is executed. For example there is the question as to how the expansion of a machine park in a production system affects the total production. The question can be answered with both approaches. The following report is looking in depth at the analytical method of queueing theory.

One method of performance analysis of open queueing networks is the decomposition method. In this method, a network consisting of 1,…,N nodes is examined; the nodes being modeled as queueing systems. The jobs enter the network from outside; after having ran through the network they leave it. Such networks are called open networks. The decomposition method cuts up the network in single components, allowing an examination of its single nodes.

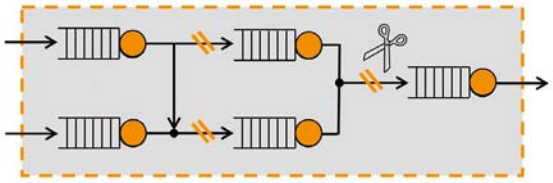

The difficulty here is that the flows between the nodes are unknown. With the help of the decomposition method, limit theorems and the theory of renewal processes this unknown parameters can be determined. Only then it is possible to execute the performance analysis of the single queueing systems by the composition of the determined parameters. The performance analysis of the entire network is the result of the analyzed single network components.

State of the art

The decomposition method was first established by Kühn[1], Chandy/Herzog/Woo[2] and Whitt[3] in the 70s and 80s. The method considers open queueing networks which consist of so-called G/G/c queueing systems. It covers the single class case and the multi-class case. In 2011 the method was further developed by Hanschke/Zisgen[4]. They considered open queueing networks consisting of G/G/c queueing systems with group arrivals and batch services. However, the decomposition method from Hanschke/Zisgen only covers the single class case. Within the scope of the project was its expansion to the multi-class case [5].

Multi-class queueing system

The considered open queueing networks consist of multi-class queueing systems with group arriv-

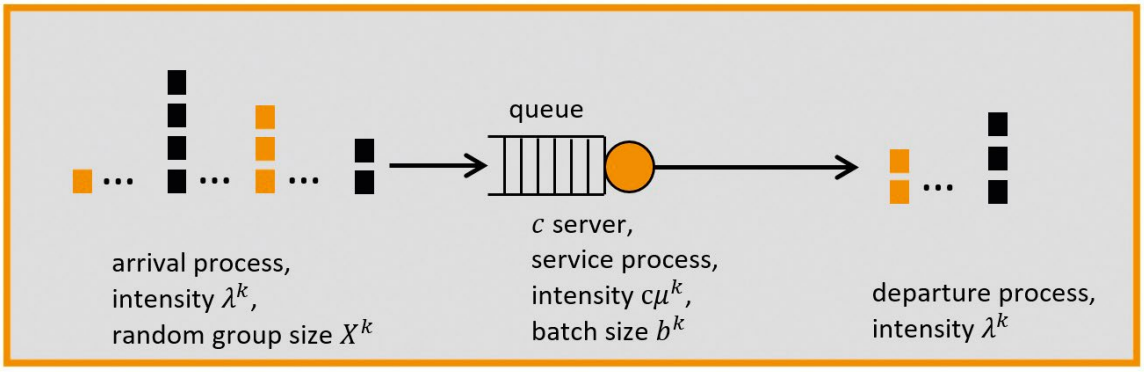

als and batch services. First, a single queueing system is examined which consists of a queue and a number of servers.

The jobs enter the queueing system in random group sizes, X. The occurrence of the groups forms the arrival processes. Since we assume the multi-class case, each class of jobs has its individual arrival process, I. If the groups reach the queueing system, the groups are sorted into unmixed batches. In the case of one server being inactive, an incoming batch can be served. Otherwise the batch joins the queue. This will also apply to jobs that are not numerous enough not suffice for a batch. The queue has an unlimited capacity. The batches in the queue are served according to the First Come First Serve principle. It is assumed that all c servers can handle batches of all classes of jobs. The service times form the service process, S. As during the arrival process, each class of jobs has its own individual service process. If a batch has been completely served, it immediately leaves the queueing system. The leaving of batches describes the departure process, D, of a queueing system.

We assume general distributions for the arrival and service processes. General distributions are usually described by their expected value and their variance. The considered systems fulfill the assumption that their utilization is less than 1, $\rho<1$. This means that in a sufficient large observation period more jobs are served than they arrive. Systems fulfilling this assumption are usually stable. In addition to the stability assumption, it is also assumed that the arrival and the service processes are independent. With regard to the classes of jobs the arrival processes as well as the service processes are independent.

Currently, an explicit analytical solution to this class of queueing systems of the steady state and transient state probabilities of waiting time, queue length and number of jobs in system is unknown. Within the scope of the project only the time-independent behavior of such systems is of interest. Since no exact solution of the steady state probabilities are known, approximations must be used. The used approximation is based on a formula of Allen and Cunneen [6].

$$E[N] = E[Z_\infty^\Sigma] + \frac{\rho^\Sigma C(c,\rho^\Sigma)}{1-\rho^\Sigma} b^\Sigma \left(\frac{SCV[I^\Sigma] + SCV[S^\Sigma]}{2}\right) k_{KLB} + b^\Sigma c\rho^\Sigma + E[Y_\infty^\Sigma]$$

The formula uses that the arrival processes I can be described as renewal processes. Under the heavy traffic assumption the service processes S can also be described as renewal processes. The heavy traffic assumption describes that the servers of the systems are always active and the queueing system runs rarely idle.

Renewal processes are described by their intensity and their variance. In case of an arrival process the intensity is denoted by λ and in case of a service process by μ.

This class of queueing systems covers the modeling approach grouping a set of jobs according to characteristics into classes of jobs. If for example a production system is considered, the jobs may differ in their occurring frequency, their batch sizes

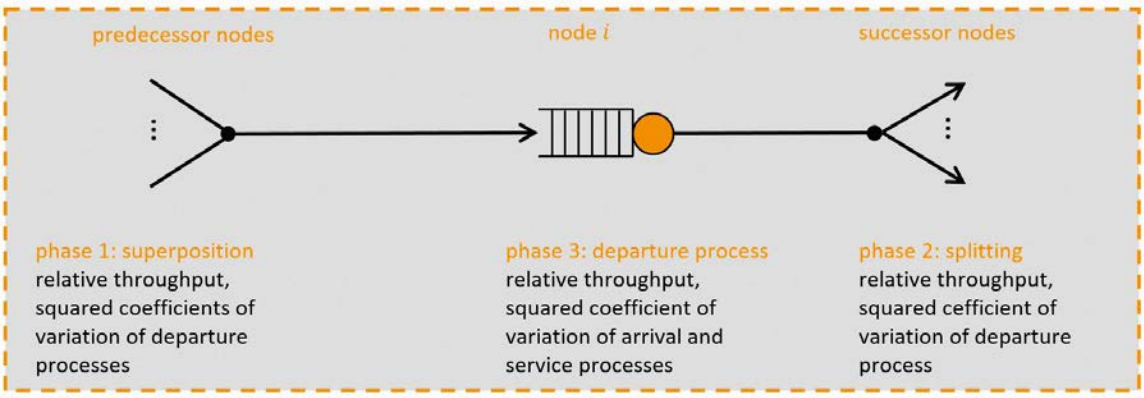

and their service times. Therefor it is attempted to summarize the jobs in classes having all the same mentioned characteristics or at least very similar ones.

Decomposition method

The execution of the decomposition method for open multi-class queueing networks with batch processing is conducted in two steps. In the first step the intensities of the renewal processes describing the flows between the queueing systems are determined. In the second step the stochastic variablities of the renewal processes are calculated. It has to be considered that the renewal processes are affected by superpositions and splittings. In the case of the decomposition of multi-class queueing networks the method provides two groups of sets of linear equations which have to be solved to determine the unknown parameters intensity and stochastic variability.

In the first step the sets of linear equations are set up which determine the relative throughput of the queueing systems with the help of traffic equations. The relative throughput indicates how many batches leave the considered node per time unit on average.

$$\tau_i^k = p_{0i}^k \frac{b_0^k}{b_i^k} + \sum_{j=1}^{N} p_{ji}^k \tau_j^k \frac{b_j^k}{b_i^k}, \quad \begin{matrix} \tau_0^k := 1, \\ i,j = 1,\dots,N \\ k = 1,\dots,K \end{matrix}$$

The relative throughput is denoted by τ and is calculated from two terms. The first term determines the relative throughput at a node from outside the network. The subsequent sum calculates the relative throughput which reach the node from other nodes. The terms include the transition probabilities to the considered node and the ratio between the incoming group sizes and batch sizes. The transition probabilities are denoted by p and the incoming group sizes and the batch sizes are denoted by b. The index i refers to the batch size of the considered node and the index j refers to the incoming group sizes or the batch sizes of the predecessor nodes.

If a number of classes of jobs are defined in the model, a set of linear equations occurs for each class of jobs. The solutions of the sets of linear equations are analytically exact. The determined relative throughput are then factored with the intensity of the input of the network, $\lambda_i^k = \lambda_0^k \tau_i^k$. The results provide the required intensities of the arrival processes.

The second step of the decomposition method is divided into three phases and has the goal to approximate the squared coefficient of variation.

The first phase maps the incoming arrival processes at a considered node to a superposition. To describe the superposition with regard to the classes of jobs denoted by $k=1,\dots,K$, the relative throughput which has already been determined and the squared coefficient of variation of the departure processes of the predecessor nodes are needed.

In order to form the superposition of the arrival process, first the counting process N for the associated renewal process I is described.

$$Var[N_{i,t}^k] = \lambda_i^k SCV[I_i^k]t$$

The counting process N can also be represented by the splitting of the departure processes of the predecessor nodes of the considered node i.

$$Var[N_{i,t}^k]' = \sum_{j=0}^{N} p_{ji}^k \lambda_i^k SCV[A_{ji}^k]t$$

The required measure SCV[I_i^k] results from the equalization of the descriptions.

$$SCV[I_i^k] = \frac{1}{\lambda_i^k} \sum_{j=0}^{N} p_{ji}^k \lambda_i^k SCV[A_{ji}^k]$$

Usually the formation of the superposition only results in a renewal process in a special case (Poisson processes). That is why the decomposition method is an approximated method.

The second phase deals with the departure process of the considered node i and splits it. To describe the splitting of the departure process the determined relative throughput of the considered node i and the squared coefficient of variation of the service process are used.

The splitting of the departure process D can be considered as a Bernoulli experiment. After completion of service at a node j batches are directed to the node i with the probability p_{ji}^k and with the probability 1-p_{ji}^k they are routed elsewhere. Let V^k be a random variable that describes the number of the first batch which arrives at node i. Since we are waiting for the first success V^k is Geometrically distributed. Because of the splitting of the departure processes new interdeparture times have to be calculated. Since the process D is assumed to be a renewal process, the parameter's intensity and stochastic variability can be determined by Wald's equations.

$$E[A_{ji}^k] = \frac{1}{p_{ji}^k} E[D_j]$$

$$Var[A_{ji}^k] = \frac{1}{p_{ji}^k} Var[D_j] + \frac{1 - p_{ji}^k}{(p_{ji}^k)^2} E[D_j]^2$$

The measure SCV[A_{ji}^k] can then be calculated by

$$SCV[A_{ji}^k] = \frac{Var[A_{ji}^k]}{E[A_{ji}^k]^2} = 1 + p_{ji}^k (SCV[D_j] - 1)$$

In general the splitting of a renewal process results in a number of renewal processes. The split renewal processes have identical interdeparture times but those times are interdependent. That means the split renewal process do not have the i.i.d. characteristic, which is another reason for the decomposition method being an approximated method.

Since the service process has not been described yet, this happens in the last phase. The service process is determined approximately. Like in the first and second phase the relative throughput of the considered node is used as well as the squared coefficients of variation of the arrival process and the service process of node i. The service process also represents the departure process of a node.

The service process or departure process can be approximated by the approach of Pujolle and Ai.

$$D_j \approx \begin{cases} \frac{S_j^\Sigma}{c_j} \; mit\; Wahrscheinlichkeit\; \rho_j^\Sigma \\ \frac{S_j^\Sigma}{c_j} + I_j^\Sigma \; mit\; Wahrscheinlichkeit\; 1 - \rho_j^\Sigma \end{cases}$$

S^Σ describes the aggregated average service times of all classes of jobs, I^Σ aggregated modified interarrival times and ρ^Σ the aggregated modified utilization of the considered queueing system. By setting up the first two moments

$$E[D_j] = E[I_j^\Sigma]$$

$$E[D_j^2] = \frac{E[S_j^{\Sigma 2}]}{c_j^2} + 2(1 - \rho_j^\Sigma) \frac{E[S_j^\Sigma]}{c_j} E[I_j^\Sigma] + (1 - \rho_j^\Sigma) E[I_j^{\Sigma 2}]$$

including the case differentiation the squared coefficient of variation of the departure process can be calculated.

$$SCV[D_j] = \frac{E[D_j^2]}{E[D_j]^2} - 1 = (\rho_j^\Sigma)^2 SCV[S_j^\Sigma] +$$

$$(1-\rho_j^\Sigma) SCV[I_j^\Sigma] + (1-\rho_j^\Sigma)\rho_j^\Sigma$$

There are other approaches to approximate the departure process, for example Whitt [3], Chylla[7] and Kühn[1] whose results only differ slightly regardless of the configuration of the queueing network [8].

If the phases are inserted successively into each other, a set of linear equations for each class of jobs is formed. The sets of linear equations contain only two unknown parameters: The squared coefficients of variation of the arrival processes of the nodes and the aggregated variant of those measures.

phase 1: $$SCV[I_i^k] = \frac{1}{\lambda_0^k \tau_i^k} \sum_{j=0}^{N} p_{ji}^k \lambda_0^k \tau_j^k SCV[A_{ji}^k]$$

phase 2: $$SCV[A_{ji}^k] = 1 + p_{ji}^k (SCV[D_j] - 1)$$

phase 3: $$SCV[D_j] = (\rho_j^\Sigma)^2 SCV[S_j^\Sigma] + (1-\rho_j^\Sigma) SCV[I_j^\Sigma] + (1-\rho_j^\Sigma)\rho_j^\Sigma$$

The aggregated squared coefficient of variation can be approximated by the following formula.

$$\mathrm{SCV}[\mathrm{I}_j^\Sigma] \approx \sum_{k=1}^{K} \frac{\lambda_i^k}{\sum_{k=1}^{K} \lambda_i^k} \frac{E[X_j^k]}{b_j^k} \left(SCV[X_j^k] + SCV[I_j^k]\right)$$

In summary the execution of the decomposition method provides an approximate description of the renewal processes between the queueing systems in an open queueing network. Then the performance measures of the single queueing systems can be calculated in the context of the network by using the formula from Allen and Cunneen and the performance analysis of the network can be determined.

Numerical results

The report presents a selected configuration that is representative of many other configurations.

The configuration is based on the reference model that represents networks. Two different classes of jobs were considered which differ in their service times at the nodes, in their transition probabilities and in their occurring frequency. We assume the same batch sizes for the classes of jobs at a node. The network consists of six nodes. The nodes 1, 3 and 5 are single server systems and the nodes 2, 4 and 6 are multi server systems. All queueing systems which are represented by the nodes have a high system utilization except the nodes 3 and 5. These nodes have a medium system utilization. Due to the assumed medium system utilization the configuration violates the assumption that the flows between the nodes are renewal processes. At the nodes 2, 4 and 5 the assumption of renewal processes is also violated. The average arrival group size at the mentioned nodes exceeds the average batch size.

$$E[X_2^1] = 5.00, E[X_2^2] = 5.00$$
$$E[X_4^1] = 4.81, E[X_4^2] = 6.14$$
$$E[X_5^1] = 5.75, E[X_5^2] = 5.49$$

This has the consequence that the sorting of an arrived group into unmixed batches takes place at the same time. So there are several renewals at a time. In addition the nodes 2, 5 and 6 are affected by splittings and the nodes 4, 5 and 6 are affected by superpositions. For the splitting the assumption of the i.i.d. characteristic no longer

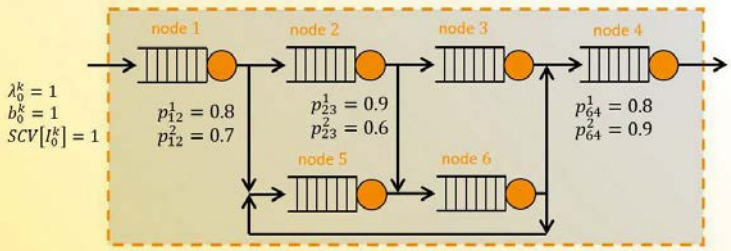

$SCV[S_i^k] = 0.5$

node 1	$c_1 = 1, b_1^k = 5, \rho_1^\Sigma = 0.8$
node 2	$c_2 = 3, b_2^k = 3, \rho_2^\Sigma = 0.9$
node 3	$c_3 = 1, b_3^k = 4, \rho_3^\Sigma = 0.6$
node 4	$c_4 = 5, b_4^k = 1, \rho_4^\Sigma = 0.8$
node 5	$c_5 = 1, b_5^k = 3, \rho_5^\Sigma = 0.5$
node 6	$c_6 = 2, b_6^k = 10, \rho_6^\Sigma = 0.7$

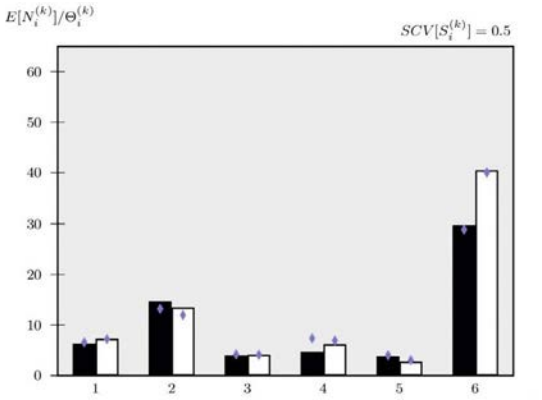

exists for renewal processes and the superposition usually does not produce a renewal process.

The listed properties of the configuration suggest that especially the nodes 2, 4 and 5 are affected by deviations of the approximations from reference values of the simulation.

The simulation was implemented by the Monte Carlo simulation. The simulations provide the point estimators and the associated confidence intervals.

The graphic preparation of the results of simulation and approximation shows the behavior of the simulation and of the decomposition method relating to the network.

The bars represent the analytical results. The black ones represent the first class of jobs and the white ones the second class of jobs. The diamonds represent the point estimators from the simulation. The decomposition method closely imitates the behavior of the simulated queueing systems in the context of the network. Larger deviations can only be observed at the nodes 2 and 4.

Conclusions

In spite of many violations of assumptions that are required by the decomposition method the method is very robust. This robust behavior can be observed for similar configurations. The deviations of the analytical method from the simulation results decreases if less assumptions are violated. The further development of the decomposition method also has its limitations. If different batch sizes for each class of jobs at a node are assumed additionally, the decomposition method is not able to represent the behavior of the queueing systems in the network adequately.

References

[1] Paul J. Kuehn. Approximate Analysis of General Queueing Networks by Decomposition. Communications, IEEE Transactions on, 27(1):113-126, 1979.

[2] K. M. Chandy, U. Herzog and L. Woo. Approximate Analysis of General Queueing Networks. IBM J. Res. Dev. 19, 1:43-49, 1975.

[3] Ward Whitt. The Queueing Network Analyzer. Bell System Technical Journal, 62(9):2779-2815, November 1983.

[4] Th. Hanschke and H. Zisgen. Queueing networks with batch service. European Journal of Industrial Engineering, 5(3):313-326, 2011.

[5] Wiebke Klünder. Dekomposition von Mehrprodukt-Warteschlangennetzwerken mit Batch-Processing. Dissertation, 2018. TU Clausthal. 978-3-86948-667-3.

[6] Tobias Gröger. Warteschlangensysteme mit Gruppenankünften, Gruppenbedienung und heterogenen Kunden. TU Clausthal, Diplomarbeit, 2007.

[7] Peter Chylla, Zur Modellierung und approximativen Leistungsanalyse von Vielteilnehmer-Rechensystemen, Dissertation, TU München, 1986

[8] Wiebke Klünder, Horst Zisgen, Thomas Hanschke. Decomposition of open queueing networks with batch service. Jahrbuch 2015/16 des Simulationswissenschaftlichen Zentrums Clausthal-Göttingen, 66-69, 978-3-946340-79-9

Project data

The project is funded from SWZ with a 0.5 TV-L E13 staff positions since April 2014 at the site Clausthal. Involved scientists are:

Prof. Dr. Thomas Hanschke
Research Group Stochastische Modelle in den Ingenieurwissenschaften
Institute of Applied Stochastics and Operations Research
Clausthal University of Technology

Dr. Wiebke Klünder
Research Group Stochastische Modelle in den Ingenieurwissenschaften
Institute of Applied Stochastics and Operations Research
Clausthal University of Technology

Solving Robust Optimization Problems by Iterative Approaches

Stephan Westphal, Anita Schöbel, Julius Pätzold

Abstract

In this paper we analyze the number of iterations needed in cutting plane approaches for solving robust combinatorial optimization problems theoretically and experimentally. We give four different bounds and show in the experiments when these bounds are attained. We especially investigate the number of iterations required for two different combinatorial optimization problems as well as for two different robustness concepts. We furthermore prove bounds on the number of iterations if the exact optimization steps in the cutting plane approach are only solved approximately. In our experiments we further investigate the effects of these enhancements on the number of iterations.

1 Introduction

Almost every optimization problem suffers to some extent from uncertainty. In mathematics there exist different approaches and hence research fields to overcome this issue. The advantage and importance of the field of robust optimization in comparison to other fields such as stochastic optimization is that it does not take any distribution assumptions to the data into account. Instead, robustness concepts are defined to measure the performance of a solution in its worst case. Robust optimization started with the work of Soyster [Soy73] and was extensively researched later, e.g., in [GL97, BTN98, BTN00, BS04, BTGN06], see [BTGN09] for a compendium on results for strict robustness and [KY97] for algorithms and applications for strict and regret robustness, and [GS16] for a survey on less conservative robustness concepts.

Robust versions of optimization problems are mostly hard to solve, especially if the underlying optimization problem is already hard. To overcome this issue there exist two main approaches: Robust reformulations and iterative cutting plane approaches. In this work we investigate the latter approach which is known under many names. [MB09] define a cutting set method for robust convex optimization problems, [ABV09] describe a relaxation procedure for min-max regret versions of combinatorial optimization problems, [BDL16] give a computational comparison of exact reformulations against cutting plane methods for robust mixed integer linear optimization problems. Behind their different names lies the same basic approach. A crucial point that is often emphasized when using this approach is the relatively small number of iterations this cutting plane approach needs, in order to obtain an optimal robust solution. Investigating this property serves as the focus of this paper.

The remainder of the paper is structured as follows. In Section 2 we introduce the notion for robust optimization and repeat the two most common concepts of strict and regret robustness. The cutting plane approach for robust optimization is revisited in Section 3. We summarize its basic properties and analyze how many iterations are needed in the cutting plane approach from a theoretic point of view. In Section 4 we propose two enhancements of the cutting plane approach in which we do not solve the two underlying optimization exactly, but only approximately. We investigate convergence and the number of iterations needed for these enhancements. Section 5 then evaluates the performance of the cutting plane algorithm and its enhancements for the minimum spanning tree and the traveling salesman problem. We in particular investigate convergence and the number of iterations needed experimentally and relate them to the bounds proven beforehand. We finally give some conclusions and mention possible further work.

2 Robust optimization: notation and concepts

As usual in uncertain optimization (see, e.g., [BTGN09]) we consider a family of parameterized optimization problems (P(u) : u ∈ U) where $U \subseteq R^q$ is a given uncertainty set and each scenario u ∈ U defines a combinatorial optimization problem

$$P(u) \qquad \min_{x \in X} f(x,u)$$

with a deterministic and finite feasible set $X \subseteq R^n$ and an uncertain objective function $f: X \times R^q \to R$. Note that we assume the function f to be defined on R^q and not only on the scenarios u ∈ U. Let us assume that one specified nominal scenario (the most likely one, or the undisturbed one) $u_{nom} \in U$ is given.

We are interested in finding a robust solution to (P(u) : u ∈ U). In the field of robust optimization there exist many different robustness concepts. In this paper, we consider the two most frequently used ones: strict robustness and regret robustness.
Strict robustness / minmax robustness

A solution is called strictly robust (or minmax robust) if it is an optimal solution to

$$\min_{x \in X} \sup_{u \in \mathcal{U}} f(x,u),$$

see [BTGN09, Soy73].

Regret robustness / deviation robustness
A solution is called regret robust (or deviation robust) if it is an optimal solution to

$$\min_{x \in X} \sup_{u \in \mathcal{U}} \left(f(x,u) - \min_{x' \in X} f(x',u) \right),$$

see [KY97, YKP07].

Many other robustness concepts exist, among others, adjustable robustness ([BTGGN03]), light robustness ([FM09, Sch14]), soft robustness ([BTBB10]), globalized robustness ([BTBdHV17]), recovery robustness ([LLMS09, GS14, CGS17]).

An overview is given in [GS16]. For our paper we define one robust counterpart problem (RC) which covers both, strict and regret robustness:

$$(RC) \qquad g^* := \min_{x \in X} \sup_{u \in \mathcal{U}} g(x,u)$$

where

$$g(x,u) := \begin{cases} f(x,u) & \text{for strict robustness} \\ f(x,u) - \min_{x' \in X} f(x',u) & \text{for regret robustness.} \end{cases}$$

In order to guarantee the existence of an optimal solution to (RC) we assume that either U is a finite set or that $f(\cdot,u): R^q \to R$ is continuous in u for every fixed x ∈ X and that U is a compact set.

In the following sections we describe and analyze a cutting plane approach which can be used to solve (RC), and hence find robust solutions with respect to the concepts of strict and regret robustness.

3 A cutting plane approach for solving robust combinatorial optimization problems

We define the following two optimization problems. For U' ⊆ U define

$$RC(\mathcal{U}') \qquad g^*_{\mathcal{U}'} := \min_{x \in X} \sup_{u \in \mathcal{U}'} g(x,u)$$

as a relaxed robust counterpart problem in which only a subset of scenarios is considered (Solving (RC) means to find the value $g^* = g^*_U$, and

$$Pes(x) \qquad g_{\mathcal{U}}(x) := \sup_{u \in \mathcal{U}} g(x,u)$$

as the evaluation of a solution x ∈ X in its worst case. We furthermore denote for U' ⊆ U:

$$g_{\mathcal{U}'}(x) \quad := \quad \sup_{u \in \mathcal{U}'} g(x,u)$$

We collect two elementary properties below.

- For $U_1 \subseteq U_2 \subseteq U$ we have $g_{U1}(x) \le g_{U2}(x) \le g^*_U(x)$ and hence $g^*_{U1} \le g^*_{U2} \le g^*_U$.
- Let $x_{U'}$ be an optimal solution to RC(U'). Then the optimal objective value g^* of (RC) is bounded by

$$g^*_{\mathcal{U}'} = g_{\mathcal{U}'}(x_{\mathcal{U}'}) \le g^* \le g_{\mathcal{U}}(x_{\mathcal{U}'}). \quad (1)$$

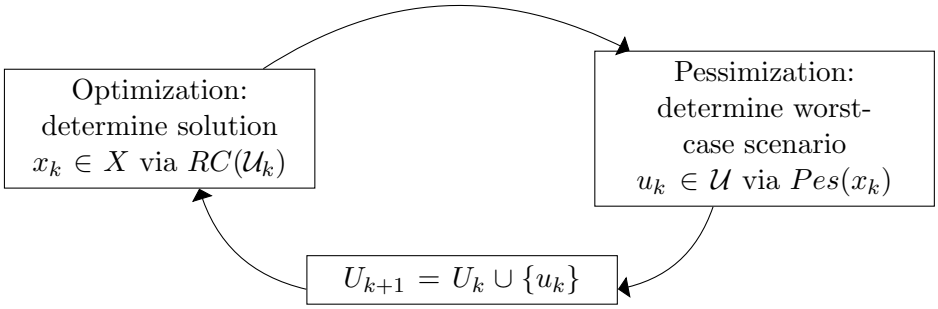

Figure 1: Basic Scheme

The proposed algorithm that solves RC constructs a sequence

$$\mathcal{U}_0 = \{u_{\text{nom}}\} \subseteq \mathcal{U}_1 \subseteq \mathcal{U}_2 \subseteq \ldots\ldots \qquad \subseteq \mathcal{U}$$

of nested scenario sets. In iteration k one finds an optimal solution xk of RC(U_k) and a worst-case scenario uk by solving Pes(x_k) which is then added to U_k in order to obtain the new scenario set U_{k+1}, see Figure1 as illustration.

The algorithm works as follows: The current best solution is stored as x_{opt} and the current best upper bound, corresponding to the objective value of the currently best found solution for each iteration is stored as ub_k. The value $gU_k(x_k)$, corresponding the optimal objective value of RC(U_k) is on the other hand the current best lower bound. The pseudo-code for this algorithm is stated in Algorithm 1.

For discussing the results of Algorithm 1 we need the following definition.

Definition 1

For a given optimization problem (RC) and some $\in > 0$, define a solution $x \in X$ to be $\in$-optimal with respect to (RC), if there is no solution $y \in X$ such that $g_U(y) + \in < g_U(x)$.

Algorithm 1: Iterative Solution Approach

Input: problem (RC), nominal scenario $u_{\text{nom}} \in \mathcal{U}$, stopping-criterion $\epsilon > 0$
Output: $x \in X$ ϵ-optimal w.r.t. (RC),
$U_0 \leftarrow \{u_{\text{nom}}\}$, $k \leftarrow 0$, $ub_0 \leftarrow \infty$
while *True* **do**
  $x_k \leftarrow$ solution to $RC(U_k)$
  if $g_{\mathcal{U}_k}(x_k) + \epsilon > ub_k$ **then**
    return x_{opt}
  $u_k \leftarrow$ solution to $Pes(x_k)$
  if $g_{\mathcal{U}}(x_k) < ub_k$ **then**
    $x_{opt} \leftarrow x_k$
  $ub_{k+1} \leftarrow min(ub_k, g_{\mathcal{U}}(x_k))$
  $U_{k+1} \leftarrow U_k \cup \{u_k\}$
  $k \leftarrow k + 1$
end

We first note correctness of the algorithm:

Lemma 2

If Algorithm 1 terminates, the returned solution xopt is ∈-optimal with respect to (RC).

Proof.
Assume the algorithm terminates in iteration k and returns some solution $x_{opt} \in X$. Then it holds that

$$g_{\mathcal{U}_k}(x_k) = \min_{x \in X} g_{\mathcal{U}_k}(x) \leq \min_{x \in X} g_{\mathcal{U}}(x) \leq g_{\mathcal{U}}(x_{opt})$$

$$= ub_k < g_{\mathcal{U}_k}(x_k) + \epsilon,$$

and hence the optimal objective value g* as well as the objective value of x_{opt} have to lie in the interval $[g_{U_k}(x_k), g_{U_k}(x_k) + \epsilon]$.

We now discuss termination of Algorithm 1 and analyze how many iterations are needed in the worst case. To this end, let l be the number of iterations of the algorithm. It is known that Algorithm 1 terminates for a finite set U and also for a finite set X. We show a bit more.

Lemma 3

Algorithm 1 stops if a scenario or if a feasible solution is found twice. Hence
1. $l \leq |U|$
2. $l \leq |X|$

Proof.
1. We show that the algorithm terminates if a scenario $u \in U$ is visited twice. To this end, let u_k be chosen as optimal solution of $Pes(x_k)$ in Step k, u_l be chosen as optimal solution of $Pes(x_l)$ in Step l and let $u_l = u_k$ for $l > k$. Then we have

$$g_{\mathcal{U}_l}(x_l) \overset{(1)}{\leq} g_{\mathcal{U}}(x_l) = g(x_l, u_l) = g(x_l, u_k)$$

$$\overset{u_k \in \mathcal{U}_l}{\leq} \sup_{u \in \mathcal{U}_l} g(x_l, u) = g_{\mathcal{U}_l}(x_l),$$

hence $g_{U_l}(x_l) = g_U(x_l)$, and the algorithm terminates.

2. We show that the algorithm terminates if a solution $x \in X$ is visited twice. To this end, let x_k be chosen as optimal solution of $RC(U_k)$ in Step k, x_l be chosen as optimal solution of $RC(U_l)$ in Step l and let $x_l = x_k$ for $l > k$. Let uk be the worst-case scenario added to U_k in Step k. Then we have

$$g_{\mathcal{U}_l}(x_l) = g_{\mathcal{U}_l}(x_k) \overset{u_k \in \mathcal{U}_l}{\geq} g(x_k, u_k) = g_{\mathcal{U}}(x_k)$$

$$= g_{\mathcal{U}}(x_l) \overset{(1)}{\geq} g_{\mathcal{U}_l}(x_l),$$

hence $g_U(x_l) = g_{U_l}(x_l)$, and the algorithm terminates.

In the next lemma, we improve the first bound $|U|$. Before doing so, let us introduce three common uncertainty sets treated in the literature:

1. Finite uncertainty $U = \{u^1, \ldots, u^N\}$
2. Interval-based uncertainty $U = [\underline{u}_1, \overline{u}_1] \times \ldots \times [\underline{u}_M, \overline{u}_M]$
3. Polyhedral uncertainty $U = \text{conv}\{u^1, \ldots, u^N\}$

Interval-based uncertainty is a special case of polyhedral uncertainty, in which the uncertainty set is a hyperbox. Other uncertainty sets may be norm-based uncertainty, ellipsoidal uncertainty (which is studied extensively in [BTGN09]), or Γ-uncertainty (see, [BS04]) which is also a special case of a polyhedral uncertainty set.

Let ext(A) denote the extreme points of the set A. With the notation used above we see that the number of extreme points for an interval-based uncertainty set is 2^M, and for a polyhedral uncertainty set it is N.

Lemma 4

$l \leq |\text{ext}(\text{conv}(U))|$

if one of the following two assumptions holds:
- $g(x,\cdot)$: conv(U) → R is strictly quasiconcave in u for every fixed $x \in X$.
- $g(x,\cdot)$: conv(U) → R is quasiconcave in u for every fixed $x \in X$ and an algorithm is used for solving $Pes(x_k)$ which returns an extreme point of the feasible (convex) set.

We remark that, e.g., the simplex algorithm and also interior point methods are examples for algorithms always returning extreme points of

the (polyhedral) feasible set even if non-extreme points are also optimal.

Proof.
First, note that for quasiconcave functions we can always optimize over the convex hull of U without changing the result, i.e.,

$$\sup_{u\in\mathcal{U}} g(x,u) = \sup_{u\in conv(\mathcal{U})} g(x,u)$$

if g(x,u) is quasiconcave in u for fixed x: Clearly, ≤ holds. To see that also ≥ holds, let $\bar{u} \in$ conv(U), i.e., there exists a convex combination $\bar{u} = \sum_{i=1}^{N} \lambda^i u^i$ with some N ∈ IN and $\lambda_i \geq 0$, $u^i \in U$ and $\sum_{i=1}^{N} \lambda_i = 1$.

We then have

$$g(x,\bar{u}) = g\left(\sum_{i=1}^{N} \lambda_i u_i\right) \leq \max_{i=1,\dots,N} g(x,u^i) \leq \sup_{u\in\mathcal{U}} g(x,u),$$

hence we obtain $\sup_{u\in conv}(U)\ g(x,u) \leq \sup_{u\in U} g(x,u)$.

Using the argument once more for U':=ext(U) we receive that

$$\sup_{u\in\mathcal{U}} g(x,u) = \sup_{u\in conv(\mathcal{U})} g(x,u) = \sup_{u\in conv(ext(\mathcal{U}))} g(x,u) = \sup_{u\in ext(\mathcal{U})} g(x,u)$$

for quasiconcave functions. For maximizing a quasiconcave function over a convex set, we hence know that there always exists an extreme point which is optimal. We distinguish two cases:

- Either g(x,u) is strictly quasiconvex. Then all maximizers of Pes(x) are at the extreme points of conv(U).
- Or g(x,u) is quasiconvex and an algorithm for solving Pes(x) is used which returns an extreme point of conv(U).

In both cases, u_k is chosen from ext(conv(U)) in every iteration k and the algorithm stops if ext(conv(U) ⊆ U_l for some iteration l (since it terminates if a scenario is visited twice according to Lemma 3), i.e., after at most |ext(conv(U))| iterations.

The previous result is in particular useful if uncertainty sets with infinite cardinality are considered such as polyhedral, interval-based or Γ-uncertainty. In order to apply the result to strict or regret robustness we next investigate under which assumptions on the original function f(x,u) the function g(x,u) is quasiconvex for fixed x.

Corollary 5

- **For strict robustness:** Let f(x,·): conv(U) → IR be quasiconcave in u for every fixed x ∈ X.
- **For regret robustness:** Let f(x,·): conv(U) → IR be affine linear in u for every fixed x ∈ X.

Then the function g(x,u) is quasiconcave in u for fixed x. In particular, the number of iterations of the cutting plane approach is bounded by |ext(conv(U))|.

Proof.
The results for strict robustness are clear. For regret robustness, recall that

$$g(x,u) = f(x,u) - \min_{x'\in X} f(x',u)$$

is quasiconcave since the minimum of a (finite) set of affine linear functions is convex, hence g is quasiconcave as the sum of an affine linear and a concave function.

4 Enhancements of the cutting plane approach

In this section we study what happens if we do not solve RC(U_k) and Pes(x_k) optimally, but only approximately. We consider the following four variations:

- ex-ex:
  Solve both, (RC) and (Pes) exactly in each iteration. This has been done in Algorithm 1.
- ex-app:
  Solve (RC) exactly, but (Pes) approximately. In other words: We do not determine a worst-case scenario in (Pes(x_k)) but just a scenario u which is worse than all scenarios in U_k.
- app-ex:
  Solve (RC) approximately, but (Pes) exactly. In other words: We do not find the best possible solution x_k to RC(U_k) but just a solution which is better than a (global) upper bound.
- app-app:
  Solve both problems approximately as described in app-ex and ex-app.

In order to formalize the approaches we need the following approximate versions of (RC) and (Pes).

Definition 6

For a given problem RC(U') and some upper bound ub we define the approximation version of RC(U') to be the decision version of RC(U') with decision value ub (stating infeasibility if no solution with value strictly less than ub can be found):
A-RC(U',ub)
Does there exist $x \in X$ s.th. } $gU'(x) < ub$?

Similarly, for a given problem Pes(x) and some lower bound lb we define the approximation version of Pes(x) to be the decision version of Pes(x) with decision value lb (stating infeasibility if no solution with value strictly greater than lb can be found):
A-Pes(x,lb)
Does there exist $u \in U$ s.th. } $g(x,u) > lb$?

We now formulate a version of the cutting plane algorithm, where both RC(U_k) and Pes(x_k) can be chosen to be solved approximately. The pseudo-code is stated in Algorithm 2.

Like in Algorithm 1 we start with some nominal scenario u_{nom}, solve a relaxed version of the original optimization problem, and get a solution x_k. For this solution we try to obtain a worst case scenario u_k and add it to the set of considered scenarios. The extension to Algorithm 1 is that one now can choose between four different variations of the algorithm by setting the two parameters RC-EX and PES-EX, and hence decide which of (RC) and (Pes) should be solved approximately. Setting RC-EX to 1 and PES-EX to 1 yields again Algorithm 1.

What differs in Algorithm 2 is that the stopping criterion can not be stated as easily as in Algorithm 1 because of the following reasons: If (RC(U_k)) is solved approximately the value $gU_k(x_k)$ is not necessarily a lower bound on the optimal objective value. If on the other hand Pes(x_k) is solved approximately, we have a similar behaviour: Only when A-Pes(x_k, $gU_k(x_k)$) is infeasible it is ensured that $gU_k(x_k)$ (and therefore $gU(x_k)$) is an upper bound for $g(x_k,u)$ and hence for the whole problem RC(U).

Because of this behaviour the algorithm keeps track of the best "true" upper bound, denoted by ubk. This upper bound is only updated when either Pes(x_k) is solved exactly and a better objective has been found or if A-Pes(x_k,$gU_k(x_k)$) is infeasible and $gU_k(x_k) < ub_k$. It can therefore be observed that the algorithm constructs a sequence of upper bounds

$ub_1 \geq ub_2 \geq ub_3 \ldots$

With the help of this "true" upper bound we get a stopping criterion for the case that we chose to solve (RC) approximately. If A-RC(U_k,$ub_k - \epsilon$) is infeasible, there is no better solution x_k with respect to the scenario set U_k and therefore the value $ub_k - \epsilon$ is a lower bound, whereas ub_k is an upper bound, making x_{opt} an ϵ-optimal solution.

The correctness of Algorithm 2 can hence be summed up by the following theorem:

Theorem 7

If Algorithm 2 returns a solution xopt $\in$ X, it is an ϵ-optimal solution with respect to (RC).

Proof.
Assume that in Step k of the algorithm the solution x_{opt} has been returned. First of all, the solution x_{opt} is always defined, since otherwise $gU_k(x_k) + \epsilon > ub_k = \infty$ would hold, contradicting g mapping to R.

If (RC) is solved exactly, the returned solution x_{opt} must be ϵ-optimal since it holds that

$$g_{\mathcal{U}_k}(x_k) = \min_{x \in X} g_{\mathcal{U}_k}(x) \leq \min_{x \in X} g_{\mathcal{U}}(x)$$

$$\leq g_{\mathcal{U}}(x_{opt}) = ub_k < g_{\mathcal{U}_k}(x_k) + \epsilon,$$

hence $g^* \in [gU_k(x_k), gU_k(x_k) + \epsilon]$, similarly to the argumentation for Algorithm 1.

If on the other hand (RC) is solved approximately and A-RC(U_k,$ub_k - \epsilon$) is infeasible it means that there is no solution $x \in X$ with (a lower bound on the) objective value less than $ub_k - \epsilon$ and therefore the solution x_{opt} is ϵ-optimal. Formally

$$ub_k - \epsilon \leq \min_{x \in X} g_{\mathcal{U}_k}(x) \leq \min_{x \in X} g_{\mathcal{U}}(x) \leq g_{\mathcal{U}}(x_{opt}) = ub_k,$$

and hence $g^* \in [ub_k - \epsilon, ub_k]$.

Algorithm 2: Enhanced Iterative Solution Approach

Input: problem (RC), nominal scenario $u_{\text{nom}} \in \mathcal{U}$, stopping criterion $\epsilon > 0$, parameter RC-EX stating 1 if (RC) is solved exactly and 0 if approximately, parameter PES-EX stating 1 if (Pes) is solved exactly and 0 if approximately
Output: Optimal solution $x \in X$ to (RC)

$U_0 \leftarrow \{u_{\text{nom}}\}$, $k \leftarrow 0$, $ub_0 \leftarrow \infty$
while *True* **do**
  if *RC-EX* $= 1$ **then**
    $x_k \leftarrow$ solution to $RC(U_k)$
    if $g_{\mathcal{U}_k}(x_k) + \epsilon > ub_k$ **then**
      return x_{opt}
  else
    Solve $A - RC(U_k, ub_k - \epsilon)$
    if *infeasible* **then**
      return x_{opt}
    else
      $x_k \leftarrow$ solution to $A - RC(U_k, ub_k - \epsilon)$

  if *PES-EX* $= 1$ **then**
    $u_k \leftarrow$ solution to $Pes(x_k)$
    $ub_{k+1} \leftarrow min(ub_k, g(x_k, u_k))$
    if $ub_{k+1} < ub_k$ **then**
      $x_{opt} \leftarrow x_k$
    $U_{k+1} \leftarrow U_k \cup \{u_k\}$
  else
    Solve $A - Pes(x_k, g_{\mathcal{U}_k}(x_k))$
    if *infeasible* **then**
      if $ub_k > g_{\mathcal{U}_k}(x_k)$ **then**
        $x_{opt} \leftarrow x_k$
      $ub_{k+1} \leftarrow min(ub_k, t_k)$
      $U_{k+1} \leftarrow U_k$
    else
      $u_k \leftarrow$ solution to $A - Pes(x_k, g_{\mathcal{U}_k}(x_k))$
      $ub_{k+1} \leftarrow ub_k$
      $U_{k+1} \leftarrow U_k \cup \{u_k\}$

  $k \leftarrow k + 1$
end

We now investigate termination of Algorithm 2 for the three new approaches ex-app, app-ex, and app-app. Since in combinatorial optimization problems X is finite anyway, we only need finiteness of the set U to still guarantee convergence.

Lemma 8

Algorithm 2 converges for the case that both RC(U_k) and Pes(x_k) are solved approximately if $|X|$ and $|U|$ are both finite. The maximal number of iterations I is bounded by $|X|+|U|$.

Proof. In each iteration of Algorithm 2 the problem A-Pes(x_k,gU_k(x_k)) can either be infeasible, or return a scenario u_k. If A-Pes(x_k,gU_k(x_k)) is feasible and the new scenario u_k occurs in the set of already found scenarios U_k, it leads to the contradiction

$$g_{\mathcal{U}_k}(x_k) \underbrace{<}_{u_k \text{ feasible sol. to A-Pes}(x_k,\, g_{\mathcal{U}_k}(x_k))} g(x_k,u_k) \underbrace{\leq}_{u_k \in \mathcal{U}_k} g_{\mathcal{U}_k}(x_k).$$

Therefore, if A-Pes(x_k,gU_k(x_k)) is feasible, the returned scenario has to differ from the previous ones, which can occur at most $|U|$ times.

If, on the other hand, A-Pes(x_k,gU_k(x_k)) was infeasible for some k, then all following solutions x_l have to differ from the currently found solution x_k. If this is not the case and the solution x_l is recurring, i.e. $x_l = x_k$ for some l>k, we get

$$ub_l - \epsilon \underbrace{>}_{x_l \text{ feas. sol. to A-RC}(\mathcal{U}_l,\, ub_l - \epsilon)}$$

$$g_{\mathcal{U}_l}(x_l) = g_{\mathcal{U}_l}(x_k) \geq g_{\mathcal{U}_k}(x_k) \geq ub_{k+1},$$

contradicting $ub_k+1 \geq ubl$. In other words: By the infeasibility of A-Pes(x_k,gU_k(x_k)) we know that the worst case value of x_k has been found. If the solution occurs again in the algorithm, its objective value could not have been improved. Thus the case infeasibility of A-Pes(x_k,gU_k(x_k)) can occur at most $|X|$ times.

Therefore A-Pes(x_k,gU_k(x_k)) can be at most $|X|$ times infeasible and at most $|U|$ times feasible, leading to a total number of iterations of the algorithm of at most $|X|+|U|$.

The convergence of Algorithm 2 for app-app implies convergence for all other three algorithms ex-app, app-ex and ex-ex, as the exact method could also be used to solve the problem approximately. We hence receive the following corollary.

Corollary 9

For all four variations of Algorithm 2 we have that $I \leq |U| + |X|$,

in particular the Algorithm needs a finite number of iterations if U is a finite set.

We remark that this bound cannot be strengthened to $I \leq |\text{ext}(\text{conv}(U))|+|X|$ as it was possible for ex-ex (see Lemma 4).

For the case that only one of RC(U_k) or Pes(x_k) is solved approximately, we get some of the bounds that have been proposed before for the case ex-ex of Algorithm 1 (see Lemma 3). We start with the variant app-ex.

Lemma 10

Assume that RC(U_k) is solved approximately and Pes(x_k) is solved exactly. Then the number of iterations is bounded by $|X|$.

Proof.
Assume a solution x_i that has been found in iteration i is reoccurring in a later iteration k, so assume $x_k = x_i$ for some $i < k$. Then it holds that

$$ub_k - \epsilon > g_{\mathcal{U}_k}(x_k) = g_{\mathcal{U}_k}(x_i) \geq g(x_i,u_i) \geq ub_{i+1},$$

contradicting $ub_i+1 \geq ub_k$. Therefore all x_k have to be pairwise disjoint and an upper bound for the number of iterations is given by $|X|$.

Now we turn from app-ex to ex-app and receive the following result.

Lemma 11

Assume that Pes(x_k) is solved approximately and RC(U_k) is solved exactly. Then the number of iterations is bounded by $|U|$.

Proof.
Assume that A-Pes(x_k,gU_k(x_k)) returns infeasibility. On the one hand, we know that gU_k(x_k) is a lower

bound on the optimal objective g* since RC(U_k) is solved exactly. On the other hand, infeasibility of A-Pes(x_k,gU_k(x_k)) implies that there is no scenario u ∈ U with worse objective value than gU_k(x_k). This means that gU_k(x_k) is also an upper bound on the optimal objective value g*. Formally, it holds that

$$g^* \leq g_{\mathcal{U}}(x_k) \underbrace{=}_{\text{A-Pes}(x_k,\, g_{\mathcal{U}_k}) \text{ infeasible}} g_{\mathcal{U}_k}(x_k)$$

$$\underbrace{=}_{x_k \text{ optimal for } RC(\mathcal{U}_k)} \min_{x \in X} g_{\mathcal{U}_k}(x) \leq g^*$$

and the algorithm stops as an optimal solution has been found. Therefore, the algorithm only continues if a feasible solution for A-Pes(x_k,gU_k(x_k)) is found. The scenario u_k must not be contained in U_k, because otherwise the contradiction

$$g_{\mathcal{U}_k}(x_k) < g(x_k, u_k) \underbrace{\leq}_{u_k \in \mathcal{U}_k} \sup_{u \in U_k} g(x_k, u) = g_{\mathcal{U}_k}(x_k)$$

would arise. Hence, every scenario u_k needs to differ from all previous scenarios (i.e. from all scenarios of the set U_k), which bounds the maximal number of iterations by $|U|$.

We remark that this bound cannot be strengthened to $I \leq |\text{ext}(\text{conv}(U))|$. The reason is that a solution (scenario) uk to A-Pes(x_k,gU_k(x_k)) does not necessarily have to lie on the boundary of U since (Pes) is solved only approximately and not to optimality. For an uncertainty set of infinite cardinality (irregardless of a possible finite ext(conv(U))) this could lead to an arbitrary high number of iterations.

The bounds obtained by the preceding lemmas are summarized in Table 1.

5 Computational Experiments

In this section we present various computational results obtained by implementing the presented cutting plane method. Our main focus is the investigation of the number of iterations. We chose two different combinatorial optimization problems, namely the Minimum Spanning Tree (MST) problem and the Traveling Salesman Problem (TSP).

Robust spanning tree problems have been investigated in the literature before, mainly with interval uncertainty, see, e.g., [Nik08, YKP01, KZ06, Mon06, MG05, ABV05, KMZ12] and references therein. The papers deal with preprocessing and robust reformulations. As approaches, tabu-search, Benders' decomposition, and approximation algorithms are suggested. The robust traveling salesman problem has not been studied as extensively, it is first setup and investigated for interval data in [MBMG07], more recent approaches can be found in [MB11, BCC14, CG16], see also references therein.

For both of the problems we considered the two introduced robustness concepts strict robustness and regret robustness, where the uncertainty lies in the weights of the edges in the underlying graph. We used finite, interval, and polyhedral uncertainty sets. Note that if (Pes) is solved exactly only the extreme points of a polyhedral uncertainty are of importance. When focusing on the number of iterations the results for finite and polyhedral uncertainties coincide (as long it is ensured that no point of the finite set lies in the interior of its convex hull). For both MST and TSP we assumed the underlying graph to be complete. Unless stated otherwise we used the ex-ex enhancement of Algorithm 2 and calculated an average number

Table 1: Different bounds for all four variants of Algorithm 2.

bound	assumptions	Algorithm			
		ex-ex	ex-app	app-ex	app-app
$B_1 = \lvert\mathcal{U}\rvert$	none	yes	yes	no	no
$B_2 = \lvert X\rvert$	none	yes	no	yes	no
$B_3 = \lvert\mathcal{U}\rvert + \lvert X\rvert$	none	yes	yes	yes	yes
$B_4 = \lvert ext(conv(\mathcal{U}))\rvert$	g quasiconcave	yes	no	no	no

of iterations among 20 randomly generated instances. We summarize the assumptions and specifications:

- MST or TSP
- Strict Robustness or Regret Robustness
- Polyhedral uncertainty set (unless stated otherwise)
- Complete Graph, uncertainty is in the edge weights
- Algorithm ex-ex (unless stated otherwise)
- Average number of iterations (average among 20 randomly generated instances)

All experiments were implemented with Python and Gurobi 7.0 and run on a standard notebook (4GB RAM, i3-2350M CPU @ 2.30GHz). The exact optimization problems (RC) and (Pes) were solved by Gurobi using standard integer programming formulations. The approximated versions were solved by Gurobi, too, but just by looking for a feasible solution, i.e. the objective function was set to zero.

Number of iterations for ex-ex

In the first experiment we investigated the average number of iterations of Algorithm 1 for MST and TSP with strict and regret robustness. We assumed a graph of n=7 nodes and generated different polyhedral uncertainty sets with the amount of extreme points ranging from |U|=50 up to |U|=500 with step size 50. For each size of |U| we generated 20 instances, and calculated the average number of iterations required.

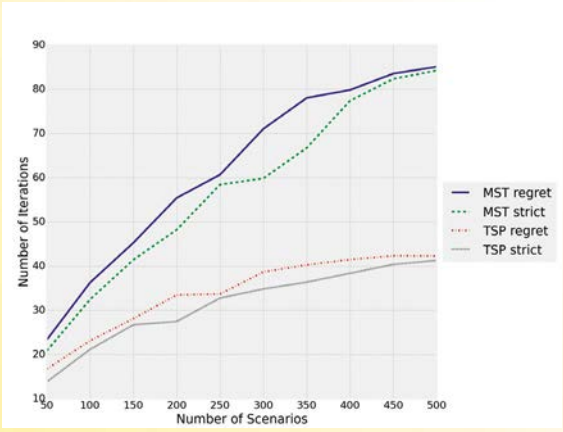

Figure 2: Comparison of MST vs. TSP and of strict vs. regret robustness for a graph of 7 nodes

What can be seen in Figure 2 is that the number of iterations is by far lower than the total amount of scenarios. The ratio between the number of iterations and the number of scenarios even decreases with an increasing size of the scenario set. It can also be seen that the finding a robust minimum spanning tree takes on average more iterations than solving the robust TSP problem. Furthermore the regret robustness concept takes a few more iterations on average than the strict robustness concept. This behaviour will now be further analyzed and explained.

Comparing Strict against Regret Robustness for ex-ex

A comparison between the average number of iterations for strict and regret robustness can already be carried out when considering Figure 2. The number of iterations for strict robustness is slightly less, but quite similar to the number of iterations for the case of regret robustness. Another interesting point considering Figure 2 is that there is a very synchronous behaviour of the curves for MST strict and TSP strict as well as of the curves for MST regret and TSP regret. This also points in the direction that the robustness concept plays a more important role for the number of iterations needed than the considered combinatorial problem.

Comparing MST and TSP

In Figure 2 we compared the average number of iterations for the MST problem and the TSP problem on a complete graph of 7 nodes. The number of feasible solutions on such a graph highly differs between the two combinatorial problems. On the one hand we have $7^5 = 16807$ different spanning trees, but on the other hand only $6!/2 = 360$ different Hamiltonian cycles. This might be an explanation for the fact that TSP requires less iterations on the same data set. To further investigate this point we compare in the following figure the average number of iterations for the MST on a graph of 7 nodes against a TSP problem on a graph of 9 nodes, since 8!/2=20160 lies approximately

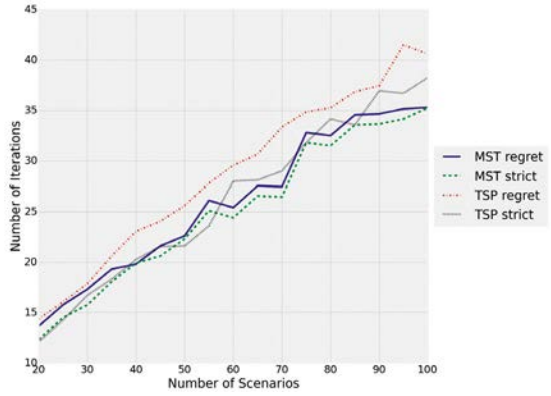

Figure 3: Comparison of TSP vs. MST but with same number of feasible solutions

in the same order of magnitude as the number of spanning trees.

One can see that now the average number of iterations for different sizes of uncertainty sets is slightly higher for the TSP than for the MST. This corresponds to the slightly higher number of feasible solutions of the problem. We conclude that the size of |X| is more relevant for the cutting plane approach than the type of the combinatorial problem.

Comparing interval against polyhedral uncertainty sets for ex-ex

The next experiments investigates differences between interval uncertainties and polyhedral uncertainties. Interval uncertainties can be considered as a special case of the polyhedral uncertainties and should hence require a quite small number of iterations. We compared different sizes of polyhedral uncertainty sets (black) against the average number of iterations required for interval uncertainties. The number of scenarios corresponds to the number of extreme points of the considered polytope.

For a graph of n=7 nodes we got an average of ≈18 iterations for interval uncertainties. This is quite a small number if compared to the set of possible $2^{21} \approx 2$ million scenarios for the case of interval uncertainties. Regarding the comparison to the case of arbitrary polyhedral uncertainty sets, one can see that for a scenario set size of approximately 30 scenarios the algorithm also takes ≈ 18 iterations, which is drastically less than 2 million scenarios.

Comparison of ex-ex, ex-app, app-ex, app-app

The final experiments investigate number of required iterations for the different approximation versions of the algorithm. To this end we considered the TSP regret problem. We first fixed the number of scenarios of the uncertainty set. Then we let the number of nodes of the underlying graph grow.

As expected, the number of iterations needed is smallest for ex-ex and highest if both problems are only solved approximately. Solving (RC) exactly and (Pes) approximately needs less iterations than solving (RC) only approximately and (Pes) exactly. Furthermore, one can clearly see that the bound $B_1 = |U| = 10$ presented lemma 11 is actually tight for ex-ex and ex-app, and does not hold for app-ex and app-app.

Next, we fixed the graph to 5 nodes and let the number of scenarios grow.

Concerning the bounds, Figure 7 shows that ex-ex and app-ex are bounded by the bound $B_2 = |X| = 12$ presented in Lemma 10, which does not hold for ex-app and app-app.

The enhancement ex-ex takes also here the least amount of iterations, but app-app does only sometimes take the most iterations. Sometimes it is passed by app-ex. The number of ex-app is always a bit higher than the number for ex-ex.
We conclude that ex-ex takes the smallest number of iterations and app-app is likely to take the highest. The number of iterations for app-ex and ex-app highly depends on the sizes of |U| and |X|.

As we now compare different methods for solving the same problem it makes sense to have a look at the runtimes of the different variations. Figure 6 shows the runtimes for the instances considered in Figure 5 and Figure 8 shows the runtimes for the instances used in Figure 7. The runtime is now not the average of the 20 instances, but its sum.

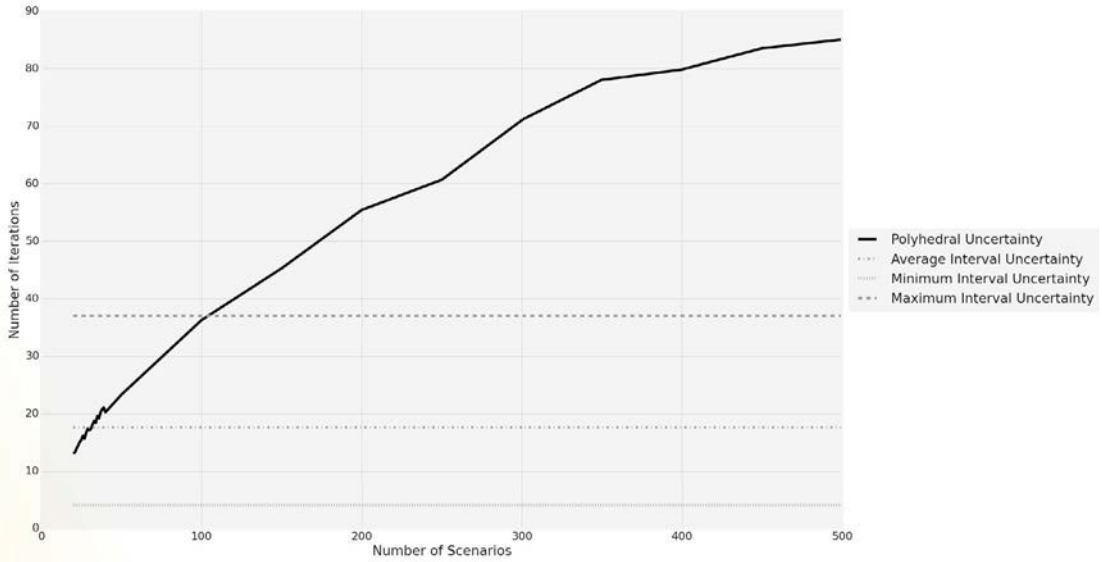

Figure 4: Comparison of interval and polyhedral Uncertainty

For the case of fixed U clear differences in runtime can only be observed from 13 nodes and higher. Here app-app and app-ex have the highest runtimes, which corresponds to their highest number of iterations in Figure 5. ex-ex and ex-app have similar and low runtimes, which also corresponds well to their low number of iterations. Therefore it can be concluded that in this case the number of iterations and the runtime behaves similarly.
For the case of fixed |X| the runtime does behave different than the number of iterations. The variation ex-app has the lowest runtimes whereas app-ex has the highest. The two cases app-app and app-ex have similar runtimes, that are lower than the ones from app-ex but higher than the ones from app-ex. The number of iterations, on the other hand, is high, if (Pes) is solved approximately. This leads to the conclusion that in the case of a small |X| (in comparison to |U|) it is beneficial for the runtimes to solve (RC) exactly and (Pes) approximately. The number of iterations, however, has no clear correlation with the runtimes.

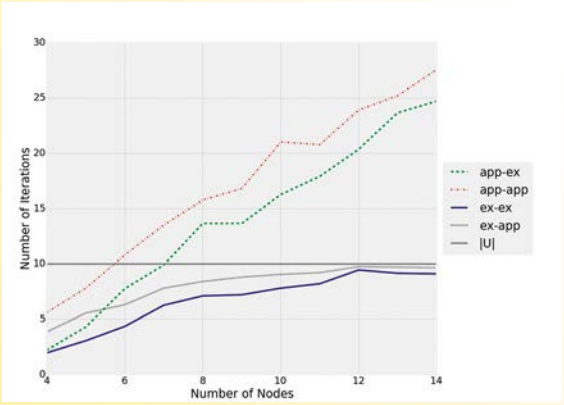

Figure 5: Number of iterations for the four variants of Algorithm 2 with fixed |U|.

6 Conclusion

In this work we investigated different properties regarding the number of iterations for cutting plane approaches to solve robust combinatorial optimization problems. On the one hand we were able to show several theoretical upper bounds, which turned out to be sharp for some instances in the experiments. On the other hand our experiments confirm the general impression that the number of iterations required for solving robust combinatorial optimization problems via cutting plane is quite small.

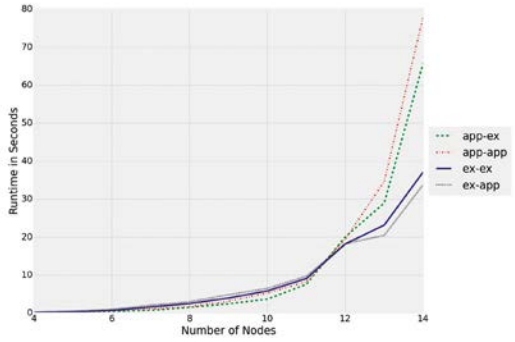

Figure 6: Runtimes for the four variants of Algorithm 2 with fixed |U|.

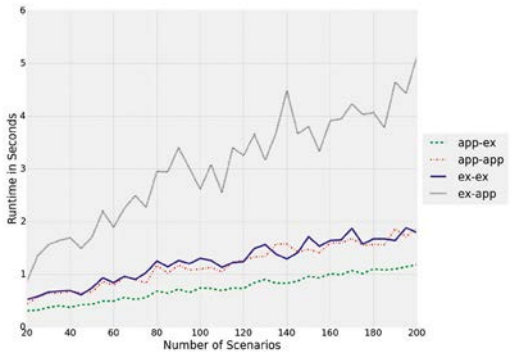

Figure 8: Runtimes for the four variants of Algorithm 2 with fixed |X|.

Furthermore the experiments shed light on the influences regarding the number of iterations. Probably the most important influence factor for the number of iterations is the problem size, in form of the values |U| and |X|, and not for example the shape of the sets U and X. The robustness concept and also the function gU are by far not as important as the sheer size of the problem. Especially the computational experiments for the presented enhancements of the cutting plane approach justify how each of them can be of practical use, when applied to the right problem setting.

Further research could be carried out on the topic of finding sharper bounds, since the gap between the best upper bound and the real number of iterations is still quite high. Then of course it would be interesting to see if there is a constructive way of bounding the number of iterations by finding a suitable subset of scenarios that leads to an optimal solution. Additionally one could further investigate the relation between the runtime of the cutting plane approach with the number of iterations. This can be done not only for the exact case, but especially for the enhancements. It would be interesting to see how runtime and number of iterations are correlated and what influences them. Finally, we work on extending our results to general mixed-integer programs and to other robustness concepts.

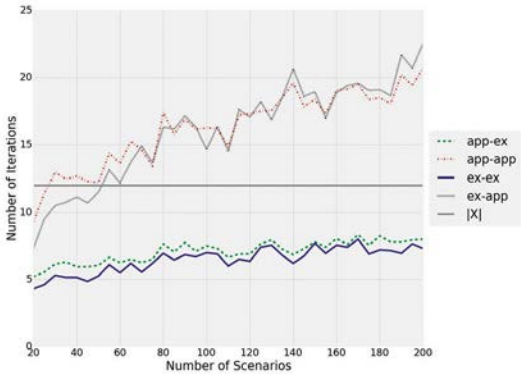

Figure 7: Number of iterations for the four variants of Algorithm 2 with fixed |X|.

References

[ABV05] H. Aissi, C. Bazgan, and D. Vanderpooten. Approximation complexity of min-max (regret) versions of shortest path, spanning tree, and knapsack. In Proceedings of the 13th annual European conference on Algorithms, ESA'05, pages 862-873, Berlin, Heidelberg, 2005. Springer-Verlag.

[ABV09] H. Aissi, C. Bazgan, and D. Vanderpooten. Min-max and min-max regret versions of combinatorial optimization problems: A survey. European Journal of Operational Research, 197(2):427-438, 2009.

[BCC14] S. Burer, N. Cho, and A.M. Campbell. Modifying soysters model for the traveling salesman problem with interval travel times. Far East Journal of Applied Mathematics, 86(2):117-144, 2014.

[BDL16] D. Bertsimas, I. Dunning, and M. Lubin. Reformulation versus cuttingplanes for robust

optimization. Computational Management Science, 13(2):195-217, 2016.

[BS04] D. Bertsimas and M. Sim. The price of robustness. Operations Research, 52(1):35-53, 2004.

[BTBB10] A. Ben-Tal, D. Bertsimas, and D. B. Brown. A soft robust model for optimization under ambiguity. Operations Research, 58(4):1220-1234, 2010.

[BTBdHV17] A. Ben-Tal, R. Brekelmans, D. den Hertog, and J.-P. Vial. Globalized robust optimization for nonlinear uncertain inequalities. INFORMS Journal on Computing, 29(2):350-366, 2017.

[BTGGN03] A. Ben-Tal, A. Goryashko, E. Guslitzer, and A. Nemirovski. Adjustable robust solutions of uncertain linear programs. Math. Programming A, 99:351-376, 2003.

[BTGN06] A. Ben-Tal, L. El Ghaoui, and A. Nemirovski, editors. Special issue on Robust Optimization, volume 107:1-2 of Mathematical Programming B. Springer, 2006.

[BTGN09] A. Ben-Tal, L. El Ghaoui, and A. Nemirovski. Robust Optimization. Princeton University Press, Princeton and Oxford, 2009.

[BTN98] A. Ben-Tal and A. Nemirovski. Robust convex optimization. Mathematics of Operations Research, 23(4):769-805, 1998.

[BTN00] A. Ben-Tal and A. Nemirovski. Robust solutions of linear programming problems contaminated with uncertain data. Math. Programming A, 88:411-424, 2000.

[CG16] André Chassein and Marc Goerigk. On the recoverable robust traveling salesman problem. Optimization Letters, 10(7):1479-1492, Oct 2016.

[CGS17] E. Carrizosa, M. Goerigk, and A. Schöbel. A biobjective approach to recovery robustness based on location planning. European Journal of Operational Research, 261:421-435, 2017.

[FM09] M. Fischetti and M. Monaci. Light robustness. In R. K. Ahuja, R.H. Möhring, and C.D. Zaroliagis, editors, Robust and online large-scale optimization, volume 5868 of Lecture Note on Computer Science, pages 61-84. Springer, 2009.

[GL97] L. El Ghaoui and H. Lebret. Robust solutions to least-squares problems with uncertain data. SIAM Journal of Matrix Anal. Appl., 18:1034-1064, 1997.

[GS14] M. Goerigk and A. Schöbel. Recovery-to-optimality: A new two-stage approach to robustness with an application to aperiodic timetabling. Computers and Operations Research, 52:1-15, 2014.

[GS16] M. Goerigk and A. Schöbel. Algorithm engineering in robust optimization. In L. Kliemann and P. Sanders, editors, Algorithm Engineering: Selected Results and Surveys, volume 9220 of LNCS State of the Art, pages 245-279. 2016.

[KMZ12] A. Kasperski, M. Makuchowski, and P. Zielinski. A tabu search algorithm for the minmax regret minimum spanning tree problem with interval data. Journal of Heuristics, 18(4):593-625, 2012.

[KY97] P. Kouvelis and G. Yu. Robust Discrete Optimization and Its Applications. Kluwer Academic Publishers, 1997.

[KZ06] A. Kasperski and P. Zielinski. An approximation algorithm for interval data minmax regret combinatorial optimization problems. Information Processing Letters, 97(5):177-180, 2006.

[LLMS09] C. Liebchen, M. Lübbecke, R. H. Möhring, and S. Stiller. The concept of recoverable robustness, linear programming recovery, and railway applications. In R. K. Ahuja, R.H. Möhring, and C.D. Zaroliagis, editors, Robust and online large-scale optimization, volume 5868 of Lecture Note on Computer Science. Springer, 2009.

[MB09] A. Mutapcic and S. Boyd. Cutting-set methods for robust convex optimization with pessimizing oracles. Optimization Methods & Software, 24(3):381-406, 2009.

[MB11] J. Majumdar and A.K. Bhunia. Genetic algorithm for asymmetric traveling salesman problem with imprecise travel time. Journal of Computational and Applied Mathematics, 235(9):3063-3078, 2011.

[MBMG07] R. Montemanni, J. Bartra, M. Mastrolilli, and L.M. Gambardella. The robust traveling salesman problem with interval data. Transportation Science, 41(3):366-381, 2007.

[MG05] R. Montemanni and L.M. Gambardella. A branch and bound algorithm for the robust spanning tree problem with interval data. European Journal of Operational Research, 161(3):771-779, 2005.

[Mon06] R. Montemanni. A benders decomposi-

tion approach for the robust spanning tree problem with interval data. European Journal of Operational Research, 174(3):1479-1490, 2006.

[Nik08] Y. Nikulin. Simulated annealing algorithm for the robust spanning tree problem. Journal of Heuristics, 14(4):391-402, 2008.

[Sch14] A. Schöbel. Generalized light robustness and the trade-o between robustness and nominal quality. MMOR, 80(2):161-191, 2014.

[Soy73] A.L. Soyster. Convex programming with set-inclusive constraints and applications to inexact linear programming. Operations Research, 21:1154-1157, 1973.

[YKP01] H. Yaman, O.E. Karasan, and M.C. Pinar. The robust spanning tree problem with interval data. Operations Research Letters, 29:31-40, 2001.

[YKP07] H. Yaman, O.E. Karasan, and M.C. Pinar. Restricted robust optimization for maximization over uniform matroid with interval data uncertainty. Mathematical Programming, 110(2):431-441, 2007.

Project data

The project is funded from SWZ with one TV-L E13 staff position since August 2015 at the sites Clausthal and Göttingen. Involved scientists are:

Prof. Dr. Anita Schöbel
Research Group Optimization
Institute for Numerical and Applied Mathematics
University of Göttingen

Martin Dahmen, M.Sc.
Research group Discrete Optimization, Institute of Applied Stochastics and Operations Research
Clausthal University of Technology

Prof. Dr. Stephan Westphal
Research group Discrete Optimization, Institute of Applied Stochastics and Operations Research
Clausthal University of Technology

Julius Pätzold, M.Sc.
Research Group Optimization
Institute for Numerical and Applied Mathematics
University of Göttingen

ASimOV: Studying the impact of passenger behavior on train delays using agent-based simulation

Sebastian Albert, Philipp Kraus, Awad Mukbil, Julius Pätzold, Jörg P. Müller, Anita Schöbel

Abstract

Delay management in rail transportation decides how to react to delays of trains. Current work on delay propagation and delay management in railway networks has hardly considered the impact that arises on train delays from passengers' behavior. In this paper, we report on advances achieved in the first funding phase of the ASimOV research project. We propose a hybrid agent-based architecture combining a macroscopic railway network simulation with a mesoscopic agent-based station / passenger simulation based on the LightJason agent platform. We provide an initial instantiation of the architecture, considering a simple platform transfer scenario; we further study how delays of incoming trains, as well as numbers and heterogeneity of passengers influence delays of departing trains. Our results support the hypothesis that passengers' behavior in fact has a significant effect on delays of departing trains.

1 Introduction

Delays are a very noticeable phenomenon in today's railway systems. Caused by source events (a track is closed, a signal fails, a train departs late because a large group is boarding), they often propagate and affect large parts of the railway network. Many mechanisms of delay propagation are well understood: A train that departs with some delay often arrives with some delay; but delays can also propagate from one train to others if punctual trains wait for delayed feeder trains (wait-depart decision), or if punctual trains must slow down because their tracks are occupied by delayed trains ahead of it (priority decision). In addition, it is known that delays may propagate due to vehicle and drivers' schedules. It is the task of delay management to keep delays small: for this purpose, delay management decisions are made at railway traffic control centers. Optimizing these decisions from the point of view of passengers (i.e., aiming at minimizing adverse effects on passengers wait and travel times), is an ongoing topic of research, see [9] for a recent survey.

However, research about delay propagation and delay management largely ignores the two relevant issues. First, in the real world, the route a passenger would take depends on the actual delays and on the delay management decisions. In many cases, waiting for the next train of the same service after missing a connection is not a good solution for passengers, because different combinations of train services may enable them to reach their destinations earlier. Only very few approaches study this observation and aim to provide corresponding models [8,20]. Here, it should also be noted that the delay of a train might even bring about new options for connections that would not be feasible under undisturbed operations.

A second aspect, which is mostly neglected in current research on delay management, relates to the behavior of passengers at the stations: What do passengers do if a transfer is likely to be missed? People may run from one platform to another in a hurry, interfering with each other, heavy luggage may slow down passengers and increase the time they need for changing trains. In addition, particular patterns of passenger flow may cause additional delays when, for instance, a steady trickle of people entering a train prevents the doors from closing – and hence the train from departing on time.

Let us consider a simple scenario to illustrate this effect: Suppose a large number of passengers disembark from an incoming train X in a station. There

are only a few minutes for reaching the platform of a connecting train, Y. Under such circumstances, it is often enough that one (fast) passenger reaches train Y on time, and before the doors close, the next passenger arrives, then the passenger after, and so on. This might lead to a delay of train Y, even if Y was punctual so far. To the best of our knowledge, there exists no previous research in delay management so far that considers delay effects as this one.

In order to deal with situations as illustrated in the above scenario, our approach is to not only simulate trains in railway networks and delays propagating between them via priority and wait-depart decisions, but we also simulate passengers to derive more realistically which effects their behavior has on train delays. This simulation includes both passenger route choices in the railway network as well as passenger movements through the stations. Thus, the aim of this research is not only to study the effect of delays on passengers but also the effect of passengers on delays. We foresee the resulting simulation model to be useful for predicting delays more realistically in specific situations. Predicting delays more precisely can help when informing passengers about options they have. Furthermore, our simulation can be used to analyze the effects of particular delay management decisions (e.g., train Y should wait for train X today) or even more general delay management strategies, and ultimately help to reduce follow-up delays in railway networks.

A topic that is closely related to the topic we study is the simulation of crowd congestion at interchange stations, as reported in [24]. In [25], the authors propose a crowd dynamics and transit network simulation platform, which can switch between different simulators. Delay propagation in the context of railway networks has been considered in [14,15] and simulated in [17]. It has also been applied to delay management, see [8] and references therein. In that work, wait-depart decisions to maintain connections for transferring passengers are considered for delay propagation, but the route choice of passengers and their behavior in stations is not dealt with.

There is a rich body of research work and tools supporting microscopic simulation of physical train movements along the tracks in a railway network; we refer to [18] for an overview. However, passengers are neglected in these simulations. Based on an analysis of existing tools and frameworks for microsimulation, we propose an agent-based modeling and simulation approach using the Light-Jason framework (see Section 3 for related work and details) since it provides a flexible, scalable architecture and can link microscopic, mesoscopic and macroscopic elements.

In Section 2, we introduce the simulation model combining a macroscopic railway network model with a microscopic model of passengers within stations. These two models get connected when passengers board or disembark: train doors and platforms serve as interfaces between the models. Section 3 describes the agent-based simulation framework and model, and Section 4 elaborates first simulation results indicating that passengers' behavior in fact has a significant effect on delays of the departing trains. The paper ends with some conclusions and points out opportunities of further research.

2 Simulation model

2.1 Overview

Delay management problems in railway networks have been traditionally modeled macroscopically, and have been formulated and solved as integer programs (IPs). Considering pedestrians in a more realistic manner both in the train network and in the stations imposes additional requirements on modeling. For example, it is necessary to link a graph-based model for the network with a grid-based model for the station. To capture realistic fine-grained movement patterns in stations according to the pedestrians' information states, preferences, and plans, microscopic pedestrian flow models are required while a macroscopic flow simulation can be implemented for the network. Essentially, our model needs to support the "network world" and the "station world" as well as passengers moving across these worlds when entering or leaving trains.

There are different architectural approaches to integrate a macroscopic railway network simulation with a microscopic station simulation model. Firstly, two individual simulation systems can be coupled

using a co-simulation approach (e.g. [6]). Secondly, an existing simulation system could be extended by new models, capturing station and network part. Thirdly, a simulation framework can be designed from scratch based on a model that unifies the network and station models. For scalability, flexibility, integration and maintenance effort, we chose the third option aiming at a unifying agent-based model based on the agent-based platform *LightJason* (see Section 4). The key design approach is that trains, passengers, and dispatcher(s) are designed as BDI agents. Trains drive, and open or close doors; passengers travel from start to destination, move through stations and board/disembark trains. The dispatcher decides which trains wait. While maintaining different levels of detail, this solution gives a uniform view on all active simulation entities.

Section 2.2 provides more detail on how we model the railway network. We present our approach to describing railway stations and passenger behavior within railway stations in Section 2.3. Section 2.4 explains how our initial model handles the transition between the railway network and station "worlds".

2.2 Railway network submodel

For the trains macroscopic simulation, we use the *event-activity network* (EAN) formalism, i.e., we create a network consist of two types of vertices: *arrival* and *departure events* E_{arr} and E_{dep}, both of which consist of a train and a station. Edges in the EAN connect events using the following *activities*:

- *Driving activity* $\alpha \in A_{drive}$ links a departure event of a train at a station with an arrival event of the same train at its next station. This forms a train driving between two consecutive stations.
- *Waiting activity* $\alpha \in A_{wait}$ links an arrival event of a train at a station with its departure event at the same station and matches the waiting time of a train in a station to let passengers disembark and board.
- *Changing activity* $\alpha \in A_{change}$ links an arrival event of a train at a station with the departure event of another train at the same station. This corresponds to the transfer of passengers from one train to another within a station.
- *Headway activity* $\alpha \in A_{head}$ models capacity limitations of the track system. This can be either two trains driving on the same track into the same direction or two trains driving into opposite directions on a single-way track. The durati-

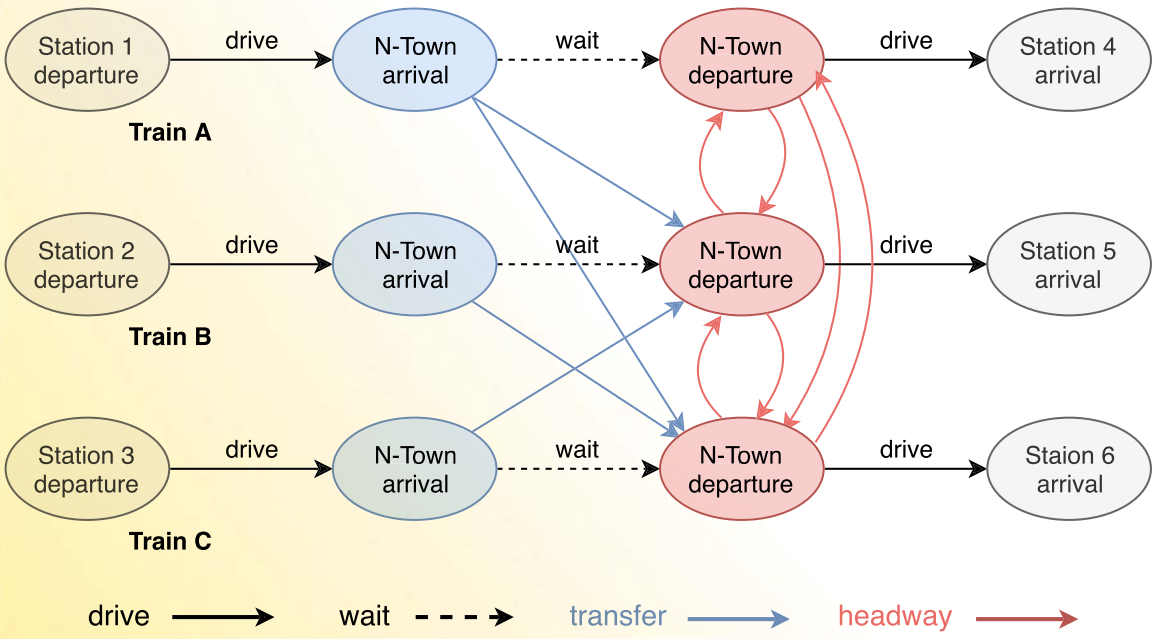

Figure 1: A small event-activity network consisting of three trains that meet at the station N-town.

on $L_{(i,j)}$ of a headway activity (i,j) means that the event j must take place at least $L_{(i,j)}$ minutes after the event i (if j actually takes place after i). We refer to [23] for details. Headway activities are used to ensure that no two trains can occupy the same platform at the same time.

Some simulation approaches, like [18], are able to route trains on the track system considering all signals, speed limits and other safety measures, such as interlocking effects of multiple trains' routes. However, since we focus on the influence of passengers' behavior, we neglect the details of the physical railway network in this first version of our work and use the macroscopic event-activity network for simulating the railway world. Figure 1 depicts a small example of an EAN with three trains.

Trains, passengers, and delays can properly be modeled using Event-activity networks. The model ensures direct visibility of *train* movements and positions. Passengers can be routed through an EAN (note that they may not use headway activities) and are allowed to change between trains by using changing activities. Delays can be propagated through the network along driving, waiting, changing and headway activities if the buffer times of each of these activities are known. In our simulation model, every train in the EAN is modeled as a separate simulation entity, or agent. The *train agents* technically know their timetable as a list of stations together with their arrival and departure times. Train agents are aware of the current time and must not depart before the respective published departure time. Their arrival at the next station occurs after the amount of time, which is calculated by the distance and their running speed, plus any additional delay that can be modeled between the two stops. As mentioned above, a detailed track simulation is currently neglected since the study of passengers at stations is our focus. Passengers are also modeled as agents. In the macroscopic railway network, they move along the network in their trains. To reach their destinations, each *passenger agent* knows their own itinerary as a list of train rides, each denoted by the train number, the station, and the departure time where they have to board or disembark. Some of them are able to adapt their itineraries when their planned journey is affected by a delay. These passenger agents model informed passengers that use their smart phones to optimize their journeys. Other passengers will stick to their itineraries, or follow the guidance given by the staff or an information board. All passengers can update their itineraries when they miss a transfer.

2.3 Railway station submodel

Following a microscopic agent-based approach, this submodel describes the physical environment of a railway station, the travel demand, and the behavior (flow) of passengers in the station. We refer to Figure 1 for a simple example scenario with two opposing entrances and platforms. The environment is modeled as a grid; travel demand is specified by origin-destination (O/D) matrices. More advanced dynamic demand models, as, e.g., provided by MATSim [11] could be used in the future. However, they are not the focus of this work.

Based on the O/D data, passengers are created with an itinerary. They are then released at the entrances of the initial station of their journey. The info sign displays information about track plans and departure times for trains. Initially, we assume that passengers are created with this information. In the future, we will investigate the case that passengers first need to obtain it by actually moving near the info sign, or that they may use mobile devices. The two entrances and exits can be used to simulate different levels of through-traffic and

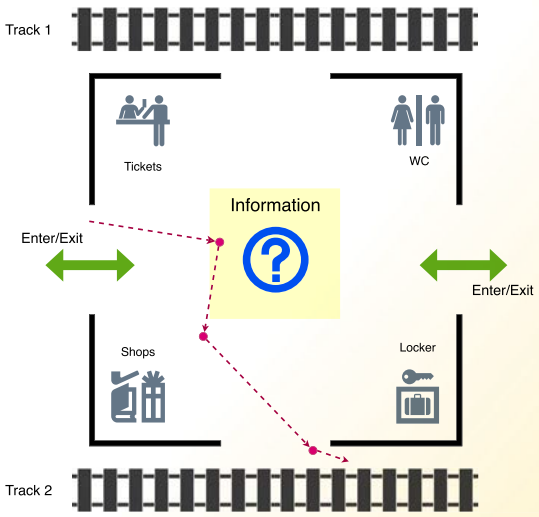

Figure 2: Exemplary station environment

their impact on delays. Based on its itinerary and departure information, a passenger decides where to go (e.g., to catch a train or to leave the station). She then plans a route and moves towards her destination. While moving, the passenger can decide to opportunistically interrupt or modify the planned route towards points of interest, e.g., to eat something (represented as dynamic internal drive to increase its energy level) or to get a newspaper (represented by a level of preference or interest). Furthermore, the movement of other passengers will also influence the passenger's trajectory; this can lead to collisions.

A cellular automaton approach [7] is used to model the flow behavior of passengers on the environmental grid. A cell can be empty or not, and it can be of different types (floor, info sign, Point of Interest (PoI), ...). According to the cell structure, discrete goal- and event-based action rules following the BDI model are applied to describe the agent-environment interactions.

To model realistic, flexible movement and routing, we use a hybrid control architecture to integrate routing and movement control as proposed in [13]: *Routing:* For each agent, individually, the Jump Point Search (JPS+) routing algorithm is used. It calculates a list of landmarks (e.g. filled dots in Figure 2) from the starting position to the goal. Those landmarks reflect unique references for each agent and we extend this as a preprocessing by defining suitable initial landmarks.

Movement control: The Social Force Model approach [12], in addition to a simple reactive collision detection[3], is applied to determine the passenger trajectory between consecutive landmarks (see the line from the entrance to the platform in Figure 2). The calculation takes the planned route of the passenger, the current situation, and other passengers into consideration[1].

In the following, we emphasize two aspects related to our agent-based simulation model: The first is our approach to solve the problem of modeling perception in a scalable fashion. The second is that we illustrate the above-mentioned BDI modeling of passenger behavior.

Dynamic perception algorithm: All passenger agents in the station update their perception in each simulation step, i.e., access the environmental state. This perception is constrained by limited ranges. We address this by enclosing the relevant simulation entity by a bounding box of configu-

Listing 1.1: Detection algorithm

```
1  input: agent PASSENGER, agent BOX
2  begin
3      LINE <- liangbarsky( PASSENGER.startposition, PASSENGER.endposition,
           BOX.topleft, BOX.bottomright )
4      LENGTH <- || LINE ||_2
5      if LENGTH = 0
6          return
7      if not BOX.contains( PASSENGER )
8          PASSENGER.trigger( "enter", BOX )
10     BOX.objects.add( PASSENGER ) ;
11     BOX.trigger( "moving", PASSENGER )
12 end
```

[1] See scenario in (2) or https://lightjason.github.io/news/2017-02-video/

rable size. This also allows a fine-grained definition of information exchange between objects. For example, the info sign box in Figure 2 can detect a passenger within its (the info sign's) bounding box. Listing 1.1 shows our algorithm, which processes the movement route of a passenger by the Liang–Barsky line-clipping algorithm [16], by which good results for detection and length calculation within the bounding box can efficiently be produced.

In each simulation step, the agent cycle executes for each agent. This leads to state information being updated, goals/events being checked, and plans expanded for each agent by, e.g., creating and instantiating actions for moving through the station while following the landmarks. In the example of the info sign, its bounding box will determine lists of passengers that entered, left, or moved through it within an agent cycle. The agent, which belongs to the bounding box, checks if another agent has left the box. Based on this information, the box state is updated. In particular, passengers who left the bounding box are informed about this by a *leave* message that may trigger new plans in the passenger agent.

Pedestrian movement: The aforementioned routing algorithm, JPS+, calculates landmarks for passengers moving through the station while simple collision detection / avoidance is factored into the environment. The detailed movement behavior of passengers in the station is expressed through a set of BDI rules, which are modeled in a rule-based scripting language (see Section 4 for details). Listing 1.2 illustrates basic elements of an exemplary BDI program consisting of one initial piece of information (= belief) and one plan.

In this example, the agent has the initial information that its train (ICE 751) will depart from platform 3. This information is expressed as a belief (line 1). Line 3 displays a plan. Plans are triggered by events, such as a new belief ('+'), retracted belief ('-') or new / retracted goal ('!'), (line 3). In the example, the goal catchtrain triggers the plan. The applicability of a plan can be further subject to additional context conditions; e.g., in line 4 it is required that the agent has the information that its train has arrived on a platform. Using logical unification (indicated by the '>>' operator), the conditions are evaluated and variables bound. Event and condition together form the *antecedent* of the plan rule; its *consequent* is the plan body, which consists of calculations, the execution of actions (e.g., the calculation of a route (line 6)), and the creation of new subgoals (line 7).

Section 3 elaborates on the principles for execution agent programs. A richer code example describing passengers' moving behavior is contained in the Appendix to this paper.

2.4 Transition between submodels

As stated so far, passengers switch between the two simulation submodels. Technically, a seamless transition between the two submodels is accomplished by modeling passengers as agents with unique identities over their complete lifecycle, and by a common object model (cf. Section 4). The doors of the trains and the platforms are also represented by agents, through which passengers switch from the railway network to the station.

Every station contains a set of uniquely named *platforms*. From a technical implementation per-

Listing 1.2: Example BDI program fragment for passenger agent

```
1  train( id("ICE 751"), platform(3) ).

3  +!catchtrain
4  : >>( train( id(T), platform(P) )
5  <-
6  route/set(P);
7  !movement/walk/forward.
```

spective, each platform maintains a collection of passengers currently standing on or moving across it, as well as a reference to any train residing at that platform. Each passenger maintains its itinerary as a list of train rides, stations, departure platforms and times. To simulate the effects of passengers disembarking and boarding, every train has a collection of *doors*. A train can only depart from a platform at a station when all its doors are closed and locked. On departure time, a command is sent to the doors to close and lock. Once all doors are locked, the train starts driving and informs the platform about the departure. Similarly, trains inform the platform, as long as they arrive at a station, about their arrival and the passengers inside itself, and unlock the doors.

Doors also maintain information about their current state, including two queues of passengers for disembarking or boarding, respectively. We assume, approximately, that a door can only be used by a single passenger at a time, and whenever the door is open and free, it will trigger either the next passenger of the disembarking queue or the boarding queue, if any, giving the priority to the disembarking passengers. To simulate the effect of the safety light-barriers installed in many trains to prevent doors from closing when there are people in it, doors keep track how long they have not been used by a passenger. A door can only close if it has not been used by a passenger for a predefined amount of time, usually a few seconds. The closing process is also simulated, which can be interrupted by a persistent passenger arriving at the door just then, forcing it to open again.

The following steps summarize the boarding procedure as performed by a passenger; the steps for disembarking from a train are analogous to those for boarding and are therefore not described:

1. Upon train announcement, check if the train is listed in the itinerary.
2. If the train is to be boarded, queue at one of the train's doors for entrance.
3. If the door is open and there are no disembarking/boarding passengers in front of the door, i.e., queues are empty, enter the train.
4. After entering (which takes a predefined amount of time), release the door. Unregister from the platform and register with the train.

3 Agent-based simulation with *LightJason*

Agent-based modelling and simulation (ABMS) [4] is a computational model for simulating autonomous (cognitive) agents and the interactions among them in a shared environment. Concepts such as reactivity, proactiveness, and social ability, as generally attributed to agents [26] are helpful for microscopic behavioral modeling. We define active simulation entities based on a BDI architecture, which allows a fine-grained modeling of their knowledge, behavior, and planning / decision-making. We refer to Section 2 for a description of the essential domain entities (agents) in our simulation scenario, i.e., passengers, trains, and the dispatcher.

The decision processes of the agents are based on individual goals and decision rules with an asynchronous concurrent execution semantics. From the modeling perspective, an argument often brought forward in favor of the MAS concept is that it allows a reduction of complexity. From the technical perspective, i.e., suitable runtime systems and frameworks, we refer to [3] for a discussion of the state-of-the-art and requirements. We summarize key requirements for a MAS simulation framework:

1. Simulate a large set of heterogeneous agents.
2. Fine-grained parameterization for modeling individual agent behavior.
3. Highly asynchronous execution mechanism.
4. High performance on executing the simulation scenarios for empirical evaluation.
5. High abstraction of software developing to separate domain-specific behavior and coding behavior.

An analysis of available agent-based modeling/programming frameworks reveals that these requirements are only partly met. Main limitations relate to scalability due to proprietary runtime systems [3]. Also, the platforms do not support state-of-the-art Object-Oriented methodologies and architectures, therefore including them in an existing code-base is very difficult since their documentation and code quality are poor. Figure 3 shows results of a benchmark comparison of the code qualities of popular open-source agent platforms[2]. It is clear that almost all platforms bring considerable numbers of errors of high and medium severity.

[2] This evaluation was performed using the tools FindBugs and J-Depend

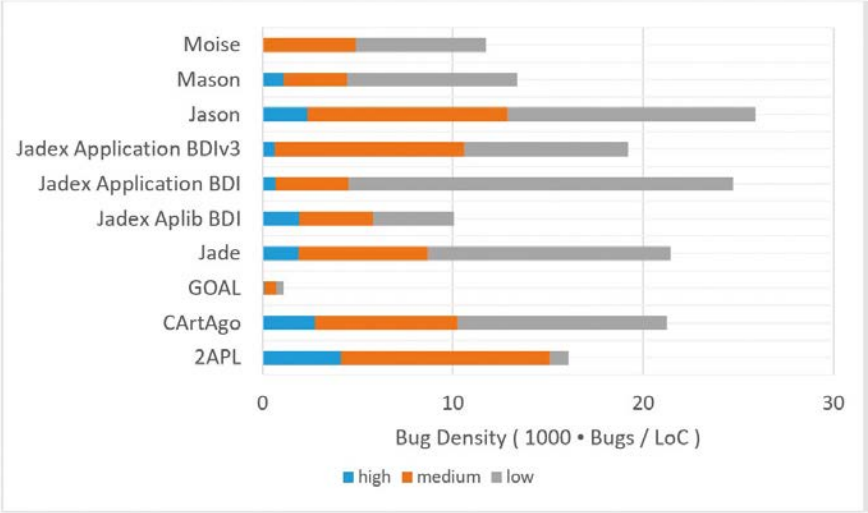

Figure 3: Bug density analysis for agent-oriented programming frameworks

This, among others, led us to develop the framework LightJason [3] from scratch. LightJason is inspired by the Jason BDI framework [5]; however, it is built on a completely new code-base and extends the descriptive language AgentSpeak(L)[19], which is used to describe agent behavior in Jason, to a newly designed language ASL+[3]. ASL+ extends the (Java-based) Object-Oriented paradigm with the BDI concept that follows the PRS execution mechanism [10]. There are a couple of features brought by ASL+, including lambda expressions, multi-plan and -rule definition, multi-variable assignments, concurrent execution mechanisms, and a fuzzy inference concept. For a brief glimpse of the ASL+ language, we refer to the example discussed in Section 2.3, Listing 1.2, and to the more complex example shown in the appendix to this paper. The semantics of plan execution in *LightJason* rests on the following design principles:

1. Multiple actions in a plan body are executed sequentially; this default semantics can be changed to parallel execution through a @Parallel annotation at the beginning of the plan specification.
2. Multiple subgoals created in a plan body are triggered concurrently; instantaneous, sequential execution can be enforced with using !!+ instead of !+.
3. Multiple matching plans are executed in parallel; synchronization can be enforced by setting context conditions.

The underlying system architecture of the *LightJason* framework is based on a layered architecture (see Figure 4) which combines functional, object-oriented, and logic programming/modeling paradigms. We refer to the *LightJason* online documentation[4] for more detailed information.

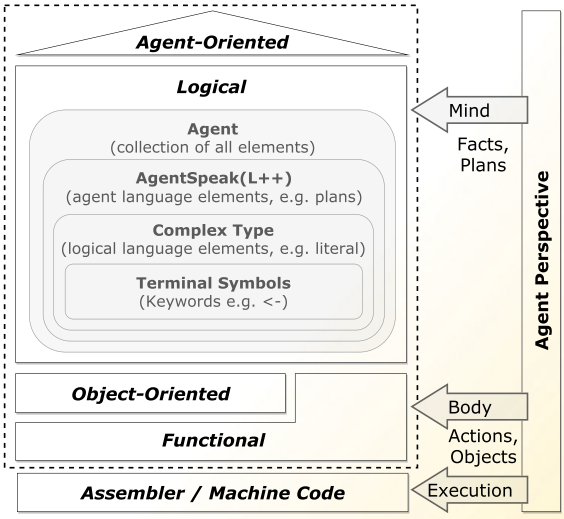

Figure 4: LightJason conceptual architecture

[3] ASL+ stands for AgentSpeak(L++).
[4] http://lightjason.org

4 Experiments

4.1 Example scenario

The first validation for the model described in Section 2 uses a small scenario in which two trains X and Y meet at a station. In this example, we simulate passengers that want to transfer from train X, scheduled to arrive at 10:00, to train Y, scheduled to depart at 10:04. The estimated average time for passengers moving from the platform of train X to that of train Y is 2 minutes. Figure [exp0] depicts the situation.

For the sake of simplicity, we assume in our example that all passengers in train X wish to continue their journeys with train Y; i.e., no other passengers disembark from train X in our station and no other passengers except those coming from train X board train Y. We also assume that for each train only one door is used to board and disembark, respectively. Even this simple situation, however, shows that the effect of passengers' behavior in the station is not negligible.

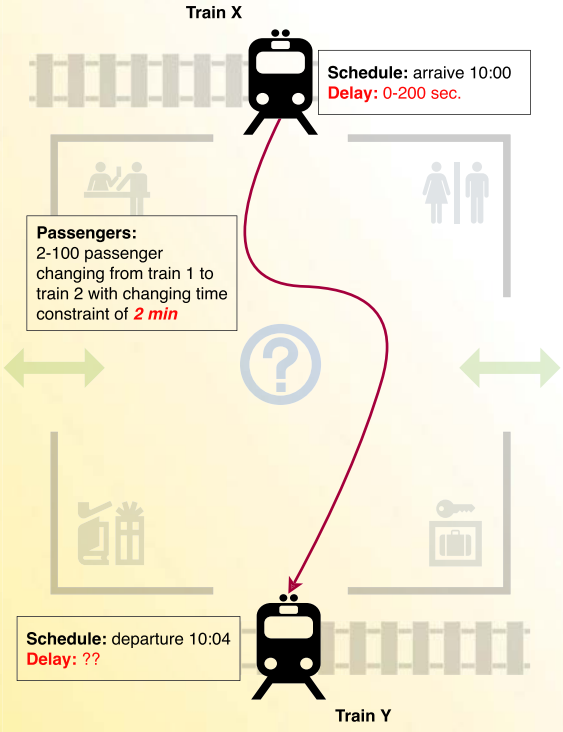

Figure 5: The simulated scenario: Passengers transfer from train A to train B in a station.

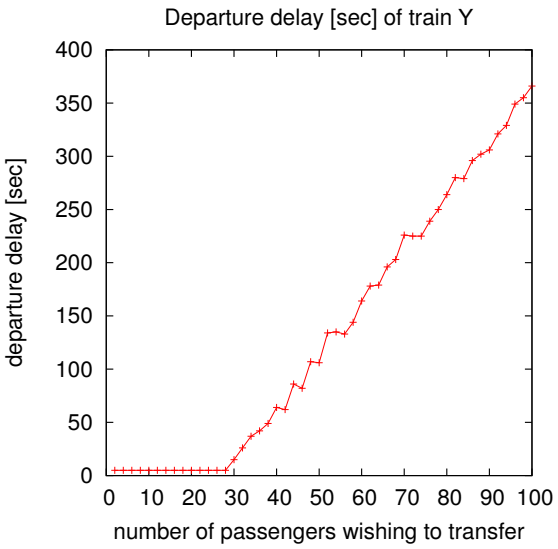

Figure 6: Departure delay of train Y with respect to the number of passengers. If more than 30 passengers wish to transfer, they delay the departing train

In the following, we consider two cases: The case where the incoming train is punctual and the case where its arrival is delayed.

4.2 Case 1: Punctual arrival of train

Here, train X is considered to arrive without delay. Consequently, in this situation one would expect that all passengers can transfer and that train Y can depart punctually. Although this would reflect the assumptions of classical delay management models, Figure 6 shows that it is not the case if many passengers want to transfer. In our simulation, the departure delay is zero if less than 28 passengers want to transfer; however, it increases if 30 or more passengers wish to transfer since they need some time to board train Y one after another.

One could argue that this effect may be negligible, as usually not too many passengers transfer to the same train, and may distribute among several doors. However, as we shall see from Section 4.3, we can expect significant effects for small numbers of passengers if train X arrives with some delay, or if passengers are not homogeneous.

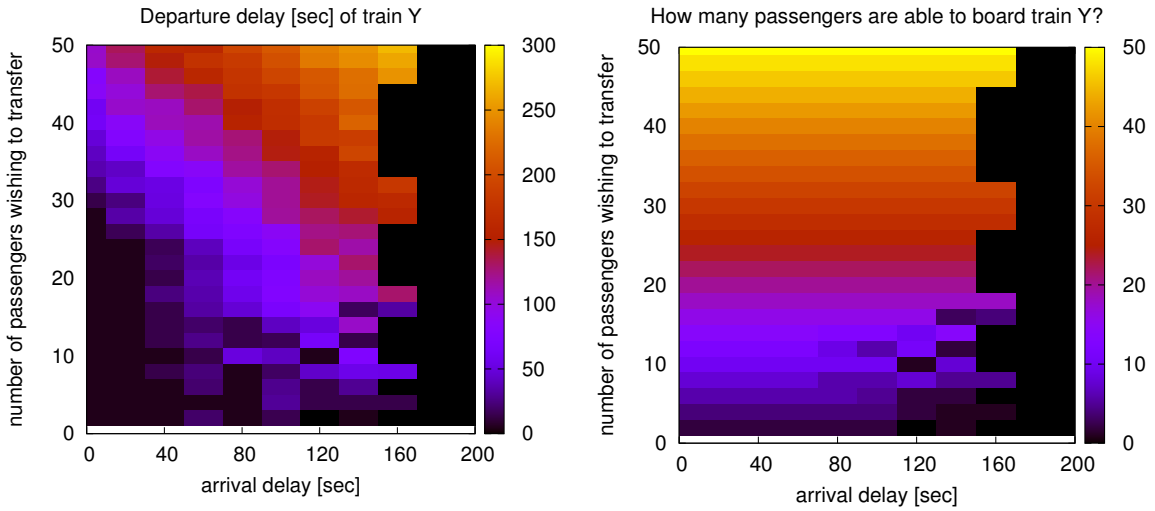

Figure 7: Departure delay of train Y (left) and number of passengers who are able to board train Y(right)

4.3 Case 2: Delayed arrival of train X

In this case, we assume train X arrives at the station with some delay. Recall that passengers need 2 minutes on average to walk from the arrival platform of train X to the departure platform of train Y, and that the scheduled time for this transfer is 4 minutes, leading to a *transfer buffer time* of 2 minutes. Therefore, it is common to assume that passengers can board train Y if the delay of train X is less than 2 minutes and that in this case all passengers make the transfer and train Y leaves on time. If the arrival delay of train X is larger than 2 minutes, classical models assume that the transfer will fail with train Y having already departed before the passengers from train X can reach its platform. This means, in both cases one may assume that train Y leaves punctually. Simulating these situations shows that all these common assumptions may be wrong, as the results in Figure 7 reveal.

Figure 7 illustrates our evaluations for different numbers of passengers, and different arrival delays of train X, namely for $n \in \{2,4,6,\ldots,98,100\}$ passengers and an arrival delay of train $X \in \{0,20,40,\ldots,200\}$ (in seconds). A glance at the left part of Figure 7 reveals that for an arrival delay of zero, we have no departure delay (graphed in black) if less than 28 passengers wish to transfer as we already know from Figure 6. If more passengers transfer, the departure delay starts to increase. We also see that for an arrival delay of more than 3 minutes (180 seconds) the departure delay of train Y is zero, since nobody reaches the platform of train Y before it leaves the station. Looking at the color-values of the heatmaps, we observe two different effects:

1. As noted in Figure 6, only one passenger can board train Y at a time; if many passengers transfer, train will be delayed. This explains that the departure delay of train Y increases with the number of passengers who need to transfer.
2. Not all passengers walk from train X to train Y with the same speed. Particularly, if many passengers wish to transfer, there may be one who is fast enough to reach train Y before its scheduled departure. While this passenger's boarding causes the door of train Y to remain open, the next one arrives and boards, too, and so on. Due to this *trickling in* effect, it is likely that most of the passengers can board even if the arrival delay of train X is larger than the 2 minutes transfer buffer time.

The right part of Figure 7 shows the number of passengers who make the transfer between train X and train Y. In case of no (or small) delay, all passengers reach Y on time and can board. If the delay starts exceeding 180 seconds, no one can

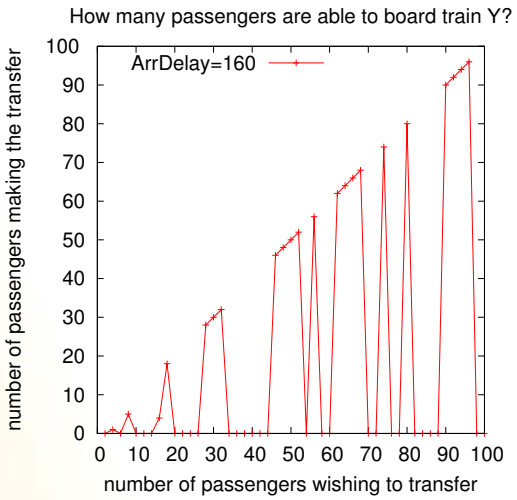

Figure 8: Number of passengers who manage to board train Y compared to number of passengers who wish to to so (for departure delay of 120 seconds).

reach the train. In between, it depends if there is a fast passenger able to reach train Y. Then it might be that all passengers can board, or that only a group of fast passengers reaches the train before it closes its doors and departs. The right part of Figure 7 shows that this effect becomes unlikely if many passengers want to transfer: In our experiments, if more than 18 passengers wish to transfer, either all of them manage to board train Y or none of them does.

Figure 8 shows an interesting case of an arrival delay of 160 seconds in more detail. This function depicts the ratio of the number of passengers who wish to transfer to train Y and the number of passengers who really manage to so. Thus, the experiments support the hypothesis that this is by chance: If there is a fast passenger who reaches train Y before it departs, we have many cases in which all passengers manage to board Y. For a small number of passengers who wish to transfer (in our figure for 16 passengers) we find that not all, but only the faster ones manage to board train Y. The specific shape of the function is random.

4.4 Heterogeneous and homogeneous passengers

Our final investigation studies the effect of heterogeneity among the group of transferring passengers. We modeled homogeneity and heterogeneity by changing the variance of the time needed for different passengers to walk from the arrival platform of train X to the departure platform of train Y. We would expect homogeneous passengers, e.g., in morning traffic, where passengers mostly carry small bags moving through the station rather quickly with approximately the same speed. During weekend travel, on the other hand, passengers are expected to behave more heterogeneously: Some carry heavy luggage and need more time to change between platforms; some travel with small children, some are elderly passengers, while others carry little baggage and may be able to run to their target platform. We simulate both the homogeneous and the heterogeneous case.

The heatmaps in Figure 9 illustrate the results for a *heterogeneous passenger group*. Here we see that it is hard to predict what is going to happen, but the outcome is random if there is a fast passenger in the group of transferring passengers who reaches the platform of train Y on time. The figure shows that this gets more likely if the number of transferring passengers increases: it is even possible that the whole group manages to board train Y if the arrival delay of train X is 160 seconds, which is considerably more than the transfer buffer time of 2 minutes.

Contrarily, Figure 10 displays the analysis for the case of *homogeneous passenger groups*. Here we observe an 'all or nothing' effect; either nobody manages to board train Y or the whole group does. Concerning departure delay (left part of Figure 10), the outcome is not random any more. Nobody is able to catch train Y if the arrival delay of train X is larger than 120 seconds, and the departure delay increases with the number of passengers who wish to transfer.

5 Conclusion and outlook

In this paper, we have been described ongoing work done in the ASimOV project. Our research

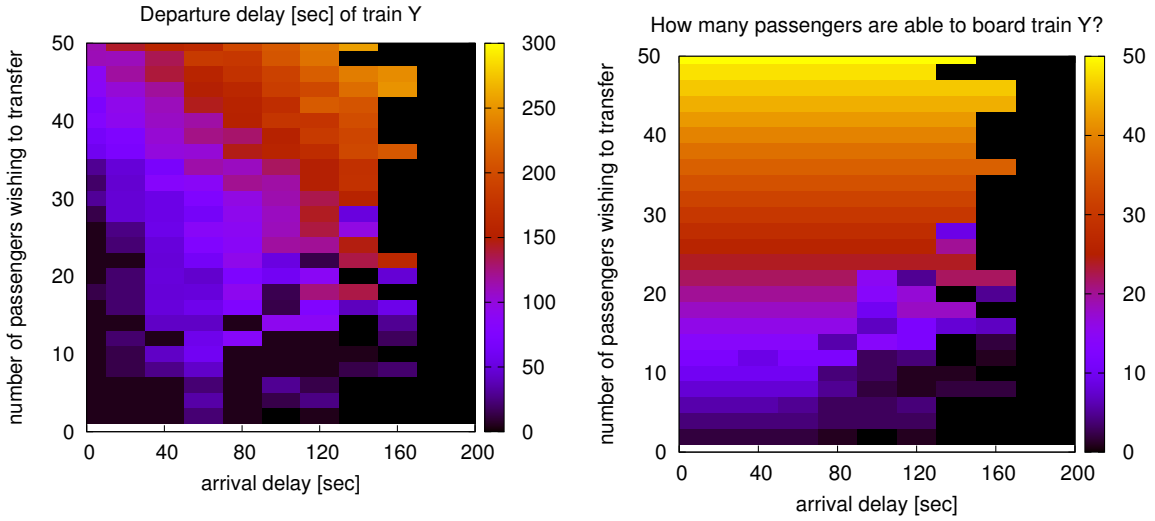

Figure 9: Departure delay of train Y (left); number of passengers able to board (right), heterogeneous case

aims to connect macroscopic railway network simulation with microscopic simulation of passengers' behavior at railway stations, put in the context of delay management. The work presented in this paper shows two basic contributions. The first contribution is a *new* conceptual model for describing the 'two worlds' of railway network and station as well as their integration in a simulation. The second contribution is that we provide insights gained from preliminary experiments that provide evidence for our hypothesis that a detailed simulation of passengers' behavior is promising in the context of delay management applications. The main result drawn from these experiments is that passengers' behavior at a station can have a significant influence on the departure delay of trains. This effect

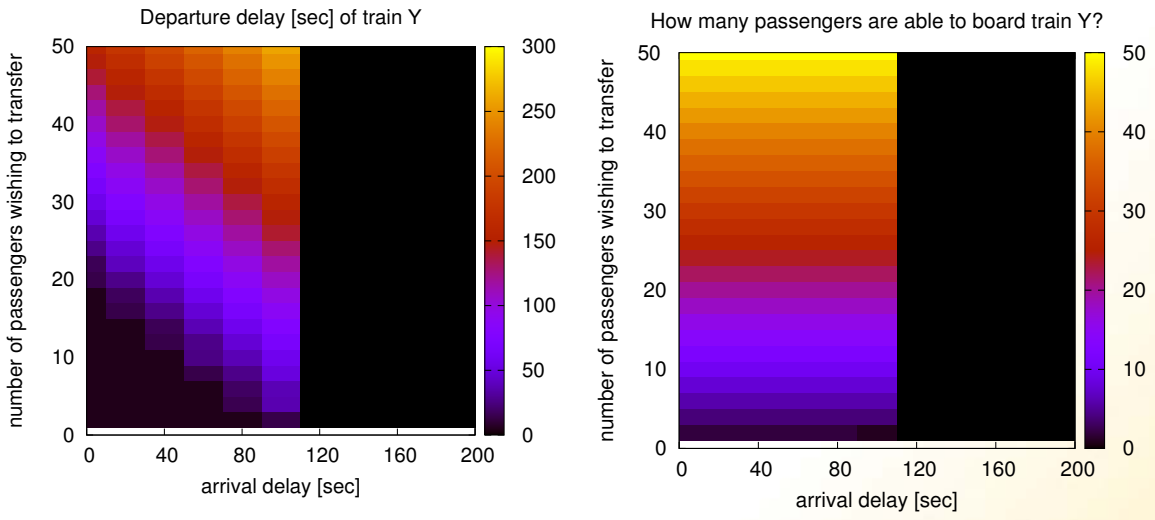

Figure 10: Departure delay of train Y (left); number of passengers able to board (right), homogeneous case

has not been considered in any delay management models we are aware of. Its intensity increases with the number of passengers wishing to transfer and with decreasing connecting times between trains. The latter is in particular the case if the train from which passengers wish to transfer (train X in our scenario, see Figure 5) arrives at the station with some delay. We have also seen that heterogeneity of the passengers plays an important role in delay creation and propagation.

We would like to point the esteemed reader's attention to the fact that, while we model individual passengers as agents in our station model, the simplifications explained for the investigated model in the reported experiments mean that our current passenger simulation is mesoscopic rather than microscopic. The movement model in the station is simplified to a stochastic queuing model (somewhat similar to that used in MATSim [11]) and does not yet consider the influence of specific features of station topology and microscopic interactions between passengers. Yet, these results form the baseline for future research directions: As a first aspect, we will increase richness and realism of passenger behavior models in the station (e.g., by considering more realistic models of passenger types, luggage, and passenger groups, as well as microscopic routing and movement control behaviours). Also boarding and disembarking on the platforms will be modeled microscopically, e.g., by considering realistic train / door topologies, but also the use of elevators, escalators or ramps to reach a platform, and more realistic behavioural features on the train. The latter also includes that passengers may dynamically change their planned itineraries, which is known to be hard to treat within optimization models (see [22]).

A second important aspect is the modeling of the information state of passengers and the impact of the informational state of passengers, e.g., through interaction with dynamic traffic signs or smartphones. A third venue of research builds on previous work on delay management (e.g., [21]) by evaluating different delay management strategies and hence help the disposition centers in taking good *wait-depart decisions*. Ongoing work uses the results reported in this paper to improve existing optimization approaches for delay management by considering the trickling-in effect examined in this paper.

6 References

[1] Ahlbrecht, T., Dix, J., Fiekas, N., Köster, M., Kraus, P., Müller, J.P.: An architecture for scalable simulation of systems of cognitive agents. International Journal of Agent-Oriented Software Engineering (IJAOSE) 5, 232265 (2016).

[2] Albert, S., Kraus, P., Müller, J.P., Schöbel, A.: Passenger-induced delay propagation: Agent-based simulation of passengers in rail networks. In Simulation Science, volume 889 of Communications in Computer and InformationScience (CCIS), 3-23. Springer, 2018.

[3] Aschermann, M., Kraus, P., Müller, J.P.: Light-Jason: A BDI Framework inspired by Jason. In: Multi-Agent Systems and Agreement Technologies: 14th Europ. Conf., EUMAS 2016, and 4rd Int. Conf., AT 2016, Valencia, Spain, 2016. LNCS, vol. 10207, pp. 5866. Springer International Publishing (2017).

[4] Bazzan, A.L.C., Klügl, F.: Agent-based Modeling and Simulation. AI Magazine 33(3), 29-40 (2013).

[5] Bordini, R.H., Hübner, J.F., Wooldridge, M.: Programming multi-agent systems in AgentSpeak using Jason, vol. 8. John Wiley & Sons (2007).

[6] Camus, B., Galtier, V., Caujolle, M., Chevrier, V., Vaubourg, J., Ciarletta, L., Bourjot, C.: Hybrid Co-simulation of FMUs Using DEV&DESS in MECSYCO. In: Proceedings of the Symposium on Theory of Modeling & Simulation. pp. 8:1- 8:8. Society for Computer Simulation International, San Diego, CA, USA (2016).

[7] Codd, E.F.: Cellular Automata. Academic Press, Inc., Orlando, FL, USA (1968).

[8] Dollevoet, T., Huisman, D., Schmidt, M., Schöbel, A.: Delay management with rerouting of passengers. Transportation Science 46(1), 74-89 (2012).

[9] Dollevoet, T., Huisman, D., Schmidt, M., Schöbel, A.: Delay propagation and delay management in transportation networks. In: et a., C.M. (ed.) Handbook of Optimization in the Railway Industry, pp. 285-317. Springer (2018).

[10] George, M.P., Lansky, A.L.: Reactive reasoning and planning. In: Proceedings of the Sixth National Conference on Articial Intelligence

- Volume 2. pp. 677-682. AAAI'87, AAAI Press (1987).
[11] Grether, D., Nagel, K.: Extensible software design of a multi-agent transport simulation. Procedia Computer Science 19, 380-388 (2013),
[12] Helbing, D., Molnár, P.: Social force model for pedestrian dynamics. Physical Review E 51, 4282-4286 (1995).
[13] Johora, F.T., Kraus, P., Müller, J.P.: Dynamic path planning and movement control in pedestrian simulation. In: van Dam, K.H., Thompson, J. (eds.) Preproc. Of 2nd International Workshop on Agent-based modelling of urban systems (ABMUS 2017). Arxiv.org, Sao Paulo, Brazil (May 2017), accepted for publication.
[14] Kircho, F.: Modelling delay propagation in railway networks. In: Operations Research Proceedings 2013. pp. 237-242 (2014).
[15] Kircho, F.: Verspätungsfortpanzung in Bahnnetzen, Modellierung und Berechnung mit Verteilungsfamilien. Ph.D. thesis, University of Technology Clausthal, Germany (2015).
[16] Liang, Y.D., Barsky, B.A.: A new concept and method for line clipping. ACM Transactions on Graphics (TOG) 3(1), 1-22 (1984).
[17] Manitz, J., Harbering, J., Schmidt, M., Kneib, T., Schöbel, A.: Source estimation for propagation processes on complex networks with an application to delays in public transportation systems. Journal of the Royal Statistical Society: Series C 66, 521-536 (2017).
[18] Pachl, J.: Railway Operations and Control. VTD Rail Publishing, Mountlake Terrace,USA, 2 edn. (2014).
[19] Rao, A.S.: Agentspeak(l): BDI agents speak out in a logical computable language. In: Agents Breaking Away, 7th European Workshop on Modelling Autonomous Agents in a Multi-AgentWorld, Eindhoven, The Netherlands, January 22-25, 1996, Proceedings. pp. 42-55 (1996), https://doi.org/10.1007/BFb0031845.
[20] Rückert, R., Lemnian, M., Blendinger, C., Rechner, S., Müller-Hannemann, M.: Panda: a software tool for improved train dispatching with focus on passenger ows. Public Transport (2017), to appear.
[21] Schachtebeck, M., Schöbel, A.: IP-based techniques for delay management with priority decisions. In: Fischetti, M., Widmayer, P. (eds.) ATMOS 2008 - 8th Workshop on Algorithmic Approaches for Transportation Modeling, Optimization, and Systems. Dagstuhl Seminar proceedings (2008).
[22] Schmidt, M., Schöbel, A.: The complexity of integrating routing decisions in public transportation models. Networks 65(3), 228-243 (2015).
[23] Schöbel, A.: Capacity constraints in delay management. Public Transport 1(2), 135-154 (2009).
[24] Shalaby, A.S., King, D., Srikukenthiran, S.S.: Using Simulation to Analyze Crowd Congestion and Mitigation Measures at Canadian Subway Interchanges: Case of Bloor-Yonge Station, Toronto, Ontario. Transportation Research Record: Journal of the Transportation Research Board 2417, 27-36 (2014).
[25] Srikukenthiran, S.S., Shalaby, A.S.: Enabling large-scale transit microsimulation for disruption response support using the Nexus platform: Proof-of-concept case study of the Greater Toronto area transit network. Public Transport 9(3) 411-435 (2017).
[26] Wooldridge, M.: An introduction to multiagent systems. John Wiley & Sons (2009).

Appendix: *AgentSpeak(L++)* code for passenger movement behavior

```
// walk straight forward towards the goalposition
+!movement/walk/forward <-
    move/forward();
    !movement/walk/forward.

// if walking straight fails, then go left
-! movement/walk/forward <-
    !movement/walk/left.

// plan for turning/walking left
+!movement/walk/left <-
    move/left();
    !movement/walk/forward.

// if walk left fails, then go right
-!movement/walk/left <-
    !movement/walk/right.

// plan for turning/walking right
+!movement/walk/right <-
    move/right();
    !movement/walk/forward.

// if walking right fails, then wait a random time
-!movement/walk/right <-
    T = math/statistic/randomsimple() * 10 + 1;
    T = generic/type/toint( T );
    T = math/min( 5, T );
    generic/sleep(T).

// if the agent has come to standstill, try to speed up
+!movement/standstill <-
    >>attribute/speed(S);
    S = generic/type/toint(S) + 1;
    +attribute/speed( S );
    !movement/walk/forward.

+!position/achieve(P, D) <-
    route/next;
    !movement/walk/forward.

// on waking up after sleeping, set speed and keep on moving
+!wakeup <-
    +attribute/speed( 1 );
    !movement/walk/forward.
```

Project data

The project is funded from SWZ with 1.5 TV-L E13 staff positions since June 2016 at the sites Clausthal and Göttingen. Involved scientists are:

Prof. Dr. Jörg P. Müller
Business Information Technology Unit
Department of Informatics
Clausthal University of Technology

Julius Pätzold, M.Sc.
Research Group Optimization
Institute for Numerical and Applied Mathematics
University of Göttingen

Prof. Dr. Anita Schöbel
Research Group Optimization
Institute for Numerical and Applied Mathematics
University of Göttingen

Demand robust arrangement of operating units and equipment by combining optimization and simulation

Uwe Bracht, Anja Fischer, Thomas Krüger, Mirko Dahlbeck, Marc Schlegel

Introduction

Globalization, an increased dynamization of markets, decreasing product cycles and increasing customer demands concerning quality and delivery reliability are only some of the challenges manufacturing enterprises have to cope with today. So manufacturing enterprises require more frequent changes in products and production programs and thus adjustments of factories and structures of production [1].

This calls for the utilization of factory planning and the tools of the digital factory [2]. Innovative ideas are needed to raise productivity and to reduce cost pressure. The planning of factory structures, starting from choosing a location to setting up departments, has an important impact for a technical and economical production process.

The layout of the departments is one of the main influencing factors for a cost efficient production and provides a basis to uphold the long-term productivity and competitiveness [3, 4]. Layout problems can be solved by heuristics and exact methods. Heuristic procedures are a standard tool used in factory planning [5, 6]. They usually allow to derive solutions rather fast but without knowledge of the quality of the solution. In contrast to this, exact solution methods are often slower and only allow to compute optimal solutions for rather small instances in reasonable time.

The layout planning process highly influences the further planning steps and the determined solution has a direct influence on the quality of the planning results and further planning efforts. So the extension of existing exact methods seems worthwhile. In order to validate the layout and its

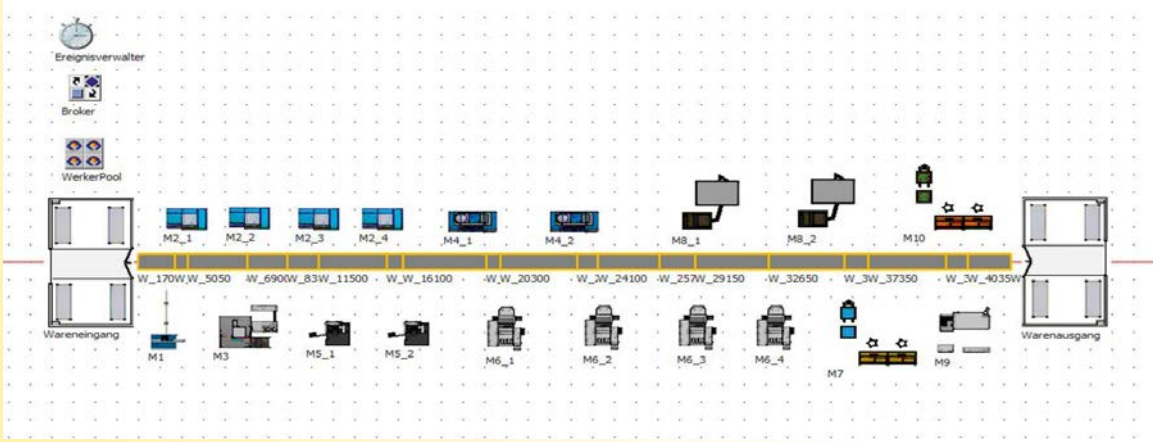

Figure 1: Simulation Model of a DRFLP Layout

Figure 2: VR-Model of a DRFLP Layout

consequences for production, we use material flow simulation and Virtual Reality (VR) [2, 9, 14]. With the material flow simulation (Figure 1), layouts are evaluated and the production processes are dynamically validated. VR enables the user to take a virtual tour in these planned layouts (Figure 2) and thus planning errors can be detected and avoided.

Layout optimization – state of research

Facility Layout Problems are a well-known field of research in mathematical optimization [10, 15]. Given a set of rectangular departments with specified sizes and input and output points as well as pairwise transport weights between them the task is to determine a non-overlapping arrangement of the departments within a facility such that the sum of the weighted distances between the output and the input points of the departments is minimized. Partially the basic structure of the layout is fixed in advance [8, 16].

Computing an optimal solution in reasonable time for practical relevant problem sizes is very difficult. Even finding good lower bounds for medium-sized instances is very challenging. For this reason, one often restricts the structure of the layout and the paths.

A well known special case of the general facility layout problem is the so called Single-Row Facility Layout Problem (SRFLP), where all departments are assigned on a single row and one measures the center-to-center distances of the departments. The SRFLP is NP-hard and by now, the largest exactly solved instance, in which methods of semidefinite optimization where used, contains 42 departments [17, 18].

In the Double-Row Facility Layout Problem (DRFLP), the departments are arranged on both sides of a common path and again one measures the horizontal center-to-center distances between each pair of departments. The DRFLP is NP-hard [7, 16]. Instances with up to 15 departments can be solved to optimality by a mixed-integer linear programming model [23].

The current best approach of [8] is able to solve DRFLP instances with up to 16 departments in at most 12 hours [8]. The idea of this approach is to enumerate over all distinguishable row assignments and to solve the DRFLP with fixed-row assignment, the so called FR-DRFLP. In [8] a strong model for the FR-DRFLP is presented which is based on betweenness and distance variables. In combination with two dummy departments which are fixed at the left and right border of the layout the betweenness variables imply an ordering of

the departments in each row and the distances to the left border are equal to the exact positions of the departments. In the following we denote the model of [8] for the FR-DRFLP as basic model because we extend this model in the next section. Unfortunately all those mathematical approaches are based on numerous assumptions and abstractions of input data. The most common assumptions are briefly explained below. It is currently assumed that the material supply point (input and output point) is in the center of a department. This assumption can lead to high deviations as the input and output points do not have to be at the same position. There are no restrictions given for the area of the factory building and for path calculations, there is just a focus on the horizontal center-to-center distances between the departments. Therefore, there is no difference if two departments are on the same or opposing sides of a path.

Due to simplification, minimum clearance conditions between departments for safety and maintenance, which are important in real environments, are not taken into account.

Extensions of the basic DRFLP model

In this section we show how to extend the model of [8] such that the resulting model is capable of important realistic aspects. Further details and proofs are given in [19]. At first, we show how to arrange the departments in a restricted area. Let the departments be given as 2-dimensional objects with given lengths and widths. In factory planning the area of a given layout is defined as the area of a minimum boundary rectangle that contains all departments. As the row assignment is fixed in the basic model the width of the layout is equal to the sum of the width of a department with the largest width in each row plus the width of the path. So we obtain a restricted area by bounding the length of the layout in an appropriate way which is possible by adding a linear inequality to the basic model.

Next we add vertical distances to the basic model measuring the center-to-center distances between two 2-dimensional departments. The distance between two departments is given as the sum of the horizontal distance between these departments plus half the width of each department and if the departments are in distinct rows we have to add the width of the path. As the row assignment is fixed we only need to add a constant to the objective value to include vertical inter-row distances. We observed that in realistic instances there often appear departments of the same type, i.e., departments that have the same length and the same transport weights to all other departments. In that case we can break symmetries and thus reduce the number of row assignments that have to be tested. Let n departments be given. In general we have to test 2 to the power of n-1 row assignments. Let a_(i) denote the number of departments of type i and let m denote the number of different department types. We proved in [14] that the number of distinguishable row assignments is at most

$$\left\lceil \frac{1}{2} \prod_{i \in [m]} (a_i + 1) \right\rceil$$

The usage of this result can be illustrated by the following example. We are given a double-row instance with 21 departments, where two departments appear four times, three departments twice and seven departments just once. Then we have to solve the basic model 43.200 times instead of more than 1 million times. If there are departments of the same type in the same row, one can break symmetries by fixing the order of these departments [14].

Usually, in factory planning the incoming and the shipping warehouse are fixed to the left and right border. In this case we can interpret the dummy departments as warehouses. Of course, we might obtain a better overall solution value if we drop the restriction on the position of both warehouses. In this case they are treated as ordinary departments that have transport connections to other departments and need a certain space.

In the classic DRFLP one can easily consider asymmetric transport weights because the distance from i to j is equal to the distance from j to i, see, eg., [20]. This situation changes if the input and output points do not lie in the center of the departments. Indeed, in our extension we can measure the distance from department i to department j as the distance from the output point of i

to the input point of j. In our extended model we add weighted ordering variables to the objective function in addition to the betweenness variables in order to include such a distance calculation. In this way asymmetric transport weights can easily be handled.

Additionally we include inner-row asymmetric clearances and in contrast to the literature we also allow the consideration of inter-row asymmetric clearances. We also include the concept of shared additional clearances. Given two neighbouring departments i and j in the same row, department i needs additional clearances on the right and j on the left, and if i lies directly left to j then the clearances can be shared. So the overall space of the layout might be decreased. For further details, we refer to [19]. Note that all these extensions can also be used for the SRFLP.

Lower bounds for the DRFLP

To the best of our knowledge combinatorial lower bounds specialized to the DRFLP are not known in the literature and lower bounds received via some branch-and-cut algorithm within a given time limit of one hour for some DRFLP formulations from the literature are rather weak.

So we focus on combinatorial lower bounds for the DRFLP which can be computed very fast. These bounds generalize the star inequalities of the minimum arrangement problem and use ideas from the scheduling literature. The main idea is to construct a layout where the sum of the weighted distances of department i to all other departments is minimized. In such a layout one department lies directly opposite to i [21] so we fix department j directly opposite to i. Then we interpret the problem of arranging the remaining departments as a scheduling problem with four machines and assign the departments via the Shortest Processing Time rule or the Smith rule (for further details we refer to [21]). Arranging every department directly opposite to i and taking the minimal objective value of these layouts leads a lower bound for the sum of the weighted distances of i to all other departments. Summing up these values for every department and dividing this value by 2 leads to a lower bound for the DRFLP.

These combinatorial lower bounds are the basis for a new distance-based integer linear program for computing even stronger lower bounds. We obtain these lower bounds by applying a branch-and-cut algorithm within a time limit of a few minutes.

Iterative combination of optimization and simulation

The extension of the DRFLP is iteratively combined with a material flow simulation as illustrated in Figure 3.

First, a planning task is solved by the DRFLP model and the layout is generated. This layout is transferred to the material flow simulator and simulation runs are performed. On the basis of the simulatively determined data, e.g., throughput times and stocks, the layout is evaluated and the need for improvements is identified.

If further improvements are necessary, the DRFLP models are extended and the solver determines a new layout solution. The DRFLP layout is valuated by simulation. The process is finished when the

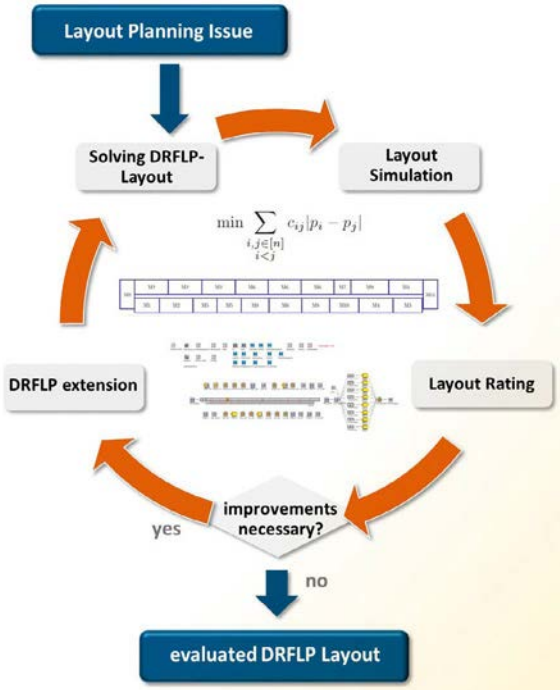

Figure 3: Iterative extension of the DRFLP Model

simulated solution fulfills all requirements. In order to make this process more efficient, a connection between DRFLP and material flow simulator must be developed. In addition, the integration of the double-row layout into the factory planning process and the use of tools and methods of the Digital Factory is required in order to exploit the potential in layout planning. To achieve this, an approach for connecting the DRFLP with the "Plant Simulation" material flow simulator is needed.

DRFLP and material flow simulation

For the connection of the DRFLP with the material flow simulation an approach was developed, which supports the iterative planning process by an automated generation of the corresponding simulation models. The concept for the automated model generation is an important element for the connection of the DRFLP and simulation. It also represents a core element of the PhD thesis of Thomas Krüger in this project. Figure 4 shows the sequence of the automated model generation. The DRFLP results are supplied in a table format, which is read in and processed by the simulator. In addition to the layout data, further information that are relevant for controlling the production processes in the simulator must be read in. Based on these data, the executable simulation models are generated automatically (see Figure 4).

The imported data have to be converted step by step into a model by different controls during the automated generation. The process consists of the following three basic steps:

1. data import
2. creation of objects, parts, resources and linking with controls
3. customizing model characteristics by selection of controls for distribution strategies and management of production processes

The user is guided through these steps by the different dialogues. An executable simulation model is then automatically generated. At this point simulations can be executed.

Figure 5 shows an example of the structure of the automatically generated model, the required data and controls.

Set up in the middle is the automated arrangement of the departments, in form of a layout variant. So the components of the simulation model can be subdivided into the following categories:

1. model building methods - orange
2. production sequence control methods - green
3. tables (input for the required information) - grey
4. results of simulation (such as data of transport distances, throughput stocks and stock movements) - light blue
5. user interface - purple

Methods for model construction are required for an automated generation of models. The methods for managing the production flow are necessary to control the individual production sequence of the goods. Both method groups use a multitude of tables, which serve as input for the required information.

In the light blue area there are the results of the simulation that are recorded during a simulation run. They contain, for example, data on transport routes, throughput stocks and stock level flowcharts.

In the user interface area, a dialog box can be used to control the model layout. The desired production program and the strategy for material flow control are then selected via drop-down lists. The system for controlling the material flow through production using a control strategy consists of the components:

– Method „target finding"
– Table "targets"
– Method "shortest processing time"

After starting the simulation, the method „target finding" is called in the outputs of the individual blocks. This happens whenever a part is ready for transport to the next location. This method checks in the table „targets" on which stations the parts have to be processed next.

If there are multiple possible successor stations (e.g. departments of the same type), the „shortest processing time" method is used to check which station offers the shortest processing time for the product. The already scheduled department

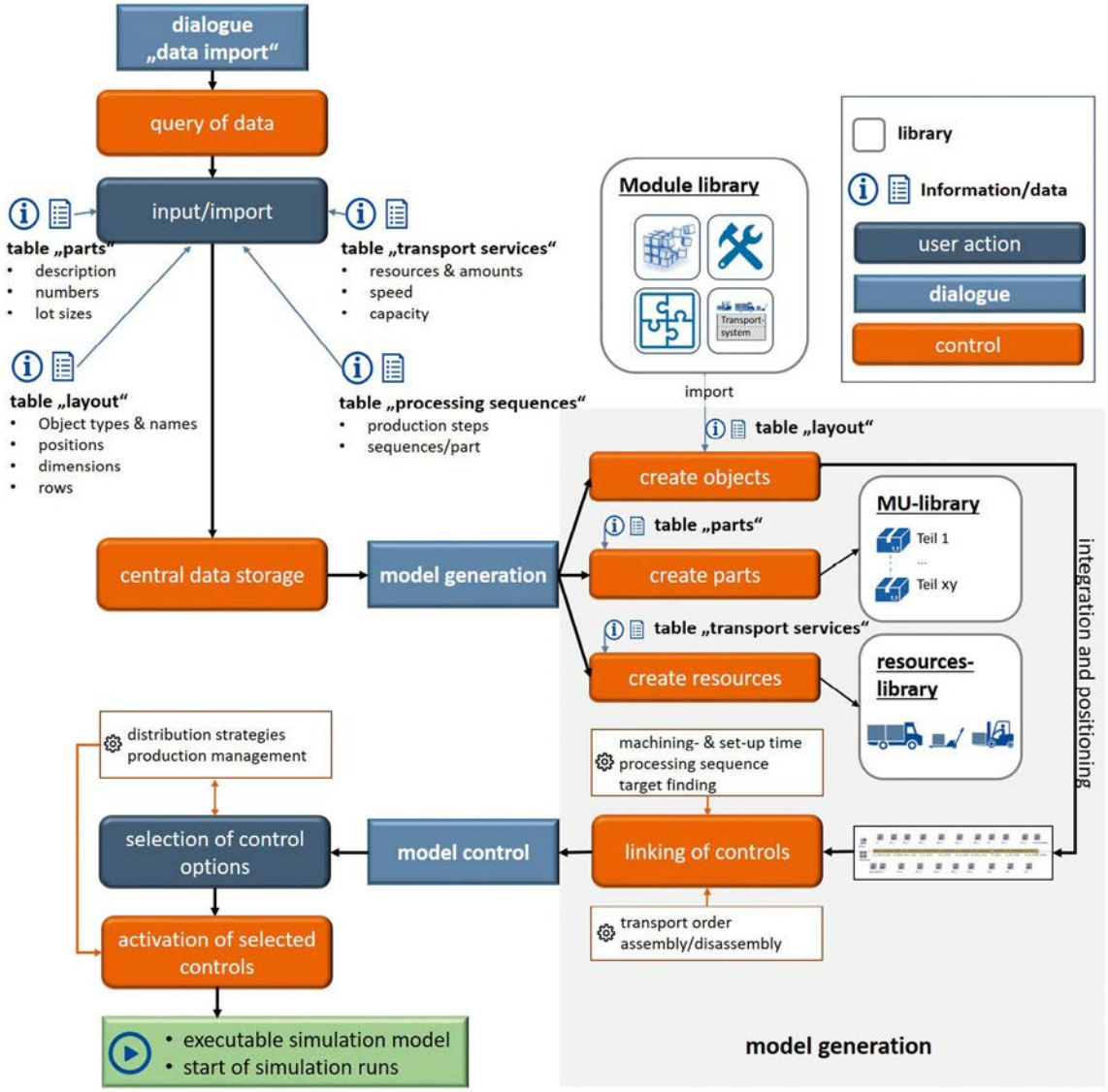

Figure 4: Procedure of the automated model generation

orders, necessary setup times or failures are taken into account. These controls are used to manage transport and processing operations in the system. The integrated methods also ensure that the correct setup and processing times are set and that statistical values such as transportation routes, capacity utilization, processing times and stock levels are recorded.

Coupling material flow simulation and virtual reality

For validation and adaptation purposes of the developed layout variants, an immersive three-dimensional environment is helpful. The IMAB offers ideal technical equipment for this with its Virtual Reality Laboratory. It consists of a VR

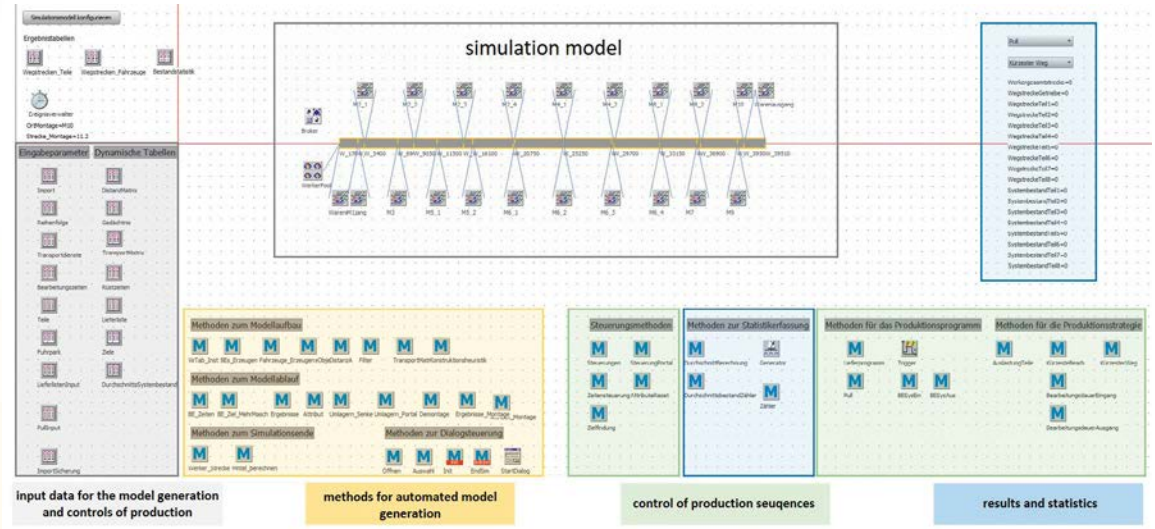

Figure 5: Structure of the generated simulation model

large-scale projection system and Head-Mounted-Displays. However, the material flow simulation program „Technomatix Plant Simulation" used in this research project does not natively support any VR display devices. Therefore, layout variants have to be modeled individually and manually in a corresponding VR software and changes in the layout have to be transferred back to the material flow simulation program in the same way.

In order to minimize the effort for visual validation, an interface was developed that automatically couples the contents from the material flow simulation program and the VR software and synchronizes any changes in real time. This can be done in both directions [22].

In addition to this synchronization, a high degree of user-friendliness should also be striven for. In order to meet the defined requirements, an overall concept was developed which can be divided into the following five steps (Figure 6):

1. Identification of required data from simulation
The first step is to examine which data have to be transferred from Plant Simulation to the VR-Environment. Position data of departments and MUs are indispensable for the representation in virtual reality, whereas processing times of a department do not have to be considered for the representation of the simulation as they are later transmitted in real time.

2. Preparation of the data in Plant Simulation
After identification of the necessary data, it has to be prepared for the respective interface in such a way that the subsequent utilization of the data can take place. For use in a VR environment a real time connection has to be established. In this project, the socket interface has been chosen to connect

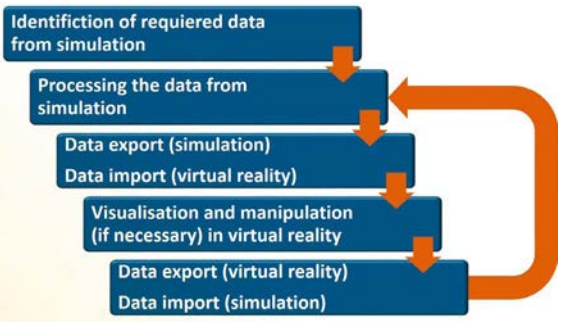

Figure 6: Steps for coupling simulation and VR

Plant Simulation to the Unreal Engine 4 (UE) which is used as VR environment. Thus, all necessary information from Plant Simulation (PS) have to be gathered from the simulation model. For this, the data have to be read from each visible object and, in case of any changes, to be updated.

3. Transmitting Data
For the exchange with the UE, PS already contains a template for the socket interfaces. So, a socket-channel to the UE can be created and data are transmitted. As already stated in the previous paragraph, all necessary data have been gathered and now have to be encoded to a common format, which the decoder in the UE is able to process. To ensure the real time connectivity, the data have to be updated each time an object in Plant Simulation has changed its position. After being transmitted, the data are used to build or update a simulation model in VR. For this, all used 3D-models have previously been filed in a library. This way, UE is able to automatically build a VR-Environment without further work by the user.

4. Visualization and manipulation in VR
After synchronization, all objects from the simulation are displayed in an immersive VR-Environment. Here, the user is able to verify the positions of all objects and is able to make changes and corrections if necessary. In this step, a high degree of user-friendliness is striven for. All actions are directly transferred back to the simulation program and do not have to be synchronized manually. Furthermore, the simulation process can be shown in real time. For this, the simulation has to be started in Plant Simulation. After that all movements of MUs are visible in VR.

5. Export from VR and import to PS
After an object has been manipulated, the updated data are decoded within this step in order to enable their utilization in Plant Simulation. In addition, a function must be created that sends the data immediately after they have been manipulated. It is then converted into the required format and the changed object receives a new position in the original simulation model.

Figure 7: VR- and simulation models in the VR-Lab

In Figure 7 we illustrate our immersive visualization. The factory including the departments are full-scale and the accessibility of the material flow offers the planners the possibility to view, analyze and design the actual appearance of the simulated factory layouts according to their ideas.

Computational results

In this section we summarize our computational results. We consider the well-known application instance [12] with 21 departments and 12 different department types mentioned in Section 'Extensions of the Basic DRFLP Model'. By using our theorem, that allows us to reduce the number of row assignments that have to be checked, we are able for the first time to solve a DRFLP instance with 21 departments in less than 14 hours. Note again that the largest double-row instance solved to optimality before contained 16 departments [8].

In the simulation we compare the exact solution with a solution found by a heuristic [5] where one has a special look on the linearity of the flows. The latter layout was improved by hand afterwards. As it is usually done in factory planning the warehouses were fixed to the border in both variants. At last we computed an optimal solution where we drop the position restrictions of the warehouses.

Our example contains eight different products which are combined in an assembly department to an end product. In all three variants we produced 36.000 end products in the simulation and determined the average transport distance of each single product as well as the total transport distance. Comparing the first two variants we observed that the solution obtained by optimization reduced the total travel distance by 4.2 % in comparison to the heuristic. If we drop the position restrictions of the warehouses we reduce the total distance traveled in comparison with the optimized layout by 31.5 % and in comparison with the heuristic layout by 34.4 %. We observed that in the optimized layouts the transport distances of single products vary significantly.

In [21] we compute lower bounds for the classic DRFLP. At first, we consider small literature instances with a known optimal solution. Our combinatorial lower bounds obtain gaps of about 50% in less than one second and our branch-and-cut algorithm within a time limit of three minutes for our ILP reduces the gaps to 28 %–34 %.

Next we consider randomly generated instances with up to 50 departments and transport densities of 10%, 50% and 100%. For each transport density we generate 10 instances and we compute the average value of the lower bounds. The integral department lengths are chosen randomly between 1 and 15 as well as 5 and 10. In order to obtain upper bounds we obtain a start layout by a heuristic of [11] and we use a 1-opt and 2-opt algorithm where in each step the exact positions of the departments are determined by solving a linear program, see [21].

Using a branch-and-cut algorithm for DRFLP formulations from the literature [7] leads to gaps of nearly 100 % for instances with more than 40 departments after a time limit of one hour. Our combinatorial lower bounds can be computed in less than 1 second and are better for almost all instances. Our branch-and-cut algorithm applied on our ILP with a time limit of 3 minutes reduces the gaps to 18-55 %. Further computational results for the space-free FR-DRFLP and for double-row instances, where all departments are of equal length, are given in [21].

Manufacturing different products

In the previous section the simulation showed that the transport distances of one product might be rather high in an optimal layout if the number of products of this type is small in comparison to the others. But high transport distances can increase the cycle time. So, for a smooth production we want to bound the transport distances associated to single products. One possibility is to use upper bounds for the transport distance of each single product. Another possibility is to set up a desired distance for each single product and to initialize a penalty function. If the desired transport distance is exceeded, we penalize this with a quadratic function and even if the transport distance is below the desired distance, we can penalize this in the objective function. This penalty function can be linearized by a piece-wise linear function, see [14].

Conclusion

We presented a new approach which combines optimization and simulation in factory planning. We restricted our attention to the Double-Row Facility Layout Problem (DRFLP) as it has a wide field of applications. We were able for the first time to solve a realistic double-row instance with 21 departments in reasonable time. In comparison with a heuristic solution our optimized solution reduced the total traveled transport distance significantly, specially when we dropped the position restrictions of the warehouses.

The DRFLP model of [8] was extended in order to cover realistic aspects. We can restrict the area of a double-row layout and we can take vertical distances into account. Now we are able to consider individual input and output points of the departments, asymmetric transport weights and asymmetric clearances. As a result, this extended DRFLP can be better used in factory planning.

Furthermore we presented combinatorial lower bounds for the DRFLP and we introduced an integer linear programing model, which is not a formulation for the DRFLP, to improve the combinatorial lower bounds. We use a branch-and-cut algorithm with a given time limit of three minutes and we obtain gaps of 45 to 55% while for instances with 40 departments or more DRFLP formulations from the literature obtain gaps of nearly 100% by using a branch-and-cut algorithm within a given time limit of one hour.

In a final step in layout planning, VR is used to validate the 3D layouts. Due to the direct data exchange, the developed connection of simulation and VR is able to implement the simulation data in the VR environment in real time. In addition to the 3D layout, the production processes can also be visualized. This is an important element for the acceptance of the planning results as all parties involved in the planning process have the same communication basis.

The extended DRFLP model in combination with the described simulation and visualization methods of the Digital Factory represents an important basis for the planning of efficient layouts.

Literatur

1. Schenk, M.; Wirth, S.; Müller, E.: Fabrikplanung und Fabrikbetrieb. Methoden für die wandlungsfähige, vernetzte und ressourceneffiziente Fabrik: VDI-Buch. Springer Vieweg, Berlin 2014.
2. Bracht, U.; Geckler, D.; Wenzel, S.: Digitale Fabrik. Methoden und Praxisbeispiele - Basis für Industrie 4.0: VDI-Buch. Springer Vieweg, Berlin 2018.
3. Rooks, T.: Rechnergestützte Simulationsmodellgenerierung zur dynamischen Absicherung der Montagelogistikplanung bei der Fahrzeugneutypplanung im Rahmen der Digitalen Fabrik. Zugl.: Clausthal, Techn. Univ., Diss., 2009. Band 20: Innovationen der Fabrikplanung und -organisation. Shaker, Aachen 2009.
4. Tompkins, J.; White, J.; Bozer, Y.: Facilities planning. Wiley, Hoboken, NJ 2010.
5. Schmigalla, H.: Fabrikplanung. Begriffe und Zusammenhänge: REFA-Fachbuchreihe Betriebsorganisation. Hanser, München 1995.
6. Kettner, H.; Schmidt, J.; Greim, H.-R.: Leitfaden der systematischen Fabrikplanung. Mit zahlreichen Checklisten. Hanser, München 2010.
7. Amaral, A.: Optimal solutions for the double row layout problem. Optim Lett 7 (2013) 2, S. 407–413.
8. Fischer, A.; Fischer, F.; Hungerländer, P.: New Exact Approaches to Row Layout Problems 2015. http://num.math.uni-goettingen.de/preprints/files/2015-11.pdf.
9. Bracht, U.; Fischer, A.; Krüger, T.: Mathematische Anordnungsoptimierung und Simulation. Ein kombinierter Ansatz zur Fabriklayoutplanung. wt - Werkstattstechnik online 107 (2017) 4, S. 200–206.
10. Anjos, M.; Vieira, M.: Mathematical optimization approaches for facility layout problems. The state-of-the-art and future research directions. European Journal of Operational Research 261 (2017) 1, S. 1–16.
11. Chung, J.; Tanchoco, J.M.A.: The double row layout problem. International Journal of Production Research 48 (2010) 3, S. 709–727.

12. Prêt, U.: Fabrikplanung (Übung) - Schneckengetriebeproduktion 2017. http://www.uwe-pret.de/fabrikplanung/skripte/stapel3/getriebe.pdf#page=2&zoom=auto,-158,843. Zugriff am 19.08.2018.
13. Schmigalla, H.: Methoden zur optimalen Maschinenanordnung. Verlag Technik, Berlin 1968.
14. Bracht, U.; Dahlbeck, M.; Fischer, A.; Krüger, T.: Combining Simulation and Optimization for Extended Double Row Facility Layout Problems in Factory Planning. In: Baum, M; Brenner, G; Grabowski, J; Hanschke, T; Hartmann, S; Schöbel, A. (Hrsg.): Simulation science. First International Workshop, SimScience 2017, Göttingen, Germany, April 27-28, 2017, Revised selected papers. Springer, Cham, Switzerland 2018, S. 39–59.
15. Drira, A.; Pierreval, H.; Hajri-Gabouj, S.: Facility layout problems: A survey. Annual Reviews in Control 31 (2007) 2, S. 255–267.
16. Anjos, M.; Fischer, A.; Hungerländer, P.: Improved exact approaches for row layout problems with departments of equal length. European Journal of Operational Research 270 (2018) 2, S. 514–529.
17. Hungerländer, P.; Rendl, F.: A computational study and survey of methods for the single-row facility layout problem. Computational Optimization and Applications 55 (2012) 1, S. 1–20.
18. Hungerländer, P.: Single-row equidistant facility layout as a special case of single-row facility layout. International Journal of Production Research 52 (2013) 5, S. 1257–1268.
19. Fischer, A.; Dahlbeck, M.: Exact Models for Extended Row Layout Problems. Working Paper.
20. Murray, C.; Smith, A.; Zhang, Z.: An efficient local search heuristic for the double row layout problem with asymmetric material flow. International Journal of Production Research 51 (2013) 20, S. 6129–6139.
21. Dahlbeck, M.; Fischer, A.; Fischer, F.: Decorous Combinatorial Lower Bounds for Row Layout Problems. Working Paper.
22. Bracht, U.; Schlegel, M.: Ein neuer Ansatz zur Modellbildung und Simulation mit VR- und AR-Brillen am Beispiel der Fabrikplanung. ASIM 2018 - 24. Symposium Simulationsrechnik (2018), S. 143–147.
23. Secchin, L.; Amaral, A.: An improved mixed-integer programming model for the double row layout of facilities. Optim Lett 13 (2019) 1, S. 193–199.

Project data

The project is funded from SWZ with 1.5 TV-L E13 staff positions since April 2016 at the sites Clausthal and Göttingen. Involved scientists are:

Prof. Dr.-Ing. Uwe Bracht
Research Group Plant Engineering, Institute for Plant Engineering and Fatigue Analysis
Clausthal University of Technology

Dipl.-Wirtschaftsing. Thomas Krüger
Research Group Plant Engineering, Institute for Plant Engineering and Fatigue Analysis
Clausthal University of Technology

Jun.-Prof. Dr. Anja Fischer
Research Group Management Science
Faculty of Business Economics
TU Dortmund University

Marc Schlegel, M.Sc.
Research Group Plant Engineering, Institute for Plant Engineering and Fatigue Analysis
Clausthal University of Technology

Mirko Dahlbeck, M.Sc.
Research Group Management Science
Faculty of Business Economics
TU Dortmund University

Simulation von Materialien

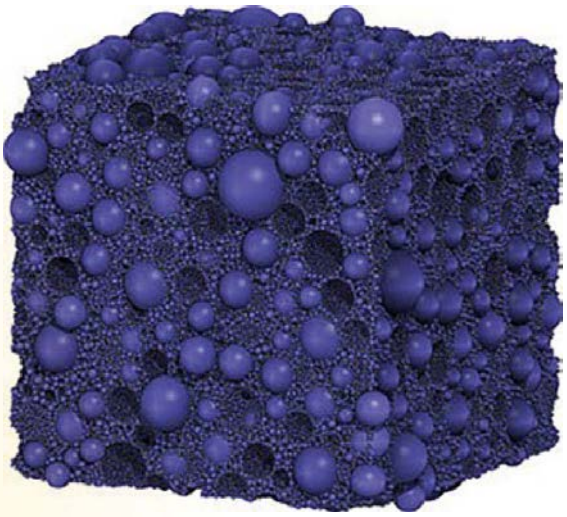

Die Fortschritte der Materialwissenschaften und angrenzender Ingenieurdisziplinen sowie Naturwissenschaften mit dem Fokus der Einbeziehung von Materialeigenschaften haben seit jeher den Entwicklungsstand einer Gesellschaft definiert. Materialwissenschaften sind gerade in der deutschen Industrielandschaft eines der zentralen Themen, welche die Grundlage für viele Innovationen in anderen Industriezweigen liefern.

In den Materialwissenschaften sowie materialorientierten Ingenieurdisziplinen und Naturwissenschaften hat sich bereits eine stark interdisziplinäre Arbeitsweise herausgebildet, welche in den stark überlappenden Bereichen „Computational Materials Science“, „Computational Physics“, „Computational Mechanics“ und „Computational Chemistry“ ausgeprägt ist. Simulationen haben sich in den Material- und Ingenieurwissenschaften und den benachbarten naturwissenschaftlichen Disziplinen zu einem lebendigen und forschungsstarken Wissenschaftszweig herausgebildet, der vermehrt auch von der Industrie wahrgenommen und aktiv gefördert wird.

Probleme der Materialwissenschaften und materialorientierten Energiewissenschaften sind sehr vielfältig und spielen sich typischerweise auf unterschiedlichsten Längen- und Zeitskalen ab. Zudem liegen die unterschiedlichsten physikalischen Ursachen vor, wie Temperatur, Strahlung, elektromagnetischer und mechanischer Felder. Deshalb zeichnet sich das Feld der Materialsimulationen durch eine Vielzahl verschiedener Simulationsmethoden aus, welche auf die jeweilige Problemklasse zugeschnitten sind:

Auf der kleinsten Längenskala werden in sogenannten ab-initio Simulationen atomare Prozesse parameterfrei auf der Grundlage von Naturgesetzen simuliert. Diese quantenmechanischen Methoden erfordern meistens Hochleistungsrechner, erlauben aber vielfältige und quantitative Aussagen zu treffen. Ein solches Programmpaket wird in Clausthal entwickelt und vertrieben.
Auf der makroskopischen Längenskala hingegen wird das Material als ein Kontinuum betrachtet, dessen Verhalten von Materialmodellen bestimmt wird. Die darin auftretenden Materialparameter müssen anhand ausgewählter Experimente mit Hilfe von Optimierungsverfahren bestimmt werden. Während eine Vielzahl von Simulationstechniken vereinheitlicht ist, kommen hierbei vorwiegend kommerzielle Programmpakete zum Einsatz. Da andererseits solche Programme auch großen Einschränkungen unterworfen sind, ist die Neu- und Weiterentwicklung von numerischen Berech-

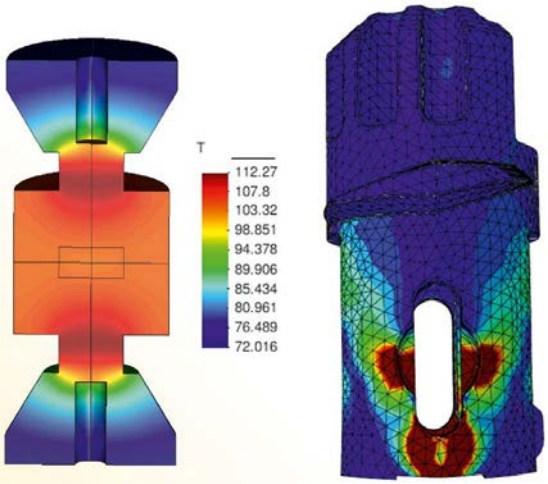

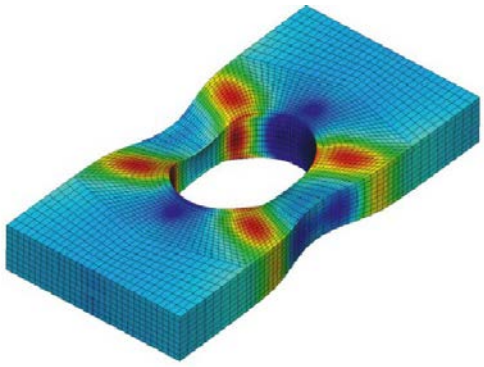

nungsverfahren erforderlich. Das Hauptinteresse bei der Anwendung kommerzieller Programme richtet sich auf die Modellierung des Problems und die Bestimmung der dabei verwendeten Parameter sowie die Validierung der Resultate. Bei der Neuentwicklung numerischer Berechnungsverfahren hingegen stehen die Analysis, die Effizienz und die Stabilität der Berechnungsmethoden und die Verifikation der Programme im Fokus.

Zwischen diesen Polen befinden sich eine Vielzahl weiterer Methoden die hier nur einige als Stichworte genannt werden sollen: Stochastische Simulationen, Molekulardynamik, Mehrfeldsimulationen, Phasenfeldtheorien, Mikrostruktursimulation von Versetzungen, Simulation chemischer Prozesse, usw.

Eine der großen Herausforderungen im Bereich Computational Materials Science“ ist daher die Multiskalensimulation, die im Idealfall von der ab-initio Simulation bis zur Simulation von Umformprozessen und Herstellungsverfahren reicht. Diese Herausforderung wird einerseits dadurch angegangen, dass Simulationsparameter gezielt von den auf atomarer Ebene bestimmten Größen über mikroskopischen Berechnungen zu den makroskopischen Simulationen durchgereicht werden. Andererseits werden unterschiedliche Simulationsmethoden in eine einheitliche Simulationsumgebung integriert, um Effekte zu beschreiben, bei denen unterschiedliche Längen- und Zeitskalen nicht mehr entkoppelt werden können. Diese Aktivitäten erfordern die Zusammenarbeit unterschiedlicher Wissenschaftsdisziplinen und profitieren von Zusammenschlüssen, wie sie im Simulationswissenschaftlichen Zentrum geplant sind.
Im Gegensatz zu etlichen anderen Anwendungen von Simulationsverfahren sind Simulationen im Bereich der materialorientierten Ingenieurdisziplinen sehr häufig dadurch gekennzeichnet, dass sie alle verfügbaren Rechnerressourcen bis an die Grenzen ausschöpfen müssen, um gewünschte Ergebnisse zu erzielen. Fragen der algorithmischen Komplexität und der Effizienz von Implementierungen sind daher für Fortschritte der Simulationsmethoden in diesem Teilgebiet von entscheidender Bedeutung.

78

Kopplung multi-physikalischer Prozesse zur Simulation von Gasbohrungen

Stefan Hartmann, Leonhard Ganzer, Jithin Mohan, Birger Hagemann

Wind- und Solarenergie können zu einem zwischenzeitlichen Überangebot an Strom führen. Eine Option zur Zwischenspeicherung der überschüssigen Energie ist die Zerlegung von Wasser in Sauerstoff und Wasserstoff durch Elektrolyse. Der Wasserstoff wird dann in unterirdischen Kavernen oder porösen Lagerstätten zwischengespeichert und bei Bedarf wieder entnommen, um ihn dann zur Methanisierung zu nutzen, in das Gasnetz einzuspeisen oder als Kraftstoff einzusetzen. Dieser Vorgang der Injektion in bzw. die Entnahme aus einem Untergrundspeicher, letzteres auch als Produktionsphase bezeichnet, führt zu dem Interesse einer ganzheitlichen Betrachtung. Hierzu wird das Gas in die Verrohrung gepresst, erhitzt sich während es um mehrere hundert Meter in die Tiefe gebracht wird und tritt an Perforationen im Rohr in das Lagerstättengestein ein. Die Perforationen sind kleine Löcher in den metallischen Rohren und den sie umgebenden Zementschichten. Ziele in diesem Projekt sind daher den Vorgang mit numerischen Hilfsmitteln zu beschreiben sowie das lokale Verhalten zur Integritätsüberprüfung der Verrohrung zu untersuchen. Da für den Gasfluss in der Bohrung, dem lokalen Verhalten des Gases an den Perforationen sowie im Gestein selbst unterschiedliche Simulationsprogramme sinnvoll sind, ist es das Ziel ein Kopplungstool für unterschiedliche Programmsysteme zu entwickeln. Zudem ist auch von Interesse wie die lokale mechanische und thermische Beanspruchung des Zements und der Rohre ist, die wiederum durch andere Berechnungsverfahren simuliert werden. Neben der Entwicklung des Kopplungstools sind insbesondere Kenntnisse des Verhaltens einzelner Unterprobleme erforderlich.

In diesem Projekt sind daher zunächst mehrere Teilprobleme untersucht worden:

1. Mathematische Formulierung der Gesamtproblematik und numerische Lösung der bei der Semidiskretisierung auftretenden Algebro-Differentialgleichungssysteme
2. Untersuchung der lokalen Spannungs- und Deformationszustände der Metallrohre sowie die sie umgebenden Zementschicht
3. Entwicklung eines Programms zur Berechnung der Rohrströmung für ein kompressibles Gas unter sich ändernden Temperaturbedingungen
4. Lokale numerische Simulation des Fließverhaltens zur Bestimmung der Druck- und Geschwindigkeitsbedingungen an den Perforationen
5. Simulation der Lagerstätte bei Injektion und Produktion.

Im Folgenden sollen kurz die einzelnen Punkte zusammengefasst werden:

Mathematische Formulierung der Gesamtproblematik

Die einzelnen Grundprobleme – Rohrströmung, thermomechanisches Verhalten der Verrohrung, Fließverhalten in der Nähe der Perforation, sowie die Gasströmung im umgebenden porösen Gestein – werden durch partielle Differentialgleichungen (PDEs) in Raum und Zeit beschrieben. Die Lösung dieser PDEs erfolgt mit Hilfe der vertikalen Linienmethode, indem zunächst die Raumdiskretisierung mit Hilfe der Methode der finiten Elemente bzw. der finiten Volumen erfolgt. Daraus entsteht ein System von algebraischen nichtlinearen Gleichungen, die mit gewöhnlichen Differentialgleichungen gekoppelt sind, was man als Algebro-Differentialgleichungssystem (DAE-System) bezeichnet. Für jedes Teilproblem entsteht ein spezielles Unterproblem, welches mit Spezialsoftware im Zeitbereich gelöst wird. Da die Teilgebiete Rohr (innen und außen), Perforationsgebiet sowie Lagerstättengestein durch unterschiedliche Lösungsverfahren behandelt werden, ist es das Ziel eine vereinheitliche algorithmische Struktur zu entwickeln. Wenn die Teillöser auf dem impliziten Euler-Verfahren basieren, lassen sich

für die Zeitintegration des DAE-Systems steifgenaue diagonal-implizite Runge-Kutta Verfahren heranziehen, um für die Gesamtproblematik höhere Genauigkeitsordnung sowie eine effiziente Zeitschrittweitensteuerung zu erhalten. Das Resultat ist ein gekoppeltes nichtlineares Gleichungssystem an jedem Zeitintegrationspunkt. Zudem sind Kopplungsbedingungen zu erfüllen, die durch geometrieerhaltende Verfahren (hier in Form eines Projektionsverfahrens) behandelt werden. Die Lösung des blockstrukturierten nichtlinearen Gleichungssystems muss mit einem Block-Gauss-Seidel-Verfahren gelöst werden, damit die entkoppelte Struktur durch die einzelnen Spezialprogramme erhalten bleibt. Die schlechte Konvergenzgeschwindigkeit des Gauss-Seidel-Verfahrens wird durch Beschleunigungstechniken (Aitken-Relaxation) erheblich verbessert. Hierzu ist ein Bericht für Anfang 2019 geplant (Mohan und Hartmann, 2019).

Lokales Spannungs- und Deformationsverhalten der Rohre

Die einzementierten Rohre, durch die das Gas strömt, werden durch Innen- und Außendruck, Eigengewicht und unterschiedliche Innen- und Außentemperaturen in Abhängigkeit der Tiefe belastet. Da sich die Metallrohre auch überlappen können, entstehen zwei- und vierschichtige Systeme aus Metall und Zement. Hierzu sind analytische Lösungen der Thermo-Elastizität hergeleitet worden, um Spannungszustände abschätzen zu können, siehe (Hartmann et al., 2018; Müller-Lohse, 2018). Auch sind hier stationäre und transiente Untersuchungen mit Hilfe von Zeitintegrationsverfahren höherer Ordnung erfolgt.

Transiente kompressible Rohrströmung

Für die Massen- und Impulsbilanz sowie Wärmeleitungsgleichung sind neben den Grundgleichungen eindimensionale finite Elemente Diskretisierungen programmiert worden, die die Rohrströmung für die Injektions- und die Produktionsphase behandeln. Hierbei ist es das Ziel diese Formulierung zunächst mit dem Programm DuMux für die Simulation der Lagerstätte zu koppeln und den Gesamtalgorithmus hierbei zu testen. Derzeit ist das eindimensionale Dreifeldproblem in der Erprobungs- bzw. Verifikationsphase.

Numerische Simulation der Perforation

Die Bohrungskomplettierung wird im Gebiet der Speicherschicht mit Löchern ausgestattet, die man als Perforationen bezeichnet. Durch diese Löcher fließt das Gas während der Produktionsphase in das Rohr bzw. wird während der Injektionsphase in die Lagerstätte gepresst. Um einerseits die Belastung auf die Bohrungskomplettierung (Stahlrohr und Zement) zu erhalten, sind Strömungssimulationen durchgeführt worden, die aufgrund von Verwirbelungen auf eine ungleichmäßige Belastung führen. Andererseits dienen die Simulationen zur Untersuchungen der Druck- und Geschwindigkeitsverhältnisse am Ein- bzw. Austrittspunkt sowie der Erfahrungssteigerung bei den dort vorhandenen Größenverhältnissen aus Perforation und Rohrdurchmesser.

Lagerstättensimulation

Die numerische Lagerstättensimulation, siehe (Hagemann, 2017), durch Einpressen von Gas sowie seiner Rückgewinnung ist das Fernziel. Derzeitige Berechnungen unterliegen einer lokalen Quelle, die die Bohrung darstellt. In einer 10m hohen und einer mehr als 1km ausgedehnten Lagerstätte sind mit dem Programmsystem DuMux erste Simulationen erfolgt, in welchem die Eigenschaften des Gases und des porösen Mediums eingehen, so dass realitätsnahe Berechnungen möglich sind.

Ausblick

Die Erkenntnisse über die Teilprobleme sind wesentlich für die kommenden Schritte. Zunächst wird die eindimensionale Rohrströmung für ein kompressibles Gas unter Temperatur mit Hilfe der Methode der finiten Elemente fertiggestellt und anschließend über ein Kopplungstool mit dem Programm DuMux gekoppelt. Hierzu werden dann zeitadaptive Berechnungen durchgeführt und das Injektions- und Produktionsverhalten von Wasserstoff in die bzw. aus der Lagerstätte behandelt.

Referenzen

Mohan, J. und Hartmann, S. (wird eingereicht, 2019): Solution techniques for coupled systems of non-linear equations. Technical report,

Faculty of Mathematics/Computer Science and Mechanical Engineering, Clausthal University of Technology (Germany).
Müller-Lohse, L. (2018): Analytische Lösung für stationäre belastete, mehrschichtige thermoelastische Rohre, Projektarbeit, Institut für Technische Mechanik, TU Clausthal.
Hartmann, S., Mohan, J., Müller-Lohse, L., Hagemann, B., Ganzer, L. (2018): An analytical solution of multi-layered thick-walled tubes in thermo-elasticity with application to gas-wells, International Journal of Pressure Vessels and Piping 161, 10 – 16.
Hagemann, B. (2017): Numerical and analytical modeling of gas mixing and bio-reactive transport during underground hydrogen storage, doctoral thesis, Clausthal University of Technology and Université de Lorraine.

Projektdaten

Das Projekt wurde von Juli 2015 bis Juni 2018 vom SWZ mit insgesamt einer TV-L E13 Stelle an dem Standort Clausthal gefördert. Beteiligte Wissenschaftler sind:

Prof. Dr. Leonhard Ganzer
Arbeitsgruppe
Lagerstättentechnik
Institut für Erdöl- und
Erdgastechnik
Technische Universität
Clausthal

**Prof. Dr.-Ing.
Stefan Hartmann**
Arbeitsgruppe
Festkörpermechanik
Institut für Technische Mechanik
Technische Universität
Clausthal

Dr.-Ing. Birger Hagemann
Arbeitsgruppe
Lagerstättentechnik
Institut für Erdöl- und
Erdgastechnik
Technische Universität
Clausthal

Jithin Mohan, M.Sc.
Arbeitsgruppe
Festkörpermechanik
Institut für Technische Mechanik
Technische Universität
Clausthal

Verteilte Multiskalensimulation zur Optimierung der Herstellung von Faserverbundwerkstoffen für den Flugzeugbau

Dieter Meiners, Dietmar P.F. Möller, Juliana Rivas-Botero, Huynh Khiem Le, Isabell A. Jehle

Faserverbundwerkstoffe gelten als Standardwerkstoffe zukünftiger Fertigungsprozesse und werden seit Jahren mit zunehmender Tendenz im Fahrzeug- und Flugzeugbau eingesetzt. Sie vereinen die Vorteile ihrer Einzelkomponenten, Faser und Kunststoff, zu einem Ganzen und zeichnen sich oft durch hohe Festigkeit, Steifigkeit und geringes Gewicht aus. Im Fahrzeug- und Flugzeugbau ist das Eigengewicht des Transportmittels proportional zum Kraftstoffverbrauch. Daher muß ein kostengünstiges Transportmittel mit geringem Gewicht zum Einsatz kommen. So verwendet man beispielsweise seit Jahrzehnten leichte Polymermaterialien sowie schwere Metallkomponenten. Neben dem Gewicht müssen die verwendeten Materialien auch spezielle Eigenschaften und Anforderungen erfüllen. Sie gehören daher zu den so genannten Funktionsmaterialien. Faserverstärkte Polymermaterialien bieten aufgrund ihres geringen Gewichts, ihrer hohen Stabilität und sicherheitsrelevanter Eigenschaften, wie der Nichtbrennbarkeit der Materialien, ein breites Anwendungsspektrum.

Bei faserverstärkten Polymermaterialien wird eine Faserstruktur in das Polymer eingebracht, um die physikalischen Eigenschaften besser an die Anforderungen anzupassen. Kostenintensive Faserwickel- und Prepreg Technologien sind die meist verwendeten Verfahren, um faserverstärkte Kunststoffe (FVK) herzustellen. Als kostengünstigere Alternativen hierzu bieten sich Infusionsverfahren, wie RTM an. Ziel ist es, dieses wirtschaftliche Bauteilherstellungsverfahren mit einem Softwarewerkzeug zu simulieren, um die Faser für eine spezielle Form-, Fasergeometrie und spezielle Polymerarten u.a. zu nutzen, ohne daß hier hohe durch Versuche verursachte Kosten entstehen.

Die Qualität des Materials hängt stark vom Druck, der Temperatur, der chemischen Zusammensetzung des Polymers und der geometrischen Form der Faserstruktur während des Herstellungsprozesses ab. Einschlüsse im Polymer durch z.B. Luftblasen reduzieren die Materialqualität. Darüber hinaus führt eine heterogene Molekularstruktur zu lokal unterschiedlichen Materialeigenschaften und kann später unter Last zum Bruch des Bauteils führen. Über die rein physikalischen Bedingungen während des Herstellungsprozesses hinaus sind in der Praxis die Fertigungsparameter von entscheidender Bedeutung. Bei einer Form für Flugzeugtüren, in die beispielsweise das Polymerharz eingebracht werden soll, sind die optimale Position der Einlaßöffnungen und der Einlaßdruck entscheidend für die Qualität des Materials der Flugzeugtür.

Die Herstellung von besonders funktionellen Faserverbundwerkstoffen mit hoher Qualität resultiert in einem multiskaligen Problem in räumlicher Dimension. Auf der untersten Ebene bestimmen Richtung und Länge, sowie die chemischen, thermodynamischen und mechanischen Eigenschaften der Polymermoleküle das Verhalten des Faserverbundwerkstoffs. Mehrere Ebenen darüber haben die hydrodynamischen Bedingungen am Einlaß des Polymers in die Form über die Einlaßdüsen Einfluß auf die Geometrie der Faserstruktur. Die Multiskaligkeit führt zu einem sehr komplexen numerischen Optimierungsproblem, da unterschiedliche physikalische und geometrische Modelle berücksichtigt werden müssen. Bei den Polymeren handelt es sich um hochviskose Flüssigkeiten, die von Temperatur und Druck abhängen und zu bestimmen sind. Darüber hinaus variiert die, für die Lösung des Modells erforderliche Diskretisierung sehr stark in ihrer räumlichen Ausdehnung.

Modellparameter zu Materialeigenschaften, wie Viskosität und Dichte bei einem bestimmten Druck und Temperatur, die das Fließverhalten des Polymerharzes bestimmen, können in einem Meß-

stand bestimmt werden. Darüber hinaus kann der Einfluß der Gewebegeometrie auf das Strömungsverhalten untersucht werden. Für die detaillierte Untersuchung der optimalen Herstellungsprozesse von Faserverbundwerkstoffen sind sowohl Messungen als auch numerische Simulationen erforderlich. Beide methodischen Ansätze kommen im Rahmen dieses Projekts zur Anwendung.

Projektdaten

Das Projekt wird seit Juli 2017 vom SWZ mit insgesamt einer TV-L E13 Stelle an dem Standort Clausthal gefördert. Beteiligte Wissenschaftler sind:

Prof. Dr.-Ing. Dieter Meiners
Institut für Polymerwerkstoffe und Kunststofftechnik
Technische Universität Clausthal

Prof. Dr.-Ing. Dietmar P.F. Möller
Arbeitsgruppe Stochastische Modelle in den Ingenieurwissenschaften
Institut für Angewandte Stochastik und Operations Research
Technische Universität Clausthal

Juliana Rivas-Botero, M.Sc.
Arbeitsgruppe Multifunktionale Leichtbau-Faserverbundwerkstoffe, Institut für Polymerwerkstoffe und Kunststofftechnik
Technische Universität Clausthal

Huynh Khiem Le, M. Sc.
Arbeitsgruppe Stochastische Modelle in den Ingenieurwissenschaften, Institut für Angewandte Stochastik und Operations Research
Technische Universität Clausthal

Isabell A. Jehle, M.Sc.
Arbeitsgruppe: Stochastische Modelle in den Ingenieurwissenschaften, Institut für Angewandte Stochastik und Operations Research
Technische Universität Clausthal

Das Virtuelle Mikroskop – Visualisierung und Inspektion der Geometrie von Partikelschüttungen

Feng Gu, Michael Kolonko, Thorsten Grosch

Zusammenfassung

Viele Materialien und Stoffe sind aus Partikeln aufgebaut, vom Beton bis zur Tablette. Manche Eigenschaften der fertigen Stoffe sind bereits stark durch die geometrischen Eigenschaften der Partikelmischungen bestimmt. Bei Beton ist z.B. die Raumausfüllung der trockenen Mischung, also das Verhältnis von Behältergröße zum Volumen der enthaltenen Partikel, ausschlaggebend für die Festigkeit des Betons nach der Aushärtung. In anderen Anwendungen, etwa bei der Herstellung von Schäumen, spielen Verteilung und Gestalt der Zwischenräume zwischen den ‚Partikeln', die in diesem Falle Hohlräume sind, eine entscheidende Rolle für die Eigenschaften des Materials.

Das Projekt „Virtuelles Mikroskop" steht in engem Zusammenhang mit dem parallel bearbeiteten Projekt „RaSim". Hier wurde für Partikelmischungen eine parallele Collective-Rearrangement Simulation auf der Grafikkarte (GPU) entwickelt. Mit deren Hilfe können mehrere Millionen unterschiedlich großer, kugelförmiger Partikel mit interaktiver Geschwindigkeit bewegt werden [1]. Dabei werden die Kugeln an zufällige Startpositionen in einem Container gesetzt und stoßen sich danach bei Überlappung solange gegenseitig ab, bis ein praktisch konvergierter, nahezu überlappungsfreier Zustand erreicht ist. Um die Qualität dieser iterativen Simulation einschätzen zu können, wurden im Projekt „Virtuelles Mikroskop" spezielle, dreidimensionale Visualisierungen entwickelt. Diese können durch den Einsatz von sogenannten Billboards mehrere Millionen Kugeln unterschiedlicher Größen mit interaktiver Geschwindigkeit darstellen (ca. 60 Bilder pro Sekunde). Dabei werden die Kugeln nur durch Quadrate gezeichnet, die

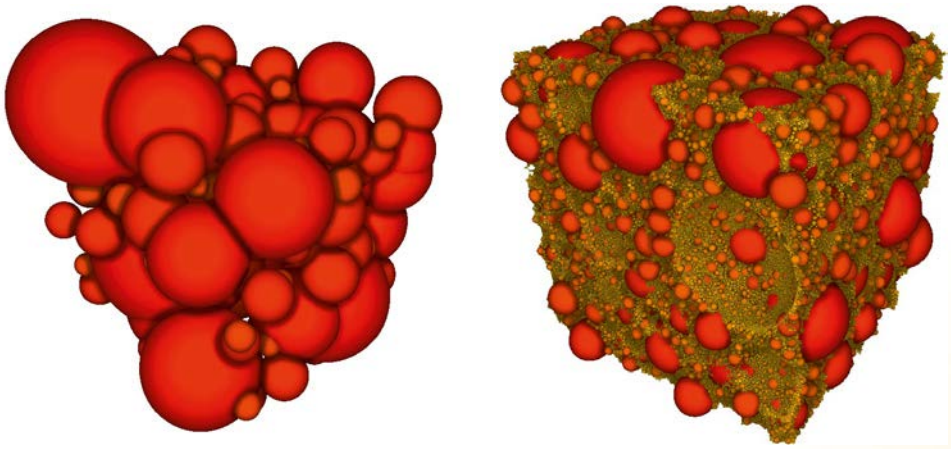

Abbildung 1: Interaktive Darstellung von 128 Kugeln (links) und 1 Million Kugeln (rechts) bei einer Geschwindigkeit von ca. 60 Bildern pro Sekunde. Der Kontaktbereich der Kugeln wird durch Screen-space Ambient Occlusion abgedunkelt dargestellt. Große Kugeln werden rot gezeichnet, kleine Kugeln sind gelb. Im rechten Bild ist der periodische Rand erkennbar: Einige Kugeln auf der Rückseite verursachen die Einbuchtungen auf der Vorderseite. Verbliebene Überlappungen zwischen den Kugeln sind bei dieser einfachen Darstellung aufgrund der gegenseitigen Verdeckung der Kugeln praktisch nicht erkennbar.

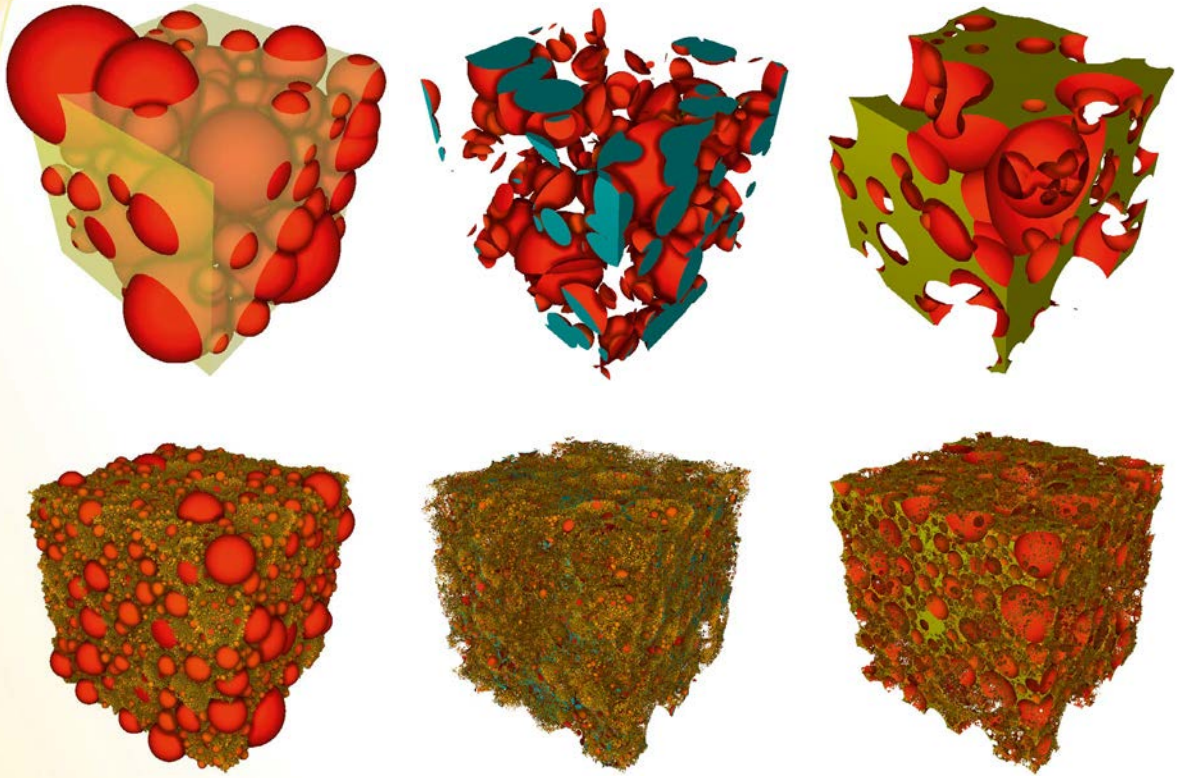

Abbildung 2: Collective Rearrangement Simulationen mit 128 Kugeln (obere Zeile) und einer Million Kugeln (untere Zeile). In der linken Spalte sind die Kugeln im Container (gelb transparent) zu sehen. In der mittleren Spalte werden die Überlappungen der Kugeln in rot dargestellt. Die blauen Bereiche sind dabei Überlappungen am Rand des Containers. Aufgrund der gegenseitigen Verdeckung der Kugeln sind diese Überlappungen in der normalen Darstellung (links) praktisch nicht zu sehen. In der rechten Spalte sind die Freiräume zu sehen.

pro Pixel wieder auf Kugelform gebracht werden. Weiterhin wird Screen-space Ambient Occlusion eingesetzt: Hier werden die Kontaktbereiche der Kugeln leicht abgedunkelt, sodass die räumliche Anordnung der Kugeln besser wahrgenommen werden kann (Abbildung 1). Die Verdeckung wird dabei pro Pixel im Bild durch die 3D-Positionen der Nachbarpixel abgeschätzt [2].

Schwerpunkt des Projekts „Virtuelles Mikroskop“ ist die interaktive Darstellung der aktuellen Überlappungsbereiche der Kugeln sowie der noch existierenden Freiräume im Container. Dies ist aufgrund der iterativen Simulation notwendig, die nicht notwendigerweise konvergiert. Gerade beim Einsatz vieler Kugeln kann es passieren, dass die Simulation in bestimmten Bereichen nicht überlappungsfrei wird. Durch parallele Programmierung auf aktueller Grafikhardware können diese Überlappungen und Freiräume für eine Million Kugeln mit einer Geschwindigkeit von 20 – 60 Bildern pro Sekunde dargestellt werden [3] (Abbildung 2). Kernidee ist hierbei der Einsatz sogenannter Pixel-Linked-Lists [4], die es erlauben, diese Bereiche pixelgenau zu zeichnen. Der Benutzer kann somit praktisch während der Simulation die aktuellen Zwischenergebnisse betrachten, d.h. die Bewegung der Kugeln sowie den Abbau der Überlappungsbereiche. Somit kann die Qualität der Simulation besser einschätzt werden als durch reine Zahlenwerte, die z.B. nur die durchschnittliche Überlappungsrate der Kugeln angeben. Die entwickelten, dreidimensionalen Visualisierungen können dabei einen besseren Eindruck der Form

der Überlappungsbereiche bzw. Freiräume geben als Standardtechniken, wie z.B. zweidimensionale Schnittebenen durch das Volumen. Weiterhin kann der Blickwinkel interaktiv verändert werden und ein zoomen in die Kugelpackung ist möglich. Auch eine Volumenberechnung der Überlappungen und Freiräume ist möglich. Schließlich ist ein Eingreifen durch einen virtuellen „Rührstab" möglich, mit dem der Benutzer nicht-konvergierte Bereiche manuell auflösen kann.

Die entwickelten Visualisierungen können auch in folgendem Video eingesehen werden: http://www2.in.tu-clausthal.de/~cgstore/publications/2017_Gu_VMV.mp4

Die aktuelle Forschung im Projekt beschäftigt sich mit der Simulation und Visualisierung von nicht-kugelförmigen Partikeln. Dies kann z.B. durch Zusammensetzung eines Partikels aus mehreren, starr verbundenen Kugeln erfolgen. Dies erhöht den Simulationsaufwand, da sowohl die Kollision der Partikel als auch die Reaktion bei Überlappung mit Translation und Rotation komplizierter wird. Weiterhin wird neben dem rein rasterisierungs-basierten Ansatz ein Ray Tracing-basierter Ansatz zur interaktiven Darstellung noch größerer Partikelmengen verfolgt. Für einen schnellen Strahltest wird hierfür eine schnelle, dynamische veränderliche Hierarchie der Kugeln entwickelt.

Literatur

[1] Zhixing Yang, Feng Gu, Thorsten Grosch, and Michael Kolonko. Accelerated Simulation of Sphere Packings Using Parallel Hardware. Simulation Science(2017), Springer

[2] Montani C., Tarini M., Cignoni P. Ambient occlusion and edge cueing for enhancing real time molecular visualization. IEEE Transactions on Visualization and Computer Graphics 12 (2006), 1237–1244.

[3] Feng Gu, Zhixing Yang, Michael Kolonko and Thorsten Grosch. Interactive Visualization of Gaps and Overlaps for Large and Dynamic Sphere Packings. Vision, Modeling and Visualization (VMV), 2017

[4] Yang J. C., Hensley J., Grün H., Thibieroz N. Real-time concurrent linked list construction on the GPU. In Proceedings of the 21st Eurographics Conference on Rendering (Aire-la-Ville, Switzerland) 2010

Projektdaten

Das Projekt wird seit September 2016 vom SWZ mit insgesamt 0,5 TV-L E13 Stellen an dem Standort Clausthal gefördert. Beteiligte Wissenschaftler sind:

Prof. Dr. Michael Kolonko
Arbeitsgruppe Stochastische Optimierung, Institut für Angewandte Stochastik und Operations Research
Technische Universität Clausthal

Prof. Dr. Thorsten Grosch
Arbeitsgruppe Graphische Datenverarbeitung und Multimedia
Institut für Informatik
Technische Universität Clausthal

Feng Gu, M.Sc.
Arbeitsgruppe Graphische Datenverarbeitung und Multimedia
Institut für Informatik
Technische Universität Clausthal

Druckinduzierte Festkörperphasenübergänge und plastische Verformung in Eisen-Kohlenstoff-Legierungen

Hoang-Thien Luu, Nina Gunkelmann

Die Analyse von Materialien unter hohen Drücken ist sowohl wichtig, um astronomische oder geophysikalische Prozesse zu verstehen, als auch von Interesse für technologische Anwendungen. So können durch Druckbelastung neue Materialien mit verbesserten Eigenschaften wie erhöhter Festigkeit entstehen.

Eisen ist eines der technologisch relevantesten Materialien und bildet die Basis moderner Stähle. Es weist einen Phasenübergang bei einem Druck von 13 GPa zu einer anderen Kristallstruktur auf: von bcc (kubisch basiszentriertes Gitter) nach hcp (hexagonal dichtest gepacktes Gitter). Bei einem bcc-Gitter kann man die periodische Struktur in kubische Elementarzellen aufteilen, bei denen sich die Atome auf den Ecken sowie in der Mitte eines Würfels befinden. Die Grundfläche der hexagonal dichtest gepackten Struktur ist ein Sechseck. Außerdem sind die Lücken zwischen den Atomen möglichst klein, das Gitter ist dichtest gepackt.

Mittels Experimenten konnten Erkenntnisse über die Phasenumwandlungen in Eisen bei hohen Drücken gewonnen werden. Experimentell können diese hohen Drücke hergestellt werden, indem mit Hilfe eines Lasers die Oberfläche des Metalls verdampft wird und der resultierende Verdampfungsdruck als Stoßwelle durch die Probe läuft (siehe Abbildung 1).

Da der Phasenübergang experimentell jedoch sehr schnell abläuft, werden Simulationen benötigt, um den Zusammenhang zwischen der Phasentransformation und den physikalischen Eigenschaften zu analysieren. Außerdem ist die Herstellung extrem hoher Drücke mit dem Computer viel kostensparender als es im Labor je möglich wäre.

Molekulardynamiksimulationen (MD) sind hier ein nützliches Tool, um diese Vorgänge auf kleinster Skala mit hoher Zeitauflösung zu beschreiben. Diese Simulationen haben den Vorteil, dass

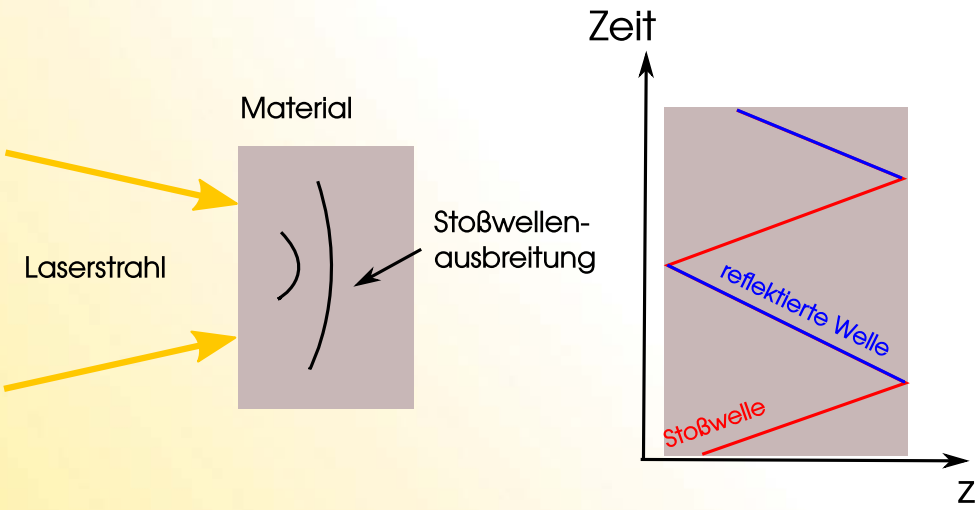

Abbildung 1: Schematischer Aufbau eines Laserstoßexperiments.

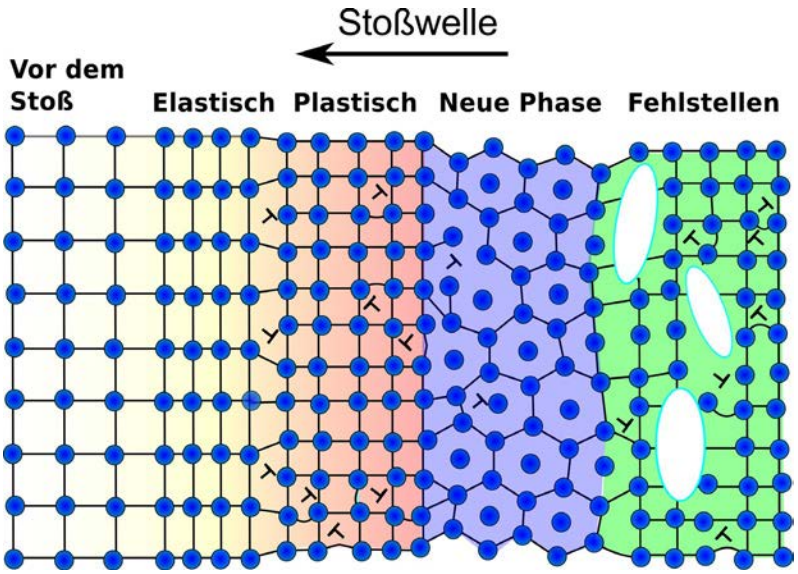

Abbildung 2: Typisches Profil einer Stoßkompression.

sie auf ähnlichen Zeitskalen ablaufen wie die beschriebenen Experimente.

Die Molekulardynamik beruht auf den Newtonschen Bewegungsgleichungen, insbesondere dem zweiten Newtonschen Gesetzes.

Ein typisches Profil eines Materials unter Stoßkompression durchläuft mehrere Zustände, welche die physikalischen und mechanischen Eigenschaften des Metalls veranschaulichen. Zuerst tritt elastische Kompression auf, gefolgt von plastischen Effekten, d.h. dauerhafter Verformung, und schließlich kann eine sogenannte polymorphe Phasenumwandlung erfolgen. Dies bedeutet, dass eine Phasenumwandlung zu verschiedenen Kristallstrukturen bei identischer chemischer Zusammensetzung stattfindet. Außerdem können sich Fehlstellen bilden. Eine schematische Darstellung kann Abbildung 2 entnommen werden.
Mit Hilfe von MD-Simulationen konnte die 3-Wellen-Struktur aus elastischer Kompression, plastischer, d.h. dauerhafter Verformung und Phasentransformation in polykristallinem Eisen bestimmt werden. Das Verständnis dieses Phasenübergangs ist wichtig, um verbesserte Materialien zu erzeugen, die bei Umgebungsbedingungen stabil sind. Hierfür wurde ein Wechselwirkungspotential generiert, welches das Wechselspiel von Umwandlung und plastischer Verformung in Eisen gut beschreibt.

Obwohl Eisen-Kohlenstoff die Grundlage des martensitischen Stahls bildet und Kohlenstoff einen entscheidenden Einfluss auf die elastischen und plastischen Eigenschaften des Metalls hat, ist dessen Materialverhalten unter Hochdruckkompression bisher kaum erforscht.

In diesem Projekt wurde das oben beschriebene Potential mit verschiedenen Potentialen für die Wechselwirkung zwischen Eisen und Kohlenstoff gekoppelt. Die mechanischen Eigenschaften von Eisen-Kohlenstoff-Kristallen wurden unter Hochdruckkompression untersucht. Damit konnte die 3-Wellen-Struktur aus elastischer und plastischer Welle und Phasentransformation bestimmt werden. Der Kohlenstoff führt in Übereinstimmung mit Experimenten zu einem erhöhten Übergangsdruck.

Projektdaten

Das Projekt wird seit September 2017 vom SWZ mit insgesamt einer W1 und 0,5 TV-L E13 Stellen an dem Standort Clausthal gefördert. Beteiligte Wissenschaftler sind:

Jun.-Prof. Dr.
Nina Gunkelmann
Arbeitsgruppe Computational
Material Sciences
Institut für Technische Mechanik
Technische Universität Clausthal

Hoang-Thien Luu
Arbeitsgruppe Computational
Material Sciences
Institut für Technische Mechanik
Technische Universität Clausthal

Simulation of Materials

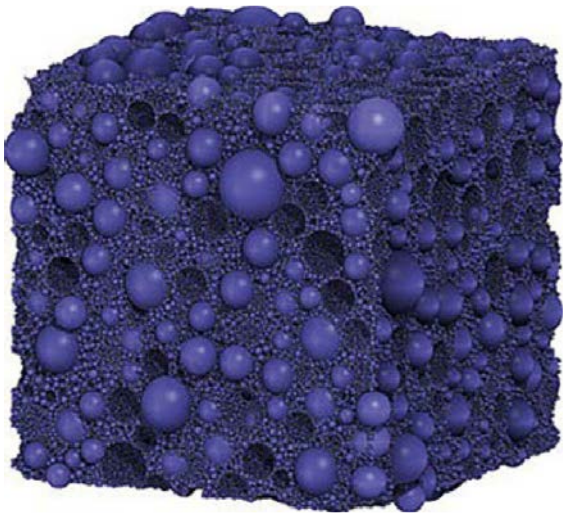

The advances in Materials Science and both related Engineering disciplines as well as Natural Sciences with focus on considering material properties always have defined the state of development of a society. Materials Science is one of the key topics in the German industrial landscape, which provides the basis for many innovations in other areas of industry.

In Materials Science and related disciplines, a highly interdisciplinary approach is already established, which is divided into the strongly overlapping areas of "Computational Materials Science", "Computational Physics", "Computational Mechanics" and "Computational Chemistry". Simulations have been developed into a living and research-oriented scientific branch in Material Science and their neighboring Natural Sciences, which is also increasingly perceived and actively promoted by the industry.

Problems in Materials Sciences and material-oriented Energy Sciences are very diverse and are typically based on multiple length and time scales. Furthermore, different physical reasons are apparent, such as temperature, radiation, electromagnetic and mechanical fields. Therefore, the field of material simulations is characterized by a variety of different simulation methods, which are tailored to the respective problem class:

On the smallest scale, atomic processes are simulated parameter-free on the basis of natural laws in so-called ab-initio simulations. These quantum mechanics methods usually require high-performance computers, but allow achieving a variety of quantitative results. Such a program package is developed and distributed in Clausthal.

On the macroscopic length scale, the material is considered to be a continuum, whose behavior is determined by material models. The material parameters, which occur in the models, have to be identified at specific experiments using optimization procedures. Since the simulation techniques are largely uniform, one concept is to draw on commercial program packages. On the other hand, these programs have limitations, so that one major goal lies in the development of new numerical methods. The main interest in applying commercial programs is the modeling of the problem, the determination of the parameters as well as validating results. In the case of code developing, the interest are seen in the analysis, efficiency and stability, and the verification of the codes.

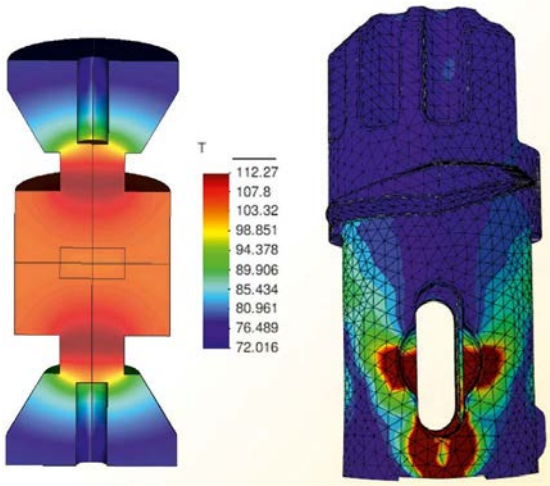

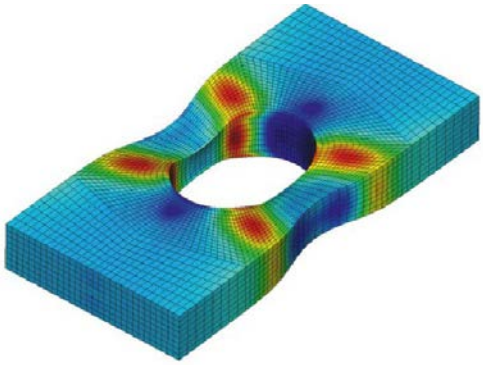

Between these poles, there are a number of other methods. Some will be listed as following: stochastic simulations, molecular dynamics, phase field methods, microstructural simulation of dislocation, simulation of chemical processes, etc.

Thus, one of the "Grand Challenges in Computational Materials Science" is the multiscale simulation, which ideally extends from ab initio simulation to the simulation of forming processes and manufacturing processes. On the one hand, this challenge is addressed by the fact that simulation parameters are deliberately transmitted from the atomic level through microscopic computations to the macroscopic simulation. On the other hand, different simulation methods are integrated into a uniform simulation environment in order to describe effects in which different length and time scales can no longer be decoupled. These activities require the cooperation of different scientific disciplines and benefit from mergers as planned at Simulation Science Center.

In contrast to several other applications of simulation methods, simulations in the field of Material Science are very often characterized by the fact that they have to exploit all available information processing resources to their limits in order to achieve usable results. Questions of algorithmic complexity and efficiency of implementations are therefore of crucial importance for the progress of the simulation methods in this area.

Coupling of multi-physical processes for the simulation of gas wells

Stefan Hartmann, Leonhard Ganzer, Jithin Mohan, Birger Hagemann

Abstract

The storage of hydrogen gas from electrolysis of water in underground caverns or porous underground formations is a viable method for storing excess energy. During periods of peak demand this stored hydrogen can be utilized to cater to the surplus energy demands. The simulation of the injection and production process with the help of open source tools is the topic of interest in this project report. Owing to the interplay of multiple physical fields in different regions using different and adapted solution schemes in each region, a coupled solution approach is required. Before developing the entire coupling scheme for simulating the in- and outflow through a gas-well, several sub-problems have been considered: first, the gas flow in the production region through the perforations in the piping is studied showing a particular flow behavior. Second, the thermomechanical behavior of the casing due to changing temperature and pressure conditions in the injection and production period is considered to obtain a first insight into the reliability (integrity) of the solid part close to the production region of the gas-well. Third, the flow behavior through the perforations in and out of the geological formation is analyzed using the open source porous medium flow solver DuMux. Fourth, a one-dimensional pipe flow problem is treated for coupling the injected gas through a pipe with the porous media solver in the underground storage. Finally, the entire equations representing the implicit time discretization schemes of the overall coupled system together with the investigation of the resulting coupling schemes combined with acceleration techniques are studied.

1. Objectives

Klaus et al. (2010) show that new energy concepts are of basic interest for storage in periods of too high energy production of renewable energy sources. In this case, there are several concepts proposed. One concept is to store hydrogen – resulting from electrolysis of water – in the geological sub-surface, (Kepplinger et al., 2011; Sherif et al., 2005). This is schematically sketched in Fig. 1. The surplus energy is drawn on to produce hydrogen, which is pressed through gas-wells into caverns of former gas reservoirs. To study the injection and production period (removal of the gas), a simulation tool for a realistic prediction is of particular interest.

There are several parts and regions of interest, which have an influence on the overall process. First, the gas flow into and out of the reservoir in the geological underground is very important, which can be treated by computational methods for porous media. We draw on DuMux (Flemisch et al., 2011) for such simulations. In this respect, several approaches and simulations have been done by (Class et al., 2009; Jiang, 2011; Hagemann et al., 2015; Feldmann et al., 2016). Since the integrity of the region close to the gas-well is of particular interest, the pressure and temperature cycles due to injecting and extracting the gas (production period) have an influence on the gas-well and the region around the gas-well. Thus,

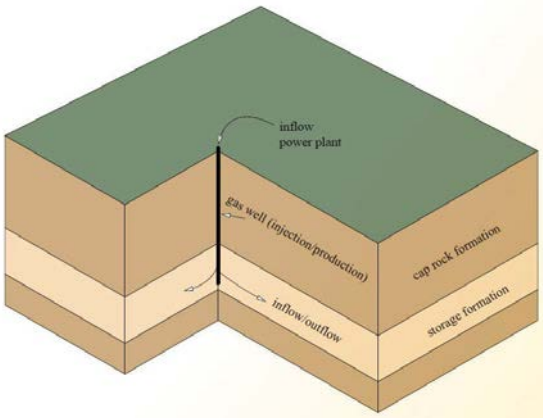

Figure 1: Underground energy storage

We gratefully acknowledge the financial support provided by the Simulation Center Clausthal - Göttingen. Furthermore, we would like to thank Lutz Müller-Lohse for providing some figures and results of a project report.

a numerical coupling tool to simulate the gas-well under temperature and pressure cycles, the gas-flow in the gas-well itself, the flow behavior close to the perforation in the gas-wells production region, which are small holes in the piping, cement and rock and the flow in the reservoir in the production and the injection periods.

2. Methods

The physical problem of injection/production of hydrogen gas to and from the surrounding geological formations can be interpreted as a surface coupling problem between three different regions. These are the fluid region comprising the conduit through which gas flow occurs, the solid region consisting of the different casings namely the surface, intermediate, and the production casings, as well as the rock region embracing the reservoir for gas storage. The casings are made of steel along with the surrounding cement between casing layers and the packer material used to seal the gas flow to the surrounding water table, see Fig. 2. The interaction between these regions has to be analyzed to answer questions on the efficiency and integrity of the gas-well. The fluid flow in the conduit is subjected to mechanical as well as thermal loads. Similarly, the casing has to sustain mechanical loads due to the injection/production process, and also to hydro-dynamical, thermal and chemical effects from the surrounding geological formations. Thus the entire physical problem leads itself to a coupled problem where methods to solve the system are driven by procedures applied in fluid-structure interaction problems. However, the solution of the overall coupling problem requires the careful analysis of several sub-problems. The sub-problems to be considered are:

(1) The effect of thermo-mechanical loads on the casing and surrounding cement,
(2) the stationary gas flux through the conduit,
(3) the flow through the perforations in the production zone, and
(4) the computation of rock region with the flow source/sink of the gas-well.

The mathematical description of each individual physical field in the sub-problems mentioned above is given by partial differential equations (PDE). These PDEs describe the variations of the primary physical quantities in space and time. To solve the entire set of PDEs, we follow the method of vertical lines as discussed subsequently.

2.1. Method of Vertical Lines.

The method of vertical lines is a technique for solving PDEs. First, the spatial discretization is carried out leading in each sub-problem – in dependence of the formulation – to systems of algebraic equations, ordinary differential equations (ODEs), or differential-algebraic equations (DAE). The second step of the method of vertical lines is to solve the resulting system of equations by non-

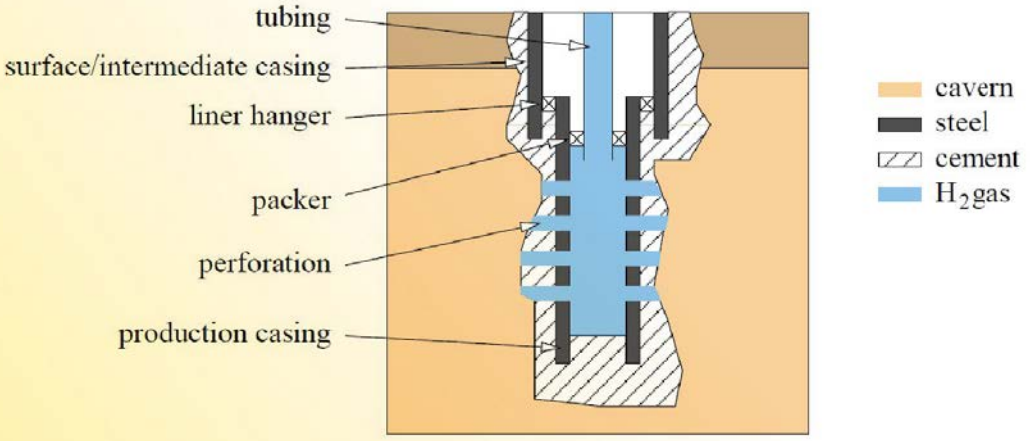

Figure 2: Principal sketch of production casing

linear solvers, or solution techniques to solve ODEs or DAEs, see, for example, (Großmann and Roos, 1994). For the sub-problems involved in the injection/production cycle in the gas-well, the PDEs are spatially discretized either by finite elements (FEM), or by finite volumes (FVM). Furthermore, we have coupling conditions between each sub-problem (sub-region) in the sense of surface coupling.

For problems of thermo-mechanics of the solid part (casing), the discretized weak form of the balance equations (quasi-static equilibrium conditions) gives the algebraic part whereas the transient heat equation represents the differential part of the DAE-system. Furthermore, when dealing with constitutive models of evolutionary-type, as it is the case for models of viscoelasticity or viscoplasticity (metal or cement plasticity), additional differential equations may arise. For the fluid solver, the application of mass balance, balance of linear momentum and energy balance leads to a pure ODE-system after spatial discretization. For the rock region, the balance laws also results in a system of ODEs. However, in the fluid as well as rock regions assumptions of incompressibility and steady flows may give rise to DAE-systems. Additional coupling constraints may also be necessary to be fulfilled at interfaces, which yield to further side conditions. The resulting DAE-systems for the three regions can be summarized as follows,

$$\begin{aligned} \boldsymbol{g}_S(t, \boldsymbol{u}_S, \dot{\boldsymbol{u}}_S, \boldsymbol{\Theta}_S, \dot{\boldsymbol{\Theta}}_S, \boldsymbol{\lambda}_S, \boldsymbol{q}, \dot{\boldsymbol{q}}) &= \boldsymbol{0}, \\ \boldsymbol{g}_F(t, \boldsymbol{\rho}_F, \dot{\boldsymbol{\rho}}_F, \boldsymbol{\Theta}_F, \dot{\boldsymbol{\Theta}}_F, \boldsymbol{v}_F, \dot{\boldsymbol{v}}_F) &= \boldsymbol{0}, \\ \boldsymbol{g}_R(t, \boldsymbol{p}_R, \boldsymbol{\Theta}_R, \dot{\boldsymbol{\Theta}}_R, \boldsymbol{v}_R, \dot{\boldsymbol{v}}_R) &= \boldsymbol{0}, \end{aligned} \tag{1}$$

where the result has to fulfill the side-conditions (interface coupling)

$$\begin{aligned} \boldsymbol{g}_{SF}(t, \boldsymbol{\Theta}_S, \boldsymbol{\lambda}_S) &= \boldsymbol{0}, \\ \boldsymbol{g}_{FR}(t, \boldsymbol{\rho}_F, \boldsymbol{\Theta}_F, \boldsymbol{v}_F, \boldsymbol{p}_R, \boldsymbol{\Theta}_R) &= \boldsymbol{0}, \\ \boldsymbol{g}_{SR}(t, \boldsymbol{\Theta}_S, \boldsymbol{\lambda}_S, \boldsymbol{p}_R, \boldsymbol{\Theta}_R) &= \boldsymbol{0}. \end{aligned} \tag{2}$$

The subscripts S, F and R represent the variables of the solid, fluid, and the rock regions, respectively. The interface conditions have two indices characterizing the interface partners.

After the spatial discretization, an efficient implicit time integrator has to be drawn on yielding a system of coupled non-linear equations. This system has to be solved at every point in time of the time integrator. We consider solvers for the aforementioned regions that are based on a Backward-Euler method, which might lead to first-order accuracy for the overall DAE-system, see (Hairer and Wanner, 1996). It has been shown by (Hairer et al., 1993 and Hairer and Wanner, 1996) that singly, diagonally implicit Runge-Kutta methods are appropriate high-order time integration schemes, which have the advantage of time adaptivity (step-size selection) without additional computational costs, and which can be chosen for sub-problem solvers, which are based on Backward-Euler implementations, see discussion in (Rothe et al., 2015a,b). The resulting coupled systems of non-linear equations for the three regions after a time integration step is given by,

$$\begin{aligned} \boldsymbol{G}_{SF}(\boldsymbol{\Theta}_{Sn+1}, \boldsymbol{\lambda}_{Sn+1}) &= \boldsymbol{0}, \\ \boldsymbol{G}_{FR}(\boldsymbol{\rho}_{Fn+1}, \boldsymbol{\Theta}_{Fn+1}, \boldsymbol{v}_{Fn+1}, \boldsymbol{p}_{Rn+1}, \boldsymbol{\Theta}_{Rn+1}) &= \boldsymbol{0}, \\ \boldsymbol{G}_{SR}(\boldsymbol{\Theta}_{Sn+1}, \boldsymbol{\lambda}_{Sn+1}, \boldsymbol{p}_{Rn+1}, \boldsymbol{\Theta}_{Rn+1}) &= \boldsymbol{0}. \end{aligned} \tag{3}$$

here, written by an Backward-Euler implementation, and the side conditions read

$$\begin{aligned} \boldsymbol{G}_{SF}(\boldsymbol{\Theta}_{Sn+1}, \boldsymbol{\lambda}_{Sn+1}) &= \boldsymbol{0}, \\ \boldsymbol{G}_{FR}(\boldsymbol{\rho}_{Fn+1}, \boldsymbol{\Theta}_{Fn+1}, \boldsymbol{v}_{Fn+1}, \boldsymbol{p}_{Rn+1}, \boldsymbol{\Theta}_{Rn+1}) &= \boldsymbol{0}, \\ \boldsymbol{G}_{SR}(\boldsymbol{\Theta}_{Sn+1}, \boldsymbol{\lambda}_{Sn+1}, \boldsymbol{p}_{Rn+1}, \boldsymbol{\Theta}_{Rn+1}) &= \boldsymbol{0}. \end{aligned} \tag{4}$$

The consideration of the side conditions can be treated using a projection technique, see (Hairer et al., 2002) or (Hartmann et al., 2008).
The solution techniques for such coupled non-linear systems involve either a monolithic or a partitioned approach. Owing to the flexibility to treat different solvers independently, a partitioned approach is favored, see, for example, (Rothe et al., 2015a). Here, non-linear GaussSeidel methods treated in detail in (Erbts and Düster, 2012; Erbts et al., 2015; Wendt et al., 2015a; Degroote et al., 2010; Joosten et al., 2009; Wood et al., 2010), which are suitable using acceleration schemes to improve efficiency and stability. A brief overview of the solution of systems of coupled non-linear equations is detailed below.

2.2. Solving Coupled Systems of Non-linear Equations

There are two basic classes of methods to treat coupled problems, namely the monolithic and the partitioned approach. In the monolithic approach, all equations from the different physical fields are solved simultaneously, and in the partitioned approach the individual systems are computed separately, commonly by specialized solvers. Although, the monolithic procedure is easier in its implementation, where the full set of non-linear equations from all contributing equations is solved with the help of a Newton-Raphson method or a similar procedure, it has disadvantages when dealing with multiple specialized black-box solvers, see (Rothe et al., 2015a) and the literature cited therein. Thus, to solve the coupled problem of injection/production, where different solvers are applied, the partitioned approach is favored, so that the systems of non-linear equations arising from each individual sub-field are treated individually with an appropriate data exchange.

Non-linear block Gauss-Seidel schemes have been utilized in a number of publications, see, for example, (Degroote et al., 2009) for solving fluid-structure interaction problems (FSI) or (Rothe et al., 2015a) and (Erbts et al., 2015) for thermo-mechanical and electro-thermomechanical problems, respectively. Sciandrone (2000) studied the convergence behavior of the non-linear block Gauss-Seidel method under convex constraints. The convergence behavior of the method was studied for an FSI model problem by Joosten et al. (2009). The benefit of adding relaxation strategies to the method is also demonstrated. To improve the fix-point behavior of the scheme, acceleration scheme are of major interest. Then, an improved stability and much better convergence properties is obtained, see, in this respect (Nobile, 2005) and (Wall, 2006) as well. The incorporation of acceleration methods helps in obtaining a better estimate to the solution increment with the previously computed solution vectors or its differences. The enhanced solution update is then utilized as the initial guess for the next Gauss-Seidel iteration. The algorithm formulation of the non-linear block Gauss-Seidel scheme with acceleration for two sub-problems (or solvers) is compiled in Tab. 1.

Table 1: Block Gauss-Seidel with acceleration schemes

Given: $\boldsymbol{f}(\boldsymbol{x},\boldsymbol{y}), \boldsymbol{g}(\boldsymbol{x},\boldsymbol{y}), \boldsymbol{x}_0, \boldsymbol{y}_0$	
repeat	$m = 0, \ldots$
	Solve first system for $\tilde{\boldsymbol{y}}^{(m+1)}$
	Compute: $\boldsymbol{f}(\tilde{\boldsymbol{x}}^{(m)}, \tilde{\boldsymbol{y}}^{(m+1)}) = \boldsymbol{0} \quad \rightarrow \tilde{\boldsymbol{y}}^{(m+1)}$
	Solve second system for $\tilde{\boldsymbol{x}}^{(m+1)}$
	Compute: $\boldsymbol{g}(\tilde{\boldsymbol{x}}^{(m+1)}, \tilde{\boldsymbol{y}}^{(m+1)}) = \boldsymbol{0} \quad \rightarrow \tilde{\boldsymbol{x}}^{(m+1)}$
	Apply acceleration scheme for $m > 2$
	Update solution vector: $\boldsymbol{x}^{(m+1)}, \boldsymbol{y}^{(m+1)}$*. Choose method*
	I. Aitken type methods
	II. Quasi-Newton method
until	stopping criterion is fulfilled

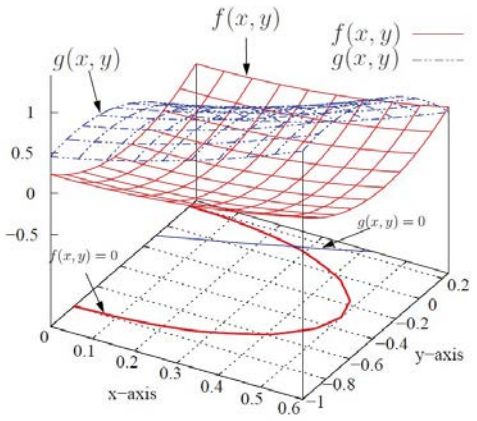

(a) Two functions and their graphical solution (contour lines for f =0 and g=0)

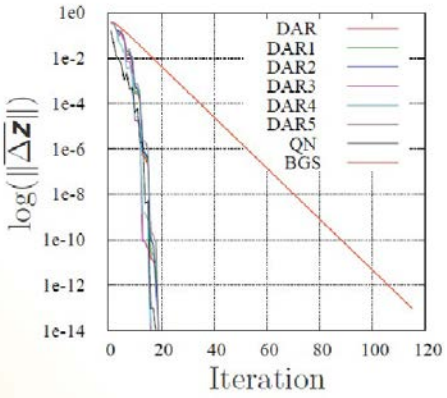

(b) Performance comparison for different acceleration methods (DAR Dynamic Aitken Relaxation, QN Quasi-Newton method, BGS block Gauss-Seidel scheme)

Figure 3: Model problem of two equations of two unknowns in (Schwarz, 1986)

two main acceleration methods namely, the Aitken-type acceleration schemes, see (Aitken, 1926; Graves-Morris, 1992; Jennings, 1971; Macleod, 1986; Zienkiewicz et al., 1988), as well as Quasi-Newton methods, see (Broyden, 1965; Nocedal and Wright, 1999; Dennis and Schnabel, 1996; Martinéz, 1994; Degroote et al., 2010), are studied within this context, see (Mohan and Hartmann, 2019). There, an example problem of Schwarz (1986) is chosen with two equations and two unknowns for comparison purposes of different solution techniques, see Fig. 3(a). Here, the example problem is divided into $f(x,y)=0$ and $g(x,y)=0$, where each function may be interpreted as a system of non-linear equations arising from some applied solver. The performance improvement for the model problem with application of acceleration methods is shown in Fig. 3(b), where the decadic logarithm of the norm of the solution increment $\bar{\Delta}z=\Delta z^{(m+1)}-\Delta z^{(m)}$ with $\Delta z^{(m+1)}=z^{(m+1)}-z^{(m)}$ and $z=\{x,y\}^T$ is plotted over the number of iterations. For details on the different acceleration methods and equations used, see (Mohan and Hartmann, 2019).

The standalone block Gauss-Seidel scheme converges to given tolerance of 10^{-14} for the difference of the solution vector Δz at 116 iterations. Drawing on the acceleration schemes, the convergence is obtained below 20 for all other acceleration schemes. Thus, a speed-up of approximately 5 is achieved. The different acceleration techniques show comparable performance. However, it has to be noted that the speed-up is specific to the model problem. It has been shown in recent studies that Quasi-Newton methods shows better performances in comparison to Aitken-type relaxation schemes for practical physical problems, see (Radtke et al.,2016, 2017; Ramiere and Helfer, 2015; Wendt et al., 2015b).

3. Numerical Examples of Partial Fields

In the following, we summarize several sub-problems apart from the pure overall numerical scheme of Section 2. These are the thermo-mechanical treatment of the piping consisting of steel and cement layers, the gas flow in the piping perforations, the entire pipe flow problem of the gas, which is pressed for several hundred meters into the underground, and the reservoir modeling.

3.1. Thermo-mechanical Properties of Piping Systems

The gas-well is composed of several layers such as the surface casing, the intermediate casing and the production casing, which are typically made of steel as shown in Fig. 2. After completion, cement is filled between each casing layer to seal the piping and to protect the piping against mechanical and chemical agencies from the formation. Furthermore, it ensures that the ground water in other sub-ground layers is not contaminated. The casing can undergo different mechanical and thermal loads such as bending and torsion. The flow of compressed gas may lead to fluctuating internal pressure loads as well as thermal loads. Similarly, owing to the surrounding geological formations further external pressure and thermal loads occur. Thus, the thermomechanical analysis of casing components with the cement layers is of particular interest. Of course, the stress states within the casing made of different layers can be obtained by finite element simulations. However, analytical solutions are of interest to obtain a faster insight into the physical problem. The underlying problem can be thought of as a multi-layered thick-walled tube. Here, we developed an analytical solution for thermo-elasticity for an axisymmetric multi-layered casing under the assumption of small strains, see (Hartmann et al., 2018). This approach has the advantage of both providing a more accurate understanding of the stress, strain, and temperature distribution in the layers concerned as well as providing a verification solution for other numerical methods. An analytical solution for a single layer under pure mechanical part is given in (Lehmann, 1984), under the assumptions of small strains and linear, isotropic elasticity. An extension to large strains in treated numerically in (Yosibash et al., 2007). Extension to multi-layered distinct elastic layers is discussed by several authors, see, for example, (Clifton et al., 1976; Yeh and Kyriakides, 1986; Bourgoyne, 1986; Bai et al., 1997; Shildip et al., 2015). For the case of an additional axial deformation this is summarized in (Hartmann and Gilbert, 2002). Several (drilling, production, installation) periods are investigated in (De Simone et al., 2017), which draw on analytically approximated results of Bradley (1979) and Fjær et al. (2008), but omitting the temperature differences in the rock formation and the internal gas

as well. Similarly to Yin and Gao (2014), Li et al. (2010) applied unequal horizontal stresses, but treated the temperature influence by an approximation – constant over the wall thickness. To provide an analytical approximation in situations with thin-walled wells, in particular, the casing itself, Teodoriu et al. (2010) developed a model with the assumptions of vanishing axial strains $\varepsilon z \approx 0$, Barlow's formulas of thin-walled tubes, and a constant mean temperature increase. These assumptions are compared to finite element simulations. Further investigations have been provided for these high temperature and high pressure conditions by (Ugwu, 2008; Bai et al., 2015a,b).

An analytical solution for the stationary thermo-mechanically coupled problem under small strains is developed for one-sided coupling. One-sided coupling implies that the stress state is coupled with the temperature whereas the heat equation is independent of the deformation. The equations for the multi-layered thick-walled tube with distinct material layers were derived under the assumption of constant deformation and temperature in the axial direction. The analytical expression is compared with the finite element simulations for the two and four layered examples above and below the packer for a representative gas-well, see Fig. 2. The governing equations and the detailed derivation is given in (Hartmann et al., 2018). The examples treated and the essential results are summarized below.

Examples

The analytical solution is utilized to determine the thermo-mechanical state of two regions above and below the packer for hydrogen injection period at a depth of 1000m from the ground level. In the examples treated, hydrogen is injected at constant pressure of 15MPa with a surface temperature of 15°C and volume flow rate of $2.97 m^3 s^{-1}$. The first region named the "two-layered casing part", which is below the packer, with the inner steel casing layer in contact with the injected hydrogen and the outer cement layer in contact with the surrounding rock formations. The second region namely the "four-layered casing part", which is above the packer with alternating steel and cement layers. In the "four-layered casing part", the inner steel casing is in contact with a static salt water column and the outer cement layer is in contact with the rock formations. The outside temperature at simulation depth is calculated to be 45°C where the effect of the geothermal gradient is considered. The radial pressure exerted on the outer casing wall by the geological formations is calculated to be approximately 10MPa with an average rock density of $2500 kgm^{-3}$ and a Poisson number of $v = 0.3$. The axial deformation on the top surface of the simulated geometry of thickness 10mm is calculated to be $w_{max} = 5 \times 10^{-3}$ mm and the no axial displacement is allowed for the bottom face. The radial distance to the inner steel casing

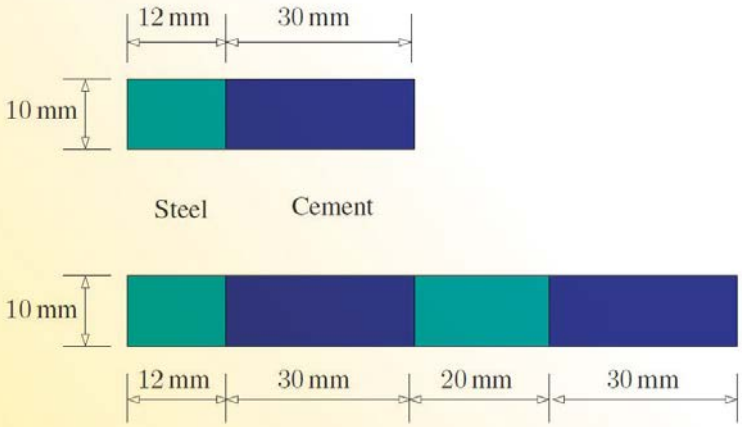

Figure 4: Top: Two-layered casing part; Bottom: Four-layered casing part

layer is taken to be 113mm for both cases. The simulated geometries for the two examples are shown in Fig. 4. The material properties for the steel and cement layers utilized for the analysis are summarized in Tab. 2.

Table 2: Material properties for steel and cement layers

Material property	Unit	Steel	Cement
Density ρ	kgm^{-3}	8000	1500
Young's modulus E	MPa	2×10^5	1.4×10^4
Poisson's ratio ν	[-]	0.2	0.35
Heat conductivity $\kappa\Theta$	$Wm^{-1}\,K^{-1}$	45	1.5
Heat expansion coefficient $\alpha\Theta$	K^{-1}	1.1×10^{-5}	1.3×10^{-5}

The temperature and pressure boundary conditions for the two-layered case are based on the properties of hydrogen gas where an ideal gas model is assumed. The internal pressure of gas is taken to be 15MPa and the temperature of 60°C is prescribed based on Ramey's equations, see (Ramey, 1962). For the four-layered casing example, the inner steel casing is in contact with the salt water column which is subjected to an internal pressure of 12MPa at a temperature of 47.3°C estimated with the steady heat equation. With these prescribed boundary conditions and material properties the thermo-mechanical state for the two examples were analyzed, see (Müller-Lohse, 2018). The essential results are summarized below.

The effect of temperature is analyzed on the stress state by comparing both the examples for purely mechanical case with the thermo-mechanical case. The radial distribution of the radial stress σr, circumferential stress σφ, axial stress σz, and resulting von Mises stress distributions σvM along with temperature Θ for the two-layered, see Fig. 5, and four-layered, see Fig. 6, casing examples are shown. Here, the dotted lines represent quantities in the pure mechanical case whereas the solid lines represent the thermo-mechanical case. In the two-layered example, the effect of thermal coupling can be seen predominantly in the axial stresses of the steel region where the difference is approximately 100MPa in the compressive sense. The circumferential stresses are only marginally affected by thermal coupling whereas the radial stresses remain largely unaffected. The axial stress has the dominant contribution which

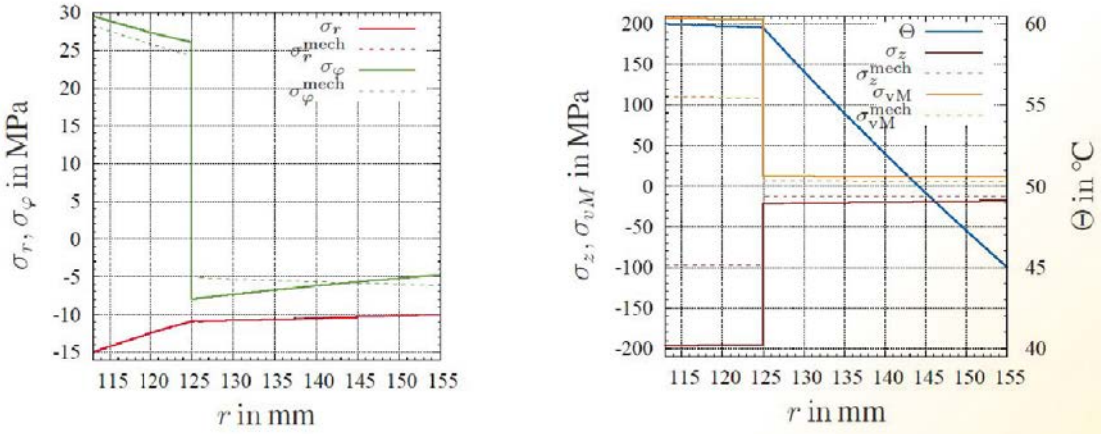

(a) Radial and circumferential stress distribution (b) Temperature, Axial and von Mises stress distribution
Figure 5: Two-layered casing part

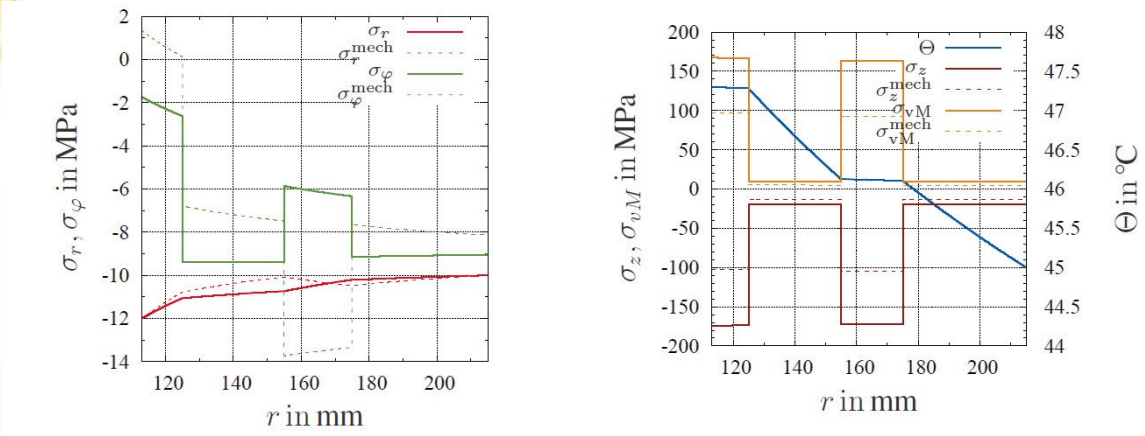

(a) Radial and circumferential stress distribution (b) Temperature, Axial and von Mises stress distribution
Figure 6: Four-layered casing part

is also reflected in the von Mises stress values. The temperature distribution shows the temperature decrease, which is largely limited to the cement layer owing to the larger heat conductivity of steel. The results for the four-layered case follow a similar trend as the two-layered example. The absolute values are lower owing to smaller differences in the pressure and temperature boundary conditions. The analytical solutions were also compared to axisymmetric simulation with FEM software ANSYS and simulation results showed good agreement with analytical solution for all the considered stress values, see (Hartmann et al., 2018).

3.2. Gas Flow at Perforations

The flow through the perforations is of interest to understand the local behavior of the flow. In order to store hydrogen in geological formations, the gas-well is perforated in this region near the cas-

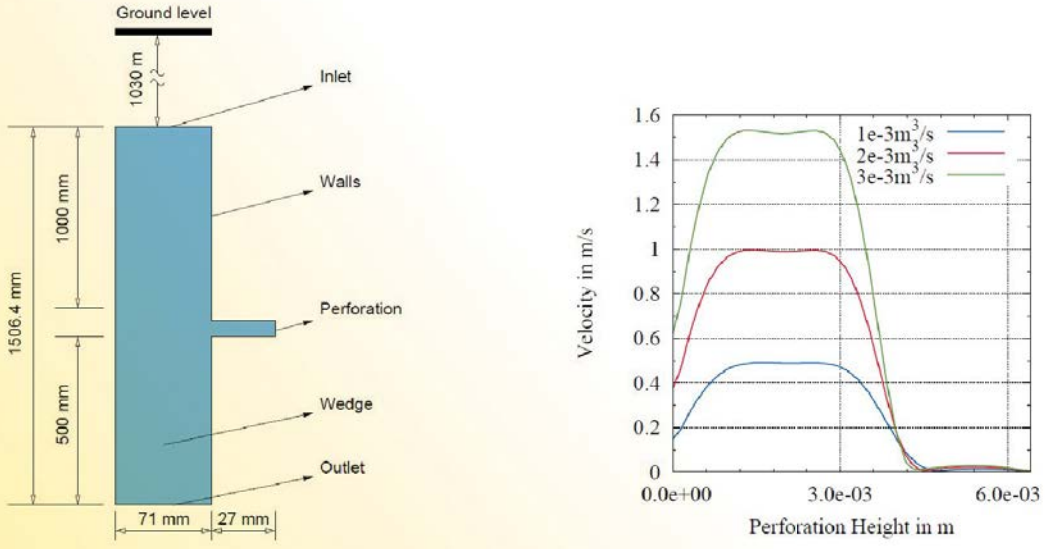

(a) Simulation geometry (b) Velocity distribution at outlet for varying injection flow rate
Figure 7: Effect of varying mass flow at perforation outlet

ing shoe. The number and size of such perforations varies as per the size of the well and the amount of storage or production required. The gas flow through the perforations is studied with help of the open source fluid solver Openfoam, which solves the Navier-Stokes equations, see (Greenshields, 2012b). The isothermal incompressible Navier-Stokes equations are solved with the help of the Semi-Implicit Method for Pressure Linked Equations (SIMPLE) algorithm as described by (Ferziger and Peric, 2012). Here, an explicit equation for pressure is obtained by taking the divergence of the discretized balance of linear momentum which is then substituted in the continuity equation for the incompressible case. The solution strategy is detailed in (Greenshields, 2012a).

Simulation Model and Results

The gas-well comprises multiple perforations. However, in order to get an insight into the flow behavior through the perforations, a single perforation with a cumulative cross section area of all the perforations is utilized for the simulation as seen in Fig. 7(a). The single perforation has a total height of 6.4mm and has a length of 27mm which is consequently the length from the production tubing having a radius of 71mm until the outer cement casing.

The region of interest is at depth of approximately 1030m from the ground level. The simulation is carried out for the injection period where hydrogen gas is injected at 15MPa. The simulated domain is assumed to be axisymmetric and is prescribed with the help of wedge boundary conditions in Openfoam with a wedge angle of 4□. A noSlip boundary condition is applied on the walls, thereby neglecting the pipe friction losses. The flow rate is prescribed at the inlet and the outlet is prescribed a static pressure boundary condition. The effect of varying injection flow rates on the flow behavior in the perforation is studied. As seen in Fig. 7(b), the increase in flow rates results increased flow velocity at the outlet. The acceleration of flow at the output is proportional to the flow rate. The effect of compressibility and effect of turbulence can also be investigated. However, in the context of the overall coupling problem of injection and production, their contributions are seen to be negligible.

3.3. Pipe Flow

The flow of hydrogen through the conduit is of primary interest in the injection or production process through the gas-well. Hydrogen is a compressible gas and hence the analysis of flow implies the study of the compressible pipe-flow problem. The conduit through which the gas flows spans hundreds of meters into the earth whereas the radius of pipe itself is in the centimeter range. The gas is injected into an underground geological formations at depth of approximately 1000m through small perforations. This entails computationally intensive CFD simulations with large disparities in mesh scales. However, we are mainly interested in the flow properties at the region close to the perforations. The full resolution of the flow over the entire length of the conduit – although interesting – is not of primary focus, especially, when coupling with other codes is also taken into account. Thus, the full 3D-flow problem can essentially be simplified to a 1D-problem of the mean flow. A finite element solution for such a problem is feasible. The use of finite elements to solve flow problems have been studied by many authors. Viscous incompressible fluids are treated with penalty function formulation by Hughes et al. (1979) and with velocity pressure finite element method by Reddy (1993). Algorithm formulations for incompressible flows using Galerkin finite elements for incompressible flow problems is detailed in Gunzburger, (2012). Compressible flows with heat transfer is treated in (Reddy and Gartling, 2010; Lewis et al., 2004). The application of nodal discontinuous Galerkin methods for compressible flow problems is detailed in (Hesthaven and Warburton, 2007).

For the solution of 1D-pipe flow, we follow the method of vertical lines as detailed in Section 2.1, where a Galerkin finite element approach for the spatial discretization and temporal discretization with Backward-Euler or high-order diagonally implicit Runge-Kutta methods are used. The governing equations and finite element procedure is detailed below.

Governing equation and constitutive relations

The compressible fluid flow is fully described by the Euler equations comprising of the continuity,

balance of linear momentum and the balance of energy given by,

$$\begin{aligned} \dot{\rho} + \rho \mathrm{div}(\vec{v}) &= 0 \\ \mathrm{div}\mathbf{T} + \rho\vec{k} &= \rho\dot{\vec{v}} \\ -\mathrm{div}\vec{q} - \frac{\alpha}{\kappa}\Theta\mathrm{div}\vec{v} &= \rho c_\Theta \dot{\Theta} \end{aligned} \tag{5}$$

The constitutive models under the assumptions of perfect inviscid gas (Euler fluid) are given by $\mathrm{T}=-\rho\mathrm{I}$ with the pressure $\rho=\rho R\Theta$ and the heat flux vector $\vec{q}=-\kappa_\Theta$ gradΘ. Here, ρ defines the density, $\vec{v}$ the velocity vector, Θ the temperature, $\vec{\kappa}$ the acceleration of gravity, c_θ the heat capacity, α the coefficient of thermal expansion, κ_Θ the heat conductivity, and R the gas constant. The complete set of equations has to be solved for the primary variables $\rho,\vec{v}$, Θ with appropriate initial and boundary conditions,

$$\begin{aligned} \frac{\partial\rho}{\partial t} + v\frac{\partial\rho}{\partial x} + \rho\frac{\partial v}{\partial x} &= 0, \\ \rho\frac{\partial v}{\partial t} + \rho v\frac{\partial v}{\partial x} + \frac{\partial p}{\partial x} - \rho k &= 0 \\ \rho c_\Theta\frac{\partial\Theta}{\partial t} + \rho v c_\Theta\frac{\partial\Theta}{\partial x} + \frac{\alpha}{\kappa}\Theta\frac{\partial v}{\partial x} - \frac{\partial}{\partial x}\left(\kappa_\Theta\frac{\partial\Theta}{\partial x}\right) &= 0. \end{aligned} \tag{6}$$

The first step in the finite element procedure is to obtain the weak form of the equations resulting in the following set of equations,

$$\begin{aligned} \int_0^L \left(\frac{\partial\rho}{\partial t}\delta\rho + v\frac{\partial\rho}{\partial x}\delta\rho + \rho\frac{\partial v}{\partial x}\delta\rho\right)dx &= 0 \\ \int_0^L \left(\rho\frac{\partial v}{\partial t}\delta v + \rho c\frac{\partial v}{\partial x}\delta v - P\frac{\partial\delta v}{\partial x} - \rho k_x\delta v\right)dx + [P\delta v]_0^L &= 0, \\ \int_0^L \left(\rho c_\Theta\frac{\partial\Theta}{\partial t}\delta\Theta + \rho c_\Theta v\frac{\partial\Theta}{\partial x}\delta\Theta + \frac{\alpha}{\kappa}\Theta\frac{\partial v}{\partial x}\delta\Theta - q\frac{\partial\delta\Theta}{\partial x}\right)dx + [q\delta\Theta]_0^L &= 0. \end{aligned} \tag{7}$$

The insertion of shape functions for the particular fields and virtual fields lead to an ODE system, which is one part of the entire DAE-system in Section 2.1.

The 1D-pipe flow code will later be coupled to the DuMux solver to simulate the complete injection/production cycle.

3.4. Reservoir Modeling

The injection or production of hydrogen through a well will result in pressure changes and consequently in fluid flow within the porous storage rock. The spreading of the hydrogen gas and pressure perturbation depends on the geometry and hydraulic properties of the storage rock and the properties of the involved fluids. Hydrogen, having a very small density and low viscosity, could tend to spread laterally very far at the top of the storage formation. For the planned coupling between fluid flow in the well and in the reservoir a simplified reservoir model was setup by using the simulator DuMux (Flemisch et al., 2011).

Governing equations

The single phase isothermal gas flow within the porous storage rock is formulated by Darcy's law,

$$v = -\frac{K}{\mu}(\mathrm{grad}\, p - \rho g) \tag{8}$$

where v is the Darcy velocity in [ms–1], K is the permeability in [m^2], μ is the dynamic viscosity in [Pas], ρ is the fluid pressure in [Pa], is the fluid density in [kgm^{-3}] and g is the gravity acceleration in [ms^{-2}]. Inserting Darcy's law into the mass balance equation leads to the following continuity equation:

$$\phi\frac{\partial\rho}{\partial t} + \mathrm{div}\left(-\rho\frac{K}{\mu}(\mathrm{grad}\, p - \rho g)\right) = q, \tag{9}$$

where ϕ is the porosity of the storage rock and q is a source or sink term. DuMux uses a cell centered finite volume scheme for the spatial discretization and an Backward-Euler integration scheme for the time discretization step. The discretization results in a system of non-linear equations at each time-step as discussed in Section 2. The number of equations is equal to the number of grid cells. The multidimensional Newton method is applied to linearize and solve the equation system iteratively. The primary variable is the fluid pressure.

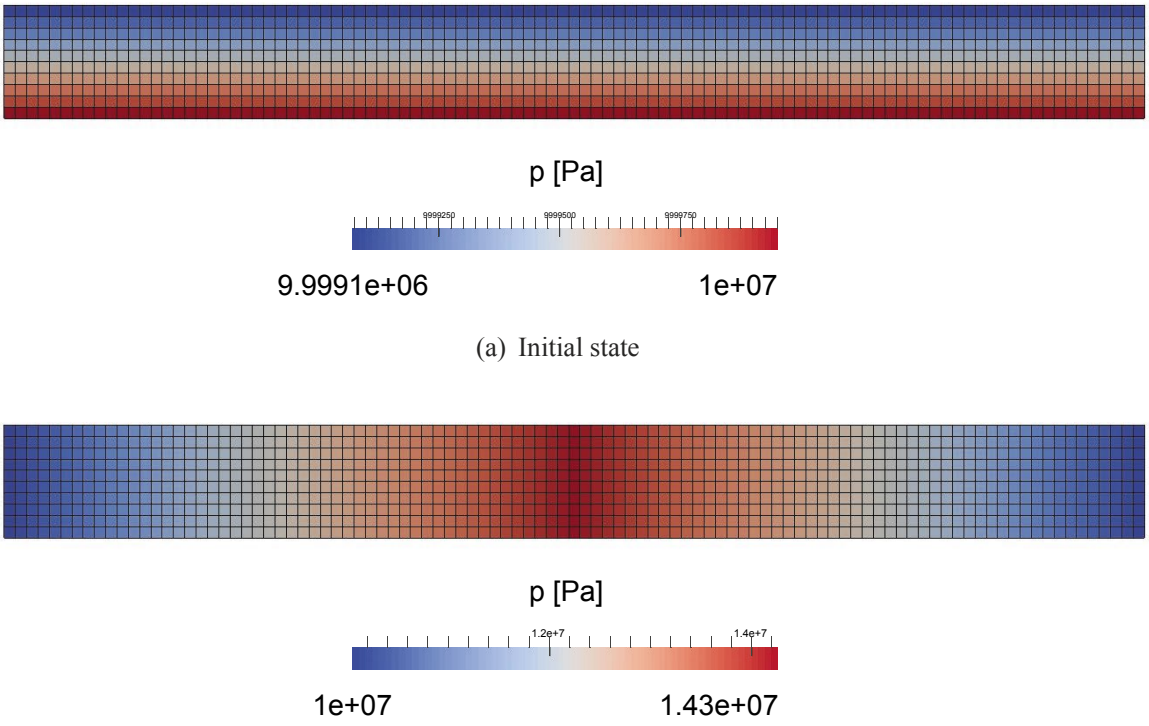

(a) Initial state

(b) After 7 days

Figure 8: Pressure distribution in the reservoir

Geometry, mesh and properties

The reservoir model has a simplified two-dimensional rectangular geometry. The horizontal dimension is 1010m while the thickness of the reservoir is 10m. For the spatial discretization the geometry is meshed by a Cartesian grid with 101 cells in the horizontal and 10 cells in the vertical direction. Consequently, each cell has a size of 10×1 m. The properties of the storage rock are homogeneous and isotropic with a permeability of 10^{-13} m^2 (≈ 100mD) and a porosity of 0.2. The density and viscosity of the fluid are correlated for hydrogen under the actual pressure and temperature conditions. The temperature is constant with a value of 40°C.

Initial and boundary conditions

The pressure is initialized to be 10MPa at the bottom of the reservoir. A hydro-static equilibrium is assumed which results in a decreasing pressure towards the top of the reservoir. However, due to the very low density of hydrogen the difference in pressure over the reservoir thickness of 10m is only 100Pa. The top and bottom edges of the reservoir are defined by Neumann boundary conditions with no flow across. In contrast, the left and right edges are set by Dirichlet boundary conditions having the initial pressure values. The gas-well is located in the center of the geometry and is assumed to be perforated over the complete reservoir thickness. The inflow or outflow of gas is modeled as source term by using the Peaceman-well model (Peaceman et al., 1983),

$$q = \frac{2\pi\rho k h_g}{\mu \ln(r_e/r_w)}(p - p_{bh}) \tag{10}$$

where h_g is the height of the grid cell in [m], r_e is the equivalent radius in [m], r_w is the geometrical well radius in [m], p is the actual fluid pressure in the well grid cell and p_{bh} is the defined bottom-

hole flowing pressure (pressure at the perforations). In the first step, the pressure at the perforations (p_{bh}) is assumed to be constant with a value of 15MPa. In the later planned coupling between well-bore and reservoir flow this value will be variable.

Results

In Fig. 8 the pressure distribution is shown for the initial state and after 7 days of hydrogen injection. In this figure the vertical axis is stretched by a factor of 10. It can be observed that the pressure in the vicinity of the gas-well increases rapidly after the injection of hydrogen has started. The grid cells containing the well are reaching an average pressure of approximately 14.3MPa after 7 days. Towards the left and right edge of the reservoir, a continuous gradient arises.

4. Conclusions

The numerical treatment of storing (injecting) and removing the gas in former gas reservoirs is a challenging task since it touches different issues. The numerical treatment requires a coupling tool to couple specialized sub-problems (pipe flow, local fluid flow, flow in porous media, ...). Thus, each sub-problem has to be treated first. This is presented in this report, where the local stress and strain state in the piping is discussed, the local flow, and the flow in the reservoir are investigated. Moreover, the basic equations of pipe flow are shown, which are necessary for coupling purposes. Finally, the overall system of differential-algebraic equations with side conditions and its possible numerical treatment are discussed occurring in the fully coupled problem. This touches essentially the numerical solution of the block-structured system of nonlinear equations and its acceleration schemes. The final coupling of all sub-problems will be the final next steps.

References

Aitken, A. (1926). On bernoulli's numerical solution of algebraic equations. In Proceedings of Royal Society of Edinburgh, 46, pages 289–305. Royal Society of Edinburgh.

Bai, M., Song, K., Li, Y., Sun, J., and Reinicke, K. M. (2015a). Development of a novel method to evaluate well integrity during CO_2 underground storage. In SPE Journal. Society of Petroleum Engineers SPE. SPE 173000.

Bai, M., Sun, J., Song, K., Reinicke, K. M., and Teodoriu, C. (2015b). Evaluation of mechanical integrity during CO_2 underground storage. Environmental Earth Sciences, 73:6815 – 6825.

Bai, Y., Igland, T. R., and Moan, T. (1997). Tube collapse under combined external pressure, tension and bending. Marine Structures, 10(5):389–410.

Bourgoyne, A. (1986). Applied Drilling Engineering. SPE textbook series. Society of Petroleum Engineers.

Bradley, W. B. (1979). Failure of inclined boreholes. Journal of Energy Resources Technology, 101:232–239.

Broyden, C. G. (1965). A class of methods for solving nonlinear simultaneous equations. Mathematics of computation, 19(92):577–593.

Class, H., Ebigbo, A., Helmig, R., Dahle, H. K., Nordbotten, J. M., Celia, M. A., Audigane, P., Darcis, M., Ennis-King, J., Fan, Y., et al. (2009). A benchmark study on problems related to CO_2 storage in geologic formations. Computational Geosciences, 13(4):409.

Clifton, R. J., Simonson, E. R., Jones, A. H., and Green, S. J. (1976). Determination of the critical-stress-intensity factor kic from internally pressurized thick-walled vessels. Experimental Mechanics, 16(6):233–238.

De Simone, M., Pereira, F. L. G., and Roehl, D. M. (2017). Analytical methodology for well-bore integrity assessment considering casing-cement-formation interaction. International Jounral of Rock Mechanics & Mining Science, 94:112–122.

Degroote, J., Bathe, K. J., and Vierendeels, J. (2009). Performance of a new partitioned procedure versus a monolithic procedure in fluid–structure interaction. Computers & Structures, 87(11):793–801.

Degroote, J., Haelterman, R., Annerel, S., Bruggeman, P., and Vierendeels, J. (2010). Performance of partitioned procedures in fluid-structure interaction. Computers & structures, 88(7-8):446–457.

Dennis, J. E. and Schnabel, R. B. (1996). Numerical methods for unconstrained optimization

and nonlinear equations, volume 16 of Classics in Applied Mathematics. SIAM Society for Industrial and Applied Mathematics, Philadelphia.

Erbts, P. and Düster, A. (2012). Accelerated staggered coupling schemes for problems of thermoelasticity at finite strains. Computers & Mathematics with Applications, 64(8):2408–2430.

Erbts, P., Hartmann, S., and Düster, A. (2015). A partitioned solution approach for electro-thermo-mechanical problems. Archive of Applied Mechanics, 85:1075–1101.

Feldmann, F., Hagemann, B., Ganzer, L., and Panfilov, M. (2016). Numerical simulation of hydrodynamic and gas mixing processes in underground hydrogen storages. Environmental Earth Sciences, 75(16):1165.

Ferziger, J. H. and Peric, M. (2012). Computational methods for fluid dynamics. Springer Science & Business Media.

Fjær, E., Holt, R. M., Horsrud, P., Raaen, A. M., and Isnes, R. R. (2008). Petroleum related rock mechanics, volume 53 of Developments in Petroleum Science. Elsevier, Amsterdam, 2 edition.

Flemisch, B., Darcis, M., Erbertseder, K., Faigle, B., Lauser, A., Mosthaf, K., Müthing, S., Nuske, P., Tatomir, A., Wolff, M., et al. (2011). Dumux: Dune for multi-{phase, component, scale, physics,} flow and transport in porous media. Advances in Water Resources, 34(9):1102–1112.

Graves-Morris, P. R. (1992). Extrapolation methods for vector sequences. Numerische Mathematik, 61(1):475–487.

Greenshields, C. J. (2012a). The Open Source CFD Toolbox-Programmer's Guide.

Greenshields, C. J. (2012b). The Open Source CFD Toolbox-User's Guide.

Großmann, C. and Roos, H. (1994). Numerik partieller Differentialgleichungen. Teubner Verlag, Stuttgart.

Gunzburger, M. D. (2012). Finite element methods for viscous incompressible flows: a guide to theory, practice, and algorithms. Elsevier.

Hagemann, B., Rasoulzadeh, M., Panfilov, M., Ganzer, L., and Reitenbach, V. (2015). Mathematical modeling of unstable transport in underground hydrogen storage. Environmental Earth Sciences, 73(11):6891–6898.

Hairer, E., Lubich, C., and Wanner, G. (2002). Geometric Numerical Integration. Springer, Berlin.

Hairer, E., Norsett, S. P., and Wanner, G. (1993). Solving Ordinary Differential Equations I. Springer, Berlin, 2nd revised edition.

Hairer, E. and Wanner, G. (1996). Solving Ordinary Differential Equations II. Springer, Berlin, 2nd revised edition.

Hartmann, S. and Gilbert, R. R. (2002). Identifiability of material parameters in solid mechanics. Archive of Applied Mechanics, 88(1):3–26.

Hartmann, S., Mohan, J., Müller-Lohse, L., Hagemann, B., and Ganzer, L. (2018). An analytical solution of multi-layered thick-walled tubes in thermo-elasticity with application to gas-wells. International Journal of Pressure Vessels and Piping, 161:10–16.

Hartmann, S., Quint, K. J., and Arnold, M. (2008). On plastic incompressibility within timeadaptive finite elements combined with projection techniques. Computer Methods in Applied Mechanics and Engineering, 198:178–193.

Hesthaven, J. S. and Warburton, T. (2007). Nodal discontinuous Galerkin methods: algorithms, analysis, and applications. Springer Science & Business Media.

Hughes, T. J., Liu, W. K., and Brooks, A. (1979). Finite element analysis of incompressible viscous flows by the penalty function formulation. Journal of Computational Physics, 30(1):1–60.

Jennings, A. (1971). Accelerating the convergence of matrix iterative processes. IMA Journal of Applied Mathematics, 8(1):99–110.

Jiang, X. (2011). A review of physical modelling and numerical simulation of long-term geological storage of CO_2. Applied Energy, 88(11):3557–3566.

Joosten, M. M., Dettmer, W. G., and Peric, D. (2009). Analysis of the block gauss–seidel solution procedure for a strongly coupled model problem with reference to fluid–structure interaction. International Journal for Numerical Methods in Engineering, 78(7):757–778.

Kepplinger, J., Crotogino, F., Donadei, S., and Wohlers, M. (2011). Present trends in compressed air energy and hydrogen storage in germany. In Solution Mining Research Institute SMRI Fall 2011 Conference, York, United Kingdom, Clarks Summit, PA, USA. Solution Mining

Research Institute, SMRI.
Klaus, T., Vollmer, C., Werner, K., Lehmann, H., and Müschen, K. (2010). Energieziel 2050: 100% Strom aus erneuerbaren Quellen. Umweltbundesamt, Dessau.
Lehmann, T. (1984). Elemente der Mechanik II, Elastostatik. Vieweg, Braunschweig, 2nd edition.
Lewis, R. W., Nithiarasu, P., and Seetharamu, K. N. (2004). Fundamentals of the finite element method for heat and fluid flow. John Wiley & Sons.
Li, Y., Liu, S., Wang, Z., Yuan, J., and Qi, F. (2010). Analysis of cement sheath coupling effects of temperature and pressure in non-uniform in-situ stress field. In Proceedings of International Oil and Gas Conference and Exhibition in China. Society of Petroleum Engineers SPE. SPE 131878.
Macleod, A. J. (1986). Acceleration of vector sequences by multi-dimensional methods. Communications in Applied Numerical Methods, 2(4):385–392.
Martine z, J. M. (1994). Algorithms for Solving Nonlinear Systems of Equations, pages 81–108. Springer Netherlands, Dordrecht.
Mohan, J. and Hartmann, S. (will be submitted in 2019). Solution techniques for coupled systems of non-linear equations. Technical report, Faculty of Mathematics/Computer Science and Mechanical Engineering, Clausthal University of Technology (Germany).
Müller-Lohse, L. (2018). Analytische Lösung für stationär belastete, mehrschichtige thermoelastische Rohre. Projektarbeit, Institute of Applied Mechanics, Division of Solid Mechanics, Clausthal University of Technology.
Nobile, P. C. J. G. F. (2005). Added-mass effect in the design of partitioned algorithms for fluidstructure problems. Computer Methods in Applied Mechanics and Engineering, 194.
Nocedal, J. and Wright, S. J. (1999). Numerical Optimization. Springer, New York.
Peaceman, D. W. et al. (1983). Interpretation of well-block pressures in numerical reservoir simulation with nonsquare grid blocks and anisotropic permeability. Society of Petroleum Engineers Journal, 23(03):531–543.
Radtke, L., Konig, M., and Düster, A. (2017). The influence of geometric imperfections in cardiovascular fsi simulations. Computers & Mathematics with Applications, 74(7):1675– 1689.
Radtke, L., Larena-Avellaneda, A., Debus, E. S., and Düster, A. (2016). Convergence acceleration for partitioned simulations of the fluid-structure interaction in arteries. Computational Mechanics, 57(6):901–920.
Ramey, Jr., H. J. (1962). Wellbore heat transmission. Journal of Petroleum Technology, 225:427–435.
Ramiere, I. and Helfer, T. (2015). Iterative residual-based vector methods to accelerate fixed` point iterations. Computers & Mathematics with Applications, 70(9):2210–2226.
Reddy, J. N. (1993). An introduction to the finite element method, volume 2. McGraw-hill New York.
Reddy, J. N. and Gartling, D. K. (2010). The finite element method in heat transfer and fluid dynamics. CRC press.
Rothe, S., Erbts, P., Düster, A., and Hartmann, S. (2015a). Monolithic and partitioned coupling schemes for thermo-viscoplasticity. Computer Methods in Applied Mechanics and Engineering, 293:375 – 410.
Rothe, S., Schmidt, J.-H., and Hartmann, S. (2015b). Analytical and numerical treatment of electro-thermo-mechanical coupling. Archive of Applied Mechanics, 85:1245–1264.
Schwarz, H. R. (1986). Numerische Mathematik. Teubner, Stuttgart, 1st edition.
Sciandrone, L. G. M. (2000). On the convergence of the block nonlinear gaussseidel method under convex constraints. Operations Research Letters, 26.
Sherif, S. A., Barbir, F., and Veziroglu, T. N. (2005). Wind energy and the hydrogen economy – review of the technology. Solar Energy, 78(5):647–660.
Shildip, D. U., Bhope, D. V., and Khamankar, S. D. (2015). Stress analysis of multilayer pressure vessel. Journal of Applied Mechanical Engineering, 4(2):1–6.
Teodoriu, C., Ugwu, I., and Schubert, J. (2010). Estimation of casing-cement-formation interaction using a new analytical model. In Proceedings of SPE EUROPEC/EAGE Annual Conference and Exhibition. Society of Petroleum Engineers SPE. SPE 131335.
Ugwu, I. O. (2008). Cement fatigue and HTHP well integrity with application to life of well prediction. Master's thesis, Texas A&M University,

College Station, TX, US.
Wall, U. K. C. F. W. A. (2006). A solution for the incompressibility dilemma in partitioned fluidstructure interaction with pure dirichlet fluid domains. Computational Mechanics, 38.
Wendt, G., Erbts, P., and Düster, A. (2015a). Partitioned coupling strategies for multi-physically coupled radiative heat transfer problems. Journal of Computational Physics, 300:327–351.
Wendt, G., Erbts, P., and Düster, A. (2015b). Partitioned coupling strategies for multi-physically coupled radiative heat transfer problems. Journal of Computational Physics, 300:327–351.
Wood, C., Gil, A. J., Hassan, O., and Bonet, J. (2010). Partitioned block-gauss–seidel coupling for dynamic fluid–structure interaction. Computers & Structures, 88(23):1367–1382.
Yeh, M. and Kyriakides, S. (1986). On the collapse of inelastic thick-walled tubes under external pressure. ASME. Journal of Energy Resources and Technology, 108(1):35–47.
Yin, F. and Gao, D. (2014). Mechanical analysis and design of casing in directional well under in-situ stresses. Journal of Natural Gas Science and Engineering, 20:285–291.
Yosibash, Z., Hartmann, S., Heisserer, U., Düster, A., Rank, E., and Szanto, M. (2007). Axisymmetric pressure boundary loading for finite deformation analysis using p-FEM. Computer Methods in Applied Mechanics and Engineering, 196:1261–1277.
Zienkiewicz, O., Paul, D., and Chan, A. (1988). Unconditionally stable staggered solution procedure for soil-pore fluid interaction problems. International Journal for Numerical Methods in Engineering, 26(5):1039–1055.

Project data

The project was funded from SWZ with one TV-L E13 staff position from June 2015 to July 2018 at the site Clausthal. Involved scientists are:

Prof. Dr. Leonhard Ganzer
Research Group Reservoir Engineering
Institute of Petroleum Engineering
Clausthal University of Technology

Prof. Dr.-Ing. Stefan Hartmann
Division of Solid Mechanics
Institute of Applied Mechanics
Clausthal University of Technology

Dr.-Ing. Birger Hagemann
Research Group Reservoir Engineering
Institute of Petroleum Engineering
Clausthal University of Technology

Jithin Mohan, M.Sc.
Division of Solid Mechanics
Institute of Applied Mechanics
Clausthal University of Technology

Distributed multiscale simulation to optimize the production of fiber composites for aircraft construction

Dieter Meiners, Dietmar P.F. Möller, Juliana Rivas-Botero, Huynh Khiem Le, Isabell A. Jehle

1. Introduction

Fiber composite materials have been used for years in vehicle and aircraft construction and will be used with increasing tendency. They are hybrid materials consisting of a combination of fibers and a matrix consisting of a mixture of resin and hardener. By combining the different materials, lightweight components with high specific strength and stiffness can be created.

Through the orientation of the fibers in the material, direction-dependent (non-isotropic) properties can be constructed and optimized. This is based on the interaction of the fibers which can handle tensile stress and the transmission and distribution of force through the matrix.

In addition to the high strength, resistance to corrosion and ageing as well as high damping capabilities and fire resistance are further advantages of these materials.

Fiber-reinforced composites are of great relevance for the aerospace industry, since the lightweight construction potential through energy savings and performance increases offer significant economic advantages compared to materials such as metals despite higher production costs.

1.1 Resin Transfer Molding

In aircraft construction, specific component properties and high reproducible quality are more important than large production quantities and minimum cycle times.

This qualifies the use of the resin transfer molding (RTM) process in aircraft manufacturing. The setup of the RTM production process is shown in Figure 1.

For the stresses in aviation, high mechanical strength is required, which requires a fiber volume content of 60% (ideal). This can be achieved by the compression technology of the RTM process

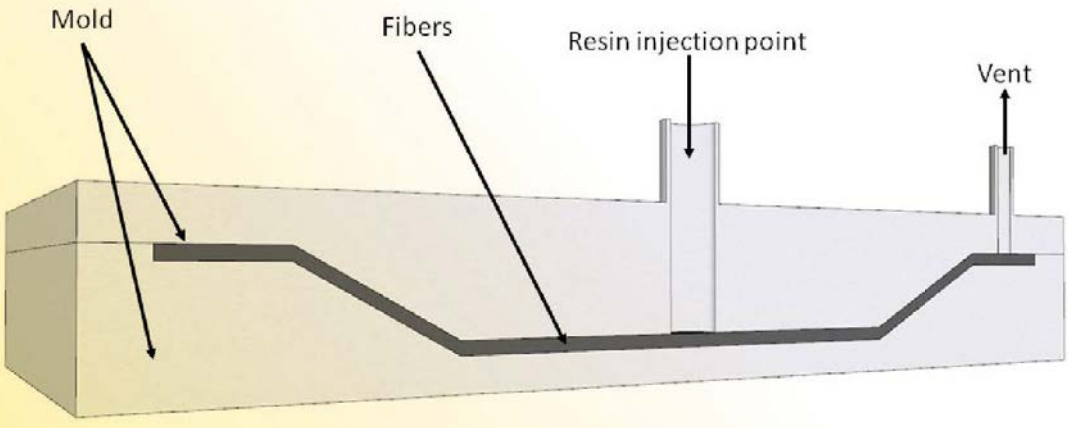

Figure 1: RTM setup

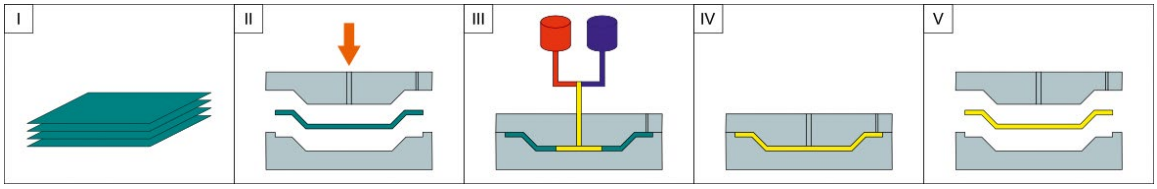

Figure 2: RTM process steps

and, in addition to good surface properties, by the double-sided contact with the molds.

The RTM production process can be divided into individual steps, as described in (AKV 2013)

At the beginning, fiber mats are cut and layered in different orientations depending on the desired component properties. (Figure 2, I), that is called lay-up. This fiber lay-up is then fixed. This can be done by sewing, weaving or gluing in combination with pressing. The result is a preform.

The preform is then inserted into the lower RTM mold. And the upper mold is closed with pressure over it (Figure 2, II). Then a resin catalyst mixture is produced by a mixer unit and injected through the resin injection point via a pump. The resin impregnates the fibers of the preform. Resin is injected at least until it exits at the vent (Figure 2, III). When the injection phase is completed, the inlet and outlet are closed and the curing phase begins. Depending on the form of the process, this can be supported by pressure increase (Figure 2, IV). The finished cured component can then be removed from the mold and passed to the finishing process. (Figure 2, V)

Voids, resin-free (dry) pores or gaps within or at the edge of the component and a heterogeneous molecular structure reduce the material stability and thus the quality of the component. In addition to the purely physical conditions during the manufacturing process, the manufacturing parameters are determining factors for the quality of the product, such as the optimal position of the inlet openings and the inlet pressure.

Important process variables are the flow front velocity, the pressure, the geometry of the mold, the roving micro structure during the process, the fiber volume content and the viscosity of the resin mixture used.

This means that the process optimization corresponds to a multi-scale problem of spatial dimensioning. The macroscopic view considers the influence of the direction and length of the fibers as well as the chemical, physical and mechanical properties of the polymer on the behavior of the fiber composite. The mesoscopic and microscopic view sees the influences of the geometry of the fiber structure and the hydrodynamic behavior of the polymer in this structure. This results in a very complex numerical optimization problem for the best possible positioning of inlet channels on the RTM mold with various dependencies on the material properties in spatial and temporal dimensions.

2. Multiphase Flow Modeling in Porous Media

2.1 General conservation Equation

Non-isothermal fluid flow in porous media can be modeled on the basis of fluid velocity, pressure and temperature into the media. In macroscopic scale, the porous model is a generalization of both, the Navier–Stokes equations and Darcy's law. The model retains both advection and diffusion terms and can therefore be used for flows in which such effects are important. In deriving the continuum equations, it is assumed that control volumes are infinitesimal and that surfaces are large in relation to the interstitial spacing of the porous medium but small relative to the scales in study. Thus, given control cells and control surfaces are assumed to contain both solid and fluid regions. This is a concept of continuum mechanics. This way, the particular details of the porous structure such as dispersion, tortuosity and

interfacial transfer between phases at the pore level are neglected.

The volume porosity φ at a point is the ratio of the volume V′ available to flow in an infinitesimal control cell surrounding the point, and the physical volume V of the cell. The general scalar advection-diffusion equation in a porous medium is introduced by (ANSYS, Inc. 2013):

$$\frac{\partial(\rho\phi\Phi)}{\partial t} + \nabla\cdot(\rho\boldsymbol{K}\cdot U\Phi) - \nabla\cdot(\Gamma^{\Phi}\boldsymbol{K}\cdot\nabla\Phi) = \phi S \quad (1)$$

where t is the time, ρ is the density, U is the velocity vector, Φ is the potential of transport, K is the area porosity tensor, Γ^{Φ} represents effective transport property and S the source term.

2.2 General Initial and Boundary Conditions

For a problem that involves partial differential equations, the solution to the problem depend on the initial and/or boundary conditions. In general, the following initial and boundary conditions can be specified for the unknown Φ.

Initial conditions, with D is the studied domain.

$$\Phi = f_1(D, t=0) \quad (2)$$

Boundary conditions

Prescribed value (Dirichlet or first kind condition)

$$\Phi = f_2(S) \quad (3)$$

where S is the boundary of the domain.

Prescribed flux (Newmann or second kind condition)

$$\frac{\partial\Phi}{\partial n} = f_3(S) \quad (4)$$

$$\frac{\partial\Phi}{\partial s} = f_4(S) \quad (5)$$

where n and s represent the normal and tangential directional vectors to the boundary S, respectively.

Mixed (Robin or third kind condition)

$$f_5(S)\frac{\partial\Phi}{\partial n} + f_6(S)\Phi = f_7(S) \quad (6)$$

The choice of one or more conditions is dependent on the problem to be solved.

Solution of a partial differential equation applied to physical problems requires physically realistic initial and boundary conditions. Fluid flow equations in porous media comprise a complicated formulation that involves elliptic, parabolic and hyperbolic terms. These different behaviors affect the way like the initial and boundary conditions in the domain must be specified. For a physical problem where fluid-fluid (liquid–gas) interface exists, the momentum flux and hence the velocity gradient in the liquid is negligible compared to that in the gas phase (because liquid viscosity is much greater than that of the gas). In addition, in transient problems the initial condition, i.e., the values of the variables, must be defined at the start of the process (t = 0).

3. Fluid flow in RTM

The reinforcement (porous) media inside the mold is initially filled with air. Resin is injected into the mold through one or more points (inlets) and air is forced out of the mold through one or more outlets. In standard RTM, the use of a single resin inlet and a single air/resin outlet is common. Resin injection through the reinforcement media can be mathematically described as a viscous fluid moving through a porous medium. The problem consists of two inviscid fluids (resin and air) flowing through a porous media contained inside the mold cavity. Different approaches can be used to model the problem. These three constraints should be discussed and compared:

a. Multi-fluid model;
b. Control Volume/Finite Element (CV/FE) based model;
c. Volume of Fluid (VOF) model.

3.1 Multi-fluid model

Macroscopic equations can be derived from the mass conservation equation:

$$\frac{\partial}{\partial t}(\phi\rho) + \nabla \cdot (\rho \boldsymbol{K} \cdot U) = 0 \tag{7}$$

and the momentum conservation equation:

$$\frac{\partial(\rho\phi U)}{\partial t} + \nabla \cdot [\rho(\boldsymbol{K} \cdot U) \otimes U] = \nabla \cdot$$

$$\{\mu_e \boldsymbol{K} \cdot [\nabla U + (\nabla U)^T]\} - \phi R \cdot U - \phi \nabla p + B. \tag{8}$$

In these equations, U is the true velocity, B is the volumetric body force, p is the pressure, μe is the effective viscosity and R represents the resistance to flow in the porous medium. This is, in general, a symmetric positive definite second rank tensor, in order to account for possible anisotropies in the resistance.

Modeling of the fluid flow strives to obtain the velocity, pressure and volume fraction (saturation) distribution of the fluid phases within the porous medium.

Neglecting body force effects, with the limit to large resistance, an anisotropic version of Darcy's law is obtained, with permeability proportional to the inverse of the resistance tensor.

$$U = -R^{-1} \cdot \nabla p \tag{9}$$

in which

$$R = \frac{\mu}{\phi K} \tag{10}$$

3.2 Control Volume/Finite Element (CV/FE) based model

The control volume/finite element method is used to discretize partial differential equations to which the conservation law applies, in this case mass conservation.

The solution of the discrete equations takes place in the center of the finite volumes, as explained in (Ferziger and Peric 2008).

The area of calculation is discretized by finite volumes. The elements can be of polygonal or

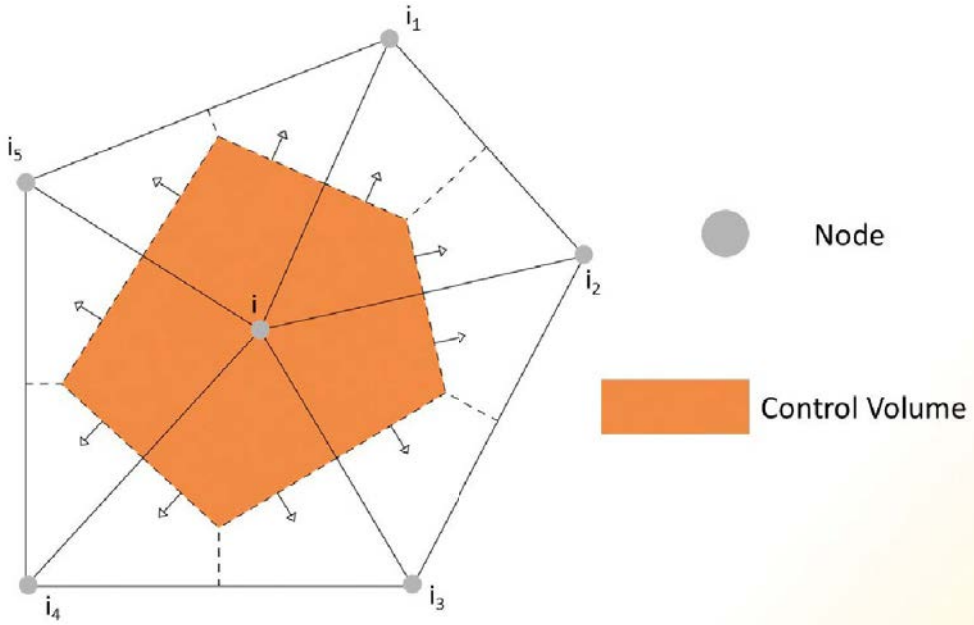

Figure 3: Discretization of the calculation area by a triangle mesh (Voller 2009)

polyhedral form. For the 2D representation of the RTM process a triangle mesh is useful.

To each node an environment is assigned, the control volume of the node.

The solution of the discrete equation of a node is the sum of the influxes and drains of fluid to and from the surrounding control volume.

The CV/FE approach allows modeling of the resin flow the porous medium consisting of fibers in the mold. Only the resin flow is considered. The presence of the medium air in the mold as well as chemical and thermal reactions is neglected. Another simplification regards the fact that the transient problem of determining resin position as a function of time inside the mold is obtained by successive solutions of a simpler steady-state problem.

The resin velocity is formulated using Darcy's Law:

$$U = -R^{-1} \cdot \nabla P \tag{11}$$

with

$$R = \frac{\mu}{K_P} \tag{12}$$

where U is the filtration velocity or Darcy flux, ∇P is the pressure drop, μ is the viscosity of the resin and K_p is the permeability.

Typical polymeric resins used in the RTM process show a non-Newtonian behavior. A Newtonian approach is suitable, largely used in the numerical investigation of RTM. Thus, assuming a Newtonian incompressible fluid we can write:

$$\nabla \cdot U = 0 \tag{13}$$

The combination of these equations results in

$$\nabla \cdot \left(\frac{K_P}{\mu} \nabla P \right) = 0 \tag{14}$$

The equation by dimension is:

$$\frac{\vartheta}{\vartheta x_i} \left(\frac{K_{P\,ij}}{\mu} \frac{\vartheta p}{\vartheta x_i} \right) = 0 \tag{15}$$

The flow through a control volume on the edge of the calculation area requires special consideration. The flows at the edges must either be known or expressed as a combination of the (unknown) inner values and the (known) boundary conditions.

The boundary conditions to be used in this equation are given.

For the injection point of the mold the boundary condition for the pressure is:

$$P = P_0 \tag{16}$$

The boundary condition for the flow front is:

$$P = P_f \tag{17}$$

Usually $P_f = 0$.

The boundary condition for the walls of the mold completes the set of equations:

$$\frac{\vartheta p}{\vartheta n} = 0 \tag{18}$$

The flow over time is represented by changes in the state of the control volumes. Each control volume must be empty, partially filled or filled. The fill factor of the control volume ranges between 0 and 1 and indicates the ratio of liquid volume to total volume.

The flow front is thus located where partially filled control volumes are present. The filling ratio of the control volumes are updated in each time step of the calculation.

The size of the time steps is adapted adaptively after each calculation. The next time step is selected so that the resin only fills one further control volume in the next calculation step, otherwise the requirement of mass preservation is not guaranteed.

As the fill ratio is uniform for the entire control volume, the net size determines the calculation accuracy.

For a more precise tracking of the flow front a higher resolution for the mesh is necessary. This topic will be solved in a follow up research work.

3.3 Volume of Fluid model

In general, the VOF (Hirt, Nichols 1981) method can be used to model multiphase flows with two or more inviscid fluids. In this model, all phases are well defined, and the volume occupied by one phase cannot be occupied by the others. The volume fraction concept is used to represent the existence of different phases inside each control volume. All the fractions are assumed continuous in space and time and their sum, inside each control volume, is equal to one. If the volume fraction of a particular phase inside a control volume is denoted as fi, then the following three conditions are possible (Srinivasan et al. 2011):

1. fi = 0: the cell is empty with fluid of phase i;

2. fi = 1: the cell is full with fluid of phase i;

3. 0 < fi < 1: the cell represents the interface between phase i and one or more other phases.

For the particular case of modeling resin and air flowing through a porous media (e.g., in RTM), only two phases are considered in the formulation. In the VOF method, only a single set of momentum and continuity equations is applied to both fluids, and the volume fraction of each fluid in every computational cell (control volume) is tracked throughout the domain. The model is composed of continuity, volume fraction and momentum equations as follows:

$$\frac{\partial \rho}{\partial t} + \nabla \cdot (\rho U) = 0 \tag{19}$$

$$\frac{\partial (\rho f)}{\partial t} + \nabla \cdot (\rho f U) = 0 \tag{20}$$

$$\frac{\partial (\rho U)}{\partial t} + \nabla \cdot (\rho U) = -\nabla p + \nabla \cdot \tau + \rho g + B \tag{21}$$

where f is the volume fraction of resin and τ is the stress tensor.

Since a single set of equations is used for both phases, average properties for ρ and μ need to be defined. These properties can be approximated as

$$p = f p_{resin} + (1 - f) p_{air} \tag{22}$$

$$\mu = f \mu_{resin} + (1 - f) \mu_{air} \tag{23}$$

The porous media (reinforcement) resistance to the flow is modeled by adding a source term to the standard momentum equation, which is actually also lead to the Darcy's Law:

$$\nabla p = \frac{\mu}{K_P} \mathrm{U} \tag{24}$$

In the VOF model, four partial differential equations must be simultaneously solved, then the solution scheme normally suffers from convergence issues. Therefore, grid refinement and time discretization constraints are required.

The VOF method could solve problems whose computational domains are divided into multi regions, filled with the reinforcement or empty, in which the resistance term turns to zero. This model is of interest for the presence of empty channels and cannot be performed with the CV/FE method.

4. Preform Geometry and Mesh Generation

When numerical methods are applied to solve a particular physical problem, it is necessary to define the grid (mesh), i.e., the numerical representation of the physical domain in the computational domain where the conservation equation can be applied. When the domain presents a complex geometry, grid generation can be a very time-consuming task. However, a well-constructed grid improves the quality of the results.

The grid can be classified by based on the logical arrangement of the control-volume as structured and unstructured grids. Structured grids are characterized by a regular arrangement of grid control-volumes. For unstructured grids, generally used for very complex geometries, there is no regularity in the arrangement of the control-volumes (cells). The grid can present uniform or non-uniform size distribution. For higher accuracy of a particular physical problem in regions where a large gradient is expected, the non-uniform grid size distribution is more effective.

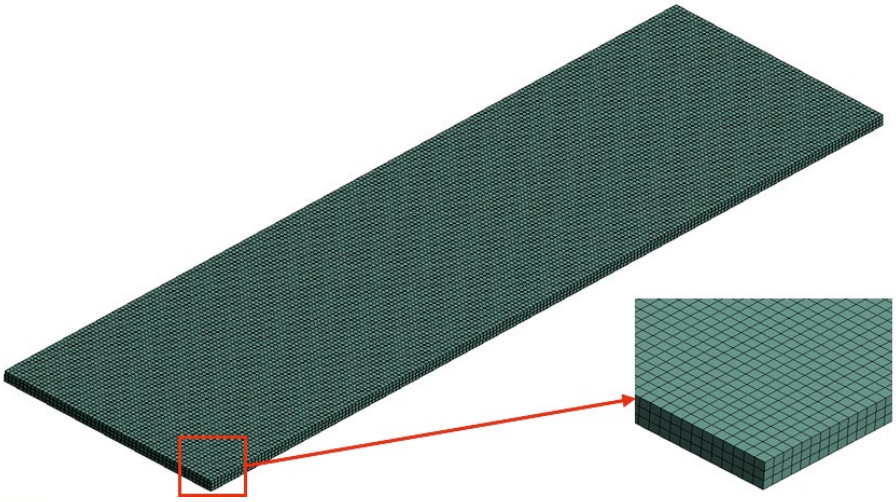

Figure 4: Mesh generation in 55x200x2.65mm domain, grid size of 1mm

For liquid composite molding, flow is transient, and mold and preform may present a very irregular shape. In this case, an adequate grid is essential to the accuracy of the solution, mainly when we apply a three-dimensional treatment. In addition, depending on the specific liquid molding technique and the particular mold design and construction being investigated, the mold may display deformation (change in relative position between the upper and lower parts of the mold) during infiltration. This brings significant challenges related to grid generation along the transient process and, because of that, research is usually considering the mold and grid to be rigid during RTM process.

5. RTM Simulations

In the liquid composite molding (LCM) process, simulations are being used mainly to verify the trial-and-error approach, which is still prevalent in the manufacturing industry. However, as the composite structures being manufactured by LCM become larger and more complex, use of process simulation may aid in improving the process design and increase the yield by counterbalancing any unforeseen disturbances that may arise during the impregnation phase.

For the application of the models and equations presented, it is necessary using a specific software package to solve them. It was considered to use two commercial software packages: ANSYS Fluent (non-RTM-dedicated) and PAM-RTM (RTM-dedicated, which would be used more in detail in the next state of the project)

In modeling by RTM, simulation software packages are used to (i) predict the resin injection profile and then be able to evaluate the filling time, that should remain below the resin curing time, (ii) predict impregnation deficient (dry) points, and (iii) determine the more suitable injection and outlet points of air/resin.

In all simulations, the preform was initially considered as having pressure (P_i), temperature (T_i), and air saturation (S_{ai}) homogeneously distributed throughout the mold with the following values: $P_i = 0$ bar, T_i at room temperature 300K and $S_{ai} = 1.0$ (consequently, resin saturation is $S_{ri} = 0.0$).

6. Experimental methods

6.1 Permeability Measurement

Permeability is a measure of the ability of porous media to allow fluids to flow through and a critical property of fiber textile that determines the flow velocity and amount of fluid in that medium. Darcy made the initial attempt to explain the fluid behavior in a porous medium by doing an experi-

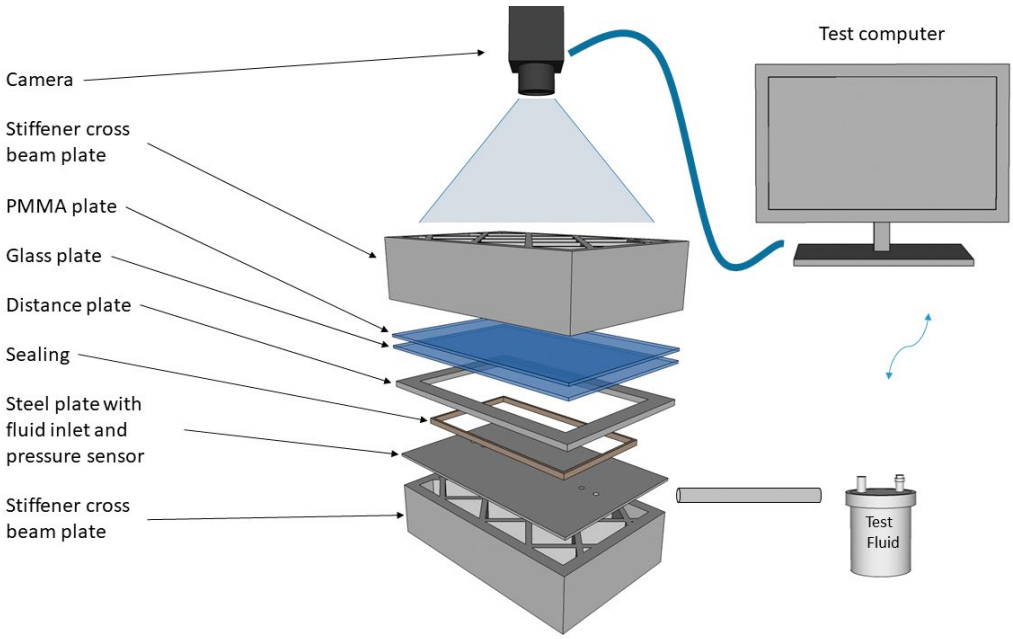

Figure 5: Permeability measurement setup (Abliz 2018)

mental study of the water flow velocity through a vertical column of sand with a known pressure gradient.

The experimental permeability determination methods are divided into two categories: saturated or stationary and unsaturated or transient permeability methods for 1D, 2D and 3D flow studies.

The flow front tracking for saturated permeability or for the volume / mass flow measurement for saturated permeability is carried out by gravimetric volume flow measurement.

The measurement of unsaturated permeability is possible in a variety of ways. All of these methods are quite similar, e.g. flow front tracking with optical, dielectric, pressure or ultrasonic sensors, etc. A common feature of all measuring setups is that the flow front of a known fluid is observed within a defined section of a textile using suitable methods. The flow front is recorded whether in one direction only (1D) or in two directions (2D) according to (Alms et al. 2010).

The main difference between different measurement set-ups is the liquid inlet. It is possible to pump the fluid either with a constant volume flow or with a constant pressure. According to (Carman 1997; Sharma and Siginer 2010; Mekic et al. 2009; Szymkiewicz 2013, Gebart 1992) and others, the method used for the measurements is not relevant. Nevertheless, it would appear advisable to adjust the measurements as far as possible to the intended application.

The laminar flow of incompressible fluids in porous media is calculated according to the Darcy's law as shown in the equation 11.

To calculate the permeability of a fabric, parameters such as the flow front over time, the pressure gradient, the viscosity of the measuring fluid (the viscosity of the resin system depends on the temperature), the cavity height and the fiber volume content are required. For the measurements several layers of fabric were placed between a metallic plate and a glass plate supported by a steel frame and the measuring liquid, in this case silicone oil AK100 from Wacker, with which the textile is impregnated as illustrated in Fig. 5.

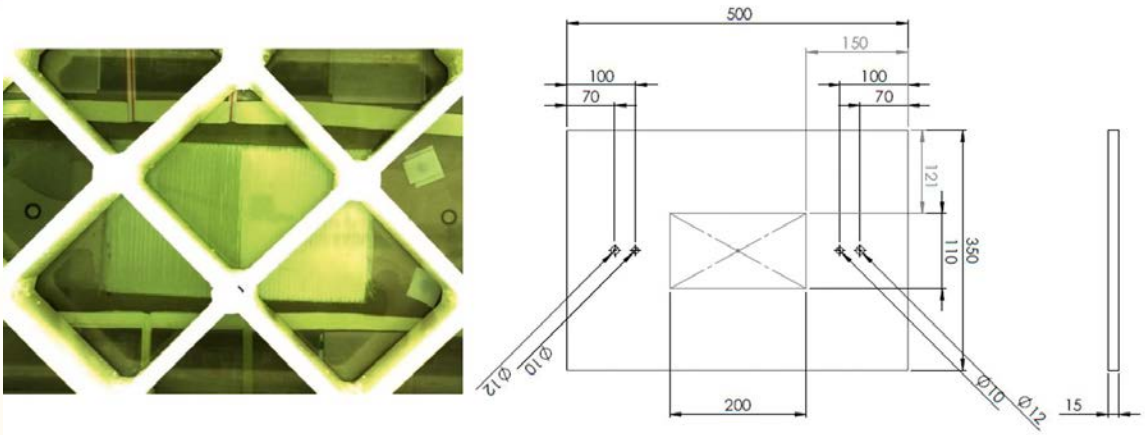

Figure 6: Permeability measurement (left, from camera view) and assembly dimensions (right)

Fig. 6 shows a camera recorded flow front with automatically activated shutter function which allows to follow the change of the flow plug over time. The more photos are taken, the higher the resolution therefore the interval time is adjustable. The interval time is adjustable. An image was taken every 5 to 20 seconds. The cavity height was measured at all four edges of the textiles and the average value was determined. The permeability of the textiles at different configurations (0°, ±45° and 90° direction, as well as symmetric quasi-isotropic configurations) at a fiber volume content of 60 % and a room temperature (20 °C).

6.2 Materials

For the Validation of the Simulation different kind of unidirectional fibers reinforcement materials are compared and characterized.

As carbon textiles we used Carbon non-crimp fabric from R&G Faserverbundwerkstoffe GmbH with different weight per unit area, 100, 200 and 400 g/m². The rovings are made of fiber with the quality ZOLTEK™ PX35 50k and Panex® 35 50k, with a filament diameter of 7.2 µm.

The glass fiber textiles are also unidirectional from HP-Textiles GmbH, with a filament diameter of approx. 10 µm with different specific weight of, 400, and 600 g/m².

In unidirectional textiles, the fibers are oriented in one direction only, which facilitates the characterization of the influence of the fiber direction on the parameters and final properties of the component as seen in the Fig 7.

The permeability, the fiber volume content (FVC) and the filament distribution are the most important parameters for the RTM process. The FVC and the draping process determine the filament spacing distribution in the final component.

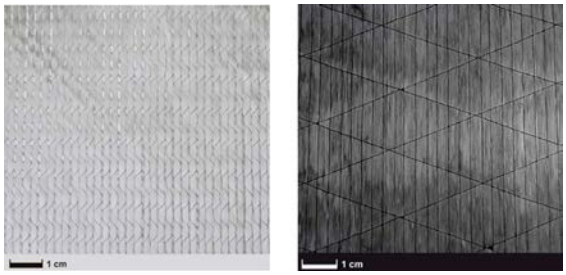

Figure 7: Glass fiber fabric (left) Carbon fiber fabric (right)

The compaction behavior, filament spacing distribution, permeability and deformation of the preform by draping on complex geometries also influence permeability and filament distribution. The draping process for complex geometries is not considered as it covers all types of deformation including compaction, consolidation, extrusion, and so forth. These deformations affect

the fabrication of composite structures, resulting in a much more complex simulation model that must take into account the differences between kinematic and mechanics-based simulation approaches described in (Potter 2015).

6.3 Characterization of the filament diameter

In order to precisely determine the fiber volume content and filament distance using optical methods, it is important to exactly determine the border and diameter of each filament, which is only possible with high-resolution microscopic methods or computer tomography (CT). However, the high local zoom leads to a restricted vision of the area of interest in the samples, which can result in an important loss of statistical information unless a lot of image material is collected and analyzed. In order to compare the influence of resolution on filament recognition and the systematic error due to sample size, the KEYENCE light microscope (VK/9710) records different types of images with different resolutions.

6.4 Characterization of fiber volume contents

The permeability of the fabric and the flow behavior of the measuring-fluid are determined by the fiber volume content (FVC). The FVC could be distinguished for the different scales in global and local FVC because of the heterogeneity of the preform structure and the macro- and micro-porous structure. The global FVC is the average value of the FVC over the entire sample structure. The local FVC shows the FVC inside the rovings. The global FVC can be calculated using the laminate thickness method according to the equation:

$$FVC = \frac{nA_w}{\rho_f h} \tag{25}$$

The FVC is equal to the product of the number of layers n an the areal weigth A_w all divided by the fiber density ρ_f and the laminate thickness h.

For carbon fiber laminates the FVC can also be determined by a chemical analysis according to DIN EN 2564:1998: aerospace series, carbon fiber laminates, determination of fiber, resin and cavity contents or for glass fiber laminates according to DIN EN ISO 1172-1998: Textile glass reinforced plastics -prepregs, molding compounds and laminates - determination of textile glass and mineral filler contents - calcination method.

Both the global and local FVC can be determined by the optical ratio of the filament volume fraction in the roving and the roving volume content (RVC) in the laminate according to the following equation:

$$FVC_R = FVF_{local} RVF \tag{26}$$

In equation (26) subscript FVC_R denotes the filament volume content in the roving, FVF_{local} the filament volume fraction in the roving and RVF the roving volume fraction.

The entire cross-section of the laminate is reconstructed from a set of high-resolution images, whereby the diameter as well as the number of filaments can be determined. This allows the local FVF of the roving to be calculated by image processing software.

7. Flow simulation results and discussion

ANSYS Fluent is a state-of-the-art Computer Aided Engineering (CAE) package for modeling fluid flow, heat transfer, chemical reactions and many other applications in complex geometries. ANSYS Fluent uses the VOF model to solve simultaneously to the momentum, continuity and volume fraction transport equations. ANSYS Fluent is strongly recommended for the solution of problems with two or more immiscible fluids where the position of the interface between the fluids and/or gases is of interest. The VOF method also allows Fluent to analyze geometries which combine porous media with open (empty) regions. Therefore, in this state of the research work, the evolution of the fluid flow front (for oil) in the experiments and simulations in ANSYS Fluent was analyzed and compared. The experimental setup is shown in Section 5, Figure 5 and Figure 6. The fluid was injected into a rectangle porous preformed fabric of 110 x 200 mm with thickness 2.265 mm and porous density of 0.4. The permeability parameter was collected by experimental results and then used in the simulation, in this

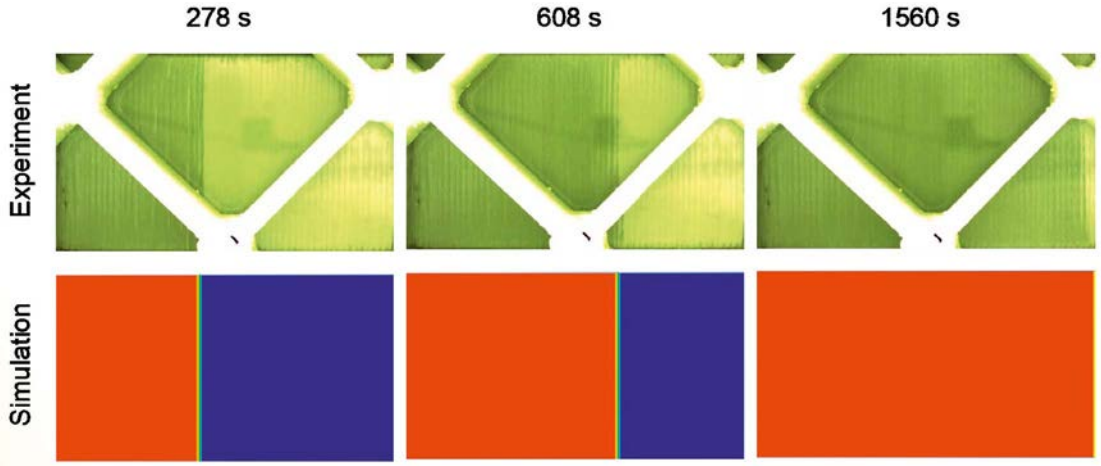

Figure 8: Evolution of the fluid flow front in 278 s, 608 s and 1560 s (red represents full of fluid, blue represents full of air)

case permeability in flow direction K = 5.29 e^{-12} m^2. The fluid in use is oil with density of 960 kg/m^3, viscosity of 0.095 Pas. The adopted boundary conditions are pressure at the inlet P = 0.91 bar. The grid generation with general size of 1 mm is used.

Figure 8 shows a comparison of the evolution of the flow front obtained by experiments and numerical simulations at three different times 278 s, 608 s and 1560 s.

The simulation results fit well with the experimental setup. But it could be seen that there are differences in flow front evolution between simulations and experiments, especially in the later time of the RTM process. It could be seen that the mold is filled faster in simulation than in experiment. In one hand, the deviations of comparing the numerical simulations may be related to an experimental setup and measurement error, as in the permeability determining, which is an importance property to the results of the numerical simulation. In the other hand, the simulations are considered as homogeneous distribution of fiber, and constant properties (permeability, porosity and viscosity), which are not always the cases in the experiment. Some sources of potential experimental errors could be (i) the visual reading of the location of the flow front (ii) the operator sensitivity to start the time measurements and (iii) the inhomogeneity in the fiber properties, which will be investigated and reported in a follow up report.

8. Outlook

Future work will focus on the calculation of the intrinsic permeability of the medium in different directions (i.e. for anisotropic porous material). For this purpose a pore scale simulation of the flow within the void space between the fabric fibers will be carried out. A pore scale simulation requires a model with much higher complexity with regard to the geometry of the porous medium.

Here, two different approaches will be pursued. On one hand, via nano computer tomography (nCT), the porous medium can be scanned and re-modelled in detail for different FVC and for the case of macroscopic obstacles embedded in the fabric. On the other hand, a porous medium can be computer generated and printed using a 3D-printer, which is available in the facilities of the Institute of polymer materials and plastics engineering, which is an innovative approach with regard to additive manufacturing approaches The reaction of the resin and the respective change in its viscosity during the curing process will be considered and incorporated in future steps in experimental design and simulation of 3D structures.

9. References

(Ablitz 2018) Abliz, D.: Functionalization of Fiber Composites with Nanoparticle-Modified Resin Systems, PhD diss, Clausthal University of technology, Papierflieger Verlag GmbH, ISBN 978-3-86948-632-1.

(AKV 2013) AKV: Handbuch Faserverbundkunststoffe/Composites: Grundlagen, Verarbeitung, Anwendungen, 4th edn. Springer Vieweg, ISBN 978-3-658-02754-4.

(Alms et al. 2010) Alms, J.B., Correia, N.C., Advani, S.G., Ruiz, E.: Experimental procedures to run longitudinal injections to measure unsaturated permeability of LCM reinforcements. FCPM Collaboration.

(ANSYS 2013) ANSYS: Fluent Theory Guide Release 15.0.

(Arranda 2017) Aranda G.S.: Contribution to the characterization of the compaction of fiber reinforcements for composite manufacturing and repair, PhD diss, Clausthal University of technology, Papierflieger Verlag GmbH, ISBN 978-3-86948-548-5,

(Carrman 1997) Carman P.C.: Fluid flow through granular beds. Chemical engineering research & desing.

(Ferziger and Pric 2008) Ferziger, J. H., Peric M.:Numerische Strömungsmechanik. Springer-Verlag, Berlin Heidelberg, ISBN 978-3-540-67586-0.

(Gebart 1992) Gebart B.R.: Permeability of unidirectional reinforcements for RTM, Journal of composite materials.

(Hirt and Nichols 1981) Hirt, C. W., Nichols, B. D.: Volume of fluid (VOF) method for the dynamics of free boundaries, Journal of Computational Physics, Volume 39, Issue 1, Pages 201-225, ISSN 0021-9991, https://doi.org/10.1016/0021-9991(81)90145-5.

(Mekic et al. 2009) Mekic, S., Akhatov, I., Ulven, C.: Analysis of a radial infusion model for in-plane permeability measurements of fiber reinforcement in composite materials: Polymer Composites, 30, 1788-1799

(Phelan 1997) Phelan, F. R.: Simulation of the injection process in resin transfer molding. Polym Compos, 18: 460-476. doi:10.1002/pc.10298.

(Potter and Ward 2015) Potter K., Ward C.: Draping processes for composites manufacture. Advances in Composites Manufacturing and Process Design, Philippe Boisse, ISBN 9781782423072

(Sharman and Siginer 2010) Sharman S., Siginer D.: Permeability measurement methods in porous media of fiber reinforced composites. Applied mechanics reviews.

(Srinivasan et al. 2011) Srinivasan, V., Salazar, A. J., Saito, K.: Modeling the disintegration of modulated liquid jets using volume-of-fluid (VOF) methodology, Applied Mathematical Modelling, Volume 35, Issue 8, Pages 3710-3730, ISSN 0307-904X, https://doi.org/10.1016/j.apm.2011.01.040.

(Szymkiewicz 2013) Szymkiewicz A.: Modelling water flow in unsaturated porous media accounting for nonlinear permeability and material heterogeneity, Springer, Berlin.

(Voller 2009) Voller, V. R.: Basic Control Volume Finite Element Methods for Fluids and Solids. Co-Published with Indian Institute of Science (IISc), Bangalore, India, ISBN 978-981-283-499-7.

Project data

The project is funded from SWZ with one TV-L E13 staff position since July 2017 at the site Clausthal. Involved scientists are:

Prof. Dr.-Ing. Dieter Meiners
Polymer Materials and Plastics Engineering
Clausthal University of Technology

Prof. Dr.-Ing. Dietmar P.F. Möller
Research group Stochastische Modelle in den Ingenieurwissenschaften, Institute of Applied Stochastics and Operations Research
Clausthal University of Technology

Juliana Rivas-Botero, M.Sc.
Research group Stochastische Modelle in den Ingenieurwissenschaften, Institute of Applied Stochastics and Operations Research
Clausthal University of Technology

Huynh Khiem Le, M. Sc.
Research group Stochastische Modelle in den Ingenieurwissenschaften, Institute of Applied Stochastics and Operations Research
Clausthal University of Technology

Isabell A. Jehle, M.Sc.
Research group Stochastische Modelle in den Ingenieurwissenschaften
Institute of Applied Stochastics and Operations Research
Clausthal University of Technology

The Virtual Microscope: Interactive Visualization of Gaps and Overlaps for Large and Dynamic Sphere Packings

Feng Gu, Michael Kolonko, Thorsten Grosch

1 Introduction and Research Goals

Particle packings form the basis of many materials from different fields like concrete, pills and tablets for medical purposes or powders for 3D printing. Important properties of the final material are determined by geometrical properties of the dry particle packing. Simulating and inspecting these packings may therefore help to develop materials with a particular desirable property.

If we approximate particles by spheres, as it is quite common in material sciences (see e.g. [20]), then the mixture is determined by its *particle size distribution* (PSD) that describes the percentage of particles for each radius.

There are several ways to simulate a packing (see e.g. [1]). If the aim is to obtain a very dense random packing, the so-called *collective rearrangement* (CR) algorithms seem to be superior. Here, a sample of spheres from the PSD is placed randomly in a container which at the beginning is chosen so small that each of the spheres must overlap with others. A repulsion between the spheres is simulated and the container is enlarged stepwise until a non-overlapping placement is reached.

As this algorithm does not aim at simulating the true physical forces that generate a packing, it is of great importance to inspect the final packing as well as its generation process to judge the quality of the simulation. It may e.g. happen, that some overlaps between spheres remain or that there are unrealistic holes in the packing. If the packing simulates a *foam*, then the spheres represent gas bubbles and the main interest is in the shape of the interstices.

Therefore the development of a flexible *visualization tool* for the simulation became necessary. It should allow the material scientist to inspect the final packing for its properties, but it should also help the developer to check the correctness of the complex simulation algorithms and the impact of their parameters.

More precisely, it should allow to navigate through the packing, select spheres, inspect its overlaps and visualize the free space. This should not only be possible for the final static packing but also during its generation to see the repulsion between the spheres and the gradual vanishing of the overlaps. Realistic simulation of e.g. concrete mixture needs huge samples of particles (see [9]). An additional challenge is the large variation of sphere sizes needed in one sample for a realistic simulation of e.g. concrete mixtures. They comprise spheres with diameters from 0.1 micrometers up to centimeters. Today, highly parallel simulations on the GPU allow one CR iteration with millions of spheres within milliseconds ([22]).

Although sophisticated methods exist to visualize the spatial placement of particles, simply drawing spheres in 3D does not show where the *remaining overlaps* or the *existing gaps* between the spheres are (see Figure 1). We therefore develop a visualization for collective rearrangement of spheres that allows a direct *rendering of gaps and overlaps*. Our method runs entirely on the GPU and supports large and dynamic sphere packings at interactive to real-time frame rates. The user can interactively inspect the current simulation and see where spheres still overlap, as well as the remaining free space between them. We demonstrate that such a visualization is more helpful than standard techniques like drawing the spheres in combination with 2D clipping planes.

These visualization tools were developed in close cooperation with a GPU-based simulation tool which is described in more detail in [22]. Similar to the former sequential simulation programs that e.g. utilized loose octrees to store the sphere locations (see [9],[15]), the GPU-based simulation also makes use of concepts from visualization so that both, simulation and visualization, use identical core data structures that can easily be exchanged between both parts of the program system.

The "Virtual Microscope" is a joined project between the Department of Informatics and the Institute of Applied Stochastics and Operations Research at TU Clausthal. This report summarizes our publication [7] which contains further details.

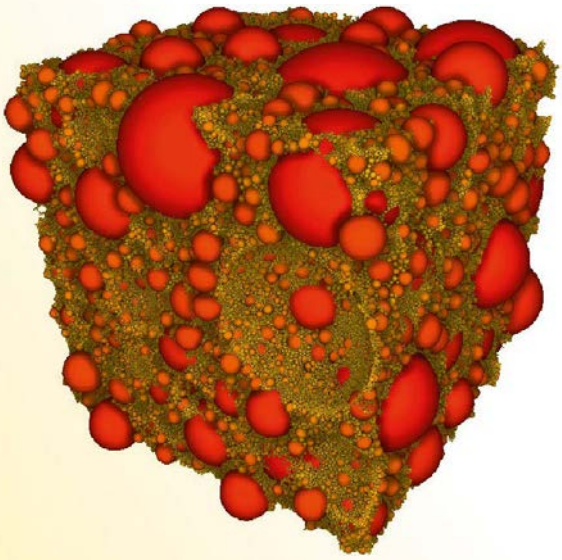

Figure 1: A sphere packing consisting of one million spheres. Large spheres are drawn in red, small spheres are drawn in yellow. The periodic boundary shows the space that spheres from the opposite side occupy. Due to the unfinished collective rearrangement process, some of the spheres are still overlapping, which is hard to see in a standard visualization.

2 Collective Rearrangement Simulation

We use collective rearrangement to determine the spatial placement of the spheres. A sequential implementation of this algorithm already existed from previous projects [16], [9]. Based on this, we developed a parallel GPU implementation of collective rearrangement which achieves interactive speed in the contemporary project "RaSim.

Given an arbitrary particle size distribution, we start with random sphere positions, and then use collective rearrangement to remove the overlaps. In this iterative process, overlapping spheres push each other away by a slight amount in each iteration. To cope with a large number of spheres, the spheres are inserted in a loose octree according to their size. In this way, possible candidates for collision are detected quickly. Our simulation uses a cubic container in combination with different border types. Beside a hard border that prevents the spheres from leaving the container, we also support a *periodic boundary* that allows a *tiling* of the sphere packing where spheres can *wrap-around* at each border. In this case, spheres intersecting the border are virtually duplicated for collision checks at the opposite border. Our method requires roughly 30 ms for one CR iteration with one million spheres and achieves good correspondence with measured densities of real materials.

3 Direct Sphere Visualization

Our method requires a visualization of spheres with pixel precision to correctly detect the existing gaps and overlaps between the spheres using a perspective projection. For a fast visualization we use billboards and start by drawing a point for each sphere [4],[5],[6],[10]. As a data structure, we use a Vertex Buffer Object (VBO) which stores position, color and radius for each sphere. We then use a geometry shader to generate a view-aligned quad for each point. To conservatively rasterize the sphere region, the quad is oriented orthogonal to the sphere center direction with a size adjusted to the sphere radius. Finally, a fragment shader is used to compute the intersection of each pixel ray with the sphere. In case of an intersection, the intersection point, the intersection normal and the sphere color are drawn into a geometry buffer. Otherwise, the fragment is discarded. Afterwards, we use deferred shading and illuminate all visible fragments based on the information in the geometry buffer (position, color, normal). Finally, we use screen-space ambient occlusion [13],[18] to display contact shadows

between nearby spheres to intensify the visual impression of the placement.

4 Voxel-based Visualization of Overlaps and Gaps

Although our visualization of spheres gives a good impression of the spatial arrangement of the spheres, it is hard to judge where the remaining overlaps and free spaces are. While this is easy to see in 2D, it is practically invisible in 3D due to the mutual occlusions of the spheres. To better evaluate the quality of the collective rearrangement, we developed a direct visualization of gaps and overlaps in 3D.

A simple solution for this problem is to use a voxel model (3D grid), such that the whole scene consists of many small cubes (voxels). Overlaps and gaps can then be drawn as voxels in different colors. Since standard solid voxelization methods [3] do not work correctly when the objects are overlapping, we developed an own parallel voxelization method for the spheres: One thread is used for each sphere which fills the corresponding voxels for the sphere. Therefore, the bounding box of the sphere is determined and afterwards each voxel inside the bounding box is tested, whether it is inside the sphere or not. Simply inverting this voxel model results in a visualization of the free spaces (gaps) between the spheres. Overlaps are also easy to detect: We simply have to check if a voxel is set multiple times. Figure 2 shows an example for a voxel-based visualization for a small number of spheres.

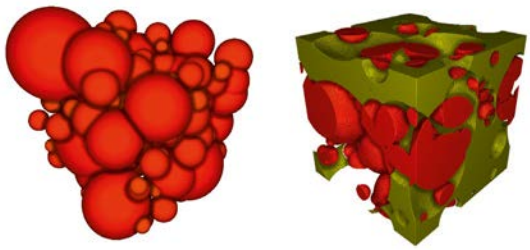

Figure 2: Left: 128 spheres. Right: Voxel model that draws the overlaps (red) and gaps (yellow) as small cubes. For a voxel resolution of 256^3, a frame rate of 10–20 frames per second can be reached.

Although the voxel model is a simple and quite fast solution, the main problem is the required memory. Since the memory grows with $O(n^3)$, the voxel resolution must be quite low: Only 512^3 voxels are possible for the typical GPU memory. Therefore, many small spheres can not be displayed correctly.

5 Visualization of Overlaps and Gaps using Pixel-linked Lists

To be able to work with a large number of potentially small spheres we decided to create this visualization directly in *screen space* with pixel precision.

GPU Linked Lists

Our work is based on the idea of GPU linked lists introduced in [21], which provides a method to dynamically construct highly concurrent linked lists on modern graphics processors. To construct a GPU linked list, two buffers are needed: One large *node buffer* which contains nodes of the linked list and another screen-sized *head pointer buffer* to store head pointers, each pointing to the start of a linked list in the node buffer, for each pixel. Figure 3 shows a small example: Here the pixel which has the value 4 on its head pointer buffer has its node information stored on the position 4 in the node buffer. This node contains a tail pointer that refers to the position of the last node that its pixel owns, which is 1 in this case. Each time a new color is written to a pixel, the global atomic counter is increased by one and a

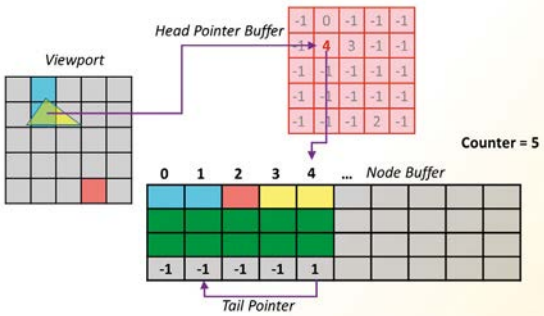

Figure 3: Calculations for a GPU linked list (based on [21]). Each column in the node buffer stands for a node. Information needed later such as index can be stored in the green parts for each node.

new node is written into the position indicated by the counter in the node buffer, with its tail pointer pointing to the position indicated by the head pointer of the pixel. If the head pointer has value –1, the tail pointer keeps its initial value –1. Then the head pointer is set to the position of the new node in the node buffer.

Spheres in Linked Lists

When applied to order-independent transparency, a GPU linked list needs 3 elements (color, depth and tail pointer) per hit point between the ray and the surface of a rendered object. This results in 12 bytes per hit point if each element requires 32 bits. In our work, we need only 16 bytes *for each pair* of hit points (enter and leave of ray-sphere-intersection). We first render all spheres and insert their enter and leave depth values in linked lists. To save GPU memory, we only store the following information for each list entry: Enter and leave depth (2 × float), the sphere index (1 × int) and the tail pointer (using 32 bits for each). The sphere index allows the implementation of a selection function, such that the user can select one overlap per mouse click and get information about the spheres that form the overlap. Besides, the sphere index is used to read the center position (3 × float) and the basic color (1 × int) for one sphere. Thus the position, normal, and color of an enter/leaving point can be calculated based on the depth value on the fly for later illumination. The depth values are stored as positive, linear z values in eye coordinates. For each of our visualizations, we first sort the depth values of each linked list along the z-axis until the surface for overlaps/gaps is found. Except of transparent renderings, we stop the sorting process at this point. We therefore need a sorting algorithm that copies the smallest element to front in each iteration, since this enables an early break of the sorting. In our work, Heapsort is applied here, since this is a non-recursive, in-place sorting algorithm which extracts the smallest element in O(log(n)) steps. Since we allow both a container with hard and periodic boundary conditions, we have to differentiate between them for visualization.

5.1 Rendering Overlaps

To detect whether there are overlapping spheres along a camera ray, we make the following observation: In case of non-overlapping spheres, we have *alternating* enter and leave points along the camera ray. Whenever two spheres are overlapping, this pattern is changing and we observe *two successive enter points*. The second enter point is the one we need to draw, as can be seen in Figure 4. Figure 5 shows a small rendering with a few spheres and the resulting overlaps. The resulting „lenses" effectively describe a CSG intersection operation [8],[17],[19].

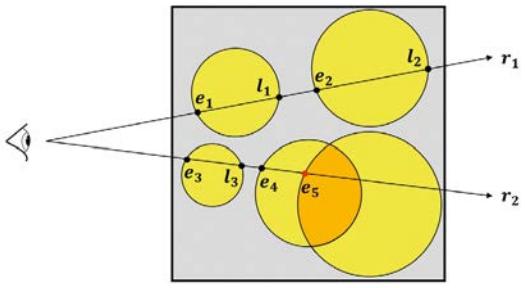

Figure 4: Rendering overlaps: For non-overlapping spheres, we have alternating enter and leave points (ray r_1). In case of an overlap, we get two successive enter points (e_4 and e_5 on ray r_2). The second enter point (e_5) is drawn. The overlap part is marked in orange.

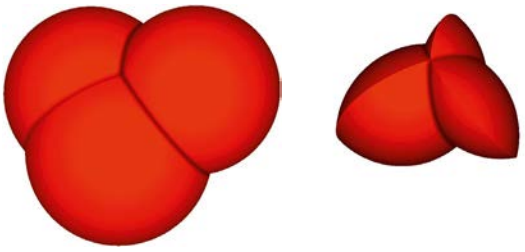

Figure 5: Three spheres and the corresponding overlap rendering.

5.2 Rendering Overlaps under Periodic Boundary Conditions

In case of periodic boundary conditions (PBCs), spheres can leave the container on each side and enter the container at the opposite side during collective rearrangement (wrap-around). PBCs have been applied extensively in theoretical modeling of crystalline solids [12], electrostatic systems

[11] and biomolecular systems [2] etc., since a large (infinite) system can be approximated by using a small part called unit cell (container).

For a correct visualization, we need to make a *virtual copy* of each sphere which intersects the border to make sure that we display all overlaps with spheres from the opposite border. Since the periodic boundary results in overlapping spheres *outside* the container we have to extend our overlap test: Detected overlaps outside the container are either discarded or projected to the container border. Figure 6 shows an example with the different cases.

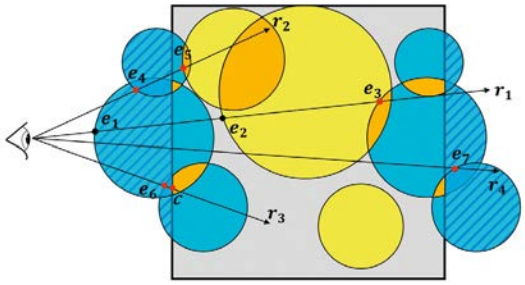

Figure 6: Different cases for rendering overlaps under pbcs. Spheres intersecting the border are virtually duplicated and drawn in blue. The parts outside of the container are marked with stripes and emerge on the opposite border. Overlaps inside the container are drawn in orange. Ray r_1 shows an overlap inside the container. Detected overlaps outside the container can be discarded: Ray r_2 detects an overlap at e_4 which is skipped and e_5 is drawn. For ray r_4, the detected overlap at e_7 is ignored because it is behind the container. Ray r_3 detects at overlap in front of the container which is projected to the border ($e_6 \rightarrow c$).

5.3 Rendering Gaps under Periodic Boundary Conditions

During collective rearrangement, it is interesting to see the empty regions where the overlapping spheres can still move into. Therefore we would like to *invert* the sphere rendering and visualize the surrounding empty space between the spheres. We use this type of visualization mainly for a periodic boundary, since a hard boundary effectively shows the container. In case of a periodic boundary, several spheres intersect the border and the visualization then shows the space between them. The basic idea to visualize this empty space is as follows: If the first intersection point along the camera rays is the container boundary, we are finished. If we first hit a sphere (which is outside the container due to the periodic boundary), we travel along the ray until we find a leave point which is *not in an intersection* between spheres. If this point is inside the container, we found the backside of the sphere that we are searching for. This point can then be rendered as the frontside of the empty space and illuminated with the inverted normal. Figure 7 shows a small example with different cases.

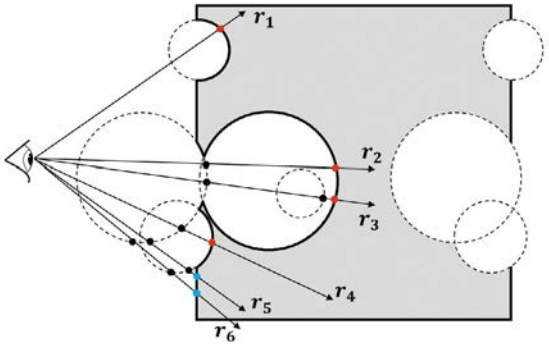

Figure 7: Different cases for rendering gaps under pbcs. Black points are visited by corresponding rays and red points stand for the surface points of gaps. Ray r_1 directly detects the first leave point as the front surface of the empty space. For rays r_2 up to r_4, several leave points must be checked until the first leave point without sphere intersection is found. Rays r_5 and r_6 detect leave points in front of the container and are therefore discarded.

Figure 8 shows a small rendering with the empty space of two spheres. This type of rendering leads to a „cheese-like" appearance, where spheric holes are extracted from the container cube, similar to a CSG subtraction operation.

6 Volume Calculation

During collective rearrangement we would like to judge whether the quality of the simulation still improves. In this case, overlapping spheres are still moving into the remaining free spaces. This means that both the total amount of overlap and

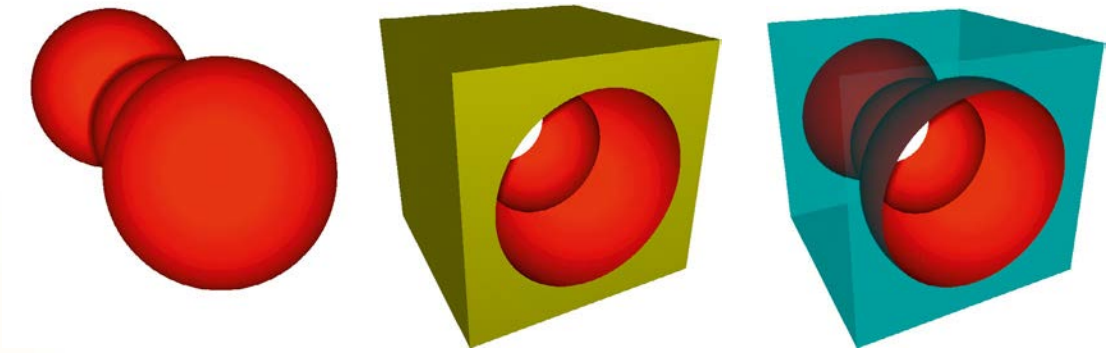

Figure 8: Rendering gaps for two spheres under pbcs: One sphere intersects the container border (left), so it is duplicated to the opposite border. Center: Resulting empty space rendering. Right: Empty space rendering with transparent container.

the amount of remaining free space decrease. The required analytic computation of the intersection volume of multiple spheres is possible, but complicated. Instead, we use the linked lists per pixel to compute the total free volume and the total overlap volume at pixel precision. The basic idea is to compute the volume for each pixel as a sum of cuboid (orthographic) or frustum (perspective) volumes, resulting from the stored depth values. If the used sphere packing contains spheres smaller than a pixel, we use *tiled rendering* in combination with an orthographic projection. The tile resolution is then adjusted, such that the smallest spheres are still larger than a pixel.

In the following, we assume a viewport resolution of w×h pixels. To determine the volume V of a pixel, we start with 0 and compute the volume by iterating through the linked list. The total volume is then determined as the sum of all pixel volumes.

6.1 Volume Calculation under Orthographic Projection

If orthographic projection is applied, the area A_p of each pixel is simply

$$A_p = \frac{(t-b)(r-l)}{hw} \quad (1)$$

where t,b are coordinates for the top and bottom horizontal clipping planes and r,l are coordinates for the right and left vertical clipping planes.

Therefore, for each pair of matched enter point with depth d_e and leave point with depth d_l, the difference $d_l - d_e$ is added to V and the sum of V over all pixels is finally multiplied by A_p given by equation ((1)) to calculate the approximated volume.

6.2 Volume Calculation under Perspective Projection

Using perspective projection with field of view angle θ and viewport aspect ratio α, the area A_p of each pixel corresponds to a rectangle with side length $2z\tan(\theta/2)/h$ in y direction and the side length $\alpha 2z\tan(\theta/2)/w$ in x direction. The pixel area can therefore be calculated as

$$A_p = \frac{4z^2\alpha\tan(\theta/2)^2}{hw} \quad (2)$$

where z is the depth value in the eye coordinate system of the point belonging to the current pixel. Under perspective projection, for each pair of matched enter point with depth d_e and leave point with depth d_l, the difference $d_l^3 - d_e^3$ is added to V and the sum of V over all pixels is finally multiplied by $4\alpha\tan(\theta/2)^2/(hw)$ based on equation ((2)) to calculate the approximated volume.

7 Results

All performance measurements were conducted on an NVIDIA GeForce GTX 1080 graphics

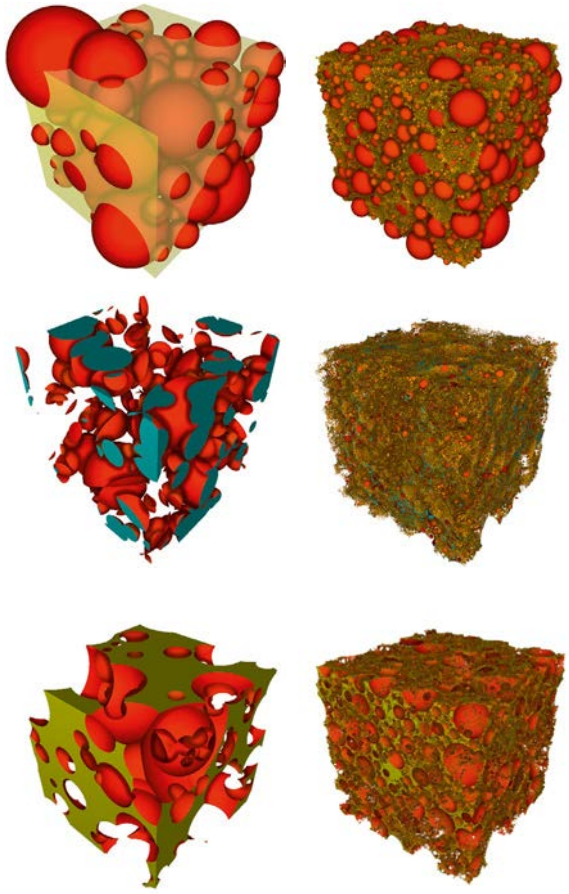

Figure 9: Overlaps (center row) and gaps (bottom row) for 128 spheres (left) and one million spheres (right). Please note that PBCs are used here, therefore some gaps and overlaps can result from spheres at the opposite border. The transparent yellow cube is the container, overlaps on the container border are drawn in blue.

card with 8 GB video RAM. The PC is equipped with an Intel Core I7-6700K processor, 4.00 GHz CPU, 32 GB RAM, running Windows 10 (x64). The viewport resolution is set to 768×768 pixels. Please see the following video for real-time frame captures: http://www2.in.tu-clausthal.de/~cgstore/publications/2017_Gu_VMV.mp4

Figure 9 shows our renderings of gaps and overlaps for different numbers of spheres. For rendering the whole container with one million spheres, the frame rate is 58 fps for the standard rendering and 45 fps for our overlaps and gaps visualization. In combination with the CR simulation, the frame rate drops to 20 fps for standard rendering and 18 fps for overlaps and gaps. Including the volume calculation requires approximately 17 ms additional time. The memory requirements for storing the linked lists are approx. 161 MB. Our largest data set contains ten million spheres. Here, we still reach a frame rate of 17 fps for the standard rendering and 11 fps for gaps and overlaps visualization. We observed that both the rendering time and the memory requirements increase linearly with the viewport resolution. Furthermore, the memory requirements increase linearly with the summed cross sectional area of all spheres.

In certain situations, it can be helpful to see a combination of overlaps and gaps in the same image. Figure 10 shows such a rendering (47 fps for one million spheres). Here, gaps from large spheres are visible as well as their overlaps with many, small surrounding spheres „on the border" of the gaps.

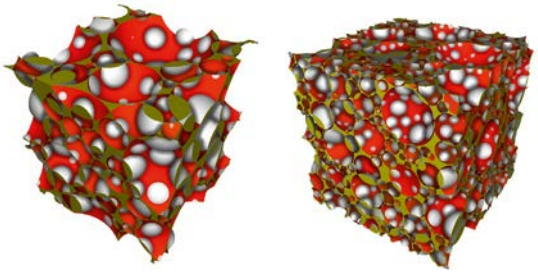

Figure 10: Combined rendering with both overlaps (drawn in grey) and gaps (drawn in red) for 128 spheres (left) and 1024 spheres (right).

The usual way to see gaps and overlaps between objects is the insertion of 2D clipping planes. Figure 11 shows a comparison between a 2D clipping plane and our 3D visualization of overlaps. Note that it is difficult to get an overview of the distribution and shape of the overlaps only based on a moving 2D clipping plane. When combined with a clipping plane, our method also shows the overlaps on the clipping plane, but in addition, the 3D structure of the overlaps behind the clipping plane. We found this a more useful combina-

tion than flying inside the 3D structure, which can become confusing. Please see the video to spot the difference between the different approaches and also the combination of our gap and overlap visualizations with a clipping plane. In addition, the video shows renderings with transparency and a user-defined virtual „stirring“ to resolve overlaps that remain after the CR simulation.

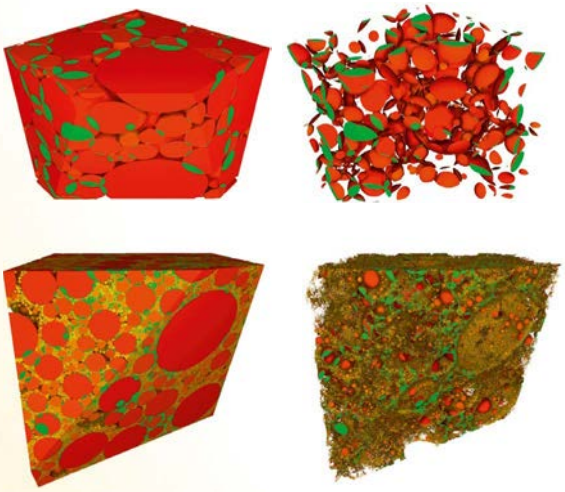

Figure 11: Comparison of our 3D overlap rendering with standard 2D clipping planes for 128 spheres (top) and one million spheres (bottom). Overlaps at the clipping plane and at the container border are drawn in green.

8 Conclusion and Future Work

We presented a new visualization technique to display overlaps and gaps in large sphere packings. For collective rearrangement simulations, this allows the user to inspect the quality of the simulation in each iteration. Our method reaches interactive to real-time frame rates for millions of spheres. Showing these structures in 3D gives a better impression of their shape than using 2D clipping planes.

As future work, we intend to integrate more realistic particle shapes, like polyhedrons [6] or collections of spheres, both in the visualization and the simulation. In case of even larger sphere packings, with many spheres that are smaller than a pixel, we examine if ray casting in combination with the loose octree can be used to display the gaps and overlaps more quickly [4]. We investigate if additional visualization techniques, like depth-aware contours or depth darkening can improve the perception of the gaps and overlaps rendering [13]. Since we detect the position of overlaps and gaps regions, repelling forces could be added in the overlap regions, as well as attracting forces in the gaps regions, to automatically improve the simulation, which could lead to a higher density of the sphere packing. Furthermore, we plan to use the visualization for other types of simulations, like random sequential addition, where spheres are attracted by gravity and roll down until they have at least three contact points, which often leaves large gaps between the spheres.

References

[1] Bezrukov, Alexander and Bargiel, Monika and Stoyan, Dietrich and others. Statistical analysis of simulated random packings of spheres. Particle & Particle Systems Characterization, 19(2):111, 2002.

[2] Cheatham, TE III and Miller, JL and Fox, T and Darden, TA and Kollman, PA. Molecular dynamics simulations on solvated biomolecular systems: the particle mesh Ewald method leads to stable trajectories of DNA, RNA, and proteins. Journal of the American Chemical Society, 117(14):4193–4194, 1995.

[3] Eisemann, Elmar and Decoret, Xavier. Single-pass GPU solid voxelization for real-time applications. Proceedings of Graphics Interface 2008, pages 73-80

[4] Falk, Martin and Krone, Michael and Ertl, Thomas. Atomistic Visualization of Mesoscopic Whole-Cell Simulations Using Ray-Casted Instancing. Computer Graphics Forum, 32(8):195–206, 2013.

[5] Grottel, S. and Krone, M. and Müller, C. and Reina, G. and Ertl, T. MegaMol – A Prototyping Framework for Particle-based Visualization. Visualization and Computer Graphics, IEEE Transactions on, 21(2):201–214, 2015.

[6] Grottel, Sebastian and Reina, Guido and Zauner, Thomas and Hilfer, R and Ertl, Thomas. Particle-based rendering for porous media. Proceedings of SIGRAD 2010: Content aggregation and visualization; November 25–26; 2010; Västerås; Sweden, number 052, pages

45–51, 2010. Linköping University Electronic Press.

[7] Gu, Feng and Yang, Zhixing and Kolonko, Michael and Grosch, Thorsten. Interactive Visualization of Gaps and Overlaps for Large and Dynamic Sphere Packings. Proc. Vision, Modeling and Visualization (VMV) 2017, pages 103-110

[8] Florian Kirsch and Jürgen Döllner. Rendering Techniques for Hardware-Accelerated Image-Based CSG. The 12-th International Conference in Central Europe on Computer Graphics, Visualization and Computer Vision'2004, WSCG 2004, University of West Bohemia, Campus Bory, Plzen-Bory, Czech Republic, February 2-6, 2004, pages 221–228, 2004.

[9] Kolonko, M. and Raschdorf, S. and Wäsch, D. A hierarchical approach to simulate the packing density of particle mixtures on a computer. Granular Matter, 12(6):629–643, Springer, 2010.

[10] Kozlikova, B. and Krone, M. and Falk, M. and Lindow, N. and Baaden, M. and Baum, D. and Viola, I. and Parulek, J. and Hege, H.-C. Visualization of Biomolecular Structures: State of the Art Revisited. Computer Graphics Forum, 36(8):178–204, 2016.

[11] de Leeuw, Simon W and Perram, John William and Smith, Edgar Roderick. Simulation of electrostatic systems in periodic boundary conditions. I. Lattice sums and dielectric constants. Proceedings of the Royal Society of London A: Mathematical, Physical and Engineering Sciences, number 1752, pages 27–56, 1980. The Royal Society.

[12] Makov, Ge and Payne, MC. Periodic boundary conditions in ab initio calculations. Physical Review B, 51(7):4014, 1995.

[13] Claudio Montani and Marco Tarini and Paolo Cignoni. Ambient Occlusion and Edge Cueing for Enhancing Real Time Molecular Visualization. IEEE Transactions on Visualization and Computer Graphics, 12:1237-1244, 2006.

[14] Mathieu Le Muzic and Julius Parulek and Anne-Kristin Stavrum and Ivan Viola. Illustrative Visualization of Molecular Reactions using Omniscient Intelligence and Passive Agents. Computer Graphics Forum, 33(3):141–150, 2014. Article first published online: 12 JUL 2014.

[15] Raschdorf, S and Kolonko, M. A comparison of data structures for the simulation of polydisperse particle packings. International journal for numerical methods in engineering, 85(5):625–639, 2011.

[16] Raschdorf, Steffen and Kolonko, Michael. Loose octree: a data structure for the simulation of polydisperse particle packings. Technical report, TU Clausthal, 2009.

[17] João Lucas Guberman Raza and Gustavo Nunes. Screen-Space Deformable Meshes via CSG with Per-Pixel Linked Lists. In Wolfgang Engel, editors, GPU Pro 5, pages 233–240. CRC Press, 2014.

[18] Tobias Ritschel and Thorsten Grosch and Hans-Peter Seidel. Approximating Dynamic Global Illumination in Image Space. Proceedings ACM SIGGRAPH Symposium on Interactive 3D Graphics and Games (I3D) 2009, pages 75–82, 2009.

[19] Jarek Rossignac and Ioannis Fudos and Andreas Vasilakis. Direct rendering of Boolean combinations of self-trimmed surfaces. Computer-Aided Design, 45(2):288–300, 2013.

[20] Salvatore Torquato. Random Heterogenous Materials: Microstructure and Macroscopic Properties, volume 16 of Interdisciplinary Applied Mathematics. Springer, 2nd edition, 2006.

[21] Yang, Jason C. and Hensley, Justin and Grün, Holger and Thibieroz, Nicolas. Real-time Concurrent Linked List Construction on the GPU. Proceedings of the 21st Eurographics Conference on Rendering in EGSR'10, pages 1297–1304, Aire-la-Ville, Switzerland, Switzerland, 2010. Eurographics Association.

[22] Yang, Zhixing and Gu, Feng and Grosch, Thorsten and Kolonko, Michael. Accelerated Simulation of Sphere Packings Using Parallel Hardware. Simulation Science (2017), Springer.

Project data

The project is funded from SWZ with 0.5 TV-L E13 staff positions since September 2016 at the site Clausthal. Involved scientists are:

Prof. Dr. Michael Kolonko
Research group Stochastische Optimierung, Institute of Applied Stochastics and Operations Research
Clausthal University of Technology

Feng Gu, M.Sc.
Research Group Graphical Data Processing and Multimedia
Department of Informatics
Clausthal University of Technology

Prof. Dr. Thorsten Grosch
Research Group Graphical Data Processing and Multimedia, Department of Informatics, Clausthal University of Technology

Pressure-induced phase transformations in Fe-C alloys: Molecular dynamics simulations

Hoang-Thien Luu, Nina Gunkelmann

1.Introduction

Iron is not only the most abundant element in both earth's crust and earth's core, but is also widely used in industry. Steels are the material of choice in a variety of applications.

Understanding the mechanical response of iron under high pressure is of particular importance. It is well known that iron has a stable body-centered cubic (bcc) crystal structure at ambient conditions. However, it transforms to the face-centered cubic (fcc) phase at a temperature above 912 °C and the hexagonal close-packed (hcp) structure under a pressure of 13 GPa[1-2]. A schematic phase diagram is shown in Fig. 1 including a sketch of the crystal structures.

Several experimental techniques such as dynamic shock wave loading[11] and rotational diamond anvil cells[10] provide insights into the mechanical response of iron under compression. Iron undergoes an elastic-plastic transition before the transformation from the bcc to the hcp structure leading to a three-wave shock structure of elastic wave, plastic wave and phase transition. The pressure-induced phase transformation in iron has been intensively investigated including experiments [3,4,5,6,7,8,9,10,11,12,13] and numerical methods, [14,15,16,17,18,19,20,21,22,23] both in single crystals and polycrystals.

In agreement with experiments, *ab initio* simulations confirm the stability of the hcp phase under pressure and provide reliable data for the development of interatomic interaction potentials. Molecular dynamics (MD) is a powerful tool to examine the transformation process and provides insights into the transformation mechanism [21,22,4,25,26] as well as the formation of twins and stacking faults in the hcp phase [17,19,20,22,27]. Recent experimental observations suggest that the transition pressure increases with increasing strain rate[11,12,28,29] and highly depends on impurity concentrations [30,31,32].

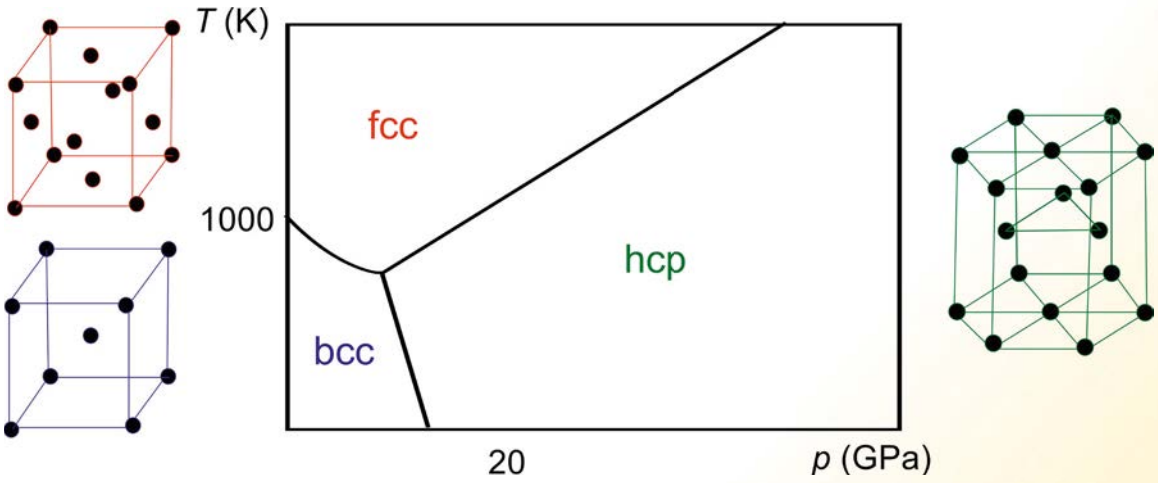

Figure 1: Phase diagram of iron and sketch of the crystal structures.

Furthermore, alloying elements in iron can change the mechanical properties dramatically[33]. Atomistic simulations were performed to study the mechanical behavior of Fe-Ni [34,35,36], Fe-Cu [37-38], Fe-Cr[39] and Fe-P[40]. The behavior of Fe-C systems is of particular important because carbon forms the basis of steels. Molecular dynamics studies report strong influences of carbon on elastic properties[41], properties of edge and screw dislocations [42-43] and austenitization temperature, [44,45] in reasonable agreement with experiments.

However, the role of carbon in the pressure-induced transformation process is still unclear. In this project, we employ MD simulations to study the behavior of pure iron and Fe-C under dynamic loading at high pressure. We describe details of our simulation method, interaction potentials and sample generations in section 2. Results and discussions are reported in section 3. To validate our potentials, we calculate lattice parameters in subsection 3.1 and equilibrium transformation pressures in subsection 3.2. In subsection 3.3 and 3.4 the mechanical response of pure iron and Fe-C single crystals under hydrostatic compression at high strain rates is studied. The influence of carbon on the material behavior of polycrystalline iron under homogeneous uniaxial compression is reported in section 3.5. We compare our results with experimental data.

2. Simulation method

2.1 Interaction potentials

Interatomic interaction potentials are used to calculate the forces between atoms, their potential energies and the trajectory of atoms by solving the second Newton's equation:

$$\boldsymbol{F}_i = m\ddot{\boldsymbol{r}}_i.$$

The potential energy E_{pot} ($\{r_1..r_N\}$) results from the interaction $\phi(r_{ij})$ of atom i with each other atom j. From

$$\boldsymbol{F}_i = \frac{-dE_{\mathrm{pot}}}{dr_i},$$

with the distance between atoms r_{ij}, we follow:

$$E_{\mathrm{pot}}(\{r_1..r_N\}) = \sum_{ij} \varphi(r_{ij}).$$

For metal systems, it is appropriate to approximate the presence of the electron cloud by the so-called embedded-atom method (EAM) which includes pair-wise interaction as well as the contribution of the electron cloud. The total energy of an atom i is given by:

$$E_i = \frac{1}{2}\sum_{i\neq j} \emptyset_{\alpha\beta}(r_{ij}) + F_\alpha\left(\sum_{i\neq j}\rho_\beta(r_{ij})\right)$$

where the pair potential interaction is defined by $\varnothing$ and the contribution of the electron cloud is described by the embedding energy F_α which is a function of the electron density ρ_β.

Iron is one of the most studied elements and there are various Fe interatomic potentials to study different aspects of the material behavior. A large fraction of iron potentials have been created for understanding radiation damage and the generation of point defects at low temperatures. Some potentials were developed to study thermal properties and aim at correctly describing the melting transition[19]. There are several potentials which reproduce the temperature-induced phase transition from bcc to fcc[44,46].

However, only a few potentials accurately predict the behavior of iron under high pressure. Among these, we can mention the Voter potential[47], the new Ackland potential[22], and the Lee potential[48]. Recently, Gunkelmann et al.[22] benchmarked various Fe potentials. The authors found that under equilibrium conditions, the Mendelev potential predicts 57.1 GPa as transformation pressure, more than four times larger than results from experiments and DFT calculations. The Voter potential[47] provides a transformation pressure at 8.1 GPa, lower than the experimental prediction, and there is no evidence of plasticity before the phase transformation[21]. This potential does not perform well in describing the mechanical response to compression: it overestimates grain boundary sliding resulting in material softening

and unrealistic temperature increase. In addition, a large amount of fcc is given instead of the experimentally expected hcp phase. The potential by Lee[48] also shows a reasonable threshold transformation pressure, but models dislocation properties less accurately. Only the new Ackland potential[22] fairly describes both the plastic behavior and the phase transformation.

Thus, the modified Ackland potential[22] is a good candidate for studying the mechanical response of iron under extreme pressure conditions. We coupled the Ackland potential for Fe-Fe interactions together with three well-known Fe-C potentials: the pair potential by Johnson[49], the EAM potential by Hepburn and Ackland[50], and a modified version of the Becquart potential [51-52].

The Johnson potential[49] accurately predicts the energetically favorable carbon interstitial site, the activation volume and energy of the migration of carbon and the binding energy of the C atom to a vacancy. However, C-C interactions are excluded. From *ab initio* data, Becquart et al.[51] derived an EAM potential which correctly describes the tetragonal distortion of the bcc lattice by the addition of carbon, C-vacancy binding energies and the diffusion of carbon in ferritic iron. It also reproduces the diffusion barrier under external load. Later, the Becquart potential[51] was updated because the original potential predicted a saddle point which deviates from the experimentally described tetrahedral position[52]. The new potential improves the energy landscape around this saddle point. Hepburn and Ackland[50] generated a more realistic Fe-C potential incorporating short ranged covalent bonded carbon atoms. The potential is based on DFT calculations and was fitted to reproduce the energetic behavior of C interstitials. It fairly describes the interaction of carbon atoms with a wide range of defects in the iron matrix, and it reproduces the solubility of carbon in the iron matrix. It has been implemented in the LAMMPS compatible format EAM/FS.

In the following, the terms Ackland+Becquart, Ackland+Hepburn, and Ackland+Johnson refer to the potentials, which couple the modified Ackland potential[22] for the Fe-Fe interaction with the Fe-C interaction potential from Becquart[52], Hepburn[50] and Johnson[49], respectively.

2.2 Sample generation

We construct cubic Fe single crystals consisting of 250.000 iron atoms with an edge length of 14 nm.

The Voronoi construction method[53] was employed to generate a polycrystalline iron sample with 64 grains and approximately 2 million iron atoms in a cubic box with a length of 30 nm. For the Voronoi construction method, seeds are randomly inserted in the crystal. Polyhedrons are constructed such that each point in the polyhedron is closer to its central seed than to all other points. The edges of the polyhedron are the grain boundaries of the crystal. Although the structure of the grains can deviate from realistic samples, this method is frequently used. In a future investigation, we aim at constructing grains that are more realistic by simulating solidification of melted Fe-C crystal.

To study the impact of carbon, we randomly added C atoms achieving almost the maximum solubility of carbon in α-iron. We deleted all C atoms overlapping with the Fe matrix. In detail, pairs of Fe and C atoms whose distance of separation is smaller than the sum of their radii are searched for, and C atoms are removed. After this step, both single and polycrystals contain 0.1 at.% C.

Note that using this method the crystals will not be tetragonally distorted by carbon. The tetragonal distortion of Fe-C can be explained by the Bain transformation from fcc to bcc: Before the transition, the carbon atoms are in the octahedral interstitial sites of the fcc phase: in the middle edges and in the center of the cell. So, after transformation, the C atoms are distributed in octahedral sites of the bcc phase, aligned preferably along one axis. Since the carbon atoms are larger than the corresponding octahedral sites, the crystal will be tetragonally distorted.

To prevent any carbon-carbon interactions, the minimum distance between carbon atoms is 0.6 nm. At the end, carbon atoms are randomly distributed in iron single crystals and polycrystals.

In the beginning, carbon atoms are not located at their preferred stable positions. Therefore, a careful relaxation is needed to assure that C atoms

occupy their energetically favorable positions: the octahedral interstitial sites. The relaxation is also essential to equilibrate grain boundaries. Note however that segregation of carbon at grain boundaries in the polycrystalline samples is not considered in this study.

To relax our system, the samples were subjected to a high temperature annealing process at 80 % of the melting temperature during 100 ps. The heating and cooling ramps were performed during 5 ps. During the relaxation process, the pressure in all three normal directions of the system is kept at zero bar using a Nosé-Hoover barostat. This scheme has been frequently used to relax polycrystalline α-iron[22,23]. At the end of the relaxation process, the total energy per atom of all samples decreased by more than 0.05 eV/atom. The final temperature was 10 K. In Fe-C, carbon atoms inside the grains migrated to octahedral interstitial site (O-site). The tetrahedral sites (T-site) are found to be unfavorable for carbon atoms.

Note that sometimes several minima exist for the geometry of the octahedral site. Those secondary minima are frequently found for the Hepburn-Ackland potential. In a paper by Janßen et al.[54], it was found that structures containing secondary minima lead to strongly deviating values of the elastic constants. Although the probability that the relaxation procedure described above converges to the global minimum tends to 1 as the time to cool the system approaches infinity, the configuration still takes the risk to end up in secondary minima because of the limited time scale in MD simulations. Accordingly, an analysis is planned where different minimization schemes are compared to globally optimized interstitial sites of carbon atoms using exact methods of discrete optimization.

The transformation pressure of iron single crystals depends on its orientation[19]. Therefore, we implemented hydrostatic compression at a strain rate of 1×10^9 s^{-1} for single crystalline iron, with a maximum strain of 10 %.

For polycrystalline iron, uniaxial compression with the same strain rate was applied achieving a maximum strain of 20 %. We did not control the temperature during the deformation process to account for plasticity driven temperature effects. Simulations have been performed with the open source code LAMMPS[55]. To minimize the influence of surface effects we used periodic boundary conditions for all samples. Atom types were detected by adaptive Common Neighbor Analysis (CNA)[56] as implemented in OVITO[57].

3. Results

3.1 Lattice parameters

As explained above, carbon changes the lattice structure of iron because the carbon atoms are larger than the corresponding interstitial sites. There exist two types of interstitial sites in bcc and close-packed crystal structures of iron: tetrahedral and octahedral sites. The O-site is smaller than the T-site in bcc iron, unlike for close-packed iron. However, octahedral sites are always energetically preferred for carbon in iron.[41,49,58,59,60]

To validate the potentials, the dependence of the lattice parameters on carbon concentration in α-iron at 300 K and γ-iron at 1185 K was studied. These temperatures were adopted to compare our results with available experimental data. A single carbon atom was set in an octahedral position in the middle of an bcc or fcc crystal, which contained 64-1000 unit cells for bcc and fcc 27-729 unit cells for fcc with the same lengths in each normal direction resulting in 128-2000 iron atoms for bcc and 256-4000 atoms for fcc. We performed molecular dynamics simulations under NPT conditions for 200 ps using a timesteps of 1 fs within periodic boundary conditions.

The lattice parameters were obtained by averaging data from the last 100 ps of the simulation. Fig. 2 shows a sketch of the octahedral site in bcc and fcc iron together with the predicted lattice parameters as function of carbon concentration, in comparison with available experimental data from Cheng et al.[58]. For the bcc crystal structure at 300 K, the Ackland+Hepburn potential overestimates the lattice parameter along the c-axis. The two other potentials, Ackland+Becquart and Ackland+Johnson potentials, are in better agreement with the experiment[58]. For the lattice parameter along the a-axis, the Ackland+Becquart

potential nearly perfectly reproduces the experimental data[58], whereas the other potentials underestimate the lattice parameter. From Fig. 2 (bottom) we observe that the experimental fcc lattice parameters by Chen et al.[58], Seki and Nagata[61], Kahn et al.[62] and Hummelshøjj et al.[63] are fairly reproduced by the Ackland+Becquart potential, whereas the expansion of the lattice is slightly underestimated by the other potentials. Note that the differences are only 0.1%.

Altogether, these results indicate that carbon atoms distort the surrounding iron atoms resulting in a tetragonal distortion of the bcc lattice structure and lattice expansion of the fcc lattice. The Ackland+Becquart potential is in almost perfect agreement with experimental results for bcc and fcc iron.

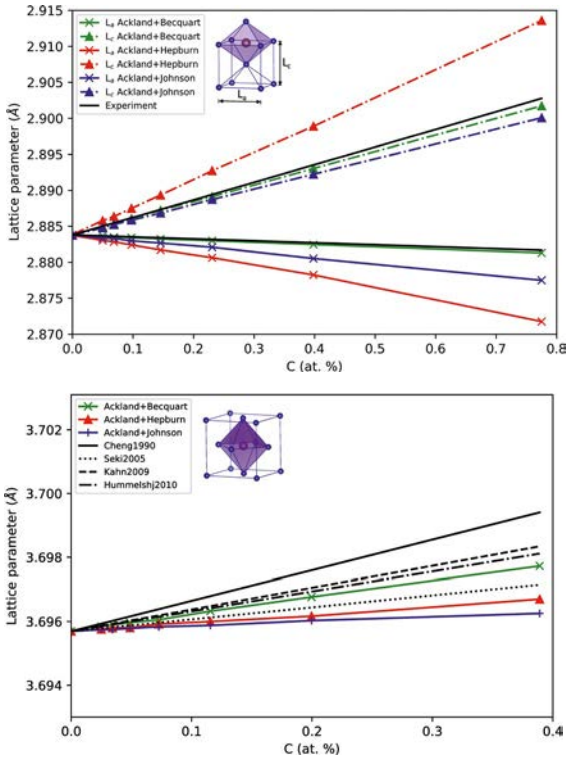

Figure 2: Lattice parameters as a linear function of carbon concentration for bcc iron at 300 K (top) and fcc iron at 1185 K (bottom). The data were evaluated by the Ackland+Johnson, Ackland+Hepburn, and Ackland+Becquart potential presented as dotted, dashed dotted, and solid lines. The experimental data is presented by solid black lines.

3.2 Transformation pressure

We used the Gibbs free energy to evaluate the phase stability under high pressure p, and the transformation pressure in iron carbon:

$$G = U + pV - TS = H - TS$$

where U is the internal energy of the system, V the volume, S the entropy and H the enthalpy. The phase with minimal Gibbs free energy is the stable phase. By evaluating the Gibbs free energy of bcc and hcp versus pressure, the transformation pressure in iron is usually identified in density functional theory[15,64] and in MD[22]. For T=0, the intersection of both enthalpies is identified as transformation pressure.

We used the Gibbs free energy to evaluate the phase stability under high pressure, and the transformation pressure in iron. We performed computations at 0 K to eliminate the entropy. Enthalpies at 10 K are almost identical to enthalpies at 0 K. The transformation energy barrier is highly dependent on impurities[65].

The transformation path of the bcc/hcp phase transformation is shown in Fig. 3 (a). The transformation process necessitates the atomic movement of iron atoms in (011) plane[5,66,67].

There are three layers of atoms belonging to the (011) plane: Atoms marked by 1-3, 4-10, and 11-13 belong to top, middle, and bottom layers, respectively. During the transformation process in in Fig. 3a, atoms in the center plane are contracted along the [001] direction and the lattice expands along [110]. Top and bottom layers behave similarly and atoms glide along the [110] direction. The O-site in bcc iron is bounded by six atoms as shown in Fig. 3b. After the transformation, five out of these six atoms form two T-sites. As stated above, the O-site is energetically favorable for carbon in contrast to the tetrahedral position in bcc iron[41,49]. However, it is not known which interstitial site will be favorable in hcp iron after the transformation process from bcc to hcp. Based on the schematic transformation path, the carbon atoms in the O-site in bcc iron tend to be trapped in the T-site in hcp iron before carbon will migrate to its preferred position. Thus, we evalu-

ate the influence of carbon on the transformation pressure of iron for two different situations: Carbon atoms are trapped in tetrahedral positions or are located in octahedral sites after the transformation.

To measure the transition pressure, we hydrostatically compress iron carbon single crystals of the same configuration as described in subsection 3.1, 64-1000 unit cells for bcc and hcp iron. A single carbon atom was placed centrally in an octahedral position in bcc iron. Both positions, octahedral and tetrahedral, were considered for hcp iron. The internal energy, pressure and volume change during hydrostatic compression were recorded to calculate the Gibbs free energy of the system. For each potential, three free enthalpy surfaces were constructed, one for bcc iron (bcc-O) and two other surfaces for hcp iron with carbon in either an octahedral (hcp-O) or a tetrahedral (hcp-T) positions.Each surface is a function of carbon concentration and pressure. Similar to their counterpart closed-packed fcc phase, the hcp-O enthalpy surface is below the hcp-T surface, and these two enthalpy surfaces are nearly parallel to each other (see Fig. 4 below).

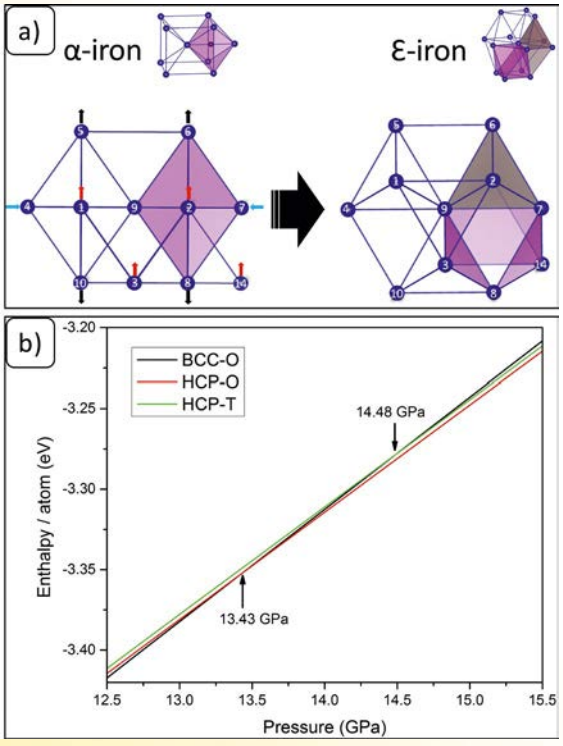

Figure 3: Schematics of pressure-induced phase transformation in iron. Purple and brown areas represent the octahedral site of the crystal structure. The mechanism includes a combination of shuffle (red arrows), dilatation (black arrows) and contraction (blue arrows) of iron atoms on (011) plane (top). Predicted transformation pressures of carbon in octahedral sites in the bcc crystal structure transforming either to octahedral or tetrahedral sites in hcp (bottom).

The reason is that carbon impurities are more stable in the hcp O-site. The intersections between bcc-O and hcp-T/hcp-O surfaces were identified as the transformation pressures at equilibrium conditions. Note that the effect of carbon migration during transformation is not considered in this method.

Under equilibrium conditions, the transformation pressure of pure iron is 13.75 GPa for the potential used in this study[22].

We calculated the Gibbs free energy for both cases: C in octahedral sites in hcp or in tetrahedral sites. The results are shown in Fig. 3 (b) for the concentration of 0.22 at. % C for the Ackland+Becquart potential. We can depict two intersection points at equilibrium conditions. The smaller value corresponds to carbon at O-sites before and after the transformation and the elevated transformation pressure belongs to carbon at O-site in bcc and T-site in the hcp phase. Our result shows clearly that the threshold pressure is increased if carbon is trapped in the tetrahedral position during transformation.

Fig. 4 shows the transformation pressures versus carbon concentration for both interstitial sites. For pure iron, the transformation pressure is at 13.75 GPa, in good agreement with experiments[29] giving a transformation pressure in iron single crystal under slow strain-rate compression of around 14.26 GPa.

Our result shows that the transformation pressure decreases with increasing carbon concentration if carbon is situated in an octahedral site before and after the transformation. If carbon is located in a tetrahedral site after transformation, we observe

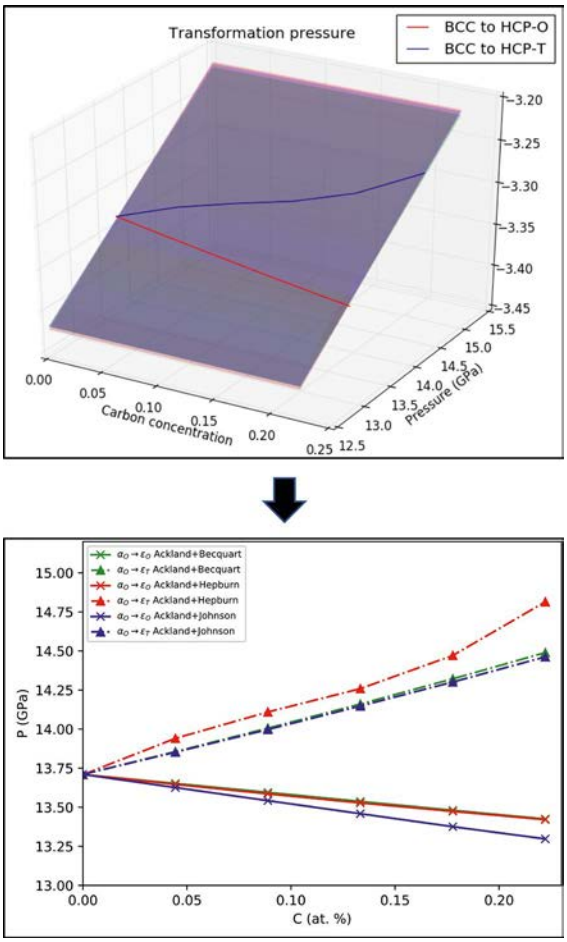

Figure 4: Enthalpy surfaces and transformation pressure in bcc iron with small C concentrations identified by the intersection of bcc and hcp enthalpies versus pressure at 0 K. Carbon is located in the octahedral sites in bcc iron and either octahedral or tetrahedral sites in hcp iron.

the opposite behavior. The three different potentials show a similar behavior as illustrated in Fig. 4. It has been shown by experiments[31,32] that the transformation pressure increases with increasing carbon concentration. A reason could be that the transformation energy barrier is increased by carbon because the bcc-hcp transformation process is hindered by multiple impurities. This explanation is consistent with the report of Hennig et al.[65], who found that carbon increases the transformation pressure in titanium. As a consequence, carbon does not freely migrate during transformation, and may be trapped at tetrahedral sites. However, in real Fe-C the increase in transformation pressure could also arise from the interaction of dislocations with carbon atoms. Dislocations can be temporarily pinned by alloying elements requiring additional stress to move the dislocations. The reduced dislocation mobility has strong implications on the mechanical properties of Fe-C and may lead to increased transformation pressures.

3.3 Single crystals under hydrostatic compression

We display snapshots of the evolution of close-packed crystal structures including hcp and fcc phases (stacking faults) in iron and Fe-C single crystals under hydrostatic compression in Fig. 5. We observe many hcp embryos at a strain of 4.1% in both models; these embryos grow substantially in pure iron while the growth of this phase is hindered by carbon in the Fe-C sample. For pure iron, the phase is almost fully developed at 5% while for Fe-C the growth mechanism is delayed. Carbon decelerates the diffusionless transformation process supporting our hypothesis that C atoms are trapped in tetrahedral sites during the transformation from bcc to hcp.

The pressure and temperature history of pure iron single crystals and Fe-C crystals during hydrostatic compression are shown in Fig. 6. The pressure history clearly shows two inflection points, the first peak is the elastic plastic limit and the second peak is the transformation pressure for the transition from bcc to hcp. Recent laser ramp-compression experiments[11,29] in iron at high strain rates show a three-waves structure of elastic wave, plastic wave and subsequent plastic wave. Note that the three-wave structure of iron strongly depends on grain size and compressive strain rate. At a strain rate less than $1x10^6$ s^{-1}, the response of iron is driven by thermal activation. At higher strain rates, the growth of the new phase is limited by the so-called phonon drag.[68] Here, the dislocation mobility becomes limited through energy dissipation off phonon modes. Since martensitic interphase dislocations govern the growth of the hcp phase the phase transition pressure increases for these high strain rates.[11] This is the reason why MD simulations of single crystal nickel[69], and copper[70] under external load

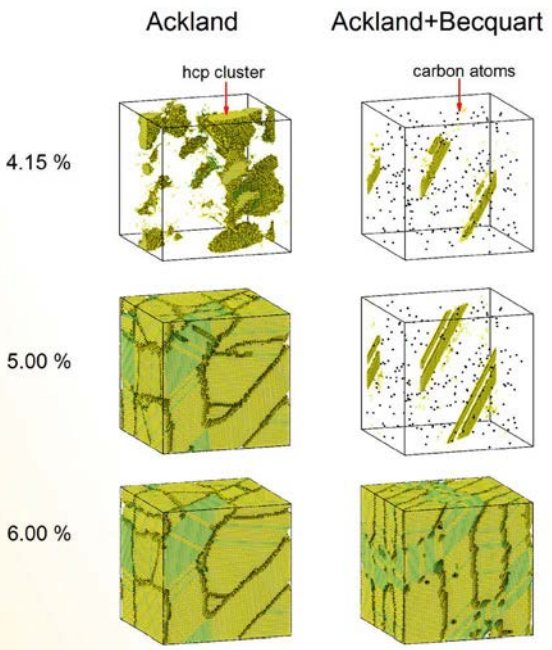

Figure 5: Snapshots showing the development of close-packed crystal structures in pure iron and Fe-C single crystals under hydrostatic compression by using the Ackland potential for Fe and the Ackland+Becquart potential for Fe-C. Crystal types were identified by aCNA in OVITO. Yellow: hcp; green fcc; black: carbon atoms. The compressive strain increases from the left to the right.

show that the yield stress increases with increasing strain rate. Hardening effects of the surrounding matrix of the new hcp phase were also found by atomistic simulations[71]. Under high strain rate compressive loadings, the elastic-plastic limit and the transition pressures for single crystals are significantly elevated in comparison to the ones at their equilibrium conditions as predicted by the Gibbs free energy.

Fig. 6 shows that the elastic-plastic transition pressure for pure iron single crystals is 26.7 GPa using the Ackland potential. This is close to the value of 22.3 calculated by the fitting equation for high strain-rate data of shock-loaded iron from Smith et al. [29] using a grain size of 14 nm. The elastic limit decreases witch carbon content. We find elastic-plastic pressures of 23.3, 22.7, and 22.5 GPa for Ackland+Becquart, Ackland+Hepburn, and Ackland+Johnson potentials, respectively. The results confirm that carbon is associated with the stability of bcc iron[44,60].

Bcc iron transforms to hcp iron at a pressure of 39.3 GPa in pure iron. The result is very close to the experimental result of 38.4 GPa[11] which was obtained by laser and magnetic ramp-compression techniques for iron with a purity of 99.995% under compressive strain rates of $3x10^8$ s^{-1}.

Recent experiments show that pure iron undergoes a pressure-induced phase transformation at 25 GPa[14] at the same strain rate. Our transition pressure smaller than the result from the fitting equation by Smith et al.[11] of 47.9 GPa fitted to high-strain rate data of magnetic ramp compression. A recent MD study by Wang et al.[21] finds a transformation pressure of 31 to 33 GPa in single crystal iron. However, the authors have not observed plasticity before the phase transformation.

From Fig. 6 we depict transformation pressures of 57.9, 52.8 and 61.1 GPa in Fe-C for Ackland+Becquart, Ackland+Hepburn, and Ackland+Johnson potentials, respectively. We conclude that carbon slightly decreases the Hugoniot elastic limit, but significantly increases the transformation pressure in iron. These results support the experimental observations by Hennig et al.[65], and Koepke et al.[32].

Plasticity driven temperature changes are shown in Fig. 6, right. At around 3 % strain, the elastic-plastic limit is reached, where we observe a sudden increase in temperature. In pure iron single crystals at 3-4 % strain, the temperature is larger than in Fe-C samples because of the nucleation of closed-packed clusters which is delayed for Fe-C. During compression, the temperature increases considerably from initially 10 K to values up to 250 K. Dislocation motion and the phase transformation contribute to increased thermal energy. The growth rate of close-packed clusters dramatically increases at a strain of 4.2 % for pure iron and above 5 % for Fe-C samples. The sudden rise in temperature with the phase transition is consistent with findings from experiments[72] and MD simulations.[26,27]

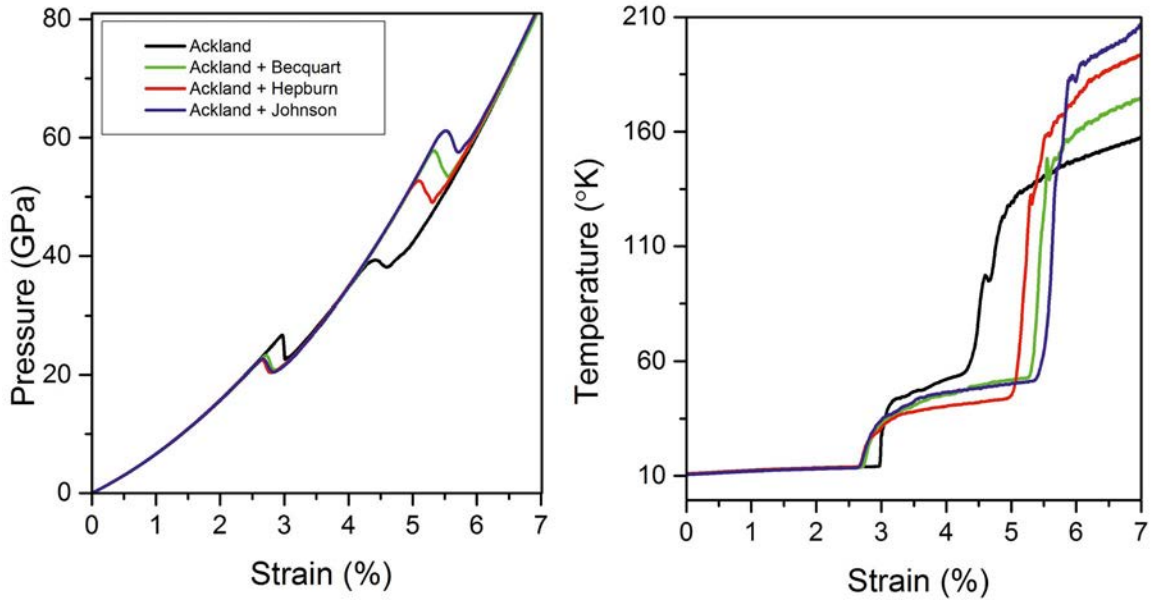

Figure 6: Pressure and temperature history of pure iron single crystals and Fe-C crystals during hydrostatic compression versus strain.

3.4 Twins and stacking faults

Stacking faults and twins have been found in both experiment[13,73] and MD simulations[19,74], for diffusionless transformations from bcc iron to close-packed γ or ε-iron. Stacking faults are defects which characterize the disordering of crystallographic planes and are thus planar.

The interface between two close-packed clusters is identified as twin boundary, if one of the two crystals is a mirror of the other. Twins were found by Kauda et al.[17] in compression simulations in iron single crystals.

We observe a large amount of stacking faults and twins in Fe single crystals, in agreement with MD studies[25]. At a strain of 10 %, we display twin boundaries and stacking faults for pure iron in Fig. 7 (top) and for Fe-C crystals in Fig. 7 (bottom). For Fe-C crystals, we observe a considerably increased amount of twins and stacking faults in comparison to the samples for pure iron. To further analyze the generation of stacking faults, we calculated the stacking fault energy (SFE) of hcp-to-fcc versus C content for the potential by Ackland+Becquart. We rigidly displaced two halves of a hcp crystal and monitored the energy change versus displacement. We find that the stacking fault energy increases with C content. However, we observe a larger amount of stacking faults in the Fe-C samples. A reason could be that the temperature is larger for our iron carbon system resulting in a decreased SFE.

3.5 Polycrystalline Fe-C under uniaxial compression

Plasticity and phase transformations in iron have been studied in detail by using several iron potentials[22]. Under uniaxial compression, plasticity in the form of dislocation activity was observed, just before the phase transformation takes place. Later, by using shock loading[23], the nucleation of mixed dislocations at the grain boundaries propagating through the grains was studied. Here, simulated X-ray diffraction has displayed clear evidence of the hcp phase and enabled direct comparison with experimental data.

In this project, we analyze the influence of 0.1 at.% C to the plastic response of polycrystalline iron samples using the potentials Ackland+Becquart, Ackland+Hepburn, and

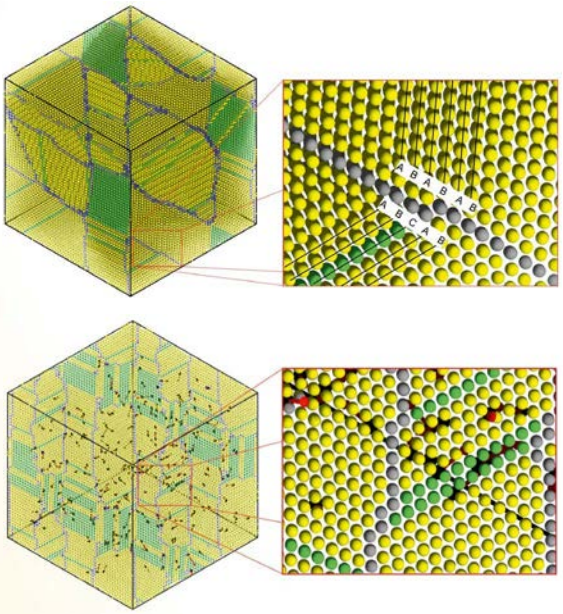

Figure 7: Top: Pure iron single crystals at 10 % strain. Atom types are detected by adaptive CNA[56]. Yellow, green and grey color represents hcp-iron, fcc-iron and disordered atoms, respectively. Bottom: Carbon atoms (black atoms) with their displacement vectors (red arrow) in iron single crystals under 10% strain using Ackland+Becquart potential. The number of twins and stacking faults is higher than for pure iron.

Ackland+Johnson. We use the von Mises stress to identify the yield stress in polycrystalline Fe-C which characterizes the onset of plasticity. Fig. 8 shows temperature and von Mises stress versus strain for uniaxially deformed Fe and Fe-C samples.

The von Mises stress linearly increases between 0.0 % and 2.5 % strain, corresponding to the elastic response of iron and Fe-C polycrystals. The elastic regime is followed by plastic deformation with a maximum in stress around 5 GPa and subsequent relaxation. We cannot pinpoint the phase transformation from this figure because of the presence of plasticity. Plasticity occurs here in the form of grain boundary sliding and rotation and dislocation emission. Grain boundary sliding is a process where grains slip past each other, driven by rotational or translational strain jumps. Since the total shear stress is driven by grain boundary sliding and dislocation activity, it can help suppressing dislocation-based plasticity.

The temperature versus strain remains almost constant up to the elastic limit and then rapidly increases due to plastic heating up to values of nearly 100 K at 9 % strain. At this strain, the phase transformation takes place and the slope of temperature versus strain increases because the phase transformation generates thermal energy. As a consequence, the von Mises stress drops down to values slightly above 2 GPa. We do not observe large differences in temperature and stress of pure iron and Fe-C samples. A reason could be that we did not consider segregation of carbon at grain boundaries which is known to increase the strength of iron carbon[75]. The Fe-C crystals using the potentials Ackland+Becquart and Ackland+Hepburn show only a marginally higher von Mises stress than the results for pure iron between 2 and 12 % strain.

At temperatures less than 150 K, the strengthening of iron by carbon interstitials may be understood from the increase of the sessile-glissile energy barrier of dislocations.

At a strain of 12 %, hcp clusters continue to grow until the boundaries reach other hcp clusters. The interfaces act as twins, which propagate through the crystal at higher strains. Similar to the behavior for iron single crystals, the number of twins is larger in Fe-C samples than in pure hcp iron. This causes a lower von-Mises stress compared to pure iron above 15 % strain as shown in Fig. 8. The results for all three Fe-C potentials show the same behavior.

Plastic activity only occurs in a narrow spatial regime.

Fig. 9 shows a slice of thickness 1.5 nm of the pure iron sample at a strain of 7 %, in a region where there is only plasticity, just before the phase transition starts. Dislocations shown are in the bcc phase. Fig. 9 shows several dislocation segments consistent with the response of iron under shock compression[23]: We observe straight screw dislocations crossing the grains. Mixed dislocations are usually nucleated at a grain boundary

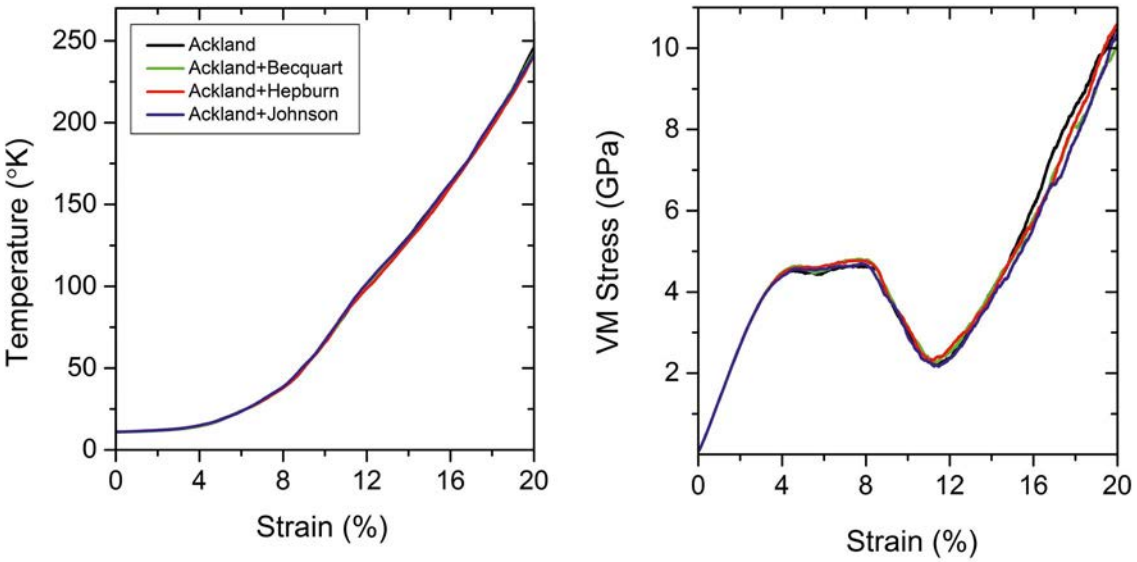

Figure 8: Temperature and von Mises stress versus strain of polycrystalline iron and Fe-C.

and propagate through the grain until they reach the opposite boundary where the dislocations are absorbed. This agrees with electron microscopy of plastically deformed metals where mostly screw dislocations are found[76].

Note that we do not observe intergranular dislocations. Inside the grains, we also find several vacancies. The number of dislocations identified by DXA is slightly larger in pure iron than in Fe-C. This could also be a reason that phase transformation is delayed suggesting that dislocations alleviate the transformation. Dislocations could act as nucleation centers for the growth of the hcp phase because the lattice distortion induced by the stress around dislocation configurations assist in the nucleation of hcp embryos.

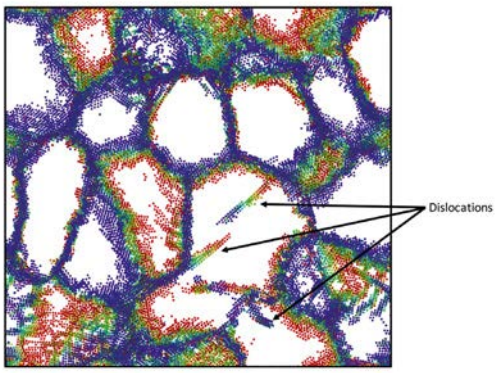

Figure 9: A slice of polycrystalline Fe sample at a depth of 13 nm with a thickness of 1.5 nm at a strain of 7 %. Atoms belonging to grain boundaries, or dislocations or interfaces are shown. The color indicates the depth of atoms, blue: front, red: bottom.

Fig. 10 shows a comparison of snapshots in polycrystalline iron and Fe-C during transformation at a strain of 9%,12 % and 18 % using the Ackland and the Ackland+Becquart potential, respectively. In pure iron, the close-packed structures start to grow from grain boundaries. In Fe-C samples, the evolution of close-packed structures is similar to the growth mechanism of the iron sample. However, it can be seen that carbon hinders the development of closed-packed phases such that the total amount of close-packed phases is smaller for Fe-C at 8 % strain. At 12 % strain, the hcp phase is almost fully developed for both crystals. This result is consistent with our finding for the phase transformation in Fe-C single crystal.

4. Conclusions

MD simulations were employed to investigate the behaviour of Fe-C systems under high pressure.

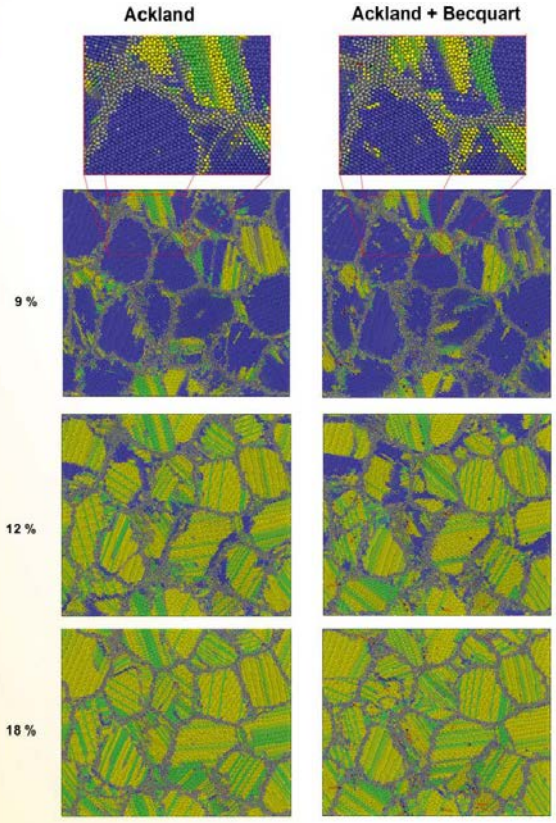

Figure 10: Snapshots showing phases of iron and iron-carbon at 9 %, 12 % and 18 % strain, using the Ackland and the Ackland+Becquart potential for polycrystalline iron and Fe-C, respectively. Blue: bcc; yellow: hcp; green: fcc; grey: grain boundaries, black: carbon, red: displacement vectors. Atom types are identified via adaptive CNA analysis[56].

We have coupled a recently developed Fe interatomic EAM potential, which faithfully describes the $\alpha \rightarrow \varepsilon$ transformation in iron, with several well-known Fe-C potentials. The potentials accurately describe the tetragonal distortion of the lattice with increasing carbon concentration in agreement with experimental data. Our results show that although the octahedral site is energetically favorable for carbon in hcp iron, C atoms could be trapped in tetrahedral sites during the transformation. This could be a reason for the increasing transformation pressure with increasing carbon concentration.

We observe a three-wave profile demonstrating that the phase transformation is preceded by plasticity. The elastic-plastic transformation occurs at 26.7 GPa and the phase transformation from bcc to hcp is at 39.3 GPa. Our results are consistent with experimental data, reporting that the transformation pressures for iron increase at high strain rate deformation due to phonon drag. The elastic-plastic transformation is decreased due to the influence of carbon on the phase stability of bcc iron. Carbon increases the transformation energy barrier, and thus increases the Fe-C phase transformation pressure.

In addition, we found an increased amount of stacking faults and twins for Fe-C samples. Finally, we have shown that interstitial carbon reduces the von Mises stress in transformed phase because of increased twinning.

Future investigations will cover the influence of carbon segregation at grain boundaries and non-equilibrium MD simulations where the dynamic wave profile might change the evolution of the microstructure. Using accelerated MD methods, carbon diffusion could be studied for smaller strain rates which could have significant impact on high-pressure dynamics. The recovery of loaded samples will also be studied to evaluate the material strength of recovered samples which could be highly influenced by carbon.

5. References

1 E. Pereloma and D. Edmonds, Phase Transformations in Steels, vol. 1 (Woodhead Publishing Limited, 2012.
2 E. Pereloma and D. Edmonds, Phase Transformations in Steels, vol. 2 (Woodhead Publishing Limited, 2012).
3 D. Bancroft, E. L. Peterson, and S. Minshall, J. Appl. Phys. 27, 291 (1956).
4 F. P. Bundy, J. Appl. Phys. 36, 616 (1965).
5 H. K. Mao, W. A. Bassett, and T. Takahashi, J. Appl. Phys. 38, 272 (1967).
6 W. A. Bassett, T. Takahashi, and P. W. Stook, Rev. Sci. Instrum. 38, 37 (1967).
7 P. M. Giles, M. H. Longenbach, and A. R. Marder, J. Appl. Phys. 42, 4290 (1971).
8 W. A. Bassett and E. Huang, Science 238, 780 (1987).

9 H. Nguyen and N. C. Holmes, Nature 427, 339 (2004).
10 Y. Ma, E. Selvi, V. I. Levitas, and J. Hashemi, J. Phys. Condensed Matter 18, S1075 (2006).
11 R. F. Smith, J. H. Eggert, D. C. Swift, J. Wang, T. S. Duffy, D. G. Braun, R. E. Rudd, D. B. Reisman, J. P. Davis, M. D. Knudson, et al., J. Appl. Phys. 114, 223507 (2013).
12 S. J. Wang, M. L. Sui, Y. T. Chen, Q. H. Lu, E. Ma, X. Y. Pei, Q. Z. Li, and H. B. Hu, Sci. Rep. 3, 1086 (2013).
13 J. C. Crowhurst, B. W. Reed, M. R. Armstrong, H. B. Radousky, J. A. Carter, D. C. Swift, J. M. Zaug, R. W. Minich, N. E. Teslich, and M. Kumar, J. Appl. Phys. 115, 113506 (2014).
14 P. Söderlind, J. A. Moriarty, and J. M. Wills, Phys. Rev. B 53, 14063 (1996).
15 M. Ekman, B. Sadigh, K. Einarsdotter, and P. Blaha, Phys. Rev. B 58, 5296 (1998).
16 H. C. Herper, E. Ho_mann, and P. Entel, Phys. Rev. B 60, 3839 (1999).
17 K. Kadau, Science 296, 1681 (2002).
18 L. Huang, N. V. Skorodumova, A. B. Belonoshko, B. Johansson, and R. Ahuja, Geophys. Res. Lett. 32, 1 (2005).
19 K. Kadau, T. C. Germann, P. S. Lomdahl, and B. L. Holian, Phys. Rev. B 72, 064120 (2005).
20 K. Kadau, T. C. Germann, P. S. Lomdahl, R. C. Albers, J. S. Wark, A. Higginbotham, and B. L. Holian, Phys. Rev. Lett. 98 (2007).
21 B. T. Wang, J. L. Shao, G. C. Zhang, W. D. Li, and P. Zhang, J. Phys. Condensed Matter 22, 435404 (2010).
22 N. Gunkelmann, E. M. Bringa, K. Kang, G. J. Ackland, C. J. Ruestes, and H. M. Urbassek, Phys. Rev. B 86, 144111 (2012).
23 N. Gunkelmann, E. M. Bringa, D. R. Tramontina, C. J. Ruestes, M. J. Suggit, A. Higginbotham, J. S. Wark, and H. M. Urbassek, Phys. Rev. B 89, 140102 (2014).
24 W. W. Pang, P. Zhang, G. C. Zhang, A. G. Xu, and X. G. Zhao, Sci. Rep. 4 (2014).
25 N. Gunkelmann, D. R. Tramontina, E. M. Bringa, and H. M. Urbassek, J. Appl. Phys. 117, 85901 (2015).
26 J. L. Shao, P. Wang, F. G. Zhang, and A. M. He, Sci. Rep. 8 (2018).
27 N. Gunkelmann, D. R. Tramontina, E. M. Bringa, and H. M. Urbassek, J. Appl. Phys. 117, 85901 (2015).
28 B. J. Jensen, G. T. Gray, and R. S. Hixson, J. Appl. Phys. 105, 103502 (2009).
29 R. F. Smith, J. H. Eggert, R. E. Rudd, D. C. Swift, C. A. Bolme, and G. W. Collins, J. Appl. Phys. 110, 123515 (2011).
30 F. S. Minshall, Response of Metals to High Velocity Deformation, vol. 9 (Interscience Publishers, Inc., Estes Pack, Colorado, 1961).
31 T. R. Loree, C. M. Fowler, E. G. Zukas, and F. S. Minshall, J. Appl. Phys. 37, 1918 (1966).
32 B. G. Koepke, R. P. Jewett, W. T. Chandler, and T. E. Scott, Metall. Mater. Trans B 2, 2043 (1971).
33 C. Moosbrugger, Atlas of stress-strain curves (ASM International, 2002).
34 E. Sak-Saracino, and H. M. Urbassek, Eur. Phys. J. B 88, 169 (2015).
35 G. Bonny, R. C. Pasianot, N. Castin, and L. Malerba, Philos. Mag. 89, 3531 (2009).
36 G. Bonny, R. C. Pasianot, and L. Malerba, Model. Simul. Mater. Sci. Eng. 17, 025010 (2009).
37 R. C. Pasianot and L. Malerba, J. Nucl. Mater. 360, 118 (2007).
38 G. J. Ackland, D. J. Bacon, A. F. Calder, and T. Harry, Philos. Mag. A 75, 713 (1997).
39 E. Sak-Saracino and H. M. Urbassek, Int. J. Modern Physics C 27, 1650124 (2016).
40 G. J. Ackland, M. I. Mendelev, D. J. Srolovitz, S. Han, and A. V. Barashev, J. Phys. Condensed Matter 16, S2629 (2004).
41 N. Gunkelmann, H. Ledbetter, and H. M. Urbassek, Acta Mater. 60, 4901 (2012).
42 R. G. Veiga, M. Perez, C. S. Becquart, C. Domain, and S. Garruchet, Phys. Rev. B 82, 054103 (2010).
43 R. G. Veiga, H. Goldenstein, M. Perez, and C. S. Becquart, Scr. Mater. 108, 19 (2015).
44 E. Sak-Saracino and H. M. Urbassek, Philos. Mag. 94, 933 (2014).
45 B. Wang, E. Sak-Saracino, N. Gunkelmann, and H. M. Urbassek, Comp. Mater. Sci. 82, 399 (2014).
46 R. Meyer, P. Entel, Phys. Rev. B 57 5140 (1998).
47 R. J. Harrison, A. F. Voter, and S. P. Chen, Atomistic Simulation of Materials: Beyond Pair Potentials, 1 (A Division of Plenum Publishing Corporation, 1994).
48 T. Lee, M. I. Baskes, S. M. Valone, and J. D. Doll, J. Phys. Condensed Matter 24, 225404 (2012).

49 R. A. Johnson, G. J. Dienes, and A. C. Damask, Acta Metall. 12, 1215 (1964).
50 D. J. Hepburn and G. J. Ackland, Phys. Rev. B 78, 165115 (2008).
51 C. Becquart, J. Raulot, G. Bencteux, C. Domain, M. Perez, S. Garruchet, and H. Nguyen, Comput. Mater. Sci. 40, 119 (2007).
52 R. G. Veiga, C. S. Becquart, and M. Perez, Comput. Mater. Sci. 82, 118 (2014).
53 G. Voronoi, J. Reine Angew. Math. 136, 67 (1909).
54 J. Janßen, N. Gunkelmann and H.M. Urbassek, Philos. Mag. 96, 1448 (2016).
55 S. Plimpton, J. Comput. Phys. 117, 1 (1995), http://lammps.sandia.gov.
56 A. Stukowski, Modell. Simul. Mater. Sci. Eng. 20, 45021 (2012).
57 A. Stukowski, Modell. Simul. Mater. Sci. Eng. 18, 15012 (2010).
58 L. Cheng, A. Böttger, T. H. de Keijser, and E. J. Mittemeijer, Scr. Metall. et Mater. 24, 509 (1990).
59 D. E. Jiang and E. A. Carter, Phys. Rev. B 67, 214103 (2003).
60 D. J. Hepburn, D. Ferguson, S. Gardner, and G. J. Ackland, Phys. Rev. B 88, 024115 (2013).
61 I. Seki and K. Nagata, ISIJ International 45, 1789 (2005).
62 H. Kahn, G. M. Michal, F. Ernst, and A. H. Heuer, Metall. Mater. Trans. A 40, 1799 (2009).
63 T. S. Hummelshøj, T. L. Christiansen, and M. A. Somers, Scr. Mater. 63, 761 (2010).
64 L. Vocadlo, J. Brodholt, D. Alfè, M. J. Gillan, and G. D. Price, Phys. Earth Planet. Inter. 117, 123 (2000).
65 R. G. Hennig, D. R. Trinkle, J. Bouchet, S. G. Srinivasan, R. C. Albers, and J. W. Wilkins, Nat. Mater. 4, 129 (2005).
66 F. Wang and R. Ingalls, Phys. Rev. B 57, 5647 (1998).
67 M. Friak and M. Sob, Phys. Rev. B 77, 174117 (2008).
68 M. Grujicic and G. B. Olson, Interface Sci. 6, 155 (1998).
69 M. F. Horstemeyer, M. I. Baskes, and S. J. Plimpton, Acta Mater. 49, 4363 (2001).
70 V. Dupont and T. C. Germann, Phys. Rev. B 86, 134111 (2012).
71 N. Amadou, T. De Resseguier, A. Dragon, and E. Brambrink, Phys. Rev. B 98, 024104 (2018).
72 V. D. Blank and E. I. Estrin, Phase transitions in solids under high pressure (CRCg Press, 2013).
73 G. E. Duvall and R. A. Graham, Rev. Mod. Phys. 49, 523 (1977).
74 M. I. Baskes and R. A. Johnson, Modell. Simul. Mater. Sci. Eng. 2, 147 (1994).
75 M. Yamaguchi, Metall. Mater. Trans. A 42, 319 (2010).
76 C.-H. Lu, B. A. Remington, B. R. Maddox, B. Kad, H.-S. Park, S. T. Prisbrey, and M. A. Meyers, Acta Mater. 60, 6601 (2012).

Project data

The project is funded from SWZ with one W1 and 0.5 TV-L E13 staff positions since September 2017 at the site Clausthal. Involved scientists are:

Jun.-Prof. Dr.
Nina Gunkelmann
Research Group Computational Material Sciences
Institute of Applied Mechanics
Clausthal University of Technology

Hoang-Thien Luu
Research Group Computational Material Sciences
Institute of Applied Mechanics
Clausthal University of Technology

Verteilte Simulation

Die numerische Simulation technisch-wissenschaftlicher Probleme gehört traditionell zu den Disziplinen mit dem höchsten Bedarf an Rechenleistung. Dementsprechend werden solche Probleme auf Supercomputern mit Vektor- und Parallelrechnerarchitektur bearbeitet. Die größten Parallelrechner der Welt wurden in den USA und inzwischen in China für Simulationsanwendungen installiert. Die größten Parallelrechner in Deutschland sind deutlich kleiner und sind an den drei Standorten München (LRZ und RZG), Stuttgart (HLRS) und Jülich (FZ) konzentriert. In Niedersachsen stehen für große Simulationsaufgaben der HLRN III (Norddeutscher Verbund für Hoch- und Höchstleistungsrechnen) und zahlreiche kleinere Anlagen an universitären Rechenzentren zur Verfügung. Diese geographisch verteilten und heterogenen Ressourcen können für zahlreiche Fragestellungen besser genutzt werden. Man spricht dabei von verteilter Simulation oder Grid Computing. Der Aufwand für die Erstellung geeigneter Software und Middleware, die zwischen den Anwendungen und den Betriebssystemen sitzt, ist im Allgemeinen sehr hoch und es gibt enorme Einschränkungen für die Anwendungen. Bislang hat es sich deshalb nur in Einzelfällen gelohnt, Simulationen auf mehrere PC Cluster zu verteilen. Mit der Entwicklung leistungsfähigerer Hardware und neuer Berechnungsmethoden zeichnet es sich jedoch ab, dass der Aufwand für die Verteilung von Simulationsanwendungen auf existierende PCs und Workstations in einen Bereich kommt, wo er für viele Anwender interessant wird.

In diesem Projektbereich sollen daher Modelle und Methoden untersucht werden, mit denen Simulationen auf ein Grid verteilt werden können und die dabei entstehenden Probleme des Software-Tests und der Qualitätssicherung gelöst werden können. „Verteilte Simulation“ meint aber auch die Simulation hochgradig verteilter realer Systeme, wie z.B. Lieferketten im Supply Chain Management, die nicht durch ein herkömmliches, geschlossenes Modell erfasst werden können.

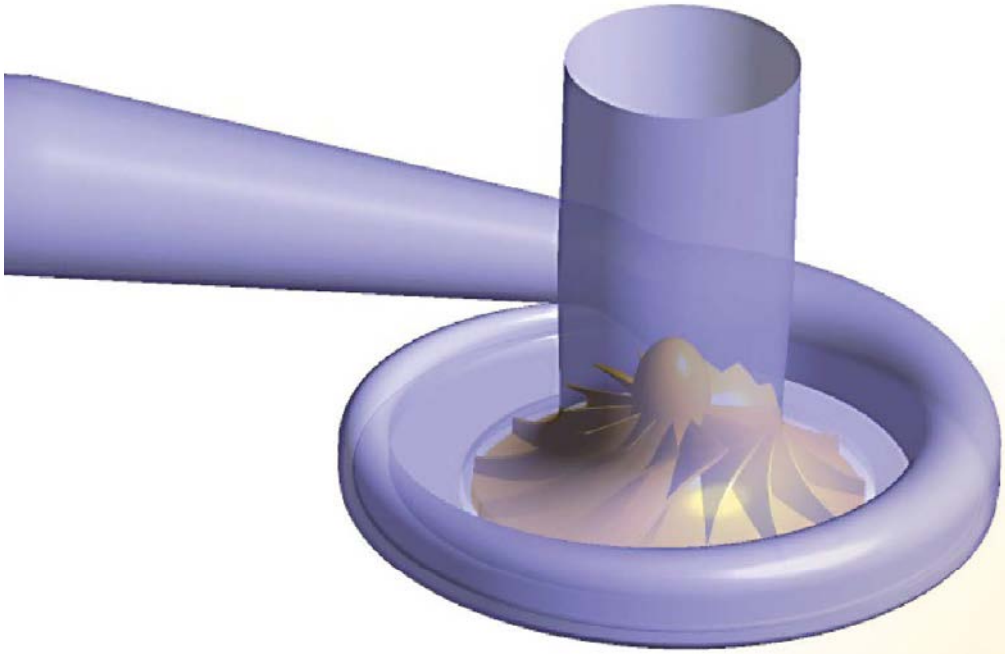

Multi-Level-Simulation using Dynamic Cloud Environments

Stefan Wittek, Johannes Erbel, Andreas Rausch, Jens Grabowski

Die Entwicklung von cyber-physikalischen Systemen erfordert die Anwendung holistischer Simulationen. Um der Komplexität dieser Systeme gerecht zu werden, streben wir eine effiziente Simulationsmethodik an. Die benötigte holistische Perspektive wird auf dem Groblevel erreicht, welches mit mehreren Modellen auf dem Detaillevel co-simuliert wird, um Teile des Systems zu fokussieren, die von besonderem Erkenntnisinteresse sind.In welche Teile „hineingezoomed" wird, ist während eines Simulationslaufes dynamisch. Dieser Dynamik wird auf Rechnerinfrastrukturebene Rechnung getragen, indem die resultierende Multi-Level-Simulation in einer Cloud-Umgebung mit dynamisch allokierten Ressourcen ausgerollt und somit die Verschwendung von Ressourcen vermieden wird.

Unsere Forschung gliedert sich in die Untersuchung der Multi-Level-Simulation und in die Entwicklung eines Deploymentansatzes zur dynamischen Ausbringung solcher Simulationen in Cloud-Umgebungen.

Ein Ergebnis dieses Projekts ist ein Ansatz zur Multi-Level-Simulationen. Die zentrale Herausforderung innerhalb des Ansatzes liegt in der Definition von Zustandsabbildungen, welche die Simulationen während der Laufzeit verbinden und die Heterogenität der Abstraktionsebenen überbrücken. Im Rahmen des Projekts haben wir nach Möglichkeiten gesucht, Techniken des maschinellen Lernens einzusetzen, um diese Abbildung mit Hilfe von nur kleinen Trainingssets zu generieren. Es zeigt sich, dass der Übergang von dem Detaillevel in das Groblevel (up) als gewöhnliches Regressionsproblem formuliert und mit entsprechenden Verfahren gelöst werden kann. Hierbei wird im Allgemeinen Information aggregiert. Deshalb kann der umgekehrte Weg (down) nicht adäquat als deterministische Funktion beschreiben werden. Dies zwingt uns dazu, auf Verfahren für das Lernen von bedingten Wahrscheinlichkeitsverteilungen auszuweichen.

Zum dynamischen bereitstellen von Cloud Ressourcen setzen wir auf einen Model-getriebenen Ansatz basierend auf dem standardisierten Open Cloud Computing Interface (OCCI) Datenmodel. Dieser Standard definiert zusätzlich zu einem erweiterbaren Datenmodel eine einheitliche Schnittstelle zum Verwalten von Cloud Ressourcen. Um das Ausführen von Multi-Level-Simulationen zu erlauben wurde im Umfang dieses Projekt eine Erweiterung für OCCI entwickelt, welche das Darstellen und Ausführen von Workflows in der Cloud erlaubt. Hierbei ist es insbesondere mögliche spezifische Infrastruktur Anforderungen für individuelle Aufgaben des Workflows zu definieren. Um die Ausführung dieser Workflows zu erlauben wurden unter anderem ein adaptives Deployment Verfahren entwickelt, sowie ein Verfahren zum Verwalten von monitoring Sensoren in der Cloud, welche die gesammelten Daten in einem OCCI Laufzeitmodel widerspiegeln können.

Das das Projekt Multi-Level-Simulation, welches durch das simulationswissenschaftliche Zentrum finanzierte wurde, stellte den Rahmen für unsere Arbeiten da. Es wurde am 31.12.2018 erfolgreich abgeschlossen.

Publikationen

[a1] Wittek, S., Göttsche, M., Rausch, A., Grabowski, J., 2016. Towards Multi-Level-Simulation using Dynamic Cloud Environments, Proceedings of the 6th International Conference on Simulation and Modeling Methodologies, Technologies and Applications (SIMULTECH 2016), Lisbon, Portugal, July 29-31, 2016. SciTePress 2016, ISBN 978-989-758-199-1.

[a2] Wittek, S., Rausch, A., 2018. Learning state mappings in Multi-Level-Simulation. Communications in Computer and Information Science (Vol. 889). Springer, Cham. https://doi.org/10.1007/978-3-319-96271-9_13

[a3] Erbel, J., 2017. Declarative Cloud Resource Provisioning Using OCCI Models, INFORMATIK 2017, 2017
[a4] Erbel, J., Korte, F., Grabowski J. 2018. Comparison and Runtime Adaptation of Cloud Application Topologies based on OCCI, Proceedings of the 8th International Conference on Cloud Computing and Services Science (CLOSER 2018)
[a5] J. Erbel, F. Korte, J. Grabowski. Scheduling Architectures for Scientific Workflows in the Cloud, Proceedings of the 10th System Analysis and Modelling Conference (SAM 2018), 2018

Einreichungen

[a6] Erbel, J., Wittek, S., Grabowski, J., Rausch A., 2019. Dynamic Management of Multi-Level-Simulation Workflows in the Cloud. Submitted to: Clausthal-Göttingen International Workshop on Simulation Science
[a7] Erbel, J., Brand, T., Giese, H., Grabowski, J., 2019. OCCI-compliant, fully causal-connected architecture runtime models supporting sensor management. Submitted to: 14th Symposium on Software Engineering for Adaptive and Self-Managing Systems (SEAMS 2019), 2019

Studentische Arbeiten

[a8] Tasik, R., 2016. Agent-based Simulation of Workflow Scheduling and Cloud Deployments, Bachelorarbeit im Studiengang Angewandte Informatik am Institut für Informatik, ZAI-BSC-2016-17, ISSN 1612-6793, Zentrum für Informatik, Georg-August-Universität Göttingen.
[a9] Erbel, J., 2017. Comparison And Adaptation Of Cloud Application Topologies Using Models At Runtime, Masterarbeit im Studiengang Angewandte Informatik am Institut für Informatik, ZAI-MSC-2017-23, ISSN 1612-6793, Zentrum für Informatik, Georg-August-Universität Göttingen.

Awards

„Best Poster Award“ für die Präsentation des Papers „Towards Multi-Level-Simulation using Dynamic Cloud Environments“ auf der 6th International Conference on Simulation and Modeling Methodologies, Technologies and Applications (SIMULTECH 2016)

Projektdaten

Das Projekt wurde von August 2015 bis Juli 2018 vom SWZ mit insgesamt einer TV-L E13 Stelle an den Standorten Clausthal und Göttingen gefördert. Beteiligte Wissenschaftler sind:

Prof. Dr. Andreas Rausch
Software Systems Engineering
Institut für Informatik
Technische Universität
Clausthal

Stefan Wittek, M.Sc.
Software Systems Engineering
Institut für Informatik
Technische Universität Clausthal

Prof. Dr. Jens Grabowski
Arbeitsgruppe Softwaretechnik
für Verteilte Systeme
Institut für Informatik
Universität Göttingen

Johannes Erbel, M.Sc.
Arbeitsgruppe Softwaretechnik
für Verteilte Systeme
Institut für Informatik
Universität Göttingen

Cloud-Efficient Modelling and Simulation of Magnetic Nano Materials

Pavle Ivanovic, Harald Richter

Zusammenfassung

Aufgrund des riesigen technologischen Fortschritts in den letzten Jahrzehnten, ziehen magnetische Nanomaterialien wegen ihrer hohen Dichte und ihrer permanenten Speicherkapazität ein großes Interesse an Computerdesign an. Sie gelten als die Zukunft vieler Speicherchips und können die vorhandenen Gegenstücke auf Siliziumbasis ersetzen. Um physikalische Zustände, die auf den Nanobereich auftreten, genau zu modellieren, müssen jedoch rechenintensive Simulationen durchgeführt werden. Komplexe Simulationen erfordern jedoch kostspielige Geräte wie Parallel- oder Supercomputer, die eine allgegenwärtige Einschreibung in die Wissenschaft verhindern. Unser Projektziel ist die Beschleunigung des Fortschritts in diesem vielversprechenden Bereich durch die Schaffung von Tools und Infrastruktur für einen effizienten und kostengünstigen Einsatz magnetischer Nanomaterialsimulationen. Der Bericht ist folgendermaßen strukturiert: Im ersten Kapitel werden die Wichtigkeit und die praktischen Anwendungen von magnetischen Nanomaterialien erläutert. Es wird vorgeschlagen, dass der neue simulative Ansatz erweiterte Cloud-Infrastrukturen für die Ausführung von Simulationen verwenden sollte. Außerdem werden aktuelle In-Cloud-Kommunikationsprobleme sowie die Vorteile von In-Cloud-Berechnungen diskutiert. In Kapitel 2 wird der Stand der Technik des vielversprechendsten mikromagnetischen Lösers beschrieben, der Magpar ist. In diesem Bericht haben wir außerdem einen kurzen Überblick über die wichtigsten Technologien und Softwarelösungen gegeben, die für effiziente Simulationen in einer Cloud-Umgebung erforderlich sind, z. B. OpenStack, ivshmem und mvapich2-virt. Nach einer kurzen Projektgeschichte werden wir in Kapitel 3 den wissenschaftlichen Fortschritt in drei Schritten vorstellen. Im ersten Schritt wird unser Umbau von Inter-VM Shared Memory, auch ivshmem genannt, zusammen mit einer ausführlichen Implementierungsbeschreibung gegeben. Darüber hinaus schlagen wir eine erweiterte, einseitige MPI_Put-Funktion in Form eines Wrapper-Codes mit integrierten Linux-User IO (uio) und Spinlock-freier Synchronisation vor. In einem zweiten Schritt werden wir eine umfassende ivshmem-Integration in OpenStack vorstellen, dass das am weitesten verbreitete Cloud-Betriebssystem in der Open Source-Domäne ist, sowie Cloud Tuning-Methoden wie etwa das CPU-Pinning und die ordnungsgemäße Zuweisung von NUMA. Schließlich wird im dritten Schritt eine Beschreibung des Wiederaufbaus von Magpar und seiner Cloud-Integration gegeben. Wie in früheren Fällen, zeigen wir verschiedene Variationen in der Verwendung von Kommunikationskanälen und können somit die Wichtigkeit einer ivshmem-Einsatz demonstrieren. Im Kapitel 4 werden umfassende Ergebnisse der Leistungstests dargestellt und anhand der in Kapitel 3 beschriebenen Implementierungsschritte beschrieben. Insgesamt können wir zeigen, dass erhebliche Leistungsverbesserungen erzielt werden, wenn die herkömmliche TCP/IP-Kommunikation durch unseren Geschwisterteil von ivshmem ersetzt wird. Die Verbesserungsfaktoren liegen zwischen 3-10 für die Kommunikation zwischen VMs ohne Cloud und zwischen 3-6 mit OpenStack als Cloud-Betriebssystem. Bei Magpar-Simulationen erhalten wir einen Verbesserungsfaktor für die verstrichene Rechenzeit von 1,4 bis 6. Der Projektbericht endet mit einer Schlussfolgerung und einer umfassenden Referenzliste.

Projektdaten

Das Projekt wurde von August 2015 bis Juli 2018 vom SWZ mit insgesamt 0,5 TV-L E13 Stellen an dem Standort Clausthal gefördert. Beteiligter Wissenschaftler ist:

Prof. Dr. Harald Richter
Arbeitsgruppe Technische Informatik und Rechnersysteme
Institut für Informatik
Technische Universität Clausthal

Dipl.-Ing. Pavle Ivanovic
Arbeitsgruppe Technische Informatik und Rechnersysteme
Institut für Informatik
Technische Universität Clausthal

Numerisch intensive Simulation auf einer integrierten Recheninfrastruktur

Alexander Bufe, Fabian Korte, Christian Köhler, Gunther Brenner, Jens Grabowski, Philipp Wieder

Zusammenfassung

Die Anwender von Simulationssoftware sind angesichts der heterogenen Infrastruktur, wie sie oft in heutigen Rechenzentren vorzufinden ist, mit der Aufgabe konfrontiert die am besten geeigneten Rechenressourcen für ihren Anwendungsfall sowie die Skala, auf welcher diese bereitzustellen sind, zu bestimmen, letztendlich aber auch die technischen Details für ihre Verwendung zu erlernen, was in jedem Fall eine Investition von Zeit voraussetzt.

Die von uns gewählte Kombination aus Anwendungsfall, zunächst betrachteter Infrastruktur und technischem Ansatz um diese auf einfache Art und Weise verfügbar zu machen ist durch mehrere Forschungsdisziplinen motiviert:

Aus ingenieurwissenschaftlicher Sicht ist das Ziel des Projektes, das Verständnis von Strömungsprozessen in komplexen Geometrie in zu untersuchen. Dabei stand in der ersten Phase des Projektes die Untersuchungen von Stofftransport und Umwandlungsprozessen in porösen Medien im Vordergrund, begründet durch den Bedarf in der chemischen Verfahrenstechnik Katalysatoren mit optimierter geometrischer Struktur zu entwickeln. In der zweiten Phase des Projektes wurde der Einsatzbereich der entwickelten Verfahren erweitert, um Strömungen im Kontext der Medizintechnik und Biomechanik zu untersuchen. Auch hier steht die Berechnung von Transportvorgängen in komplexen Geometrien im Vordergrund. Exemplarisch werden die Strömungen in den oberen menschlichen Luftwegen, d. h. Nase und Nasennebenhöhlen betrachtet, die durch eine komplexe, verästelte geometrische Struktur gekennzeichnet ist.

Die relevanten mathematischen Methoden aus der numerischen Strömungsmechanik schließen insbesondere die Lattice-Boltzmann Methode (LBM) unter Anwendung adaptiver Gitterverfeinerung ein. Diese müssen jedoch noch weiterentwickelt werden um auch für die technisch relevanten porösen Strukturen die auf sehr unterschiedlichen Längenskalen ablaufenden Prozesse auflösen zu können.

Die durchgeführten Simulationen dienen hierbei nicht nur zur Verbesserung des ingenieurwissenschaftlichen Verständnisses, sondern auch zur Evaluation der weiteren in diesem Projekt durchgeführten Entwicklungen. Sie sind hierfür hervorragend geeignet, da sie eine Vielzahl von Anwendungsfällen mit unterschiedlichen Anforderungen an die Infrastruktur darstellen. Parameterstudien, bei denen das gleiche Programm mehrmals mit einem anderen Parameter gestartet wird, stellen beispielsweise wesentlich andere Anforderungen an die Netzwerkverbindung als eine einzelne Simulation mit einem einzigen großem Rechengebiet und der Übergang vom Entwicklungs- in den Produktivbetrieb kann eine Verwendung anderer Ressourcen sinnvoll sein.

Aus Sicht der der Informatik ist ein Aspekt die Parallelisierung des Simulationscodes um die Methode auf aktuellen HPC Clustern mit GPU-Beschleunigerkarten anwendbar zu machen. Außerdem sollte die Möglichkeit die Fähigkeiten moderner heterogener Infrastrukturen, insbesondere IaaS Clouds und HPC Cluster, zu nutzen dem Simulationsanwender auf einfach nutzbare Weise zugänglich sein einschließlich einer automatischen Auswahl der am besten geeigneten Ressource. Eine zentrale Komponente der im Rahmen dieses Projektes durchgeführten Entwicklungen ist die Verteilungsschicht („Distribution Layer“), welche die Aufgabe übernimmt zwischen den Applikationsmodellen für Simulationscode auf der einen Seite und den verschiedenen Ressourcentypen auf der anderen Seite zu vermitteln, ob diese nun auf einer Cloud basieren oder HPC Cluster mit evtl. Beschleunigerkarten sind. Dazu werden die Anforderungen an die Resource direkt modelliert

und mit den auszuwerten und eine sinnvolle Wahl unter den verfügbaren Ressourcen zu treffen.

Die Kombination aus einem Applikationsmodell mit gewählten Parametern und dem Infrastrukturmodell liefert anschließend u.a. die instanzierten Modelle, die für Verteilungs-, Ausführungs- und Abwicklungsschritte relevant sind, welche durch den Simulationsanwender per Kommandozeilenschnittstelle ausgelöst werden können.

Projektdaten

Das Projekt wird von März 2016 bis Februar 2019 vom SWZ mit insgesamt 2 TV-L E13 Stellen an dem Standort Clausthal gefördert. Beteiligte Wissenschaftler sind:

Prof. Dr.-Ing. Gunther Brenner
Arbeitsgruppe Strömungsmechanik
Institut für Technische Mechanik
Technische Universität Clausthal

Prof. Dr. Ramin Yahyapour
Arbeitsgruppe Praktische Informatik
Institut für Informatik
Georg-August-Universität Göttingen

Prof. Dr. Jens Grabowski
Arbeitsgruppe Softwaretechnik für Verteilte Systeme
Institut für Informatik
Georg-August-Universität Göttingen

150

Überwachung von Softwarequalität mithilfe von Agenten-basierter Simulation

Jens Grabowski, Stephan Waack, Jürgen Dix

Einleitung

Die Qualitätssicherung von Softwaresystemen ist eines der Forschungsgebiete, das in den letzten Jahrzehnten an Popularität dazugewinnen konnte. Mittlerweile ist Software zu einem essentiellen Bestandteil des alltäglichen Lebens geworden. Die Komplexität von Software steigt an, was auch daran liegt, dass bestehende Softwaresysteme kontinuierlich den aktuellen Anforderungen angepasst und erweitert werden müssen. Aus diesem Grund besteht großes Interesse an der Überwachung der Qualität eines Systems während dessen Evolutionsprozesses sowie der Vorhersage der Qualität für einen konfigurierbaren Projektverlauf. Je eher ein Projektmanager auf ein Problem hingewiesen wird, umso eher kann er darauf reagieren und entsprechende Gegenmaßnahmen einleiten. Dies könnten z.B. Veränderungen an der Zusammensetzung des Entwickelteams sein. Durch die Wahl eines simulationsbasierten Ansatzes können unterschiedliche Szenarien durchgespielt und deren Resultate miteinander verglichen werden. Durch die Entwicklung einer verteilten Plattform ist es zudem möglich, größere Projekte sowie komplexere Abläufe und Kommunikation widerzuspiegeln.

Ansatz

Unser Ansatz besteht aus drei unterschiedlichen Forschungsbereichen: Datengewinnung aus Software Repositorien, Agenten-basierte Modellierung und Simulation, Bewertung mittels bedingter Markovscher Zufallsfelder.

Zu Beginn des Projekts haben wir Fragestellungen wie zum Beispiel die Auswirkung des Wegfalls eines Hauptentwicklers beantwortet, um die generelle Aussagekraft der Simulation zu testen. Im weiteren Verlauf des Projekts haben wir das getestete Simulationsmodell immer weiterverfeinert, um es realistischer zu machen. Dafür haben wir ein dynamisches Entwicklerverhalten, die Beschreibung und Auswirkung von Commit-Mustern und die Evolution der Softwaregraphen verfeinert. Um Fragen zu beantworten, wird als erstes wird ein Agenten-basiertes Modell erstellt. Um das Modell zu parametrisieren, benötigen wir Daten, die aus ausgewählten Open Source Repositorien gewonnen werden. Mit den daraus geschätzten Parametern kann die Simulation ausgeführt werden. Sollte das Modell noch nicht zur Fragestellung passen, kann es beliebig angepasst werden bis es zu einer Antwort führt. Abschließend werden die simulierten Ergebnisse mit Hilfe von bedingten Markovschen Zufallsfeldern bewertet. Wie diese drei Bereiche zusammenspielen, mit der Absicht die Qualität eines simulierten Softwareprojekts zu bewerten, wird im Folgenden genauer beschrieben.

Verantwortlich für den Evolutionsprozess von Software sind Entwickler und ihr Commit-Verhalten. Eine Generalisierung von Entwicklern ist nicht möglich, da die Arbeit von Individuen oft vom Durchschnitt abweicht. Aus diesem Grund werden Entwickler in verschiedene Typen eingeteilt. Die Klassifizierung basiert auf den Daten der Repositorien und jeder Typ weist eine andere Commit-Häufigkeit sowie eine andere Wahrscheinlichkeit einen Fehler in der Software zu beheben auf. Da das durchschnittliche Verhalten, zu einem, zu linearen Wachstum geführt hat, wurde ein dynamisches Modell basierend auf Hidden-Markov-Modellen eingeführt, welches des Entwicklern erlaubt in ihrer Aktivität zu schwanken, d.h., mal mehr und mal weniger zu arbeiten.

Um Qualitätsaussagen über die Software machen zu können, benötigen wir die Anzahl der Fehler, die einer Datei zugeordnet sind. Dazu werden

unterschiedliche Fehlertypen sowie deren Entstehungsraten ermittelt.

Um Abhängigkeiten zwischen Dateien zu beschreiben wird ein sogenannter Change-Coupling-Graph benutzt. Jeder Knoten repräsentiert eine Datei und jedes Mal, wenn Dateien zusammen in einem Commit verändert werden, wird eine neue Kante zwischen ihnen gezogen. Existiert bereits eine Kante, so wird ihr Gewicht erhöht. Diese Netzwerke und dessen Veränderungen über den Projektverlauf werden ebenfalls aus den Software Repositorien gewonnen. Enthaltene Cluster stellen logische Unterteilungen der Software da, wie z.B. Module oder Pakete. Eine weitere Verfeinerung besteht darin, das Commitverhalten mit Mustern zu beschreiben, die z.B. ein Refactoring oder einen Bugfix bedeuten. Diese Muster wirken sich dann auch direkt auf den Change-Coupling-Graph aus und können mittels Graphtransformationen beschrieben werden.

Passend zu der oben genannten Fragestellung wird ein Agenten-basiertes Simulationsmodell entwickelt und mit den Daten aus den Repositorien parametrisiert. Ein Agent ist ein Individuum, das autonom in seiner Umgebung agiert. Es wird zwischen aktiven und passiven Agenten unterschieden. Die aktiven können den Zustand der passiven verändern, umgekehrt geht das nicht. Wir haben nur einen aktiven Agententyp, den Entwickler. Passive Agenten sind unter anderem Dateien und Fehler.

Zu Beginn der Simulation wird eine bestimmte, feste Anzahl von Entwicklern jedes Typs instanziiert. Diese sind dann, beschrieben durch ihr jeweiliges Commit-Verhalten, verantwortlich für die Entstehung der Software. Des Weiteren können mit einem Commit auch Fehler behoben werden. Ob ein Fehler gefixt wird ist abhängig vom Fehlertyp, Entwicklertyp und Vernetzungsgrad der fehlerbehafteten Datei.

Um die simulierte Software bewerten zu können, wird jede Datei vorläufig als akzeptabel oder problematisch gekennzeichnet. Diese Kennzeichnung basiert auf der Anzahl und dem Typ der einer Datei angehefteten Fehler. Der simulierte, gekennzeichnete Change-Coupling-Graph dient als Grundlage für die weitere Auswertung.

Der Zustand der simulierten Software wird mit bedingten Markovschen Zufallsfeldern bewertet. Hierbei fließen auch Abhängigkeiten zwischen den Dateien in die Bewertung ein. Hat z.B. die Datei A eine schlechte Qualität und die Datei B hängt von A ab, so ist die Qualität von B davon beeinträchtigt. Des Weiteren sollen größere, zusammenhängende Teile der Software eine homogene Bewertung erhalten.

Ergebnisse

Basierend auf durchgeführten Fallstudien konnten wir nachweisen, dass Agenten-basierte Simulation ein vielversprechender Ansatz zur Softwarequalitätssicherung ist. Mit dem hier beschriebenen Ansatz ist es möglich einen Qualitätstrend eines Softwareprojekts, bezüglich einer konkreten Fragestellung, zu analysieren. Mithilfe des erarbeiteten Simulationsmodells lassen sich eine Vielzahl verschiedener Fragestellungen beantworten wie z.B., die Auswirkungen der Teamkonstellation, also das Hinzufügen oder den Wegfall von Entwicklern am Projekt. Das eingeführte dynamische Entwicklerverhalten zeigt sich in der Simulation so, dass realistischere, weniger idealisierte Kurven für den Projektverlauf entstehen.

Die Einführung von Veränderungsmustern erlaubt eine feingranulare Simulation des Change-Coupling-Graphen insofern, dass der gezielte Einsatz die Auswirkungen von z.B. Refactorings zur Reduktion der Komplexität besser dargestellt werden können.

Publikationen

Steffen Herbold, Fabian Trautsch, Patrick Harms, Verena Herbold, Jens Grabowski.
Experiences With Replicable Experiments and Replication Kits for Software Engineering Research, Advances in Computers, Vol. 113, Elsevier, 2019

Marlon Welter, Daniel Honsel, Verena Herbold, Andre Staedler, Jens Grabowski, Stephan Waack. *Assessing Simulated Software Graphs using Conditional Random Fields*, Post-Proceedings of the Clausthal-Göttingen International Workshop on Simulation Science 2017, Springer, 2018

Daniel Honsel, Niklas Fiekas, Verena Herbold,

Marlon Welter, Tobias Ahlbrecht, Stephan Waack, Jürgen Dix, Jens Grabowski. *Simulating Software Refactorings based on Graph Transformations*, Post-Proceedings of the Clausthal-Göttingen International Workshop on Simulation Science 2017, Springer, 2018

Philip Makedonski, Verena Herbold, Steffen Herbold, Daniel Honsel, Jens Grabowski, Stephan Waack. *Mining Big Data for Analyzing and Simulating Collaboration Factors Influencing Software Development Decisions* , To appear in: Social Network Analysis: Interdisciplinary Approaches and Case Studies, CRC Press, 2016

Verena Herbold, Steffen Herbold, Jens Grabowski. *Learning from Software Project Histories: Predictive Studies Based on Mining Software Repositories* , European Conference on Machine Learning and Principles and Practice of Knowledge Discovery (ECML-PKDD) - NEKTAR Track , 2016

Daniel Honsel, Verena Herbold, Marlon Welter, Jens Grabowski, Stephan Waack. *Monitoring Software Quality by Means of Simulation Methods*, 10th International Symposium on Empirical Software Engineering and Measurement (ESEM) - Short Paper , 2016

Verena Herbold, Steffen Herbold, Jens Grabowski. *Hidden Markov Models for the Prediction of Developer Involvement Dynamics and Workload*, 12th International Conference on Predictive Models and Data Analytics in Software Engineering (PROMISE) , 2016

Verena Herbold, Daniel Honsel, Jens Grabowski, Stephan Waack. *Developer Oriented and Quality Assurance Based Simulation of Software Processes*, Proceedings of the Seminar Series on Advanced Techniques & Tools for Software Evolution (SATToSE), 2015

Verena Herbold, Steffen Herbold, Jens Grabowski. *Intuition vs. Truth: Evaluation of Common Myths about StackOverflow Posts*, The 12th Working Conference on Mining Software Repositories (MSR) - Challenge Track , 2015

Verena Herbold, Daniel Honsel, Steffen Herbold, Jens Grabowski, Stephan Waack. *Mining Software Dependency Networks for Agent-Based Simulation of Software Evolution*, The 4th International Workshop on Software Mining (SoftMine), 2015

Verena Herbold. *Statistical Learning and Software Mining for Agent Based Simulation of Software Evolution*, Doctoral Symposium at the 37th International Conference on Software Engineering (ICSE), Florence, Italy , 2015

Verena Herbold, Daniel Honsel, Jens Grabowski. *Software Process Simulation based on Mining Software Repositories*, The Third International Workshop on Software Mining (SoftMine), 2014

Philip Makedonski, Fabian Sudau, Jens Grabowski. *Towards a Model-based Software Mining Infrastructure*, ACM SIGSOFT Software Engineering Notes 40(1) , ACM , 2015

Fabian Trautsch, Steffen Herbold, Philip Makedonski, Jens Grabowski. *Addressing Problems with External Validity of Repository Mining Studies Through a Smart Data Platform*, 13th International Conference on Mining Software Repositories (MSR), 2016

Philip Makedonski, Jens Grabowski. *Weighted Multi-Factor Multi-Layer Identification of Potential Causes for Events of Interest in Software Repositories*, Proceedings of the Seminar Series on Advanced Techniques & Tools for Software Evolution (SATToSE), 2015

Präsentationen

Evolution of Change Coupling Graphs, Tobias Ahlbrecht, Jürgen Dix, Niklas Fiekas, Jens Grabowski, Verena Herbold, Daniel Honsel, Stephan Waack, Clausthal-Göttingen International Workshop on Simulation Science 2019

Stipendien

ACM SIGSOFT Travel Grant: $1.200 für Verena Honsel zur Teilnahme an der International Conference on Automated Software Engineering (ASE) inklusive des Workshops on Software Mining (SoftMine) 2015 in Lincoln, Nebraska, USA

Preise

ACM SIGSOFT Distinguished Paper Award auf der MSR 2016 für das Paper „Adressing Problems with External Validity of Repository Mining Studies Through a Smart Data Platform“

Projektdaten

Das Projekt wird seit April 2016 vom SWZ mit insgesamt 1,5 TV-L E13 Stellen an den Standorten Clausthal und Göttingen gefördert. Beteiligte Wissenschaftler sind:

Prof. Dr. Jens Grabowski
Arbeitsgruppe Softwaretechnik für Verteilte Systeme
Institut für Informatik,
Universität Göttingen

Prof. Dr. Jürgen Dix
Arbeitsgruppe Computational Intelligence
Institut für Informatik
Technische Universität Clausthal

Prof. Dr. Stephan Waack
Arbeitsgruppe Theoretische Informatik und Algorithmische Methoden
Institut für Informatik,
Universität Göttingen

Distributed Simulation

Numerical simulation of technical and scientific problems traditionally is one of the disciplines with the highest demand of computing power. Accordingly, such problems are processed on supercomputers with vector and parallel computing architecture. The most powerful parallel computers in the world have been installed in the US and in China for simulation applications. The most powerful parallel computers in Germany are much smaller than these machines and are concentrated at three sites in Munich (LRZ and RZG), Stuttgart (HLRS) and Jülich (FZ). In Niedersachsen there are HLRN II (North German Network for High-Performance Computing) and many smaller systems in university computer centers available for large simulation tasks. These geographically dispersed and heterogeneous resources can be used more efficiently for numerous questions. This is referred to as distributed simulation or grid computing. Unfortunately generally the effort needed to create the software and middleware that sits between applications and operating systems is very high and there are enormous constraints on the applications. Therefore it has paid only in individual cases, to distribute simulations on multiple PC clusters so far. However, with the development of more powerful hardware and new calculation methods, it is apparent that the effort to distribute simulation applications to existing PCs and workstations is an area where it is of interest to many users.

In this project area we will examine models and methods with which simulations can be distributed on a grid and the resulting problems of software testing and quality assurance can be solved. "Distributed Simulation" also means the simulation of highly distributed real systems, such as Supply chains, supply chain management, which cannot be detected by a conventional, closed model.

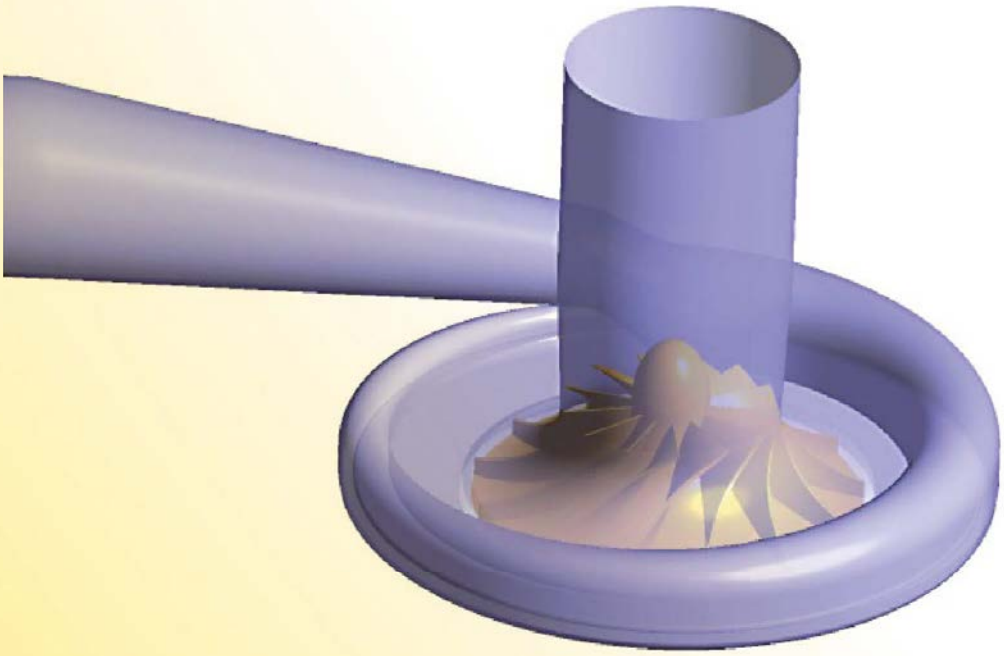

Multi-Level-Simulation using Dynamic Cloud Environments

Stefan Wittek, Johannes Erbel, Andreas Rausch, Jens Grabowski

Introduction

Cyber physical systems (CPS) consist of numerous physical and software components. Autonomous cars and automated logistic facilities are examples of such systems. The engineering of CPS is a difficult task due to the complexity of these systems. Simulation has become a core method in engineering. The complexity of a system is abstracted into an executable model that allows us to evaluate designs without the need of building physical prototypes. This reduces the costs and effort involved in this task.

Applying simulation to CPS provides numerous chances. Aside from the possible reduction of prototyping effort, the product can be improved and its costs can be lowered. Real-time simulations can be employed at runtime to infer from a few measurement points to numerous virtual sensors located among these physical sensors. This allows to reduce the amount and quality of sensory used, which in turn leads to efficient designs. The cost of the system can also be lowered by allowing deviation in the physical part of the CPS.

Nowadays the simulation of complex systems is done according to specific simulation questions. Scenes are modelled in a particular domain containing only one area of the system using a specific modelling technique. An example of this is the model of a single site within a complex supply chain. By doing this, the interdependency between these scenes and its environment is lost.

Simulation for CPS must be both: Holistic enough to capture the dependencies between its components, but only as complex as feasible, regarding modelling effort and computation times. Figure 1 describes this Tradeoff in more detail. In the figure,

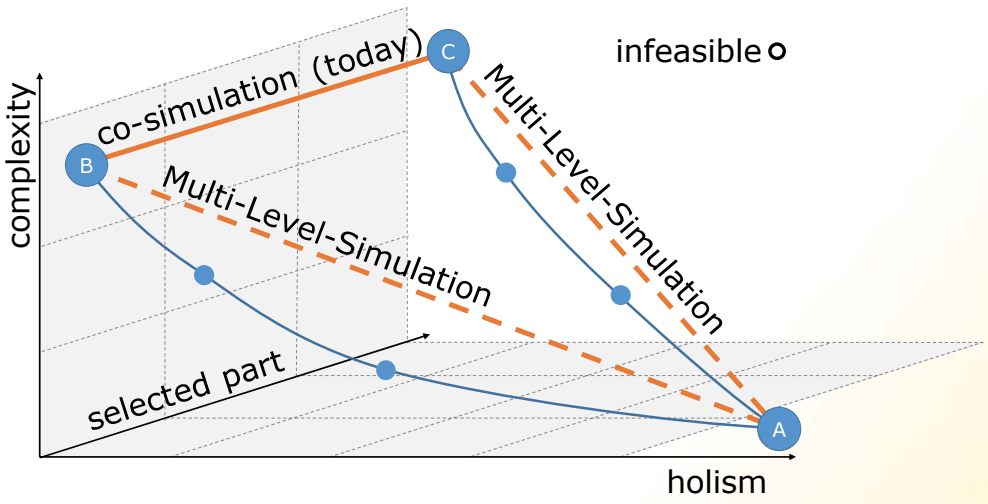

Figure 1: Tradeoff between complexity and holism in simulation.

simulation scenes are depicted as dots and arranged according to their complexity and holism (x- and y-axis). Without considering the available resources, a simulation of the whole system that is modeled, using the most detailed technique available, to provides the potentially most accurate results. Under restricted resources and for larger systems, such a simulation is infeasible. Instead, the whole system can only be simulated using a coarse simulation (A). If more detail is needed to answer specific questions, only a smaller portion of the system can be considered, ultimately leading to a very small part of the system using the most detailed technique (B). Such a zoom-in could be done with any part of the system, i.e. (C). But, since these scenes are simulated independently, interdependencies between them are lost. To acquire a more holistic view, these scenes can be connected directly using a methodology or by building interfaces between these scenes and employing co-simulation. Both approaches are difficult, expensive and often only valid for particular instances of these scenes.

Within the research project Multi-Level-Simulation we aim for a simulation methodology that is efficient regarding complexity. We simulate the CPS on multiple levels of abstraction. On a coarse level, the whole CPS is modelled using a simple semantic (A). To answer questions that require more detailed simulations, only relevant areas of the system are chosen to be co-simulated on more detailed levels (B,C). Which area is relevant may vary during the course of the simulation. To reflect this, the connected detail simulations may change dynamically. Complex simulations are resource intensive and need proper computation infrastructures. If the simulation is dynamic as proposed, this infrastructure needs to be dynamic as well.

In a traditional computing infrastructure setting, the resources have to be designed for the worst case, i.e. to satisfy the requirements of the most resource-intensive possible simulation run in order to generate its results in an acceptable time frame. This poses no problem for simulations with homogeneous requirements. However, for cases where the resource utilization is highly heterogeneous, as in the case of our simulation methodology, the computing infrastructure that accommodates the worst case is vastly oversized for the average simulation, resulting in a low overall utilization and thus cost inefficiency.

A better choice for the computing infrastructure of this use case is one that allows to reserve and release resources on-demand to dynamically match the requirements of the simulation. The Cloud Computing paradigm that has emerged and matured in the last few years matches this need. Thus, we developed an approach to deploy and execute simulations on a Cloud platform in order to achieve a timely as well as cost-efficient solution.

Related Research

In this section we describe research related to our project. The co-simulation of heterogeneous systems is the aim of a variety of tools and frameworks. A selection of these works is presented. The idea to simulate systems on different levels of abstraction can be found in several approaches. Some focus on certain application domains while others aim to provide a general framework. We will discuss both directions. Cloud infrastructures in general and the deployment and optimization of simulations are an active research field. We will provide a brief overview and discuss known approaches in this field.

A variety of works focus on the co-simulation of different simulations tools. Examples of this are the High Level Architecture specification for simulation interoperability[4] , the Functional Mockup Interface standard for model exchange and co-simulation [1] and the Mosaik Simulation API [13]. Another approach is to integrate different simulation semantics into a single tool. The Ptolemy project is an example for this approach [6]. All these works aim towards a holistic simulation of the system under investigation. The simulation of different abstraction levels is only addressed in terms of tool integration. The task to provide proper interfaces to connect simulation on different levels has to be done by the modeler.

Much effort is put into approaches that provide such concepts for specific domains such as material flows [5][8], traffic [2] or agent based behavior simulation [3]. They center on the dynamic switching of abstraction levels of model parts at runtime. To do so, explicit mappings between the states of different levels are provided. These mappings are tightly bound to the domain and the simulations they connect and are not designed to be generalizable.

Some research is conducted investigating more general concepts for the problem. The approach of Dynamic Component Substitution describes a co-simulation as a set of connected software components communication through given interfaces [11]. Switching a part of the simulation to a more detailed version corresponds to substituting one component with another. Both components are required to have the exact same interfaces. This is a critical limitation. If the components are situated on different levels of abstraction, it is plausible to expect the same for their interfaces. Multi Resolution Entities [12] define a mapping that is used to synchronize the simulation state on different levels. These mappings are defined as invertible to use them in both directions. This requirement is only met, if no information is lost mapping a detailed state to a more coarse state, which does not apply in general, as we will describe in Section 3. The concept of Multi Resolution Modelling Space introduces adapters between the interfaces and several mappings between the states of simulations on different levels [7]. However, the problem of information loss is not addressed in this approach.

Our approach of Multi-Level-Simulation is different from these approaches, because it does not force the engineer to tailor the coarse level simulations into components connected by interfaces. We consider this approach as too inflexible. The coarse level can be modeled with no dependency on the detailed level. In fact, even cutting arbitrary parts out of existing coarse level simulations to be linked to a detailed level is possible. The detailed simulations are linked to a single simulation on the coarse level using only a state synchronization mechanism. This mechanism also addresses the problem of information loss.

Simulations with a dynamic resource requirement rely on dynamic adaptive systems such as the cloud computing infrastructure. This infrastructure pools large amount of physical hardware to allow users to dynamically rent computing resources on demand [22]. Thus, a dynamic scaling of applications can be performed in the cloud [9].

Moreover, approaches exist that consider the execution of simulation workflows using elastic cloud infrastructure. Vukojevic-Haupt et al. [14] describes an approach provisioning a workflow execution middleware on demand. In their approach, however, specific infrastructure requirements cannot be specified. Another approach tackling this issue is presented by Qasha et al. [10] extending the Topology and Orchestration Specification for Cloud Applications (TOSCA) [23] standard for the execution of workflows. Nonetheless, TOSCA does not define a uniform interface that corresponds to its datamodel, compared to other cloud standards like the Open Cloud Computing Interface (OCCI) [19], making it difficult to perform adaptive actions at runtime.

Multi-Level-Simulation

One of the main results of this project is our approach for Multi-Level-Simulation. This approach is the result of the analysis of our lift example described in [a1]. To evaluate and further evolve this approach we looked at a second example the supply chain example. The most challenging part of this approach is the definition of the state map-

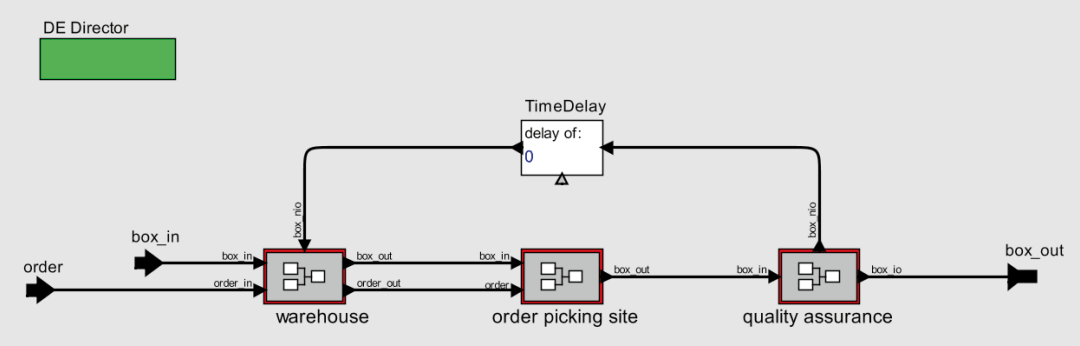

Figure 2: Model of the supply chain using Ptolemy.

pings *up* and *down* which connect the simulations during runtime. Within the project we investigated a machine learning approach to generate this mappings using only small labeled training sets provided by the user. In this section of the report, we describe the supply chain example in more detail, give a brief overview of the Multi-Level-Simulation approach and discuss our insights on learning up and down.

Supply Chain Example

This section describes the supply chain example used as a second case study.

A planner is commissioned to prepare a rough draft for a supply chain. In order to evaluate whether this design meets its requirement, a model of the supply chain is created and then simulated.

The supply chain will consist of three sites. The first site is a warehouse. Here the goods stay until they are ordered. In the second sites, an order picking, they are combined into shipments. In the third sites, quality assurance, the picked shipments are subjected to an inspection. This is to identify possible defects before they are shipped to the customer. Figure 2 shows a screenshot of this supply chain model build within the project using the Ptolemy framework [6].

The rough draft defines a specification framework for the individual sites. The simulation of the supply chain suggests that if the sites comply with this framework, requirements can be fulfilled.

How the sites should look in concrete terms, in order to comply with this framework, however, is still open. In a later step, detailed designs of the sites are developed. They describe concrete realizations of the sites. An example of this is the detailed design of order picking.

The order picking site must again meet specific requirements derived from the rough draft so the supply chain as a whole meets its requirements. However, it is not clear whether the planner's detailed design will achieve this. To be able to evaluate this within a simulation, the planner models the detailed design of the order picking site.

The planner has completed the detailed design for order picking and evaluated it in a simulative manner. Figure 3 contains a screenshot of an implementation of the model.

The planner considers the order picking to be the most important location in the supply chain. For this reason, a more detailed investigation of how the site designed in detail interacts with the other sites is needed.

Both models are in themselves unsuitable for answering the simulation question of the planner. For this reason, the planner is looking for a way to combine the models within a Multi-Level-Simulation.

Multi-Level-Simulation approach

This section summarizes our Multi-Level-Simulation approach. An in depth description can be found in [a2]. It is worth noting that the notation changed slightly since this publication.

A model is composed of a defined set of state variables. The assignment of this variables is altered during runtime by a simulation function. This func-

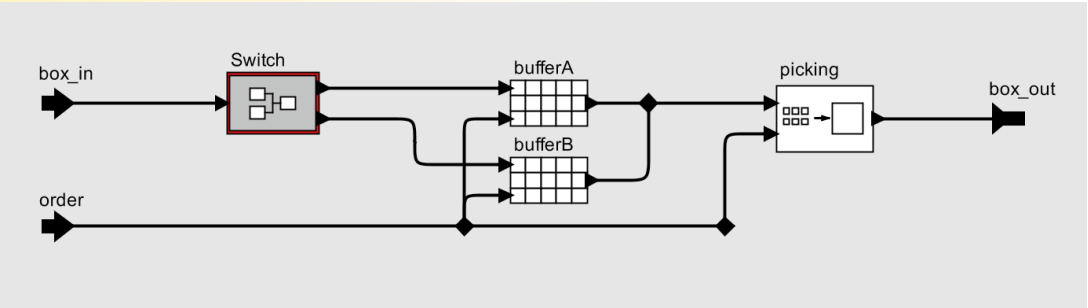

Figure 3: Model of the order picking site using Ptolemy.

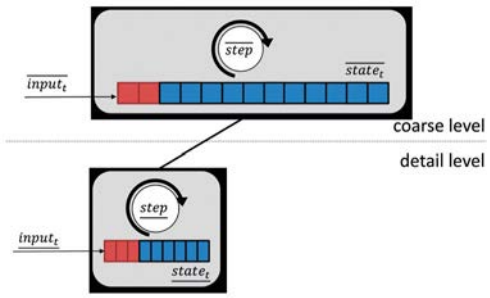

Figure 4: Structure of a Multi-Level-Simulation

tion takes the current state and some inputs provided by an environment to progress the simulation. A Multi-Level-Simulation consist of at least two such models which reside on different levels of abstraction. Figure 4 shows the structure of such an Multi-Level-Simulation. In the figure input variables, state variables and the step function of the coarse level model are depicted using a line on top, while the corresponding parts of the detailed model are denoted using a line at the bottom.

The behavior of such a simulation is depicted in Figure 5. Each simulation step of the Multi-Level-Simulation is composed of the three intermediate steps distribution, parallel execution and integration.

In the distribute step, $\overline{state^t}$ and $\overline{input^t}$ of the coarse level are mapped to the detailed level using the mapping and are than integrated (>>) into $\underline{input^t}$ and $\underline{state^t}$ of the details level. In the execution step both simulation proceed in time using their simulation functions $\overline{step}$ and $\underline{step}$. This may happen in parallel. In the Integration step, the new state of the detailed level $\underline{state^{t+1}}$ is mapped to the coarse level using up and than integrated into the state the new state of the coarse level $\overline{state^{t+1}}$. The integration operator simply overwrites a specific set of variables.

Learning State Mappings

This section details our endeavor to employ machine learning technics to learn up and down.

The up mapping mimics the model abstraction relation between the variables of the detailed and the coarse level. This relation can be described as an equivalence relation $\sim\alpha$ among assignment of this variables of the detailed level model. All states, which are consider the same if mapped to the coarse level are equal with respect to $\sim\alpha$. All members of an equivalence class implied by the relation must be mapped to the same coarse state by up.

Such an up mapping can be acquired using state of the art techniques for regression. In [a2] we investigate the performance of several such techniques on a variety of data sets, including the lift example.

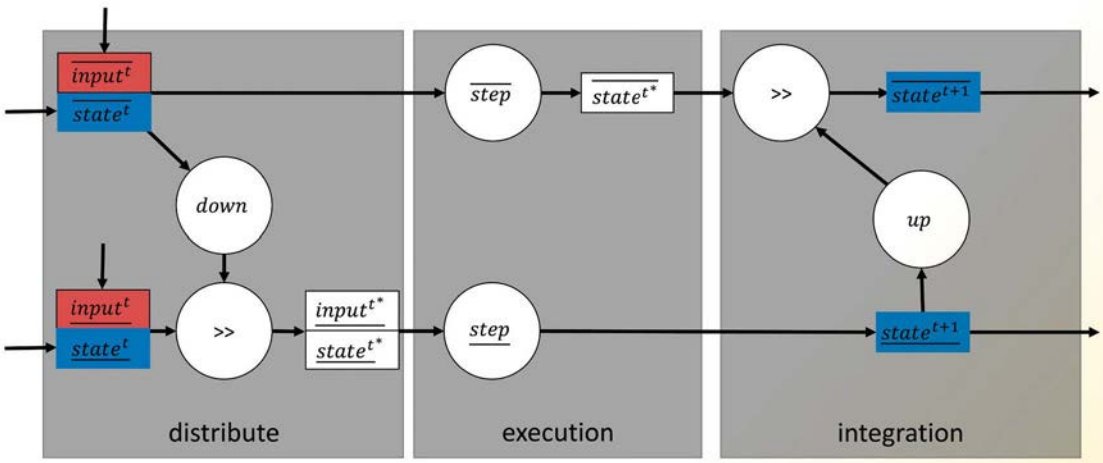

Figure 5: Behavior of a Multi-Level-Simulation.

The very same techniques perform very poorly on down. As it turns out, down is not a mapping at all. To illustrate this, lets consider the supply chain Multi-Level-Simulation described above. An example of states that need to be mapped are the boxes stored in the warehouse. The coarse level describes them only by their volume, while the detailed levels models them using their three dimensions. It is obvious that there are infinitely many combinations of this three dimensions of the detailed level that correspond to the same volume on the coarse level. All such boxes are considered equal with respect to $\sim\alpha$.

$$\begin{pmatrix}1\\4\\2\end{pmatrix} \sim_\alpha \begin{pmatrix}2\\2\\2\end{pmatrix} \sim_\alpha \begin{pmatrix}1\\0.5\\16\end{pmatrix} \sim_\alpha \dots$$

And all such goods are mapped to the same state on the coarse level by up.

$$up\left(\begin{pmatrix}1\\4\\2\end{pmatrix}\right) = up\left(\begin{pmatrix}2\\2\\2\end{pmatrix}\right) = up\left(\begin{pmatrix}1\\0.5\\16\end{pmatrix}\right) = 8$$

If down is a mapping, then by definition there is one single combination of dimensions that a particular volume is mapped to.

$$down(8) = \begin{pmatrix}2\\2\\2\end{pmatrix}$$

This would lead to a system in which for each equivalence class of $\sim\alpha$ only a single detailed state is considered, while all other members of this class are ignored. This would invalidate the simulation result significantly.

And this is also the reason for the poor performance of regression techniques on this problem. Regression, by definition, aims to find a mapping.

To overcome this limitation, we consider down as an nondeterministic sampling of an conditional probability density function p $(\underline{state^t}|\overline{state^t})$.. Our experiments show, that mixed density networks [17] and stochastic feed forward neuronal networks [18] perform reasonably well to estimate such a sampling using labeled training data.

A Dynamic Cloud Environment for Multi-Level-Simulations

To cope with ever changing workloads, the virtualization of hardware is indispensable due to its dynamic and scalable nature. This capability forms the essence of cloud computing in which large amounts of computing resources are pooled together in order to be rented by consumers [22] . For the deployment and execution of Multi-Level-Simulations in the cloud, we utilize the concepts of *Model-Driven-Engineering* allowing users to define *models* depicting simulation tasks and the required cloud architecture. To build these models, we utilize and extend the *Open Cloud Computing Interface* (OCCI) [19] a cloud standard providing a datamodel and interface to manage cloud deployments. In the following, we introduce the concepts and developed tools used to dynamically deploy and execute Multi-Level-Simulations in the cloud using OCCI.

Modeling Cloud-Deployments

To access cloud resources in a provider independent way standards like OCCI emerged [19]. OCCI is developed by the *Open Grid Forum* (OGF) and defines an extensible datamodel as well as a uniform interface to manage cloud resources. This datamodel got implemented as a metamodel by Merle et al. [17], i.e., a formal language for cloud deployments. Around this metamodel an OCCI toolchain [18] emerged granting users access to a textual and graphical editor to design cloud deployments in form of OCCI models. Moreover, as part of this toolchain a server is provided that forwards incoming OCCI requests to the cloud. To deploy and execute a Multi-Level-Simulation in the cloud we utilized this standard and its metamodel to create workflow models that can be enacted over OCCI's standardized interface. Thus, a user can define in detail which infrastructure and applications are required for the simulation using a standardized metamodel. Moreover, due to OCCI's uniform interface requests can be performed adapting the cloud deployment at runtime.

A Workflow for Changing Infrastructure Requirements

Even though, OCCI defines an interface that allows to provision infrastructure [21] and deploy applications [20] on top of it, it does not allow to define a sequence of tasks to be executed on top of the provisioned infrastructure. Therefore, we extended the metamodel of OCCI, as described in [a5], to allow

users defining workflows for arbitrary infrastructure and configuration requirements. Therefore, a language is created that allows to fulfill the individual infrastructure requirements of each step in a Multi-Level-Simulation. Currently, only workflows building a directed acyclic graph are supported. To give a brief example, Figure 6 shows a workflow comprising a Task **A** requiring a single VM and storage, while Task **B** and **C** together require three VMs. For each of these infrastructure requirements a user can define arbitrary applications running on top of it using common configuration management scripts like ansible.

In addition to these workflows, we developed a *workflow engine*, shown in Figure 6, which combines the information contained within the design time workflow, defined by the user, with a *runtime model* representing the current cloud deployment. Using both information, we adapt the deployed infrastructure to the needs of each individual task in the workflow. Thus, the overall provisioned resources for a workflow can be reduced while giving users access to define arbitrary infrastructure and application configurations.

After the workflow has been defined it serves as input for the workflow engine. As a first step the sequence of tasks to be performed are transferred into the runtime model. It should be noted, that this sequence of workflow tasks can be adapted at runtime.

Thereafter, the components of the workflow engine, *task enactor* and *architecture scheduler*, take care of the workflow's execution. Both components are part of the workflow engine's self-adaptive control loop periodically monitoring the runtime model for the current state of the workflow. The architecture scheduler analyzes the current state of the cloud deployment, e.g., the amount and configuration of active VMs and networks, and the task enactor checks the state of each task in the workflow, e.g., whether it is scheduled, active, or finished. Based on this runtime information it is analyzed and planned which task is ready for its execution and which cloud architecture is currently required. Furthermore, each component is responsible to perform the execution of the planned changes.

The task enactor checks which task has to be executed and whether its required architecture has already been deployed. If both criteria are met the task enactor triggers the execution of a task over the OCCI interface by performing a start action for the corresponding element in the runtime model. This operation is then forwarded to the specific VM in the cloud responsible for executing the task. In the example shown in Figure 6, the architecture for Task **A** is currently deployed and provisioned allowing the task enactor to execute it, as shown in the right part of the figure.

While tasks are triggered via the task enactor, the architecture scheduler identifies the exact infrastructure configuration required at each point in time. E.g., at the start of the workflow the architecture scheduler ensures that only the infrastructure for task **A** is provisioned including a VM and a storage. Therefore, an OCCI model representing the required architecture at each point in time is created over a model transformation merging the infrastructural needs of, e.g., task **B** and **C**. To provision the identified cloud architecture model, we developed a *models at runtime* (M@R) engine which generates and executes an adaptation plan as explained in the following section.

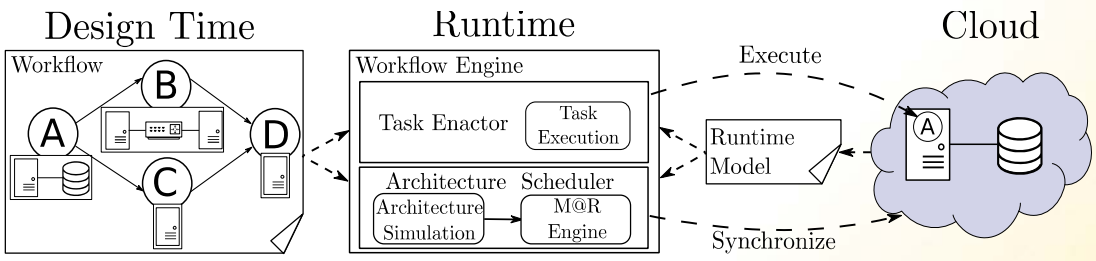

Figure 6: Cloud workflow overview.

Enacting and Adapting Deployment Models

As OCCI specifies a uniform interface that corresponds to its datamodel, requests to manage cloud resources can be directly derived from user defined OCCI models. However, the requests and the order in which they have to be performed to adapt a running system is not given. Thus, we developed a M@R engine [a4, a9] to automatically adapt running cloud infrastructures by comparing the current to the desired state of the cloud deployment and derive adaptive actions.

This engine is comprised of three major steps as shown in Figure 7 Deployment engine overview. The extraction of the current state in the cloud in form of an OCCI runtime model, the comparison to the desired state, and finally the execution of required adaptation steps.

As a first step a runtime model is *extracted* using the OCCI interface. Thus, access to the model representing the current state in the cloud is granted. Thereafter, the extracted runtime model is compared to the user's target model. Hereby, the elements of the target and runtime model are compared based on their id and attributes. Finally, the elements of both models are separated into four categories: *old elements*, *new elements*, *missing elements*, and *updated elements*. Old elements, are elements are the same within the OCCI target and runtime model thus they are ignored by the adaptation steps. New elements are elements from the target model currently not present in the runtime model thus requiring a request to create them. Missing elements are elements not present in the target model but in the runtime model thus requiring a request to delete them. Finally, updated elements are elements present in both the target and runtime model but with different kinds of configurational attributes thus requiring a request to update their attributes or state.

After the comparison, the adaptation steps take place. First, every element from the missing elements gets deprovisioned. Thereafter, the updated elements get updated, and finally the new elements get provisioned. While the deprovisioning and update phase trivially perform requests to adjust the runtime model, the provisioning phase identifies dependencies within these requests by performing model transformations on the target model as described in [a3]. Therefore, two model transformations are performed. The first transformation creates a provisioning order graph out of the OCCI model describing the dependencies to create each OCCI element. For example, before a network link can be attached to a VM, the network as well as the VM need to be started. Thereafter, this dependency graph is transformed into an UML activity diagram serving as provisioning plan which represents the sequence of requests to be performed. Finally, the provisioning plan is interpreted and executed bringing the cloud deployment into the state defined by the user.

Using the adaptive capabilities of this engine, we only have to define the cloud architecture model required in each step of the Multi-Level-Simulation workflow. However, in order to derive more sophisti-

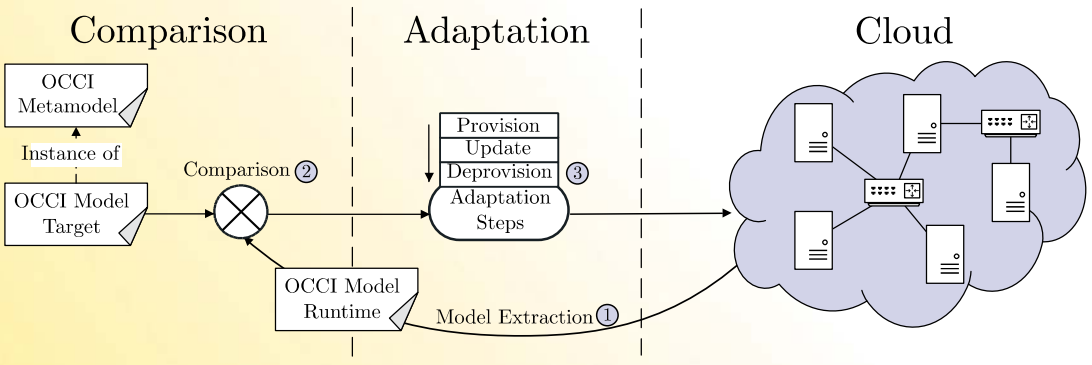

Figure 7: Deployment engine overview.

cated cloud configurations monitoring information is required that not only reflects the infrastructure and application topology of the cloud deployment, but also operational information, e.g., the state of an application or the CPU utilization of VM. Therefore, we developed an approach reflecting this kind of information in an OCCI runtime model as discussed in the following section.

Model Driven Monitoring

Even though, we are able to define workflows and automatically enact them using the workflow and models at runtime engine we currently only consider information regarding the deployed cloud infrastructure and application topology. Thus, we do not have access to operational information, i.e., information about application specific behavior or even the CPU utilization of different VMs running in the cloud. Therefore, in [a7] we developed a monitoring extension for OCCI. This extension allows users to define and manage their own sensors over OCCI's uniform interface, as well as reflect their gathered results directly in the runtime model. This extension enables OCCI runtime models to serve as a knowledge base with a single point of access for self-adaptive control loops such as the one represented within the workflow engine. Moreover, it allows to define adaptive monitoring features to only gather information about the system when it is required. Thus, sensors can be created to monitor Multi-Level-Simulation giving information when to perform a coarse or fine grained simulation. Using this information, we integrate higher abstracted workflow concepts such as loops and decision nodes as described in [a6].

Status and Outlook

The project Multi-Level-Simulation provided the funding for or research. It ended on 31.12.2018. All Work packages were concluded and all of the projects milestones met. Although the project was a success, number of new questions have been raised in the course of the project. In this section we want to discuss some of them as areas of further research.

While the described learning techniques perform well on the examples and on other low dimensions data sets, they only reach limited results on higher dimension data. We are considering to construct a method equivalent to a kernel density estimation employing silverman's rule-of-thumb to directly learn a nondeterministic down. This method is supposed to perform well even on high dimensional data. Details on this approach are to be published.

Multi-Level-Simulation seams to be applicable in the area of simulation based optimization. Here a heuristic searches for an optimal set of model parameter with respect to an objective function. The Multi-Level-Simulation is used to evaluate the objective function of a given set of parameters. The heuristic will try many of such parameter sets and cause a huge amount of simulation runs in the process. Thus the gain in efficiency regarding model complexity a computation caused by the Multi-Level-Simulation approach will multiply in an optimization scenario. Such a multi-level-optimization approach would extend the Multi-Level-Simulation and although have a significant impact on the infrastructure layer. Thus, further investigations are required.

Currently, we are able to define and execute workflows for Multi-Level-Simulations in a cloud environment. Therefore, an OCCI model has to be created describing the individual infrastructural requirements of each step in the simulation. To dynamically adjust the provisioned cloud resources during a workflows execution a models at runtime engine is used. In future work, we integrate the recently developed OCCI monitoring approach with our workflow engine to derive more sophisticated solutions for required cloud infrastructures at each step of the workflow.

References

[1] Blochwitz, T., Otter, M., Akesson, J., Arnold, M., Clauss, C., Elmqvist, H., Friedrich, M., Junghanns, A., Mauss, J., Neumerkel, D., 2012. Functional mockup interface 2.0: The standard for tool independent exchange of simulation models, Proceedings of the 9th International MODELICA Conference. Munich, Germany, doi: 10.3384/ecp12076173.

[2] Claes, R. and Holvoet, T., 2009. Multi-model traffic microsimulations, Proceedings of Winter Simulation Conference. Austin, Texas, pp. 1113–1123.

[3] Navarro, L., Flacher, F. and Corruble, V.,

2011. Dynamic Level of Detail for Large Scale Agent-Based Urban Simulations, in AAMAS '11: The 10th International Conference on Autonomous Agents and Multiagent Systems. Richland, SC: International Foundation for Autonomous Agents and Multiagent Systems (AAMAS '11), pp. 701–708.

[4] Dahmann, J. S., Fujimoto, R. M. and Weatherly, R. M. ,1997. The Department of Defense High Level Architecture, Proceedings of the 29th conference on Winter simulation - WSC '97.

[5] Dangelmaier, W., Mueck, B., 2004. Using Dynamic Multiresolution Modelling to Analyze Large Material Flow Systems, Proceedings of the 36th Conference on Winter Simulation, WSC '04. Winter Simulation Conference. Washington, D.C., pp. 1720–1727.

[6] Eker, J., Janneck, J.W., Lee, E., Liu, J., Liu, X., Ludvig, J., Neuendorffer, S., Sachs, S., Xiong, Y., others, 2003. Taming heterogeneity - the Ptolemy approach. Proc. IEEE 91, pp. 127–144.

[7] Hong, S.-Y., Kim, T.G., 2013. Specification of multi-resolution modeling space for multi-resolution system. SIMULATION 89, 28–40. doi:10.1177/0037549712450361.

[8] Huber, D., Dangelmaier, W., 2011. A Method for Simulation State Mapping Between Discrete Event Material Flow Models of Different Level of Detail, Proceedings of the Winter Simulation Conference, WSC '11. Phoenix, Arizona, pp. 2877–2886.

[9] Lorido-Botrán, T., Miguel-Alonso, J., Lozano, J. A., 2012. Auto-scaling Techniques for Elastic Applications in Cloud Environments. Technical Report: University of the Basque Country, pp. 11 – 14. doi:10.1145/2611286.2611314.

[10] Qasha, R., Ca□a, J., Watson, P., 2015. Towards Automated Workflow Deployment in the Cloud using TOSCA. In 2015 IEEE 8th International Conference on Cloud Computing, pp. 1037-1040.

[11] Rao, D.M., 2003. Study of Dynamic Component Substitutions (Dissertation). University of Cincinnati.

[12] Reynolds, Jr., P.F., Natrajan, A., Srinivasan, S., 1997. Consistency Maintenance in Multiresolution Simulation. ACM Trans Model Comput Simul 7, pp. 368–392. doi:10.1145/259207.259235.

[13] Schütte, S., Scherfke, S., Tröschel, M., 2011. Mosaik: A framework for modular simulation of active components in Smart Grids, IEEE 1st International Workshop on Smart Grid Modeling and Simulation, SGMS 2011, pp. 55-60.

[14] Vukojevic-Haupt, K., Karastoyanova, D. Leymann, F, 2013. On-demand Provisioning of Infrastructure, Middleware and Services for Simulation Workflows. Proceedings of SOCA.

[15] Bishop, C., 2013. Mixture Density Networks. Journal of Chemical Information and Modeling, 53(9), 1689–1699. https://doi.org/10.1017/CBO9781107415324.004

[16] Tang, Y., Salakhutdinov, R. (2013). Learning Stochastic Feedforward Neural Networks. Nips (Vol. 2), pp. 530–538. https://doi.org/10.1.1.63.1777

[17] Merle, P., Barais, P., Parpaillon, J., Plouzeau, N. and Tata, S., 2015. A Precise Metamodel for Open Cloud Computing Interface. IEEE 8th International Conference on Cloud Computing, New York, pp. 852-859. doi: 10.1109/CLOUD.2015.117

[18] Zalila, F., Challita, S., Merle, P., 2017. A Model-Driven Tool Chain for OCCI. 25th International Conference on Cooperative Information Systems (CoopIS), Rhodes, Greece.

[19] Open Grid Forum, Open Cloud Computing Interface – Core, available online: https://www.ogf.org/documents/GFD.221.pdf, last retrieved: 01/20/2019

[20] Open Grid Forum, Open Cloud Computing Interface – Platform, available online: https://www.ogf.org/documents/GFD.227.pdf, last retrieved: 01/20/2019

[21] Open Grid Forum, Open Cloud Computing Interface – Infrastructure, available online: https://www.ogf.org/documents/GFD.224.pdf, last retrieved: 01/20/2019

[22] Mell, P. and Grance, T., 2009. The NIST definition of cloud computing. National institute of standards and technology, 53(6), p.50.

[23] Organization for the Advancement of Structured Information Standards, Topology and Orchestration Specification for Cloud Applications, available online: https://docs.oasis-open.org/tosca/TOSCA-Simple-Profile-YAML/v1.2/os/TOSCA-Simple-Profile-YAML-v1.2-os.pdf, last retrieved: 01/20/2019

Project data

The project was funded from SWZ with one TV-L E13 staff position from August 2015 to July 2018 at the sites Clausthal and Göttingen. Involved scientists are:

Prof. Dr. Andreas Rausch
Software Systems Engineering
Department of Informatics
Clausthal University of Technology

Stefan Wittek, M.Sc.
Software Systems Engineering
Department of Informatics
Clausthal University of Technology

Prof. Dr. Jens Grabowski
Research group for Software Engineering for Distributed Systems
Institute of Computer Science
University of Göttingen

Johannes Erbel, M.Sc.
Research group for Software Engineering for Distributed Systems
Institute of Computer Science
University of Göttingen

Cloud-Efficient Modelling and Simulation of Magnetic Nano Materials

Pavle Ivanovic, Harald Richter

1 Introduction

Following the huge technological progress in last decades, magnetic nano materials are attracting significant interest in computer design, because of high densities and permanent storage capabilities. They are considered to be the future of many memory chips and can replace the existing silicon-based counterparts. However, in order to precisely model physical conditions that occur on the nano scale, computationally demanding simulations have to be conducted. Complex simulations, however, require expensive equipment, such as parallel or super computers, which hinders a ubiquitous enrolment in science. Our project goal is to accelerate progress in this promising field by creating tools and infrastructure for an efficient and cost-effective employment of magnetic nano material simulations. The report is organised as follows: in the first chapter, the importance and practical applications of magnetic nano materials are explained. It is suggested that the new simulative approach should use augmented cloud infrastructures for running simulations. Additionally, current intra-cloud communication-problems are discussed, as well as the benefits incurred by in-cloud computations. In chapter 2, the state of the art of the most promising micro-magnetic solver is given which is Magpar [1]. Also, we have provided in this report a short overview of key technologies and software solutions that are necessary for efficient simulations in a cloud environment which are OpenStack [2], ivshmem [3] and mvapich2-virt [4]. In chapter 3, after a short project history, we will present the scientific progress by means of three steps. In the first step, our rebuild of inter-VM shared memory, also known as ivshmem, is given together with a detailed implementation description. Additionally, we will suggest an augmented, one-sided MPI_Put function in form of a wrapper code with built-in Linux user IO (uio) drivers and spinlock-free synchronisation. In the second step, we will present a comprehensive ivshmem integration into OpenStack, which is the most widespread cloud operation system in the open source domain, as well as cloud tuning methods, such as cpu-pinning and proper NUMA [5] allocation. Finally, in the third step, a description of rebuilding Magpar and its cloud integration is given. As in previous cases, we show several variations in communication channel usage, and can thus demonstrate the importance of an ivshmem deployment. In chapter 4, comprehensive performance tests results are presented and described by means of the implementation steps outlined in chapter 3. All in all, we can show that significant performance improvements are achieved if traditional TCP/IP communication is replaced by our sibling of ivshmem. Improvement factors range between 3-10 for Inter-VM communication without cloud and between 3-6 with OpenStack as cloud OS. For Magpar simulations, we obtain an improvement factor in elapsed computing time of 1.4-6. The project report ends with a conclusion and a comprehensive reference list.

1.1 Motivation

Magnetic nano materials [6] are thin layers (1-100 nm) or small areas (1-100 nm2) of specific materials such as iron, cobalt, nickel, gadolinium or dysprosium, which are elements. Alternatively, the materials can also be composed of alloys, such as samarium-cobalt or neodymium-iron-boron, or ceramics, such as iron oxide or barium carbonate. The common property of these materials is that elementary magnets that are smaller than 1nm in size exist in them. Usually these tiny magnets are randomly oriented in the material, and have no globally orientated magnetic field. However, each elementary magnet can be oriented in a desired direction by means of an external magnetic write-field. Because of that property, magnetic nano materials are important in technology, since they

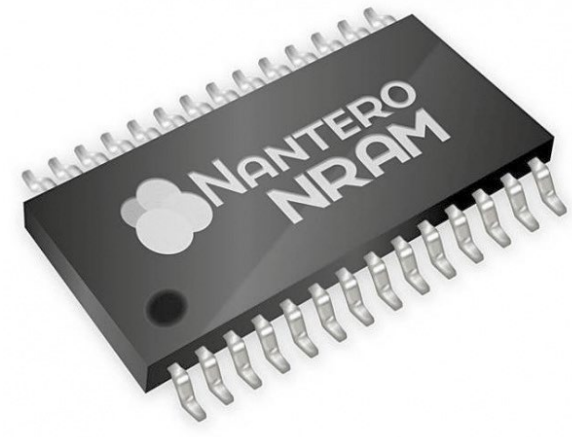

Figure 1: Example for a Magnetic RAM chip

cannot only be employed as high-capacity computer-storage but also as tiny switching. Physicists consider such materials as the computer's components of the future, albeit they are already now in commercial usage in hard drives and so-called magnetic RAM chips (MRAMs) (fig. 1).

Especially interesting and challenging in the field of magnetic nano materials is the research direction of "Spintronic". Spintronic may deliver the ultimate density for bit storage, because it uses the orientation of a single electron's spin to store a bit as "up" or "down" spin. Additionally, Spintronic has the potential to provide for the smallest switching elements, coming in trillions of transistors on the same chip and operating under very low power. Because of these perspectives, research in magnetic nano materials is important and should be fostered.

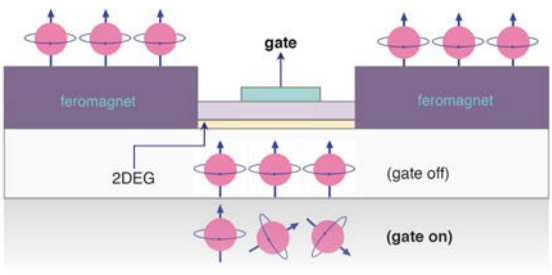

Figure 2: Spintronic - ultimate bit storage and small low-power switching-elements

Unfortunately, research in that field requires special equipment, such as scanning tunnel microscopes and ultra-high vacuum laboratory-setups, together with access to a supercomputer or parallel computer. The latter two are needed to simulate in 2D or 3D space and in time certain materials on a nano or even pico meter scale. Because of the resulting financial and organizational hurdles, such research is limited to a smaller circle of scientists and it is thus not open to a worldwide community, which delays progress.

1.2 Simulative Approach

For this project, we have created our own cloud in order to run simulations by solving complex partial differential equations that are the key to Magnetic Nano materials. The goal of this project is the replacement of expensive parallel supercomputers by more affordable and accessible cloud systems.

During our research, we have found only few software solutions that match the criteria of open-source and the possibility of parallel execution on multiple cores/CPUs. Unfortunately, none of the few was designed for running in a cloud environment. The reason for this are the inefficient scaling which clouds exhibit when going from small to large numbers of cores/CPUs or when going from small to large problem sizes. The observed and measured high-latency for inter-server communication is the main reason for this behaviour. Firstly, processes that are placed on the same server but on different VMs, cannot communicate with each other via shared memory in their server because of the strict and full inter-VM isolation that comes with the VM and cloud paradigms. Secondly, processes which are distributed on a local and on remote servers cannot communicate efficiently with each other because of the lack of built-in support in the cloud for low-latency high-bandwidth networks such as Infiniband [7], e.g. On the other hand, clouds are presenting nowadays the most cost-efficient way of computing, compared to own hardware installations. Finally, a cloud is typically an easily accessible platform. For example, with Amazon Web Service (AWS), clients can rent Teraflops or Terabytes of computing power and storage respectively for only a few Euros as monthly fees. With these price/performance figures in mind, scientists can try to focus in research more on cloud

computing approaches. Additionally, we will show subsequently that engaging a private cloud together with proper middleware can provide to the scientist similar performance as a parallel computer, but at lower costs and with higher flexibility.

2 State of the Art

2.1 Simulating Magnetic Nano Materials

Magpar was an open-source finite-element package written in C++ for micromagnetics until it got broken because of newer releases of Linux. It uses mesh geometry files and material parameters as input for solving on a parallel computer various micro- and nanomagnetic problems, such as the computation of the static energy minimization, of dynamic time integration, of exchange energy and of the effect external write fields have. In addition, Magpar consists of rich libraries for the geometry modelling of the material input, and for post-processing the output. Moreover, it has support for a highly efficient numerical-solution of the Landau-Lifschitz-Gilbert Equation (LLE) [8] for both, stiff and non-stiff problems, which is mandatory for micro- and nanomagnetic simulations. Additionally, its main competitor Nmag [9] cannot provide the same or a comparable efficiency and scalability for parallel execution. However, Magpar has also its downside: parallelisation is based on the obsolete mpich2 standard, and many old links and symbols were broken or whole libraries were missing with the advent of newer Linux updates, because the software was and is not maintained any more, although being good.

2.2 OpenStack

OpenStack is an open-source cloud-computing operating system written in Python that has a comprehensive set of services and tools, which are every 6 months further developed via new releases. Its constituting parts are first the software on the so-called controller node, and second the components for its "compute nodes". On the controller node, the main component is a cloud-wide process-scheduler called "Nova". The compute nodes in turn have "Neutron" [10] as their main part, which provides for virtual networks between virtual cores (so-called vCPUs) and VMs, as well as for a real network between physical servers and the Internet. Additionally, there exist several virtual storage capabilities for compute nodes, such as Cinder and Swift for example. Finally, the controller node has an administrator GUI called "Horizon dashboard", together with diverse management tools, such as the „Ceilometer" for performance measuring, for example.

2.3 Inter VM Shared Memory – ivshmem

Ivshmem is a highly efficient shared-memory mechanism that allows zero-data-copy for VM-to-VM and VM-to-Host communication, as long as it takes place in the same server. By installing ivshmem, users can avoid substantial overhead created by the KVM/QEMU [11] hypervisor/emulator and by memory virtualisation, because no internal data buffer is needed for data exchange. This has a huge impact on bandwidth and latency for inter-VM communication, which made ivshmem second to none with respect to performance. It is created by means of libvirt [12], a user library for KVM/QEMU that enables an efficient management of the configuration parameters of the created VMs. Although accessible through a command line interface (CLI), parameters for the input to libvirt are typically defined by XML files. After its creation, ivshmem becomes available to user-space applications in the guest OS of a VM in form of memory in a virtual Peripheral Components Interface (PCI) device. The result is that two or more user applications in different VMs of the same server can directly communicate with each other by accessing the shared memory, thereby circumventing the isolation between VMs that is otherwise omnipresent.

2.4 MVAPICH2-virt

MVAPICH2-virt [4] is a free MPI-3 software package from the Ohio State University/USA that we used for our modified MPI implementation. Its most important feature is the built-in support for ivshmem. Furthermore, because of the fact that MVAPICH2-virt was initially developed for Infiniband networks only, it requires a manual installation process along the guidelines of the most-important Infiniband manufacturer, which is Mellanox Corp. This is accomplished by means of special APIs instead of standard OFED verbs [13], which

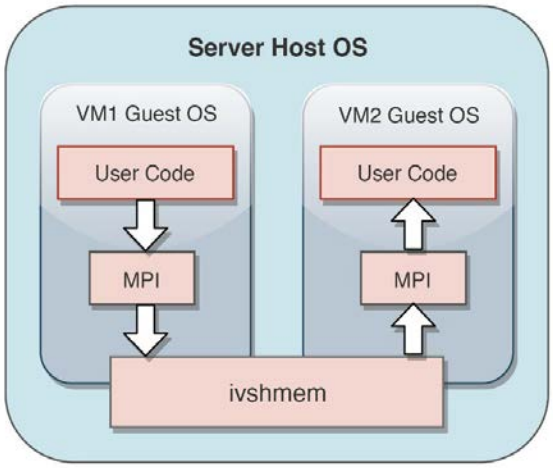

Figure 3: Architecture of ivshmem

are used otherwise as device driver for Infiniband. MVAPICH2-virt does not come with its source code, which removes flexibility in the utilisation of different communication channels and prevents insight in the underlying shared-memory (SHM) synchronisation mechanism. Moreover, it uses TCP/IP for the indispensable mutual exclusion of multiple processes when they access the same shared memory. This TCP/IP-based shared memory access-synchronization implies a high latency for each access switch.

3 Project Description

3.1 Project history

We started this project by evaluating the LLG Equation with respect to its parallel inter-process communication, in order to make its computation more efficient when being executed in a cloud. Clouds typically exhibit a high-latency low-bandwidth inter-VM communication because the communication is TCP/IP-based and also because of the overhead the cloud incurs. We investigated the performance of three solvers (Magpar, Nmag and Vampire [14]) and found out that some changes in them are desirable to achieve better performance in a cloud. The proposed changes have already been described in the previous annual report. In the second step of the project, we used our private cloud and installed the three aforementioned open-source micromagnetic solvers. The solvers were used to measure run times for demonstration examples. Then, these results were used as reference for later measurements. The difficult part in the examples was to create proper input files for each of the three solvers that can be considered as comparable to each other, although the input parameters of the solvers are not. We had to define for the solvers the same physical problem with the same size by means of different input parameters. Time-consuming was also to compare subsequently their output, because the solvers not only differed in input but also in output with respect to styles and file formats. After correct evaluation, it turned out that Vampire has to be put into another category as Magpar/Nmag, because it was created as a solver on the atom and molecule level and not on a nano- or micrometer scale which is why we were comparing later only Magpar with Nmag.

3.2 Stage 1 of the Project - Rebuilding of ivshmem with blocking synchronisation

3.2.1 State-of-the-Art before Integration

Early versions of the "Quick Emulator" (QEMU) [11] and of libvirt [12] supported ivshmem by means of a simple virtual PCI device. However, these versions did not include an efficient access synchronisation for the shared memory. However, this is indispensable for all parallel applications in High Performance Computing (HPC) that rely on shared memory. With the first ivshmem, users had as the only synchronisation means so-called spin-locks, which means to poll a status bit in a software loop until an access flag is set or reset. This resulted in many wasted CPU cycles which is intolerable for HPC. Because of that, the first version of ivshmem was not a success for HPC. Later, a better synchronisation mechanism called Shared-Memory-Server (SMS) was created which uses interrupts to communicate between the processes of a parallel user code without spin-locks. SMS became available to users as a third-party add-on.

Another issue that hampered the success of ivshmem in the past was its unfriendly user interface, which was a consequence of how the shared memory was implemented: it was created by its author as memory inside of a virtual PCI device. For that memory, the author had to create also the set of registers every PCI device must have. Three of

these registers were then used for the mentioned interrupts for SMS synchronization:

1.)A PCI-BAR0 base-address register which points to the begin of the virtual PCI device register set
2.)A doorbell register to trigger the interrupt
3.)A PCI BAR2 register, that points to the shared memory in the address space of the guest OS

The sending of an interrupt to another process of a parallel user code was triggered by writing a specific value into the ivshmem doorbell register. A change in the doorbell register was automatically detected by the underlying QEMU which then started a complicated interrupt mechanism. However, writing to a hardware register is not supported by any implementation of MPI, which is why the user interface of ivshmem had to be considered as unfriendly.

3.2.2 Functions of the SMS

The SMS is responsible for the creation and handling of virtual PCI registers created for ivshmem and managed by KVM/QEMU. It has advanced to the central hub for inter-VM SHM-based data-exchange for ivshmem. The virtual PCI registers allowed to send interrupts from one VM to another, provided that both VMs were running in the same host OS. Such interrupts can be used to synchronise ivshmem accesses between multiple read/write processes. For example, the interruption of a reading process can be used to block the reading, such that no read occurs during write, which would otherwise yield unpredictable results. Thus, interrupts free from spin locks, which consume unnecessarily CPU cycles. However, according to the author of ivshmem, the synchronization interrupts require also to wrap a parallel user application based on ivshmem into a modified user-IO device-driver (uio driver) for Linux. Such uio drivers consist always of two parts, a user part running in user-mode and a kernel part running as a Linux module in kernel-mode. Both parts cooperate with each other, thereby passing the frontier between user space and system space. Unfortunately, both parts had to be modified for usage in ivshmem. However, the modification was not well documented. Furthermore, the needed modifications were not supported by some Linux distributions. Nevertheless, the author of ivshmem based his code on interrupts for access synchronizing and on the fact that a Linux device driver stops at a read() statement which is directed to a device, if the device is not ready for being read. Linux resumes the device driver's execution, if the device has become ready. Both, the device driver's suspend and resume happens without polling, i.e. without wasting CPU time. However, it is upon the user of ivshmem to write the user-part of a Linux uio driver and to load a corresponding uio module into the kernel, which are tasks not every HPC user can accomplish. Moreover, parallel applications based on the standard Message Passing Interface (MPI) had to be changed partly, because the original MPI did not support ivshmem as communication means. Finally, with subsequent Linux releases, the address layout of the virtual PCI registers created by QEMU for ivshmem did not work anymore, with the consequence that the interruption of another process ceased to work. The result the user of ivshmem noticed was that the unblocking the other process did not work anymore. Later, a patch from the creator of ivshmem became public, and the problem could be solved.

However, another issue then showed up because QEMU and its libvirt library diverged for some time and could not cooperate with each other in many cases. Later the authors of QEMU and libvirt fixed also this problem.

The current state is that all issues were repaired, and that SMS has become an official part of QEMU. This part is now called ivshmem-server.

3.2.3 Integration of ivshmem and uio Driver with MPICH

For our project, we had to integrate ivshmem and a proper uio driver into our MPICH code that was created by following MPI-3 API guidelines. This required additional matching of proper versions of QEMU and libvirt such that they could cooperate with each other. We had to find-out the matching by ourselves, since it was not possible to wait for official bug fixes of QEMU and libvirt. For that purpose, we had to switch to the Ubuntu distribution of Linux in which we devised also simple HPC applications for ivshmem to make tests and to conduct performance measurements. These test apps had to be wrapped into the user part of the modified uio driver, and a corresponding uio module had to

be patched into the Ubuntu kernel, which was also not user-friendly.

3.2.4 Patching the User and Kernel Parts of uio Device Driver

The patching the two parts of user and kernel of a standard uio driver was necessary because the parts must accomplish two tasks for ivshmem:

1.) They have to map virtual ivshmem PCI registers into the address space of the parallel user code, so that it can access ivshmem from user space
2.) They have to send and receive interrupts for those VMs that host the parallel user application as distributed MPI processes.

3.2.5 Final Constellation of MPICH and ivshmem

In this project, we have patched and successfully loaded uio module, together with its ivshmem kernel counterpart and therefore rebuilt the broken libraries. Also, proper versions of QEMU and libvirt are found that cooperate with each other in latest stable version of Linux Ubuntu distribution. Furthermore, we have created custom performance test-code, which was integrating ivshmem, uio user drivers and MPICH parallel libraries in order to demonstrate efficiency of ivshmem-based communication. Thereby, new SHM communication mechanism based on implementation logic of single-side MPI_PUT memory access is created that could further replace inefficient TCP/IP inter-VM communication. Finally, we have achieved that blocking read feature of ivshmem works for the first time with QEMU version 2.9.50, libvirt version 2.0, MPICH version 3.2 and Ubuntu version 14.04 and integrate it in our sync mechanism.

The first key to the architecture of fig. 4 is that the address space of the MPI guest-OS application is first "mmapped" to virtual PCI-memory and then mapped to physical Linux/POSIX SHM by a 2nd mmap. Both is accomplished by the Linux mmap() call. By the tricky double mapping, access of Linux shared memory (SHM) in system space became available for user space without any system call. The second key to the architecture of fig. 4 is to replace the existing MPI_WIN_LOCK synchronisation calls in mpich-3.2 with blocking sync of ivshmem. This was necessary because MPICH does not come with ivshmem support, but with slow access synchronization based on TCP/IP.

In order to obtain the software architecture of fig. 4, we had to repair, for example, two inter-process communications: The first fix pertained to the com-

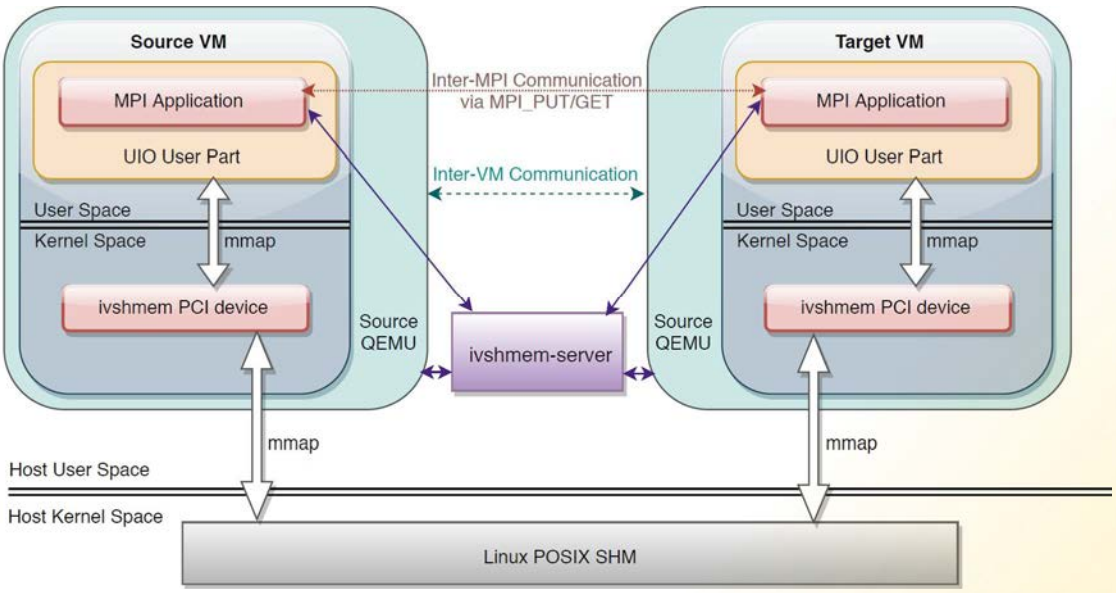

Figure 4: Software architecture of modified MPICH with ivshmem.

munication between the ivshmem-server running in the host OS and the uio driver running in a guest OSes. This communication occurs only during VM creation, and, because of that, it is not needed to make it fast. Therefore, a standard Linux socket communication was chosen because it is broadly supported.

The second fix pertained to the communication between any pair of QEMU processes running in the same host OS. Such QEMU pairs are responsible for two VMs each. The first VM hosts a sender process that wants to write to ivshmem, and the second VM hosts a receiver process that wants to read from ivshmem, potentially at the same time, which is not possible. In order to synchronize the two ivshmem accesses according to "read-after-write", that QEMU that is responsible for the sender process has to monitor whether the sender writes a bit in doorbell register. If this happens, it means that the sender wants to access ivshmem. Then, the first QEMU signals a flag via a Linux eventfd() call to that QEMU that cares for the receiver. Eventfd() was chosen by the author of ivshmem because it allows to send a signal and to listen for it without polling, i.e. without wasting CPU cycles. Subsequently, the 2nd QEMU sends in turn a Message-Signalled-Interrupt (MSI) to the receiver it cares for. The eventfd() signal is transmitted in the host OS between the two QEMUs, while the MSI is transmitted in guest OS from the 2nd QEMU to the 2nd VM in order to interrupt the receiving process. Please note, only the sequence of eventfd() and MSI was able to penetrate the perfect isolation between both VMs which otherwise exists. KVM has erected such barriers in host OS during VM creation. This way, we finally managed to restore the feature of interrupting other processes on the same server and obtained an efficient ivshmem access-synchronization for new Linux releases.

However, the integration of ivshmem with MPICH was not completed with the described action, because another problem showed up: each VM requires a modified configuration file in XML format so the the VM learns to know about the existence of ivshmem for it. This configuration file is used as input for KVM/QEMU, which is responsible for the VM. However, the manual modification of a VM XML file resulted frequently in undesirable side effects. This happened due to poor documentation of what a proper content in the XML file is, and due to many different versions of Linux, libvirt, KVM and QEMU that are on the market. By conducting multiple experiments and tests, the proper content of the XML configuration file was finally found.
This way, we finally managed to integrate blocking sync ivshmem mechanism with MPICH, and we published in [3] test measurements conducted with the described setup.

3.3 Stage 2 of the Project - Integration of ivshmem into OpenStack

3.3.1 State-of-the-Art before the Integration

OpenStack is the most widespread open-source cloud-OS, which is why we decided to integrate the ivshmem into OpenStack. However, before we could start it became clear that some cloud tuning measures would be necessary for an efficient operation of ivshmem in an OpenStack cloud. The reasons for that can be made clear if the state-of-the-art at the time we begun is considered. This state-of-the-art was as follows: First, there was a significant overhead induced by OpenStack for inter-VM communication, even on the same server. The software stack for such a situation is depicted in fig. 5. In this figure, the communication of an example HPC application is shown that is distributed onto two VMs only, each executing half of the on the same server. (A realistic application would be distributed over hundreds or thousands of VMs in many servers). However, already in the simple HPC example of fig. 5 the big software and protocol stack in the middle between the two VMs is clearly visible. This stack is added by OpenStack for security reasons and to be able to communicate between VMs via the same protocol as between VMs on different servers. This protocol is TCP/IP. As a result, the application would be hampered by the high TCP/IP latency which is not bearable for HPC.

Second, the manual update of VM configuration file proved to be even more difficult in a cloud OS than without it. The reason for that is that all VMs in the cloud are managed centrally by the Horizon dashboard of OpenStack which in turn requires a more complex VM configuration file. Additionally, the manual configuration update requires also changes of QEMU and libvirt configuration scripts. Unfortu-

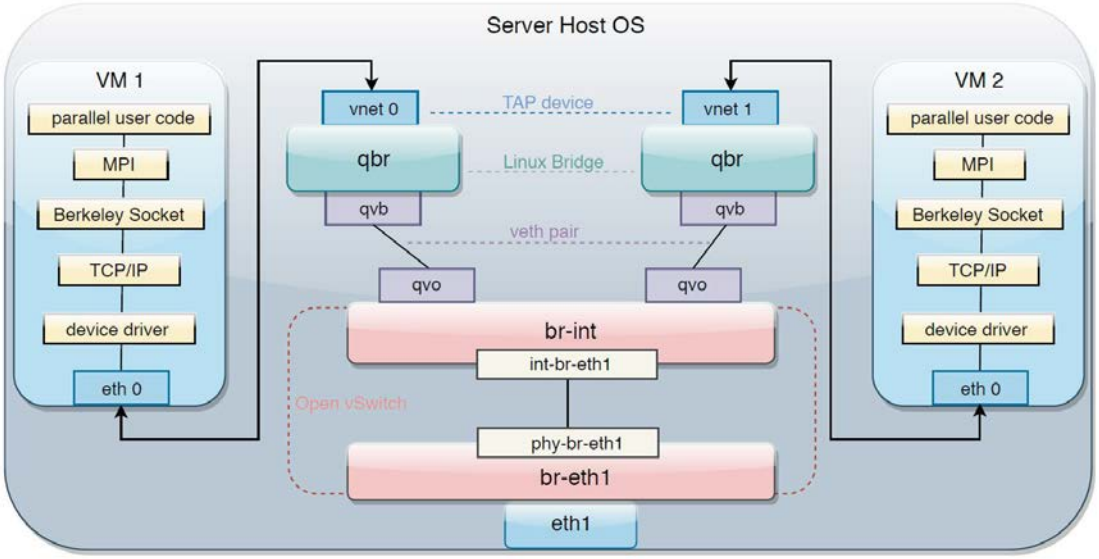

Figure 5: Software overhead in OpenStack for inter-VM communication on the same server

nately, there is only little documentation on this topic, and many parameters depend on the used Linux distribution. Finally, Linux security features such as SELinux [15] notice the efforts for change and want to prohibit them. As a result, a complex scenario of access privileges has to be erected.

Third, all servers are of the symmetric multiprocessor type (SMP) which means that multiple multicore CPUs are grouped physically around a shared main memory. A central host OS scheduler named CFS [16] periodically allocates processes, which are ready to run to available cores, and deschedules them if they are waiting for IO during execution. However, the so-called cache working set for a process has to be re-established from zero as soon as a process is allocated to a new core in another CPU, after its IO is completed. During the working-set re-establishing time, many cache misses occur which is not desirable for HPC because it slows down the application.

Fourth, OpenStack creates inside the same server one or more virtual LANs as a communication means for server-internal VMs and for external data-exchange. Such LANs are needed, in order to initialize any MPI library, such as MPICH for example, and for synchronizing between MPI processes on different servers. Therefore, defining a good virtual network configuration and topology in OpenStack plays an important role for the later HPC efficiency.

3.3.2 Cloud Tuning Measures

In order to pave the way for efficient HPC in a cloud on base of ivshmem, we did some cloud tuning first. The taken measures were paravirtualisation and CPU pinning, which are both explained subsequently.

3.3.2.1. Paravirtualisation

Paravirtualization is an efficient software solution for virtualization. In paravirtualization, all original guest-OS device-drivers are replaced by stub codes only. For example, KVM provides by means of "virtio" [17] several alternative device drivers as stubs for Linux. Virtio is a Linux kernel module and has thus kernel privileges. The alternative device drivers are called stubs because their only function is to hand-over their call parameters to QEMU and get back return results from KVM/QEMU. Stub device drivers have the same API as the original driv-

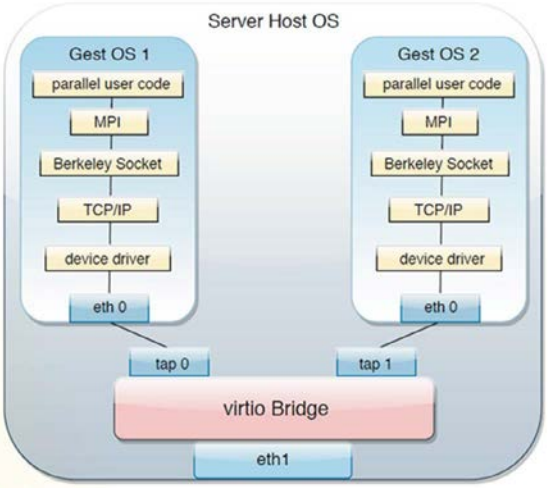

Figure 6: Software Stack for inter-VM communication with Virtio

ers, but they do not drive anything since they are running in guest OS which has no access to real hardware. In contrast to the original device drivers, stubs know that they are running in a guest OS and cooperate therefore actively with that QEMU that is responsible for the guest OS. This means, the interception of interrupts and of privileged instructions by the hypervisor is not needed any more, since the stubs do not execute them because they do not want to control real hardware. This saves many CPU cycles which is why we used paravirtualization for cloud tuning. In addition to that, the software stack between communication VMs on the same server becomes much simpler with paravirtualization, which boots performance as well. The resulting architecture is depicted in fig. 6.

3.3.2.2. CPU pinning

CPU pinning is a Linux feature that binds a process to a specific core. If the process is descheduled because of waiting for IO, it will find parts of his previous cache working set, remaining still in its core after being rescheduled. This reduces the amount of cache misses after IO is completed which speeds-up the process.

3.3.2 Results of Cloud Tuning Measures

As one of our main results, we have seamlessly implemented ivshmem into contemporary version of OpenStack and then further improved the existing Neutron network by introducing custom Virtio Bridge instead of OVS [18]. Additionally, we have presented several tuning methods, such as proper NUMA allocation and CPU pinning and therefore, adapted ivshmem to perform even better. Furthermore, we have conducted effective measurements in carefully selected configuration setups for both ivshmem and TCP/IP-based emulation of physical shared memory. All setups and methods are then evaluated and compared, showing that the best ivshmem scenario is at least three times as fast as the best TCP/IP case. Finally, our results and measurements are recognised by IEEE and published in [19].

The latest development is that a new version of QEMU makes it possible to use ivshmem in OpenStack, without a complex setup of access privileges, which was previously required for a manual modification of VM configuration files. Therefore, an average OpenStack user can now fully benefit from ivshmem and its integration in OpenStack.

3.3 Stage 3 of the Project – Rebuilding of Magpar

In the third stage of the project, we have combined our previous results and added new techniques in order to rebuild Magpar with ivshmem support by integrating it with mvapich2-virt and our private OpenStack cloud.

3.3.1 State-of-the-Art before Integration

Maintenance for Magpar stopped in 2010, and after some Linux updates the last version became broken. The reason for that was that Magpar was designed for an early release of the MPI-2 standard which used a so-called MPD [20] process manager, together with old MPI libraries.

3.3.2 Restoring Magpar

Since Magpar has shown to be the best software package for parallel execution of the LLGE solver, we decided to restore Magpar. In order to achieve this, we have re-written all Magpar installation scripts, and we searched for proper replacements for old libraries and found them. Furthermore, we decided to migrate to MPI-3, which was at that

time mpich release 3.2. The migration was a significant step because it solved two issues:

1) It replaced MPD by a more advanced successor called Hydra [21]. Hydra provides features that are important in modern HPC, such as topology-aware process binding and a GUI for process management. Furthermore, Hydra is part of the overall mpiexec [22] script, which makes running of MPI applications straightforward without knowing much technical background.
2) It introduced a new MPI communication channel called Nemesis, which is more efficient and which switches automatically from TCP/IP to standard Linux SHM if available. However, SHM via Nemesis is only possible within the same VM and not even within the same server, which is why ivshmem is still needed.

Finally, we could rebuild the whole Magpar package. Then, we repeated running our test application to verify that still the same results were computed for the same input. Our measurements showed even performance improvements compared to the old Magpar.

3.3.2 Integration of Magpar with MVAPICH2-virt.

Mvapich2-virt is intended to run mainly under a Red Hat Linux, which is why it is shipped and maintained by the Red Hat package manager RPM [23]. We examined available tools and found the proper setup to convert RPM packages into Debian software packages. Since Ubuntu is a derivative of Debian, this tool was helpful for us. Additionally, the OFED verbs library had to be replaced by a special version from the Mellanox company called Mellanox verbs, but this was unfortunately poorly documented. Furthermore, a change in the compiler script shipped with mvapich2-virt was needed as well, in order to establish correct paths between MPI libraries and the Ubuntu system binaries.

4 Performance Tests

All performance tests were conducted on our private Ubuntu cloud. In the next subchapter the features of this cloud are reported.

4.1 Hardware and Software of our Private Cloud

Our initial cloud setup included 18 old servers from Dell and Sun, comprising a total of 84 cores, 324 GB RAM and 19 TB of Disk Storage. This setup was coupled by Ethernet cards and a switch of 1 Gbits/s transmission speed. The most powerful machine we used was a server from Dell with 2 CPU sockets for Intel Xeon CPUs of type E5620@2.40GHz and four cores each. The cores are equipped with Hyperthreading, thus allowing for 2 logical processing elements per core. They included VT-x Virtualization, L1 data and instruction caches of 32 KB each, L2 caches of 256 KB each, and a shared L3 cache of 12.288 K. The size of the main memory was 32GB. The second strongest machine we used was similar to the first, but there were Xeon CPUs of type X5355@2.66GHz, and the cores were without Hyperthreading. Additionally, there was a L2 cache of 4 MB but no 3rd level cache.

4.2 Stage 1 – Performance Results after ivshmem restore

These performance measurements were performed in our strongest server with varying block sizes and by means of the following three scenarios: a) an Inter-VM communication with MPI_PUT for one-sided data exchange and with MPI_WIN_LOCK for passive remote memory access (RMA). This setup uses the MPICH Nemesis-sock channel and results in standard TCP/IP communication. b) An Inter-VM communication with our MPI_PUT and our MPI_WIN_LOCK equivalent via ivshmem and SHM synchronization. This setup required the integration of ivshmem in MPICH. c) A host-OS communication with the standard MPICH via the SHM Nemesis channel. The third scenario was used as a reference for a) and b). Results for the elapsed times are depicted in figure 7, and for bandwidths in figure 8.

The elapsed time is calculated at the sender by dividing by two the time difference between the first byte sent and the reception of a transfer-complete notification from the receiver, with SHM synchronisation included. Bandwidth is calculated by dividing the elapsed time by the respective message sizes.

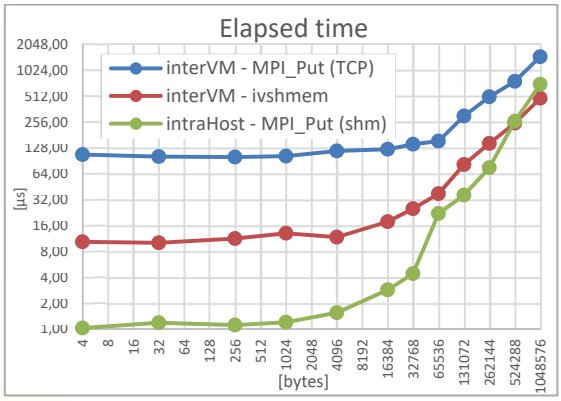

Figure 7: Measurements of elapsed time for various message sizes

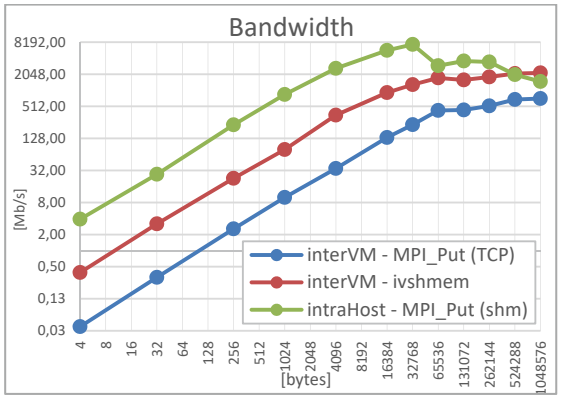

Figure 8: Results of calculated bandwidth for various message sizes

Based on these measurements, we could observe four phases in figure 7 and figure 8: I.) Phase 1 for 0 to 4 kB block lengths for the transferred message: in this phase, we can see that the SHM synchronisation time is dominating the data transfer time, because the elapsed time does not increase with an increased message size. Furthermore, the amortization costs for SHM synchronisation are decreasing with increased message size. Finally, ivshmem surpasses TCP/IP by a factor of up to ten in both, bandwidth and elapsed time, respectively. II.) Phase 2 for 4-64 kB block lengths: in this phase, we can observe that the elapsed time begins to increases with the message size, which is visible at the ivshmem curve. The maximum reachable bandwidth is approximately 7.4 GB/s at a block length of 32 KB. Also for TCP/IP, a maximum value for its linear slope is reached. The reason for the latter is that only one TCP/IP packet is needed for all message sizes. Furthermore, the curve for the elapsed time is sharply changing its slope angle. III.) Phase 3 for 64-256 kB block lengths: in this phase, we can see that a transmission saturation is reached at about 256 KB block length with data rates of 2,1 and 0,25 GBs/s. Here, ivshmem surpasses TCP/IP by a factor of four. IV.) Phase 4 for block lengths > 512kB: we can observe a declining reference curve, while ivshmem becomes the fastest communication. This is a remarkable result, because it means that virtual communication can even be faster than real communication for very large block sizes. The reason for that surprising behaviour is that ivshmem does not make any time-consuming system-call, in contrast to host-OS applications that are coupled by SHM. Also, ivshmem operates fully in user space because of mmap and the blocking-read feature, which is in the user part and thus in the user space of uio, although the SHM is physically located in host-OS system-space. This is a highly efficient method and because of that, ivshmem is second to none in HPC. As a result, the performance difference between TCP and ivshmem in phase IV is a factor of three with respect to bandwidth, although TCP implementations are highly efficient as well for large message sizes. Finally, it must be mentioned that the block length for the peak ivshmem bandwidth is also influenced by the chosen synchronization and communication type. For example, with active RMA, MPI Start-Post-Wait-Complete and point-to-point MPI_Send, the maximum bandwidth is obtained at a message size of 256kB, resulting in an ivshmem bandwidth benefit four times higher than TCP/IP.

4.3 Stage 2 – Performance Results after Cloud Tuning and ivshmem Integration

For these measurements, we used OpenStack Juno, Ubuntu 16.04 as guest OS, CentOS 7.1 as host OS, QEMU 2.9.50, libvirt 2.0, MPICH 3.2 and virtio 1.1.1 as software environment. Additionally, we sent data from one MPI process to the other, while varying its size from 4bytes to 1Mbyte. The transmission was accomplished by one-sided MPI_PUT via the standard MPICH Nemesis-sock channel. However, because Host shared memory

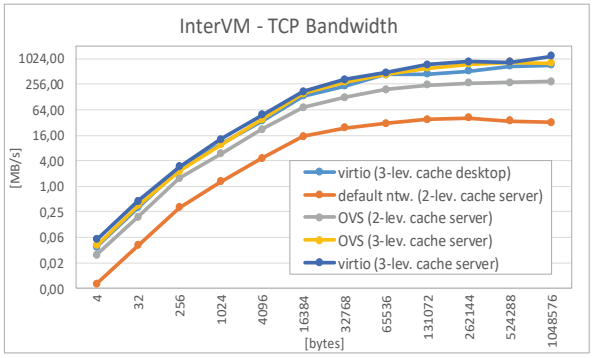

Figure 9: Elapsed times for TCP/IP-based inter-VM communication

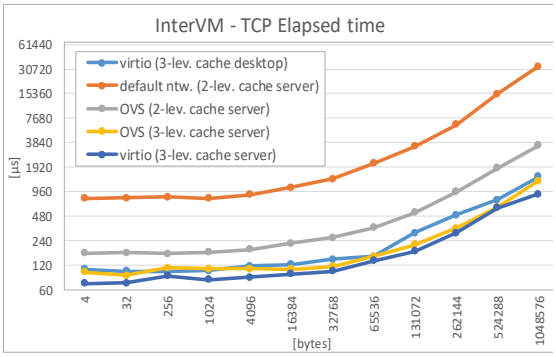

Figure 10: Bandwidth for TCP/IP-based inter-VM communication

could not be used due to VM-isolation, MPICH emulates this functionality with TCP/IP communication by sending data packets back and forth that carry shared variables.

In the first step, the influence of engaged 3rd level caching on OVS is discussed in comparison to 2nd level caching only. As reference, we used the elapsed time for transferring data in configuration where no cloud was engaged (VM only). The results are shown in the orange, grey and yellow curves of fig. 9 and fig. 10. The two orange curves depict the elapsed time and bandwidth for inter-VM data exchange with QEMU emulation of a fully virtualised network and no cloud OS. In this case, each Guest device-driver access to QEMU-emulated network device is intercepted by KVM, which is very inefficient. As one can see, if OpenStack is engaged with its paravirtualised drivers and OVS (grey curves), performance is much better than without cloud. The reason for this significant improvement lies in concept of paravirtualisation where KVM does no longer intercept Gest access to the emulated hardware. Instead, all parameters of Gest device-driver calls are forwarded directly to QEMU. Additionally, engaging 3rd level caching further improves performance (yellow curves) because of higher cache capacity and reduced access time. Similarly, replacing the server by a desktop PC (light blue curves) showed also good per-

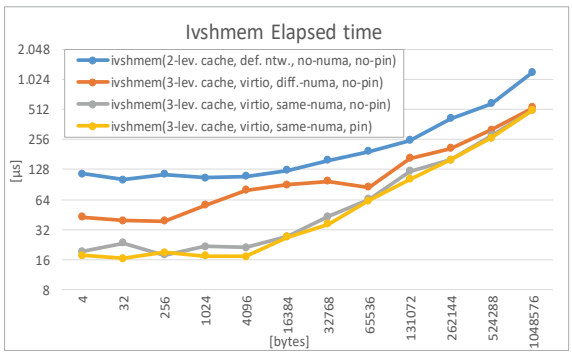

Figure 11: Elapsed times for ivshmem-based inter-VM communication

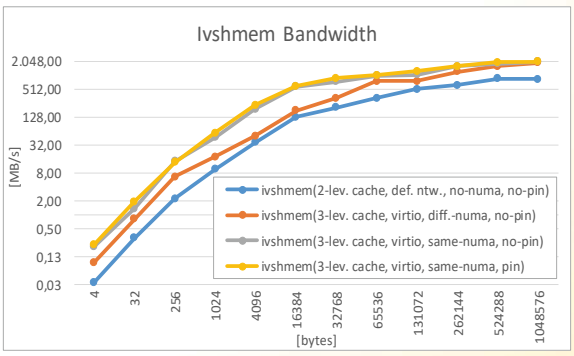

Figure 12: Bandwidth for ivshmem-based inter-VM communication

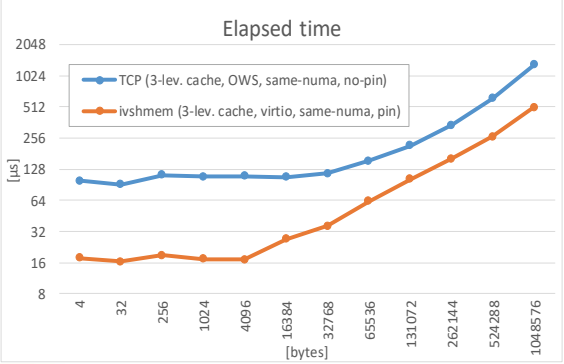

Figure 13: Elapsed times for TCP and ivshmem-based inter-VM communication

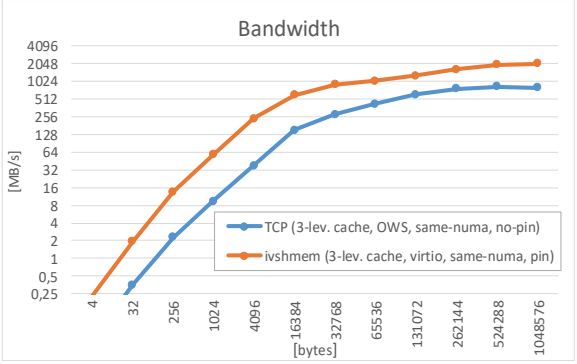

Figure 14: Bandwidth for TCP and ivshmem-based inter-VM communication

formance, but disadvantage was limited scalability and cloud incompatibility. Finally, the only measure that made significant difference was replacement of Neutron's OVS by virtio-net.

4.3.1 Tuning the ivshmem Inter-VM communication

The isolated ivshmem performance results are depicted in fig. 11 and fig. 12. The blue curves show implementation of fully virtualised or emulated TCP/IP network, which is still required for initial MPI synchronization. As shown in figures below, it has very poor performance, but far better than non-SHM solution shown in fig. 9 and fig. 10. As expected, performance improves further if the same tuning measures are engaged as before, i.e. 3rd level caching and virtio instead of OVS. The effect is shown in the orange curves. Additional gains are possible by proper NUMA allocation and CPU pinning.

4.3.1.1 Proper NUMA Allocation, no-CPU Pinning

In the grey curves of fig. 11 and fig. 12, it becomes visible that manually allocating the communicating VMs into the same non-uniform memory-access (NUMA) region yields in further significant improvements. In such a uniform memory access region, all VMs have the same access latency to the physical shared memory in host OS. On the other hand, allocating the MPI VMs to different NUMA regions leads to frequent cache misses, and data access times are not equal any more as well.

4.3.1.2 vCPU Pinning

If cache misses occur together with a rescheduling of the vCPU, that executes a VM, from one physical processing unit (i.e. core) to another, the result is a non-monotonously increasing performance for increased message size. This is noticeable in the grey curve of fig. 11 for sizes from 4B to 1KB. Therefore, each Host vCPU process was manually bound by us to a specific physical processing unit in procedure known as CPU pinning. The utmost performance boost is achievable if ivshmem is used together with 3rd level caching, virtio, proper NUMA allocation and CPU pinning. This is demonstrated by the yellow curves in fig. 11 and fig. 12. In this case, bandwidth reaches 2 GB/s for a message size of 1 MB, which is twice as much as for the best TCP/IP case. For smaller message sizes, the difference is even bigger. The results were achieved without using SR-IOV [24] as hardware accelerator for communication.

Finally, direct comparison of standard TCP/IP OpenStack cloud performance with our ivshmem integration is depicted in fig. 13 and fig. 14, for elapsed time and bandwidth respectively. Furthermore, we have intentionally selected same-NUMA region for Inter-VM measurements since NUMA allocation is performed randomly by OpenStack scheduler and therefore during each instance cre-

ation different memory region could be engaged. For the smaller size messages, synchronization is dominating communication and performance difference is factor of six in favour of ivshmem. On the other hand, further increase of message block size leads to the case that data flow becomes main contributor to overall communication time. Consequently, from this moment on the difference between two communication technologies drops to the factor of three, in case of the largest messages. This is remarkable result, considering that NUMA tuning was not applied as mentioned earlier.

4.4 Stage 4 – Performance Results after Magpar Integration

As in our initial measurements presented in previous report, we have used a cube of Permalloy with x/y/z-dimensions of 30x30x100 nm3, respectively, as ferromagnetic material. Further input configuration included magnetic saturation of 0.86e6 A/m, damping constant of 0.5 and exchange-coupling constant A=13.0e-12 J/m. As output, the time course of the magnetisation vector was calculated in the cube for the interval of 0-300 ps, which is the point in time when the Permalloy reached saturation. Finally, all measurements are performed in our strongest hardware with focus on inter-VM intra-Server communication. In order to perform the precise estimation of improvements introduced with ivshmem, we have combined three scenarios and present them together in table 1: 1) Restored original Magpar solver with mpich2 communication libraries and MPD process manager. 2) Upgraded Magpar to latest MPI-3 standard and corresponding performance optimisations. 3) Magpar integrated with mvapich2-virt and ivshmem SHM support. Furthermore, beside elapsed time T, we have provided in post-processing phase additional two parameters: speedup S and efficiency E. We calculated them in a following way: S is defined as the execution time on n vCPUs compared to that on 1 vCPU. E is defined as E = S/n and denotes the vCPUs utilization.

As visible in table 1, execution time T is almost identical in all 3 cases when sequential (1vCPU) execution was engaged, which is expected. All 3 Magpar runs occurred by using internal shared memory enhanced with VT-x hardware accelerator and therefore visible minor fluctuations could be attributed to random nature of Host Linux scheduler. On the other hand, in case of parallel execution, we could observe further improvements introduced with MPI-3 standard, especially in case of 4 vCPUs, where difference between original mpich2 and new mpich3.2 is the most visible. However, because of initial problem size segmentation and following extensive IPC, we could not achieve any speedup S greater than 1 when TCP/IP is engaged. This fact is important because it demonstrate that current cloud technologies are not suitable for HPC. Also, it is necessary to stress that focus of our measurement setup was mainly the load of Inter-VM IPC and therefore we have disregarded all parallel Intra-VM solver executions. As shown in our previous report with Intra-VM measurements, shared memory of both mpich2-shm and Nemesis-shm channels is sufficient and further improvements are not expected. On the other hand, parallel execution based on ivshmem is clearly superior and brings total speedup of more than 61%. This is significant, considering that relatively smaller problem size was used as input. However, in case of higher number of grid points, it is expected that achieved speedup would be superseded several times, as

Table 1: Comparison of different Magpar implementations

	Original (mpich2)			Improved (mpich_3.2)			Ivshmem (mvapich2)		
Setup	**T [s]**	**S**	**E [%]**	**T [s]**	**S**	**E [%]**	**T [s]**	**S**	**E [%]**
1 vCPU	84,98	1	100	85,07	0,99	99	86,80	0,98	98
2 vCPUs	97,71	0,87	43,5	92,51	0,92	46	62,14	1,37	68,38
4 vCPUs	116,01	0,73	18,25	92,66	0,92	23	52,79	1,61	40,25
6 vCPUS	292,06	0,29	4,83	273,82	0,31	5,17	52,90	1,61	28,83

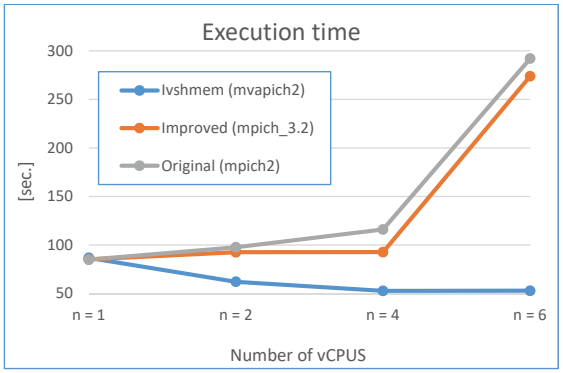

Figure 15: Magpar execution time in relation to number of vCPUs

shown in our previous measurements. Additional reason why we could not observe more than 100% speedup, as seen in pure HPC performance measurements depicted in chapters 4.1 and 4.2, is that Magpar is complex micro magnetic solver and communication is only one segment of overall execution time. Most of the time, simulation software such as Magpar, spend in computation phase.

Additional aspect of Inter-VM communication shown by these measurements is saturation of processing elements. In fig. 15, it could be observed that the best performance is reached already at 4 vCPUs in case of ivshmem and to certain extent in mpich3.2 as well. Therefore, any further increase of parallel processes employed would only deteriorate achieved performance gains. This clearly demonstrate complexity of virtualisation and amount of overhead created during Inter-VM IPCs, although the benefits of internal shared memory utilisation were not taken into consideration. As expected in cases of complex simulation software, efficiency E was dropping with every increase of processing elements (vCPUs), and ivshmem remained superior to both TCP/IP competitors. Moreover, ivshmem provided more than six times better efficiency in case of maximum number of vCPUs tested. Finally, we have achieved that Magpar was executed for the first time in OpenStack cloud environment using ivshmem for Inter-VM communication and demonstrated its supremacy over standard TCP/IP channel. Our tests showed that ivshmem brought improvements between factors of 1.4-6, depending on number of parallel elements, which is indispensable for HPC.

5 Conclusion

Magpar was a good parallel solver for the Landau-Lifshitz-Gilbert equation (LLGE) for micromagnetics until it broke in newer Linux releases. It used the message-passing interface (MPI) for high-performance computing. In this project, we have achieved that Magpar is usable again, and we improved it additionally by migrating to the MPI-3 standard. This was made possible by adapting it to the mpich-3.2 library, which was the latest stable version of MPI-3 at the time. Furthermore, we enabled for the first time Magpar to use ivshmem, which is a superior inter-VM communication means based on virtual shared memory inside of a server. Additionally we migrated Magpar to an OpenStack cloud environment. With this setup, we have achieved performance improvements of 1.4-6, depending on the number of used vCPUs hosting parallel MPI processes. This is in comparison to a Magpar execution with standard mpich2 communication channels without ivshmem. Also, we have shown that ivshmem is better for all message sizes, compared to MPI communication channels based on TCP/IP. Performance improvements are between factors of 3-10, depending on the message size. For messages bigger than 512kB and special hardware configuration, ivshmem even surpasses pure non-virtualized Linux SHM performance, which is a remarkable result. Additionally, we have introduced for the first time known tuning methods, as new features in the context of ivshmem and OpenStack, such as paravirtualization, proper NUMA allocation and CPU pinning. Finally, we have conducted runtime measurements in carefully selected configuration setups for both ivshmem and TCP/IP-based emulation of physical shared memory. All setups showed that the best ivshmem scenario is at least three times as fast as the best TCP/IP case.

6 References

[1] http://www.magpar.net/

[2] Open source software for creating private and public clouds, https://www.openstack.org/

[3] P. Ivanovic, H. Richter, Performance Analysis of ivshmem for High-Performance Computing in Virtual Machines, Proc. 2nd

International Conference on Virtualization Application and Technology (ICVAT 2017), Shenzhen, China, Nov.17-19, 2017.
[4] http://mvapich.cse.ohio-state.edu/user-guide/virt/
[5] https://en.wikipedia.org/wiki/Non-uniform_memory_access
[6] Vijay K. Varadan, LinFeng Chen, Jining Xie. Nanomedicine: Design and Applications of Magnetic Nanomaterials, Nanosensors and Nanosystems. s.l. : Wiley, November 2008.
[7] Infiniband, http://www.mellanox.com/pdf/whitepapers/IB_Intro_WP_190.pdf
[8] Lubomír Bañas, Numerical Methods for the Landau-Lifshitz-Gilbert Equation, in Zhilin Li, Lubin G. Vulkov, Jerzy Wasniewski (Eds.): Numerical Analysis and Its Applications, Third International Conference, NAA 2004, Rousse, Bulgaria, June 29 - July 3, 2004, Re- vised Selected Papers. Springer 2005 Lecture Notes in Computer Science ISBN 3-540- 24937-0, pp. 158-165.
[9] Nmag, University of Southampton, http://nmag.soton.ac.uk/nmag/
[10] Introduction to OpenStack Networking (neutron), https://docs.openstack.org/liberty/networking-guide/intro-os-networking.html
[11] S. Weil, QEMU version 2.10.93 User Documentation, https://qemu.weilnetz.de/doc/qemu-doc.html
[12] Libvirt virtualization API, https://libvirt.org/
[13] OFED verbs driver, [https://www.openfabrics.org/index.php/openfabrics-soft- ware.html
[14] Vampire,. http://vampire.york.ac.uk/features/
[15] SELinux, https://en.wikipedia.org/wiki/Security-Enhanced_Linux
[16] CFS, https://en.wikipedia.org/wiki/Completely_Fair_Scheduler
[17] Virtual I/O Device (VIRTIO) Version 1.0. Committee Specification Draft 01 / Public Review Draft 01, http://docs.oasis-open.org/virtio/virtio/v1.0/csprd01/virtio-v1.0-csprd01.pdf, Dec. 03, 2013.
[18] Open vSwitch in OpenStack, https://docs.openstack.org/liberty/networking-guide/scenario-classic-ovs.html
[19] P. Ivanovic, H. Richter, OpenStack Cloud Tuning for High Performance Computing, Proc. 3rd IEEE International Conference on Cloud Computing and Big Data Analysis (ICCCBDA 2018), http://www.icccbd.com/, Chengdu, China, April 20-22, 2018.
[20] Multi-Purpose Daemon, https://cs.mtsu.edu/~rbutler/mpd/
[21] https://wiki.mpich.org/mpich/index.php/Hydra_Process_Management_Framework
[22] https://linux.die.net/man/1/mpiexec
[23] RPM, https://en.wikipedia.org/wiki/Rpm_(software)
[24] P. Kutch, B. Johnson, SR-IOV for NVF Solutions - Practical Considerations and Thoughts, rev. 1.0, Networking Division, https://www.intel.com/content/dam/www/public/us/en/documents/technology-briefs/sr-iov-nfv-tech-brief.pdf, Feb. 23, 2017

Project data

The project was funded from SWZ with 0.5 TV-L E13 staff position from August 2015 to July 2018 at the site Clausthal. Applying scientist is:

Prof. Dr. Harald Richter
Research Group
Technische Informatik und Rechnersysteme
Department of Informatics
Clausthal University of Technology

Dipl.-Ing. Pavle Ivanovic
Research Group Technische Informatik und Rechnersysteme
Department of Informatics
Clausthal University of Technology

Numerically Intensive Simulations on an Integrated Compute Infrastructure

Alexander Bufe, Fabian Korte, Christian Köhler, Gunther Brenner, Jens Grabowski, Philipp Wieder

1 Introduction

In the SWZ-Project "Numerically Intensive Simulations on an Integrated Compute Infrastructure", researchers from the TU Clausthal, the University of Göttingen and the Gesellschaft für wissenschaftliche Datenverabeitung mbH Göttingen (GWDG) collaborate to create an infrastructure to simplify the selection and management of compute resources from heterogeneous compute service offerings which are today's reality in many data centers. As a main use case, we consider fluid flow simulations as they are conducted by the research group at the TU Clauthal.

From an engineering point of view, the aim of the project is to investigate the understanding of flow processes in complex geometries. The first phase of the project focused on the investigation of mass transport and conversion processes in porous media, due to the need in chemical engineering to develop catalysts with an optimized geometric structure. In the second phase of the project, the application range of the developed processes was extended to investigate flows in the context of medical technology and biomechanics. Here, too, the calculation of transport processes in complex geometries is in the foreground. The flows in the upper human airways, i.e. nose and paranasal sinuses, which are characterized by a complex, branched geometric structure, are examined as examples.

The relevant **mathematical methods** from computational fluid dynamics include in particular the Lattice Boltzmann Method (LBM) and

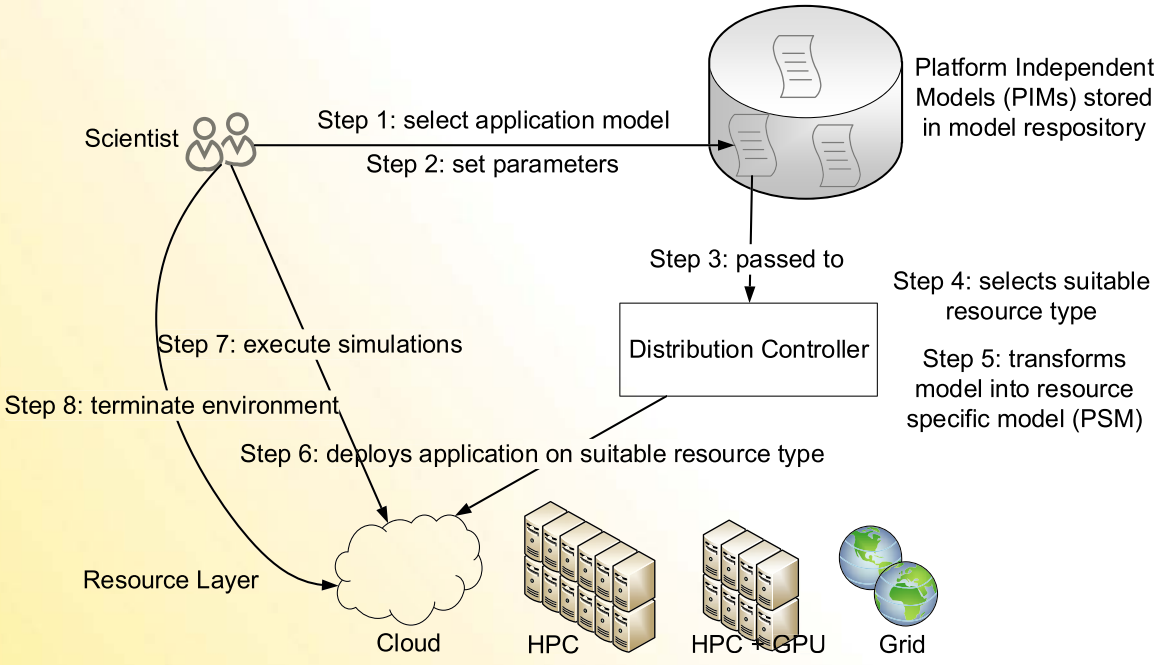

Figure 1: General workflow from the viewpoint of a simulation scientist.

its application using adaptive mesh refinement. However, these need to be developed further in order to account for the varying length scales on which processes take place in technically relevant porous media.

The simulations of flow in porous media not only have the purpose of increasing understanding of mass transport in porous media, but are also used to evaluate the developed architecture. These simulations are perfectly suitable as they cover a broad range of application cases with different requirements regarding the used infrastructure. Parameter studies for example have other requirements regarding the network connection as a single simulation of a large area or the transition from code development to actual simulations might have different resources requirements. Parallelization of the simulation code to make the method accessible to current High Performance Computing (HPC) setups featuring GPU accelerator cards is one aspect of concern from the view of **Computer Science**. Moreover, the ability to exploit the capabilities of modern heterogeneous infrastructures, including IaaS Clouds and HPC nodes, should be easily accessible available for the simulation scientist, including the automated choice of the most suitable resource type.

2 Architecture

In all parts of a numerical simulation workflow the widespread heterogeneity of IT systems comes into play: Since the computing and/or storage resources are in general not available on the simulation scientist's workstation directly, remote systems equipped with different hard- and software have to be utilized. The manageability of the entire setup is improved by making a conceptual distinction between the general involved parts, such as the desired simulation application and available types of computing resources on one side, and the concrete simulation/case/job and the instance of, e.g., a Cloud setup or an HPC-Installation. Our approach is inspired by the Model-Driven Architecture (MDA).

2.1 Model Driven Architecture

MDA is a design pattern developed by the Object Management Group (OMG), which provides an approach to tackle the complexity of heterogeneous environments by proposing the use of formal models that describe the system. These models can be analyzed on their own, for example to make high-level design decisions and/or simulate the system without real resources attached. In addition, they are best designed in a framework that allows the automatic translation of models into code. One of the modeling languages developed by the OMG is the well-known Unified Modeling Language (UML). In the context of MDA, the IT system to be modeled, i.e. the hard- and software setup, is referred to as platform. While the system's general features, such as the kind of software dependencies of a simulation application or the job scheduling system in a compute cluster are modelled with the help of so-called **Platform Independent Models** (PIM), the concrete setup intended to be deployed necessitates P**latform Specific Models** (PSM), which in this example would describe the distribution packages or environment modules to provide said dependencies and the available hardware described in the form that can be understood by the scheduling system, respectively. The crucial part of achieving automated resource deployment and execution of the simulation application can then be formulated as the task to take user input and data gathered from the system itself to transform the PIMs into PSMs. Once this part is taken care of, the PSM can be translated into the resource-native format, e.g., configuration scripts, job input data, or job scripts.

2.2 General Workflow

Figure 1 depicts the envisioned workflow from the viewpoint of the simulation scientist. A PIM encodes the structure and behavior of the simulation application in a target resource independent way and is stored in a model repository. The simulation scientist is then able to select (Step 1) and adapt (Step 2) the existing models from the repository. The selected and instantiated model is then passed to a Distribution Controller (Step 3) that evaluates the parameters of the model (Step 4), selects the suitable target infrastructure accordingly and transforms the selected model into a PSM that matches the requirements of the targeted infrastructure (Step 5). In the next step, the resource provisioning and the automated

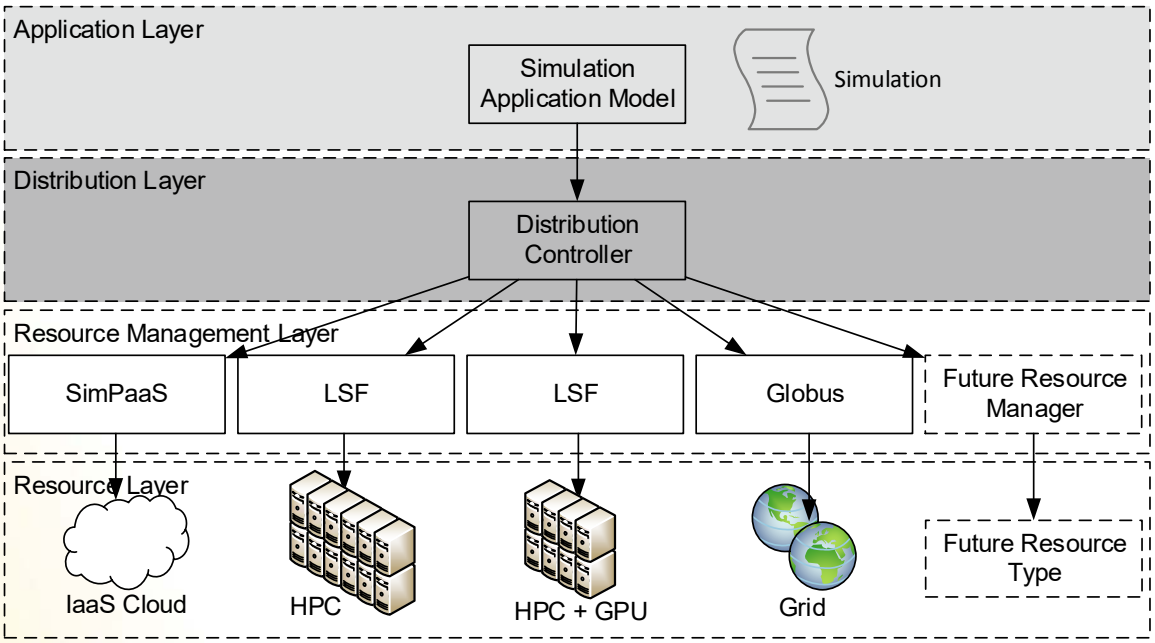

Figure 2: Overview of the architecture layers with independent models for the simulation application and the compute resources.

deployment of the simulation application on the targeted resource is triggered (Step 6). After that, the simulation scientist is given access to the provided resource via a Command Line Interface (CLI) and can execute his simulations accordingly (Step 7). When all simulation runs are done, the simulation scientist can collect the output data and triggers the cleanup and termination of the provided infrastructure (Step 8).

2.3 Architecture Layers

The layers of our architecture are shown in Figure 2. Simulation application models and those models representing abstractions of the compute resources (such as cloud-based virtual machined, HPC clusters managed by IBM LSF or GRID resources) we can choose from are depicted in separate layers because they're designed without explicit knowledge of the respective other model. This design philosophy implements the MDA principle of leveraging domain-specific knowledge: An expert for describing the resource demands of, e.g., an MPI-parallelized simulation doesn't have to know how the process distribution has to be communicated to the job scheduler, since this knowledge is the responsibility of the developer of the resource model. The distribution layer uses models from both adjacent layers to automatically generate (via a Model-to-Model (M2M) transformation) a platform-specific deployment model, which can subsequently be used (with a Model-to-Text (M2T) transformation) to generate, for example, a Cloud-deployment script or an HPC job script.

3 Modelling and Model Matching

3.1 TOSCA

In our architecture, the MDA pattern is being implemented using the Topology and Orchestration Specification for Cloud Applications (TOSCA), which is an XML-based orchestration template format also standardized by the OMG.

With the basic principle of modeling the capabilities of a cloud platform and automatically

matching them to the requirements of the desired application, TOSCA provides a framework enabling us to develop facilities for the deployment of simulations in a platform-agnostic way. The corresponding application model consist of the infrastructure, in particular the needed virtual machines, the internal and external network, the operating system images, and the application to be installed and run itself. In Figure 3 the TOSCA metamodel is shown in diagrammatic form. We're highlighting the parts most relevant to our architecture and leave a more detailed description to our SimScience 2017 publication [1]. Entity Types model the basic component types, an application, or compute resource model can be built from. Another essential part of TOSCA are Requirement and Capability Definitions which are the foundation of defining the dependencies between the resource model and the application. Concrete Entity Templates instantiate the Entity Types and define Requirement and Capability instances which we later on use to automatically match the requirements of an application to the capabilities of a resource type.

3.2 Tooling

Our tooling is build on top of the Eclipse Modelling Framework (EMF), which provides the functionality to define metamodels and generate model editors. In addition to EMF, we use Epsilon, which provides a family of languages for model querying, manipulation and transformation, and Sirius, another Eclipse project that allows to define graphical editors for EMF-based models. At the core of our modelling tool, is a metamodel, which is generated from the TOSCA schema. This generated metamodel is further enhanced with constraints formulated in the Object Constraint Language (OCL) to allow for model validation at

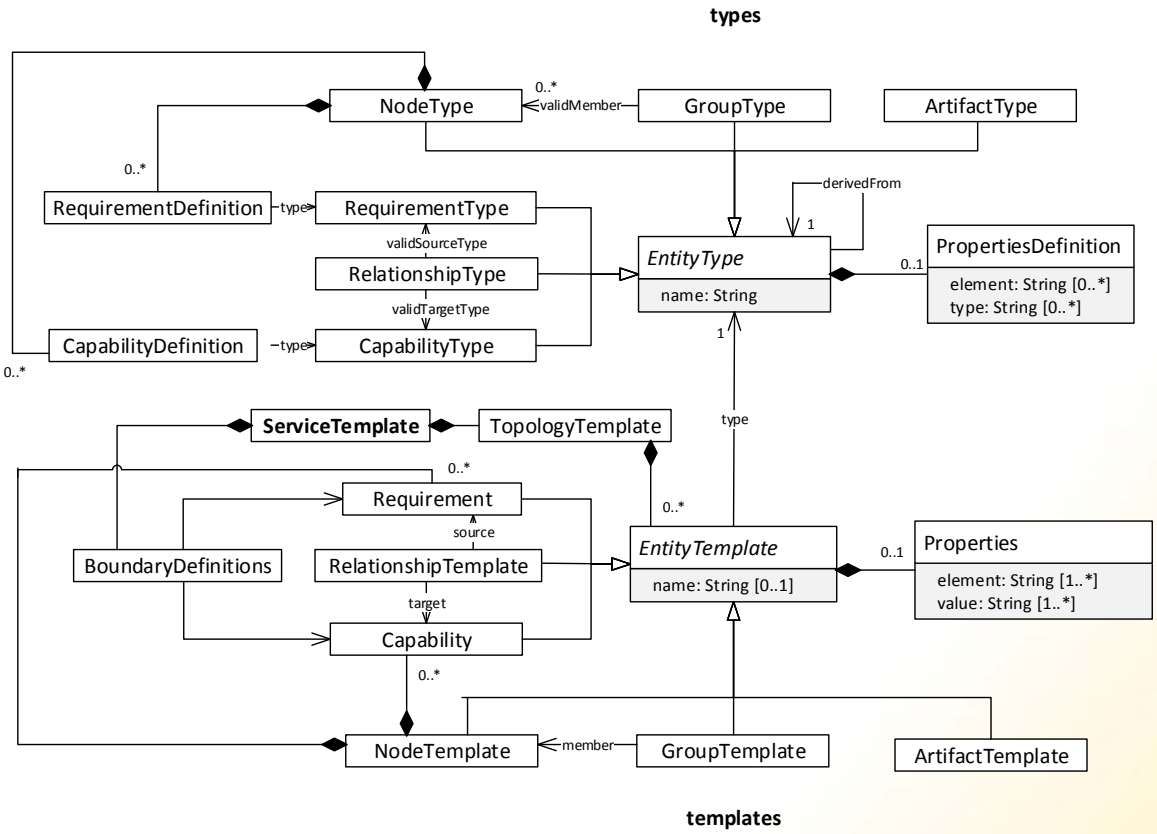

Figure 3: Simplified representation of the TOSCA metamodel.

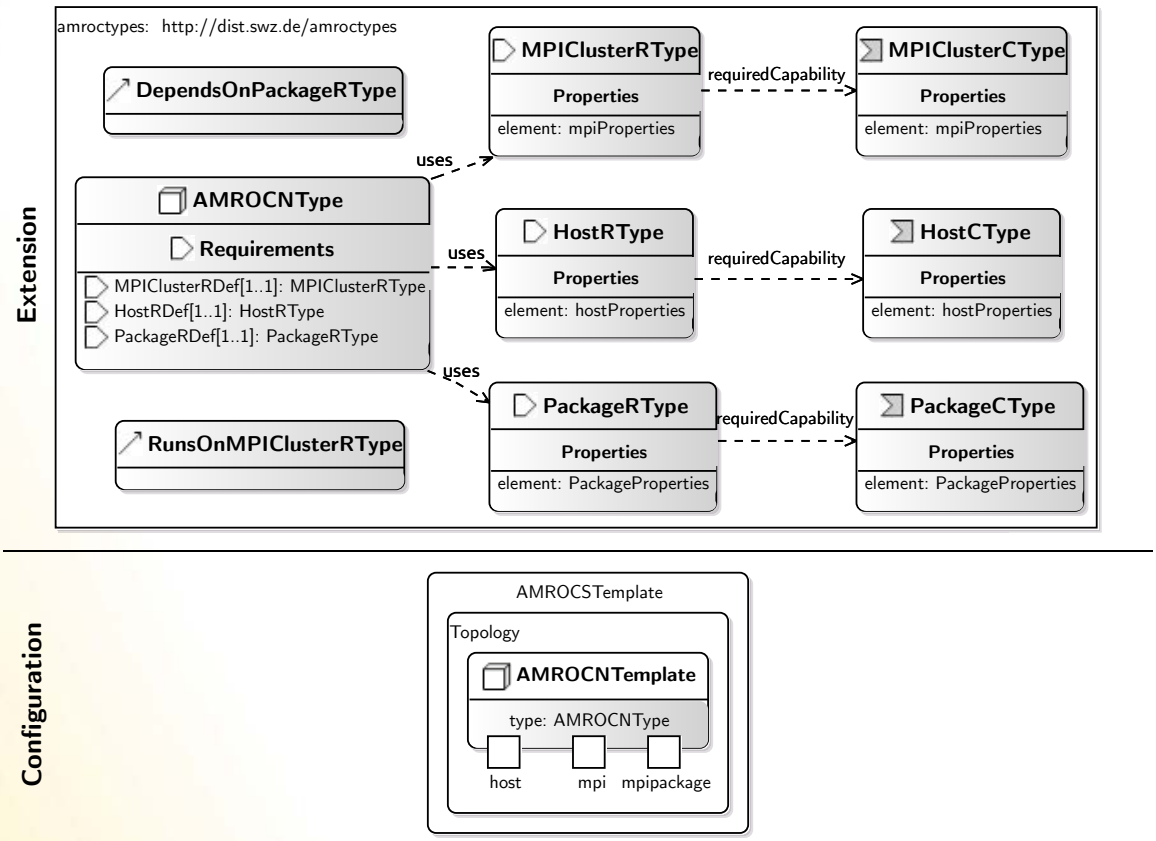

Figure 4: Graphical representation of the AMROC simulation application model.

design time. The TOSCA metamodel is used to generate Java code for the data structures to represent TOSCA elements at runtime and a simple Eclipse-based model editor.

Graphical Editors

TOSCA models potentially grow large in size and can become complex. To handle this complexity, we decided to define a graphical representation and a graphical editor with help of the Sirius framework. Furthermore, we decided to provide two different diagram types for TOSCA artifacts, a TOSCA ***Extension Diagram*** depicts only the Entity Types and a TOSCA ***Configuration Diagram*** depicts their instantiation by Entity Templates. Examples for graphical representations created with the editor are shown in the Figure 4, Figure 6, and Figure 5.

Model Validation

In addition to the graphical representation and modelling, our tooling allows for the validation of the defined TOSCA models at design time. This includes ensuring that Entity Templates reference the valid Entity Types and only expose the Capabilities and Requirements that are defined by the Entity Types they reference. The presented tooling can be used to define the application model and the resource models as exemplified in the following sections.

3.3 Application models

Our TOSCA based approach allows to define the requirements of a simulation application with help of TOSCA Requirements. As described above, the defined Requirements subsequently get matched by the distribution controller against the Capa-

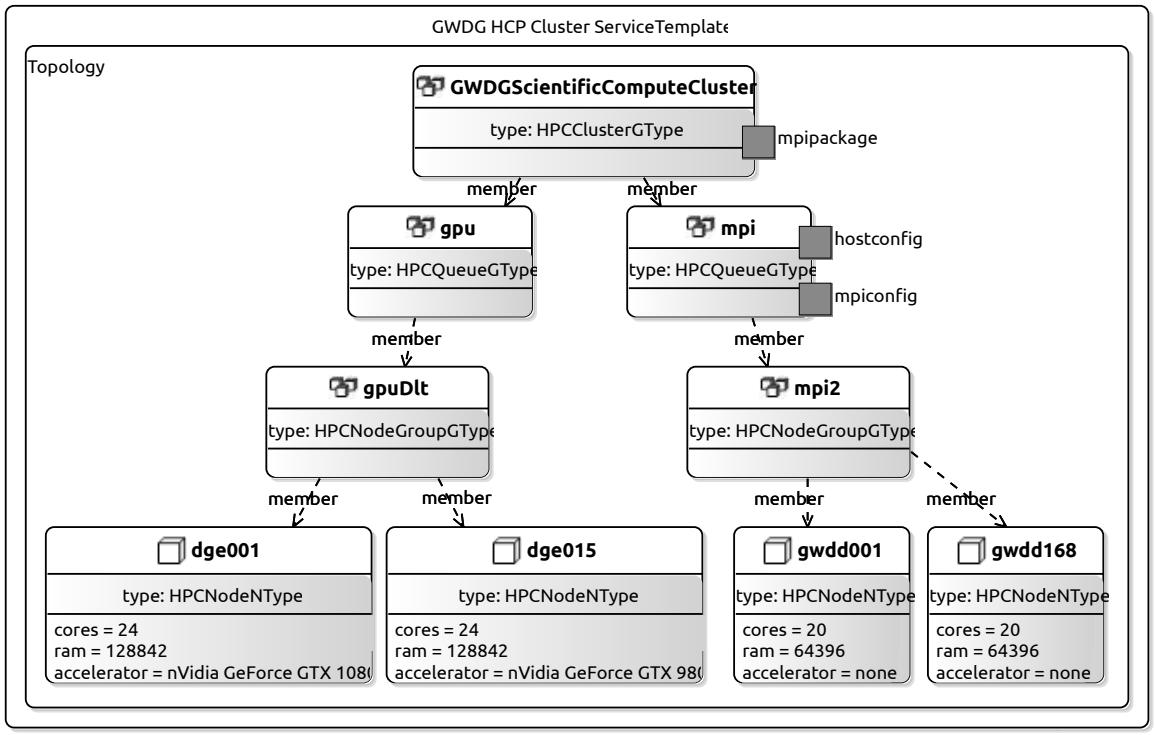

Figure 5: Graphical representation of a resource model for the GWDG HPC cluster.

bilities defined in the Resource models. Figure 4 depicts a simplified representation of the model for the software package AMROC, a tool chain for simulating fluid flows with the Lattice Boltzman Method on an adaptive mesh. AMROC uses the Message Passing Interface (MPI) for parallel computation and is designed to run on large HPC cluster.

In the extension diagram (upper part of Figure 4) new types for Nodes, Requirements and Capabilities can be designed. The example depicts the definition of a new Node Type for the AMROC software packages with additional Requirement Types that can be used to model the requirements of AMROC for an MPI cluster, a specific MPI package installation, and a certain configuration for the virtual machines. The lower part of Figure 4 shows an instantiation of the types definition in a configuration diagram. It depicts a Node Template for a specific AMROC software package instance with an instantiation of the three aforementioned requirements. The software configuration of AMROC itself is automated with help of configuration management scripts that accompany the model.

When a researcher now wants to execute a simulation, the modelled requirements of the simulation application are then used to select a suitable resource type. To provide this functionality, we model the different available resource types also with TOSCA as we will exemplify in the following.

A model for the GWDG HPC cluster

Figure 5 depicts a simplified representation of a resource model for the HPC cluster at the datacenter of the GWDG. We model the cluster itself as a set of nested Group Templates, whereby the toplevel Group Template represents the cluster itself, the Group Templates on the second level represent its queues for submitting batch jobs and Group Templates on the third level represent groups of hosts. The physical machines of the cluster are modelled as Node Templates on the lowermost layer in the figure. Since all machines

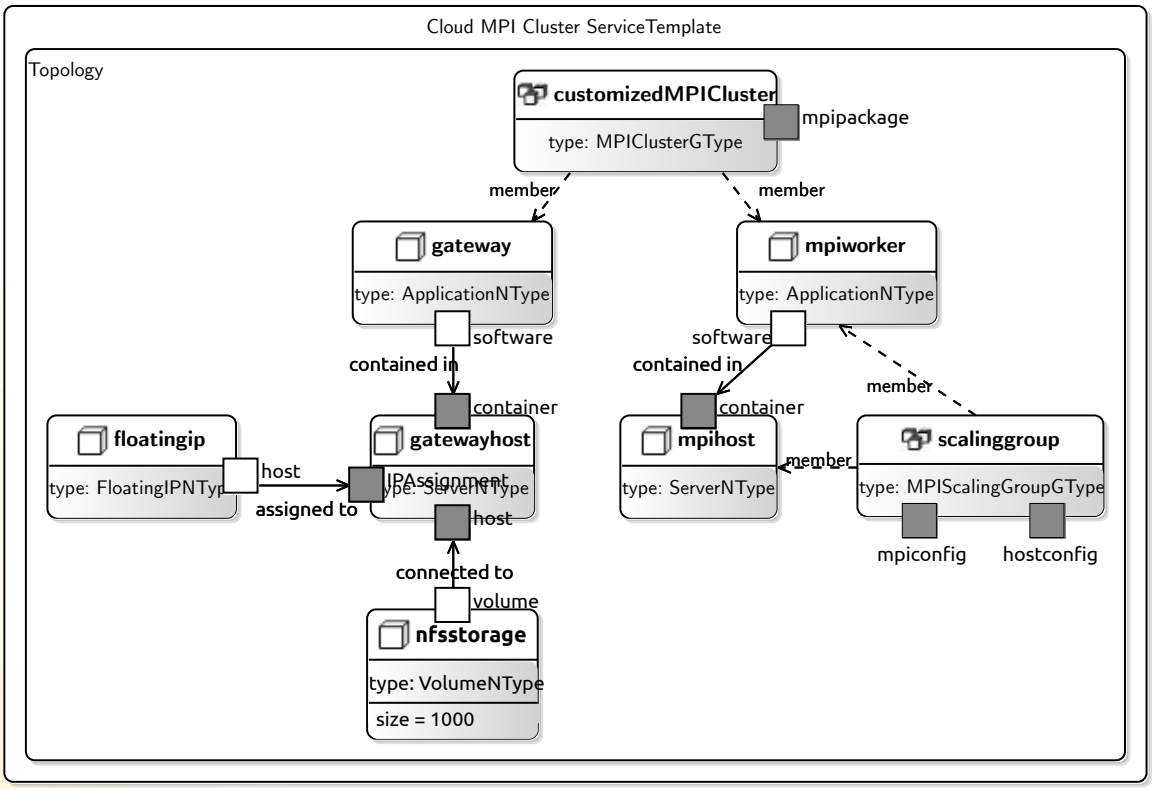

Figure 6: Graphical representation of the resource model for an MPI cluster running in the cloud.

in the cluster share the same software configuration, the availability of the specific MPI version is modelled as a Capability of Group Template representing the Cluster. The Capabilities for a certain hardware configuration and also the MPI cluster Capability itself are modelled as part of the submission queues. This allows the automatic generation of job submission scripts for a specific queue that contains the right amount and configuration of machines required by the simulation application.

A model for a cloud-based MPI cluster

Figure 6 shows a simplified representation of resource model for an MPI cluster that can be automatically deployed in a cloud environment. In contrast to the fixed setup of the HPC cluster presented in Figure 5, it is possible to provision the required number of machines directly and also configure the size of the distributed file system. The subset of the model represented in Figure 6 contains the matching Capabilities for the Requirements defined in the AMROC simulation application model. Again the Capability to provide a specific software package for running MPI is modelled as part of the cluster. This Capability is accompanied by the necessary automation scripts for installing the software package on the provisioned cloud machines. The Capability of providing the MPI cluster itself and also its hardware configuration is modelled as part of a Group Template that also allows to configure the number of MPI-enabled compute nodes that should be provisioned on-demand in the cloud.

4 Runtime and Execution

After a successful match against the Capabilities of a resource model, a PSM is automatically created by a model transformation that contains only the elements relevant for the execution at runtime, but is also enriched with platform-specific techni-

cal details. E.g., in case the targeted resource type is the cloud, this includes the information on which type and amount of which specific virtual machines to boot. For cloud resource types, this has been achieved by defining a mapping between TOSCA and the Open Cloud Computing Interface (OCCI) specification [2] and the actual refinement of OCCI to be combined with configuration management for the installation of the application [3]. Currently, we execute the simulation application after it is installed manually with help of generated job scripts. In the related SWZ-project ``Multi-Level Simulation'', an approach was developed to model and execute scientific workflows in clouds with OCCI [5] and it is planned to integrate the approach with the architecture developed in this project to allow for the execution of whole scientific workflows.

5 Distributed Simulations

5.1 Basics of LBM

In classical CFD methods, macroscopic flow variables like velocity and pressure are directly obtained from the continuity and the Navier-Stokes equation, which in turn are derived from conservation principles of mass and momentum. Typically, finite volume or finite element methods are used to discretize and solve the resulting nonlinear system of second order partial differential equations numerically. In particular, for incompressible flows special attention has to be paid for the coupling of the continuity and Navier-Stokes equation using iterative methods. As an alternative approach, the lattice-Boltzmann (LB) method is used in the present study. It originates from Boltzmann's kinetic molecular dynamics and may be understood as a discretization in space and time of the velocity-discrete Boltzmann equation. Thus, the LB method determines the probability distribution function for molecular particles with a certain velocity at a certain position in space. The macroscopic variables such as density and velocity are obtained from the moments of this distribution function. From a mathematical point of view, the LB method forms a set of first order partial differential equations. The solution algorithm is considerably simpler compared to that in classical CFD methods and there is no need for an iterative pressure-velocity coupling.

5.2 GPU Implementation and Refined Meshes

The key advantage of the Lattice Boltzmann method is the good parallelisability and easy implementation on many architectures. Since the LBM algorithm is memory bound, it profits greatly from the high memory bandwidth on GPUs.

Special data structures have been developed for efficient usage of the device memory. We use the esoteric twist data structure [10], which allows for combination of the streaming and collision step while only using a single set of distribution functions.

The usual implementation on cartesian grids has the drawback that the grid resolution cannot be changed for given reasons. Therefore we use an approach based on hierarchically refined grids. Since the shear stress is a moment of the distribution function, it can be computed locally. This information about the velocity gradient can be used for high order velocity interpolation at the level interfaces (compact interpolation) [9].

OpenCL is used for the implementation of the device code. In contrast to the proprietary CUDA it has the advantage that implementation for multiple CPU and GPU architectures are available and the code is not limited only to NVIDIA hardware.

5.3 Use Case: Pressure Drop in Packing of Spheres

Predicting the pressure drop in the flow through a particle filled reactor is of great importance in chemical engineering. When the particles are relatively large compared to the characteristic length of the reactor, the confining walls can have a great influence on the flow and thus on the pressure drop. Thus, the effect of geometry on the pressure drop in packed beds is subject of extensive research since decades. Many experimental findings and derived correlations exist which differ widely. We used a solely computer based approach to study this effect systematically. The sphere packings are created numerically. Then a mesh is generated and the flow through the bed is calculated and evaluated. This process has the

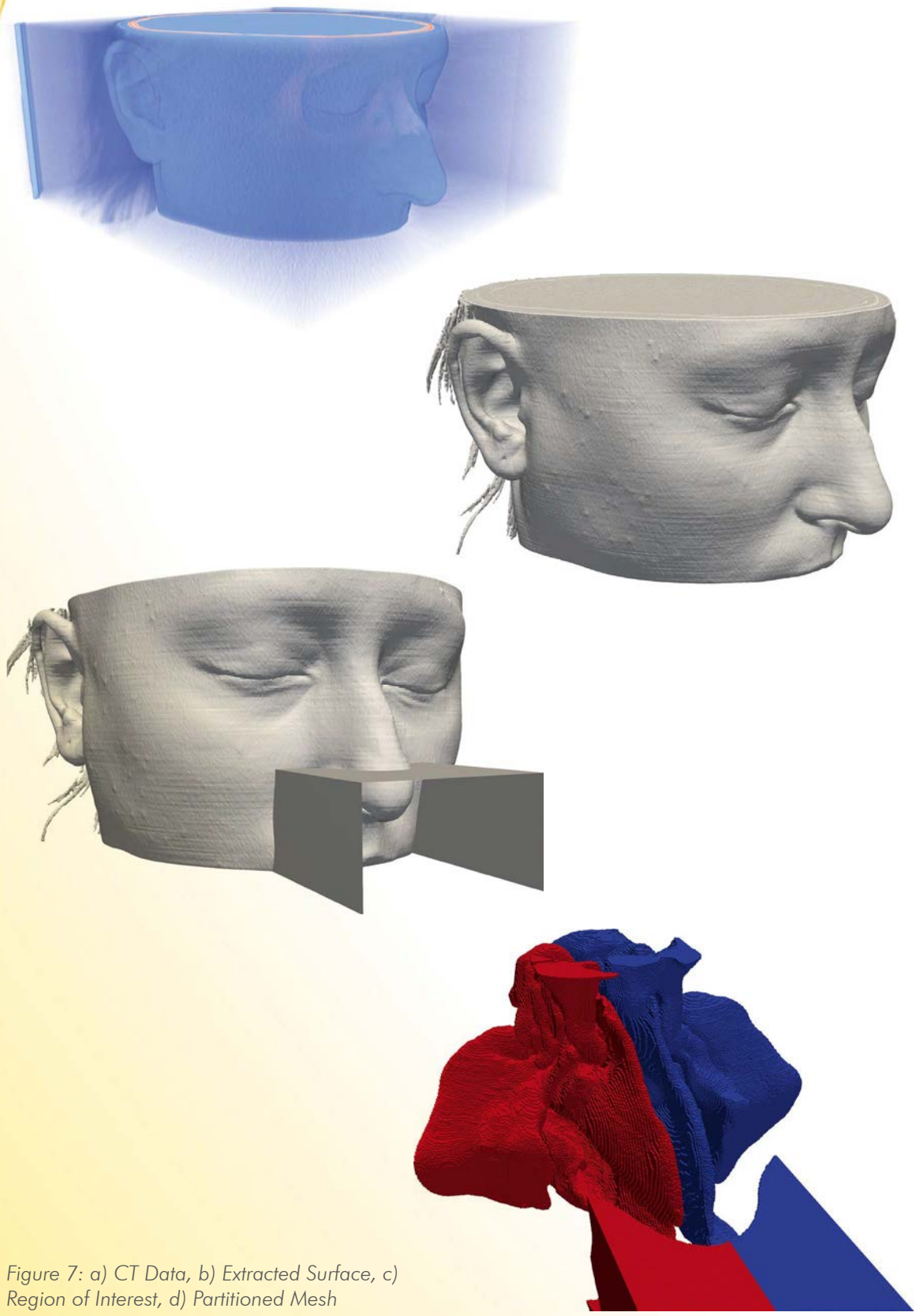

Figure 7: a) CT Data, b) Extracted Surface, c) Region of Interest, d) Partitioned Mesh

advantage, that the whole process of packing generation, mesh generation, flow calculation and evaluation can be automated allowing to study numerous cases of different geometries. The results clearly show, that the pressure drop is a non monotonic function of the reactor hydraulic diameter to sphere diameter ratio, wich is in contrast to common correlations. Furthermore, three different reactor geometries, a pipe, a channel and two infinitely extended plates, were studied in order to investigate the universality of the correlations. The results show, that for high ratios of hydraulic diameter of the reactor to sphere diameter the three geometries behave similar, whereas for small ratios the pressure drop is difficult to cast in simple correlations. Details can be found in PAPER.

5.4 Use Case: Nasal Cavity

Nasal septum deviation (NSD) is a physical disorder of the nose, involving a displacement of the nasal septum, which can cause symptoms like sleep apnea, snoring, repetitive sneezing, facial pain and nosebleeds. The connection between discomfort and the type of NSD is unknown. Since changes in the airflow by NSD are probably an important cause for the symptoms, previous studies used computational fluid dynamics to analyze the flow. Classical CFD methods require manual processing by the user thus limiting the amount of analyzable geometries. Since the human nose has high natural variations, ideally a large number of cases should be analyzed in order to obtain reliable correlations. We use a novel approach based on the lattice Boltzmann method, which does not require any user input. The goal is to transform a whole database of computed tomographic (CT) scans into fluid dynamic variables which can than be used to find reliable correlations between discomfort and fluid dynamic properties.

Running the simulation of the nasal cavity flow use case comprises several steps:

Surface Extraction
First, the CT scan (figure 7(a)) needs to be converted to a triangle mesh (figure 7(b)) which serves as input for mesh generation. The marching cubes algorithm is used for this process. The grey values in the CT scan are given in normalized Hounsfield Units so a fixed value can be used for all scans.

Mesh Generation
In contrast to finite-volume methods the refined cartesian grids needed by LBM can be created without manual user processing. In the context of NSD the mesh needs to be limited to the regions of interest. We use a heuristical approach to limit the mesh outside the head to a small area around the nose (figure 7(c)).

CFD Simulation
The flow is then calculated using our in-house LBM code on hierarchical refined grids.

Evaluation

The evaluation of the calculated flow field must also work without user interference. Some fluid dynamic numbers like pressure drop or maximal flow velocity are easy to obtain whereas other like the ratio of volumetric flows between left and right part of the nose require a more sophisticated approach. An algorithm which automatically classifies each cell as belonging to the left or right side is used to extend the possibilities for evaluation (figure 7(d)).

The different phases have different resource requirements, which are summarized in Table 1. Therefore different ressources should be used.

Table 1: Resource requirements of the different processing steps.

Processing Step	Parallelization Type	Memory Requirements
Surface Extraction	-	~ 1 GB
Mesh generation	OpenMP	~ 1 GB
CFD simulation	OpenCL	~ 10 GB (GPU)
Evaluation	-	~ 10 GB

6 Summary and Outlook

We presented our architecture for modelling and matching the requirements of a simulation application against different computing resource types, including cloud resources and HPC clusters. Our approach is inspired by the Model-Driven Architecture and uses the cloud standard TOSCA as a modelling language. This architecture is currently integrated with a model at runtime approach that automates the actual resource provisioning and deployment for the simulation application. The goal is to provide an integrated solution for modelling simulation applications, their deployment on heterogeneous compute resource types and finally their execution.

The project is currently in its final phase and we use the developed code for the pressure drop in packaged spheres and the nasal cavity use cases for the evaluation of the proposed architecture and tooling.

Project-Related Publications

More information on the architecture can be found in:

[1] F. Korte, A. Bufe, C. Köhler, G. Brenner, J. Grabowski, P. Wieder, „Transparent Model-Driven Provisioning of Computing Resources for Numerically Intensive Simulation“,, in Proceedings of the Clausthal-Göttingen International Workshop on Simulation Science (SimScience 2017), 2017.

More information on the models at runtime approach for the model execution can be found in:

[2] F. Korte, J. Erbel, J. Grabowski, „Model-Driven Cloud Orchestration by Combining TOSCA and OCCI (Position Paper)'“, in Proceedings of the 7th International Conference on Cloud Computing and Services Science (CLOSER 2017), 2017.

[3] F. Korte, S. Challita, F. Zalila, P. Merle, J. Grabowski, „Model-Driven Configuration Management of Cloud Applications with OCCI'“, in Proceedings of the 8th International Conference on Cloud Computing and Services Science (CLOSER 2018), 2018.

[4] J. Erbel, F. Korte, J. Grabowski, „Comparison and Runtime Adaptation of Cloud Application Topologies based on OCCI (Position Paper)“, in Proceedings of the 8th International Conference on Cloud Computing and Services Science (CLOSER 2018), 2018.

[5] J. Erbel, F. Korte, J. Grabowski, „Scheduling Architectures for Scientific Workflows in the Cloud“, in Proceedings of the 10th System Analysis and Modelling Conference (SAM 2018), Springer, 2018.

More information on the fluid dynamics simulations can be found in:

[6] A. Bufe, G. Brenner, „Systematic Study of the Pressure Drop in Confined Geometries with the Lattice-Boltzmann-Method“, in Transport in Porous Media, June 2018, Volume 123, Issue 2, pp 307–319

[7] S. Hofmann, A. Bufe, G. Brenner, T. Turek, „Pressure drop study on packings of differently shaped particles in milli-structured channels“, in Chemical Engineering Science 155:376-385, November 2016

[8] A. Bufe, M. Klee, G. Wehinger, T. Turek, G. Brenner (2017), „3D Modeling of a Catalyst Layer with Transport Pores for Fischer-Tropsch Synthesis“, Chemie Ingenieur Technik, 89: 1385–1390. doi:10.1002/cite.201700066

Further References

[9] M. Geier, A. Greiner, J. G. Korvink „Bubble functions for the lattice Boltzmann method and their application to grid refinement“, in The European Physical Journal Special Topics, April 2009, Volume 171, Issue 1, pp 173–179

[10] M. Geier, M. Schönherr „Esoteric Twist: An Efficient in-Place Streaming Algorithmus for the Lattice Boltzmann Method on Massively Parallel Hardware“, in Computation 2017, 5(2), 19

Project data

The project is funded from SWZ with 2 TV-L E13 staff positions since March 2016 at the sites Clausthal and Göttingen. Involved scientists are:

Prof. Dr.-Ing. Gunther Brenner
Division of Fluid Dynamics
Institute of Applied Mechanics
Clausthal University of Technology

Prof. Dr. Ramin Yahyapour
Research group Praktische Informatik
Institute of Computer Science
University of Göttingen

Prof. Dr. Jens Grabowski
Research Group for Software Engineering for Distributed Systems
Institute of Computer Science
University of Göttingen

Monitoring Software Quality Using Agent-based Simulation Models

Tobias Ahlbrecht, Jürgen Dix, Niklas Fiekas, Jens Grabowski, Verena Herbold, Daniel Honsel, Philip Makedonski, Stephan Waack

Introduction

Software Quality Assurance is a field that has risen in popularity over the last decades. Software has become an integral part of almost everybody's life, in economics, in science and in everyday life. Complexity of Software has grown and the responsibility that programs have been extended over the years. It is therefore only natural to explore ways to better monitor software quality and predict possible problems in the future. The sooner a bug or unsafe part of software code can be detected, the sooner a project manager is able to react to it and implement countermeasures. Even if there is no immediate problem with the software, the detection of unclean code can prevent problems in the future.

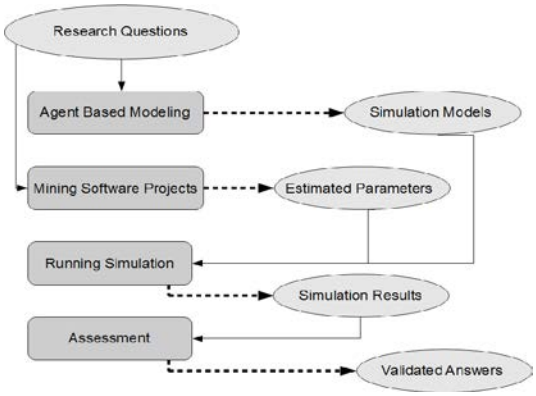

Figure 1: Process of building simulation models.

Once a problem has been identified, the next step is to find effective countermeasures (e.g., involve more developers). Due to the nature of our simulation-based approach, we can evaluate different actions that a project manager can execute and predict their impact in terms of software quality and evolution. This establishes a feedback loop for project managers for planning the software project and its resources. Within this project, we worked out different Agent-based simulation models that are able to answer different questions concerning software evolution.

Approach

In this section, we describe our approach for evaluating the trend of simulated software projects. Therefore, we propose an interaction of three different research areas.

The overall process is depicted in Figure 1. Starting with a concrete research question about software evolution in mind, e.g., how are different kinds of changes distributed over time, a tailored model is built (Agent-Based Modeling). With the model in mind, we select and mine open source software projects which helps us estimate appropriate model parameters describing the software evolution process under investigation (Mining Software Repositories). Once the model is adjusted with the estimated parameters, the simulation can be run (Running Simulation). This step also belongs to the agent-based modeling, since it gives feedback about the model itself, e.g., if it needs to be adapted, if the so gained model does not fit the real world. Finally, the simulated results get assessed in terms of their quality (Assessment).

Concretely, we use mining of software repositories to parameterize the simulation model according to one particular open source project. By this, we observe the size and effort, i.e., number of different developer types, of other open source projects with the aim of simulating them under similar settings. Then, an agent-based simulation model is used to describe the behavior of the differ-

ent developer types as well as the dependencies between software entities and developers. Finally, to evaluate the simulation, Conditional Random Fields (CRFs) are applied on the simulated software dependency graphs.

In the following, we describe the three steps in more detail.

Parameter Mining

The main driver of the simulation are the developers, which trigger the simulation by their changes on the software entities. Thus, the description of the developers as well as their contribution behavior is of great importance.

In a software project, especially in the open source context, the work of an individual often differs significantly from the average behavior. It is influenced by their experience, position, involvement in the project, and personal work style. To take this into account, we derive developer types by mining. Understanding developer roles and related contribution is important for the software development process, e.g., making trend predictions [1]. In this work, developer roles are classified based on heuristics about the commit frequency and bug fixing activity of individuals.

Since the simulation makes statements about the overall quality of a software project, the introduction of bugs is an important factor. From software repositories, one can retrieve the information, at which point in time a bug occurs or gets fixed, but often the information about the change introducing the bug is missing [2]. The current model reflects bug report and closing frequencies based on mining issue tracking systems (ITS).

To model dependencies between software entities, e.g., classes, files, and modules, we make use of change coupling networks, i.e., dependencies based on common changes. For this, we create, for example at the file level, a node for every entity, i.e., file. If two files are changed together, an edge is created and its weight increased with every further change. To reduce noise, we omit large commits. To trace the evolution of these networks, we measure the average degree, modularity, diameter, and the number of clusters over time. The degree is the number of dependencies of a node, the modularity represents an indicator of how good the graph can be divided into clusters, and the diameter describes the distance, i.e., the maximum shortest path in the whole network. The clusters are assigned by the nodes' modularity class [3]. This way, the clusters represent logical dependencies of software entities, e.g., user interface elements or tests.

Agent-Based Simulation Models

For the Agent-based simulation, we distinguish between two different models, a software evolution model and a BDI-based model. In the following, we explain both models.

Software Evolution Model

In previous work [4, 5] we presented agent-based simulation models for software processes in order to monitor the quality of the software under simulation. The aim is to assure the quality of software projects. In these models, developers work on *software entities*. Thus, it is their behavior which makes the software evolve over time and developers are the main active entities of our model. The developers' work is performed as commit. Commits can be separated into the following three actions: *create, delete, update*. Applying a commit changes the state of several software entities simultaneously and can fix a bug with a certain probability. The model is depicted in Figure 2.

Each of the four different developer types has its own commit behavior according to the effort the developer spent on the project. Bugs are divided into three different types according to their severity.

Required dependencies between entities are modeled as graphs. The most important one is the *change coupling graph*: this graph represents dependencies between software entities that are changed together several times. This means that the structure of this graph depends on the developers' commit behavior. In particular, this behavior includes the selection of the files changed together in one commit. This selection is partly based on random decisions. This means, that the simulated change coupling graph depends partly

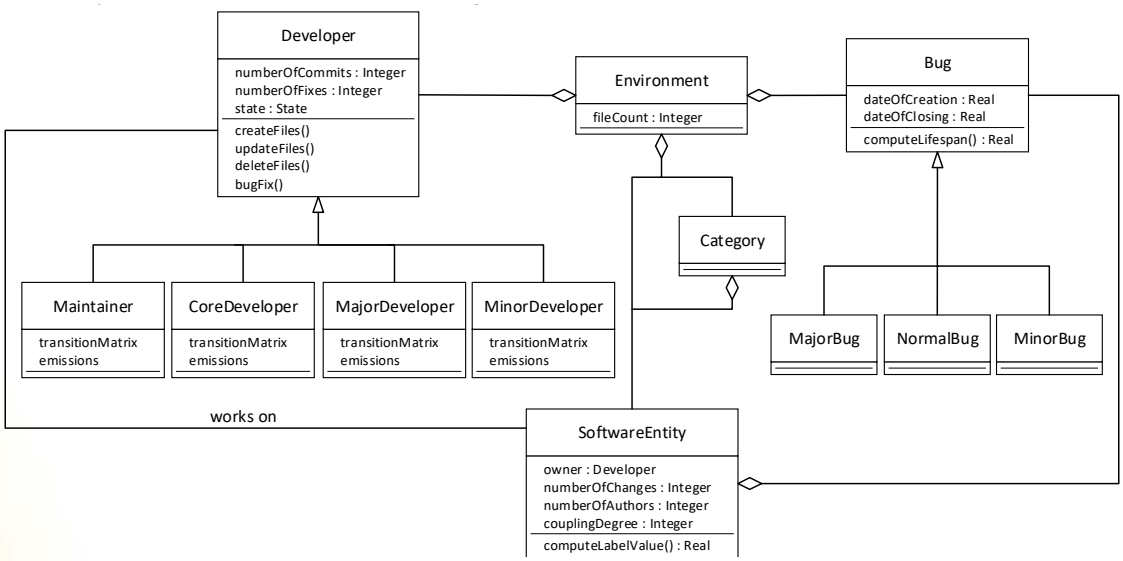

Figure 2: Agent-based simulation model for software evolution (see [1]).

on randomness. To reduce the randomness, we extend our model with refactorings. This allows us to model structural changes according to rules for certain refactoring types.

Since the change coupling graph serves as input for our assessment tool, improvements to this graph are expected to result in more accurate quality assessments of the overall software under simulation. This assessment is described in the Section Automated Assessment.

How we improve the structure of the simulated software graph using refactorings is described in more detail in the case study *Software Refactorings based on Graph Transformations*.

BDI Model

One of the challenges is to model the entity selection of a commit. Without knowledge about the intention of the developer, software entities are selected mainly randomly as mentioned in [4]. This results in significant differences between a simulated and a mined, i.e., real change coupling graph.

To reduce the coincidence, we use the prominent BDI [6] approach for selected simulation models. In such a model, developers formulate goals based on their beliefs and build plans to reach them. Beliefs are the current state of the project, represented as software metrics, as well as a parameter that can be set by the manager each time the simulation runs. Thus, we can easily compare differently configured simulation runs with each other.

Goals are, for example, add new features, fix bugs, improve the maintainability, or reduce the complexity of the project. A developer agent selects the goal based on its beliefs. From time to time, the beliefs have to be revised.

Plans are patterns that should, when applied to the software graph, achieve a goal. They can also be concatenated to reach a goal.

To get a realistic model we need a description of patterns for different source code changes like refactorings, bug fixes, or additional functionality. The formulation of them requires preliminary work in terms of mining open source repositories. Valuable information for this are, e.g. how software metrics like the complexity or the lines of code change, how many files will be touched and how the touched files are connected.

A Scalable Agent Platform

As mentioned in the introduction, available dedicated simulation platforms (like *Repast Simphony*) or general agent languages that offer declarative tools for suitable modeling (like *jason* [7] do not scale up in the number of agents and can, therefore, not be used for our purpose.

But jason-like languages do offer interesting tools that facilitate the modeling of software evolution enormously (and are also reusable).
In particular, jason, as taken off the shelf, is extremely limited in the number of agents (only a few hundred if communication is used).

In previous work [8] we have already worked on a general agent platform, *maserati*, to deploy huge numbers of agents (in the area of traffic simulation). Many techniques and design decisions will be reused. Instead of reimplementing jason from scratch, we focus on a new approach, based on *mapreduce*.

The main idea of mapreduce is to distinguish between synchronized and non-synchronized objects and then to identify parts of the simulation that are completely independent from each other and can thus be processed in parallel. Agents that are working on the same part of the world or are communicating with each other need to be synchronized among them.

The main step in our approach is to find an efficient translation from jason to mapreduce.
Previous approaches were either limited in the use of agent models or in the expressibility of the underlying language.

Our platform, in contrast, supports full jason-style agentspeak. Using mapreduce
allows us to get a linear scale-up in the number of agents.

Automated Assessment

For the assessment of the simulation results we are using Conditional Random Fields, to be precise, we are using a variant based on the Ising model [9] known from theoretical physics. Our CRF-based assessment model works on change coupling graphs, where each node of the graph represents an entity (for example a file) of the software project. The edges represent how strong the software entities are coupled, in terms of collective changes per commit.

CRFs are commonly used in bioinformatics to predict protein-protein interaction sites [10, 11]. Other fields where CRFs were applied successfully are shallow parsing [12], image labeling [13] as well as entity recognition [1]. The common ground for these application fields is the fact, that the labeling of the neighborhood of a node is a strong indicator of its own label. The same is true for software graphs: The function of a bug-free entity that resorts to a problematic entity is disturbed.

In our model, each node of the change coupling graph has a *local quality label* out of {acceptable, problematic} assigned to it, which reflects the quality of this entity. The local label is determined by the number of bugs of the underlying entity. Our method then provides a high-level quality assessment, where another *final quality label*, again out of {acceptable, problematic}, is assigned to every node. The final quality label of a node depends on the final quality labels of those nodes adjacent to it as well as on its own local quality label. This leads to a homogenization of the final quality labels compared with the local quality labels. Entire regions of the software graph can be identified as either acceptable or problematic instead of doing so for individual software entities.

We think that such a high-level assessment is more useful for project monitoring than just information about single software entities. Also note, that we use the same labels {acceptable, problematic} for the local label as well as the final label of a node. The local label of a node represents the quality of that specific piece of code, whereas the final label of a node represents its functioning and maintainability in the program including other files that influence the one in focus. If, for example, a file depends on another error-prone file, the work of that file is also flawed.

For training purposes, a standard machine learning approach using supervised learning techniques is not tractable in this case, since

there does not exist reference data for software projects, where all software entities are labelled problematic/acceptable in terms of their functioning. Therefore, we engineered a special training paradigm to determine the parameters for the Ising model. We call it Parsimonious Homogeneity Training. This training is not dependent on reference data. Instead of that it is designed to produce the following two effects. First, homogenizing the assessment of highly interconnected regions of the software graph, Second, leaving the assessment of these regions in relative independence from one another. It is crucial that the software graphs are of the following kind. The set of nodes is always decomposed into highly interconnected so-called *communities* representing logical parts of the software project. The number of edges between communities, however, is much smaller. Now we can describe the two goals of our training.

Homogenization: of communities in the software graph. The final labelling of all nodes of a community shall be mostly the same.

Independence: of communities from one another. The final labeling of the nodes in one community shall have little impact on the final labelling of nodes in another community.

Once we have broadly homogeneous classifications of communities, a comprehensible visualization of the state of the software can be reached. At that point an entire community can be reduced to the information that it is mainly acceptable or mainly problematic and thus the complexity of the assessment decreases dramatically. The second goal is the counterpart to the first, since we would end up in complete homogenization of the graph if we only had the first goal. The parsimonious homogeneity reflects our intuition that we want to homogenize parts of the graph for clarity, yet not homogenize the classification of the entire graph, as in that case we would lose too much information. We assume that problems in some part of the software (e.g. the view) does only have a small impact on other parts of the software (e.g. the controller).

Please find a detailed description of our approach containing experiments with automatically generated graphs using a stochastic block model in [15].

Case Studies and Results

The current work builds on our preliminary work where we showed the feasibility of an Agent-based simulation for software evolution, e.g., the evolution of the change coupling networks [4,5]. More on developers' contribution behavior can be found in [5]. Here, we focus on newer work built upon the experiences gained from the former studies.

Case Study 1: Dynamic Software Development Models

One of our studies [16] deals with a dynamic description of developers involvement and workload, since our preliminary studies posed a problem with the linear effort spent by developers in the simulation. To introduce more dynamics in the simulation, we employ state based probabilistic models that describe developer behavior where developers can go through states of different involvement.

Developers' actions are not solely visible in their commit behavior. Besides the Version Control System (VCS), a huge amount of data is available for analyses: Issue Tracking Systems (ITS), Mailing Lists (ML), forums, and also the activity of developers on social networks like Twitter can be traced.

However, given the whole history of a project, it is hard to derive a complete picture of the behavior of developers. Often, the different data sources have no links among each other, e.g., names and email addresses for the same developer can differ across platforms. This is often solved by tools developed for that purpose or manual mapping. To describe the evolution of development activity and involvement of developers in a dynamic way, i.e, the extent of involvement in a project varies over time, we make use of the data describing the observable behavior of developers.

We propose to employ Hidden Markov Models (HMMs) to gain insights about the underlying behavior.

We focus on analyzing the following important involvement factors for each developer over the

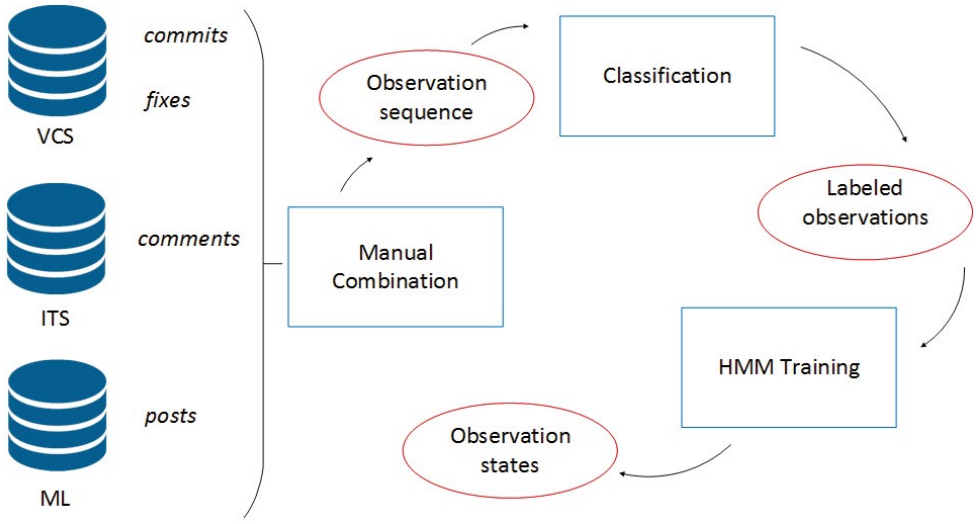

Figure 3: Data collection and processing for the learning of observation states (adapted from [5]).

time: the monthly number of commits and bug fixes, the amount of mailing list posts, and the number of comments in the ITS as observation sequence. This way, we get a broad picture of the evolution of open source software (OSS) developers.

In Figure 3, the broad learning process is illustrated. We start with a sequence of monthly activity vectors as observations retrieved from the VCS, ITS, and ML. These are manually combined. Following, we use a threshold learner and KNN (K-Nearest Neighbor) to classify the observations into low, medium, and high for each metric and with a majority vote for each observation. With the Baum-Welch and the Viterbi algorithm we calculate the transitions between the involvement states (e.g., low involvement to medium involvement) and the emissions for all states (i.e., the workloads) from the labeled observations.

We build a HMM for each developer of a project, as well as one general model for all developers. This way, we can describe the activity and workload of developers dynamically, which we will use to extend our simulation model to allow for changes in the project team during the simulation.

Results

We evaluated our approach in a case study including six OSS projects. The goal of our case study is to examine our main hypothesis, i.e., that we can describe developer contribution dynamics with HMMs and its usefulness for the prediction of developer contribution.

We trained a HMM for each developer, who performs a minimum number of actions in the project. Since we assume to derive similar models for same developer roles, we compared the retrieved models role-wise and also project-wise. Finally, we are interested to know to which extent the HMMs derived by a project are applicable for other software projects.

To assess the goodness of fit of the derived models, we measure the misclassification rate *mr* which counts the number of observations where the predicted state differs from the classification done by the threshold learner and KNN.

The mean misclassification rate of all fitted HMMs for developers' contribution behavior is $mr = 0.098$ with threshold classification and *mr*

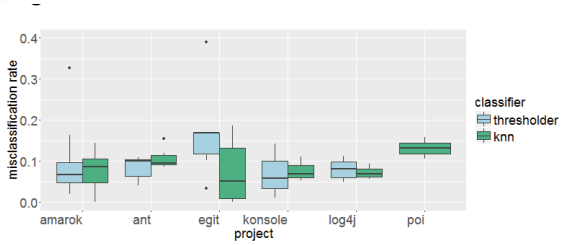

Figure 4: mr for Individual Models [5].

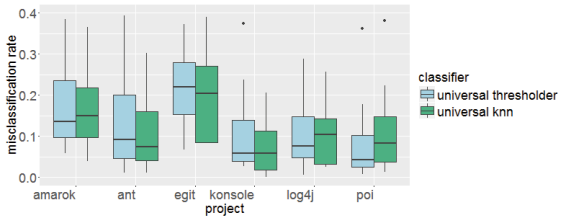

Figure 5: mr for General Models [5].

= 0.109 with KNN, i.e., the prediction performs well in general. Project-wise results are depicted in Figure 4.

The average misclassification rate using general models comes up to 14.5 % for the threshold classification and 13.5 % for the KNN classification model. Project-wise results are depicted in Figure 5.

In both cases all 106 developer models could be created. This emphasizes the major advantage of an universal model. It is appropriate for all developers, e.g., with the universal models we were successful in predicting the sequence of involvement states also for the developers, where no individual model could be calculated. In contrast to the individual models the general model performs about 5 % worse. Therefore, the general model performs well, but for an explicit description of the workload, also other factors should be taken into account.

We also started experiments with including the developer involvement states in the simulation. Therefore, we used the general models for core, major, and minor developers. Such that developers in the simulations can switch dynamically between different levels of involvement and, thus, contribute according to their state, e.g., a core developer with low involvement may only commit a few times for the respective period.

A major advantage of using the state based models for simulation is the more realistic representation of, e.g., the growth of the software system in the number of files due to the different amount of workload by the developers.

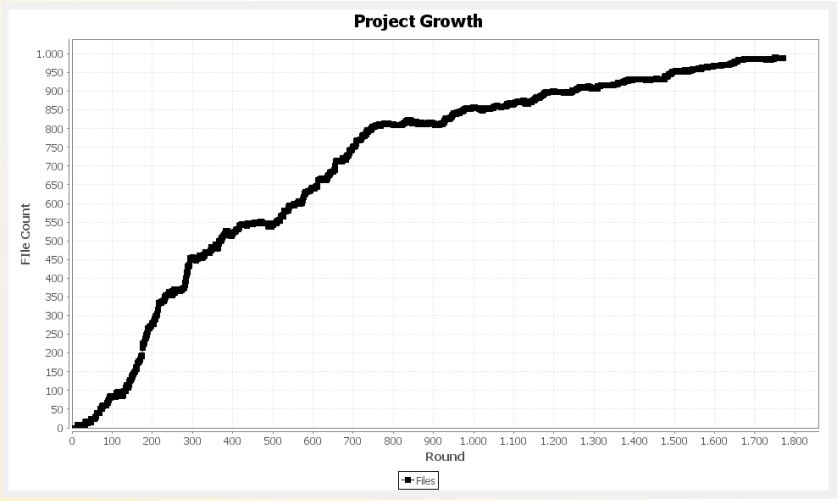

Figure 6: Simulated project growth in number of files for egit (generated from Repast Simphony).

Figure 7: Simulated developer states (average per type) for egit (generated from Repast Simphony).

Figure 6 shows the simulated project growth for parameters mined form the project *egit*. The growth trend is influenced by the work done by the different developers. Figure 7 shows the related states of all involved developers taken as the average. Note that, in *egit* only major and minor developers were detected and, thus, active in the project. The effects of developer dynamics can be retraced, e.g., in times where major developers are in average contributing highly (simulation round 200-300), the growth in number of files increases strongly.

Case Study 2: Software Refactorings based on Graph Transformations

As mentioned above, one identified challenge is to improve the structure of the simulated software graph. In order to do so, we require a more detailed description of which files are selected for a commit and how these files change. A usual approach to describe well defined code structure changes are *software refactorings*. Therefore, we propose in [17] a general model for refactorings which can be easily integrated in our agent-based model developed earlier. The main idea of this approach and some results are described below. A software refactoring is defined by Martin Fowler [18] as follows:

Refactoring means a restructuring of software without changing its behavior. The aim is to make the software more readable to developers and/or to increase the maintainability.

For reasons of clarity and limited space we will restrict the explanation of this case study to only one refactoring, namely *move method*. The entire case study ca be found in [17]. The definition of the refactoring is as well by Martin Fowler [18].

Move Method: will be applied if a method calls more methods or features of another class than from its own. It moves the method to the class with the most calls.

We are using graph transformations [19] to model structural changes to the software graph caused by the application of a software refactoring as presented in [20]. In order to do so, we have to apply two steps. First, we have to define a software graph were refactorings can be applied. Such a graph requires additional nodes and edges. Second, we have to develop transformation rules for each modeled refactoring.

The graph representing the simulated software has two node types, one representing classes and one representing methods. To model relationships between the nodes we define two edge

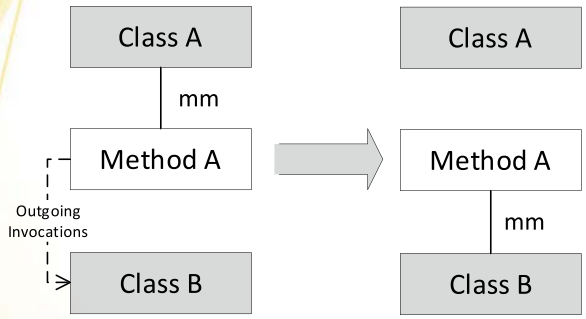

Figure 8 Transformation rule for the refactoring move method. (see [3])

types. One edge representing method membership between a method node and a class node as well as a directed edge representing method calls between two method nodes.

Based on the above described software graph we can define the following transformation rule for the refactoring move method.

The graph transformation rule for the refactoring move method depicted in Figure 3 shows how the left-hand side of the rule will be replaced by the right-hand side in the software graph. The dotted edge represents outgoing invocations, which means method calls to one or more methods of the other class.

To find a match for the rule's left-hand side, not only the structure of the software graph is considered, but also appropriate software metrics. These are, for example the coupling measured in number of outgoing invocations (NOI) for *Move Method* (see Figure 8). Furthermore, we assume that NOI of the origin class of a method will be reduced when a *Move Method* is applied.

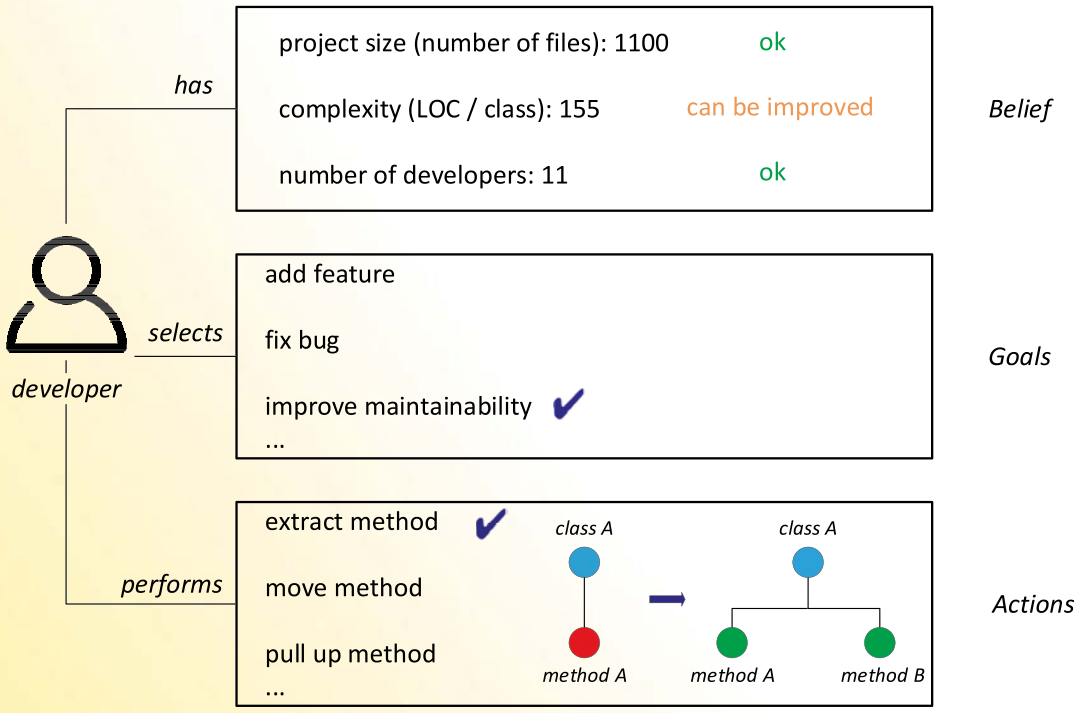

Figure 9: Example for developer's goals and plans [16]. The developer works on a method that is hard to maintain because it has too many lines of code. To improve maintainability, the developer applies the refactoring Extract Method. This means that parts of the origin method are moved to a newly created method which is called from the origin method.

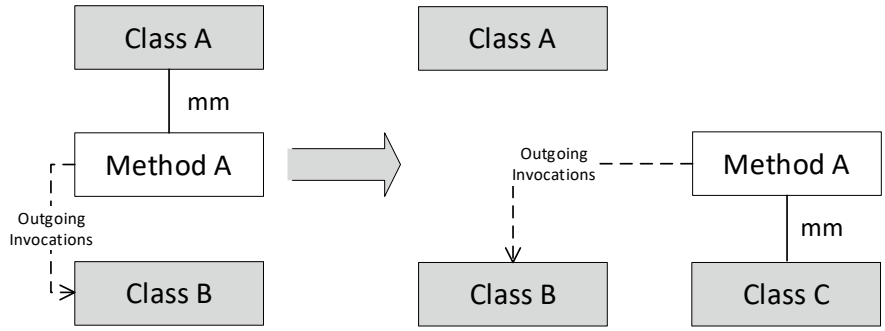

Figure 10: Alternative rule for refactoring Move Method. (see [3])

To apply the model described above to a software graph, we require detailed information about the state of the software before a refactoring is applied and how the state changes when a certain refactoring was applied. The state is represented by software metrics for size, complexity, and coupling. The framework we used to gather the required information about the analyzed software projects is described [17]. To make to mining work more efficient we are currently developing a new mining framework based on SmartSHARK [21].

For simulation purposes we are using a new developed simulation platform based on Python and Apache Spark that we presented in [22]. This platform supports the prominent BDI approach which allows us to model a detailed behavior for developers including refactorings. This means that developers formulate goals based on their beliefs and build plans to reach them.

In this example we consider the developer's goal improve maintainability, which results in applying a certain refactoring. Beliefs are the current state of the software under simulation, represented as software and graph metrics. The decision process of a developer is depicted in Figure 9.

For this case study, we analyzed and simulated three open source projects: Junit[1] - a unit testing framework for Java, MapDB[2] - an embedded database engine for Java, and the GameController[3] used for several RoboCup competitions. One notable result of analyzing these projects is the fact that only a small amount of methods are moved to already existing classes. This means that in many cases where the refactoring is applied, methods are moved to newly created classes. Due to this fact we have defined an alternative transformation rule for the refactoring move method as depicted in Figure 10.

Using the results presented above to parameterize the model gives us the ability to run the simulation with our developed simulation platform.

Figure 11 shows the simulation results for the three projects. JUnit, GameController and MapDB have similar method sizes in terms of LOC, but vastly different average method complexities to start with.

JUnit and GameController were simulated for 365 steps. The general trend is that complexity is traded for size. Note however, that LOC changes on a much smaller scale. For example, extracting a method will add new lines for the function signature, closing brace and call into the new method, but can dramatically reduce complexity. In the simulation of MapDB no further sensible refactorings were found before the predetermined step count, so the simulation ends effectively at step 265. This shows that other commit types, not based purely on refactorings, should be included in the simulation.

[1] https://github.com/junit-team/junit
[2] https://github.com/jankotek/mapdb
[3] https://github.com/bhuman/GameController

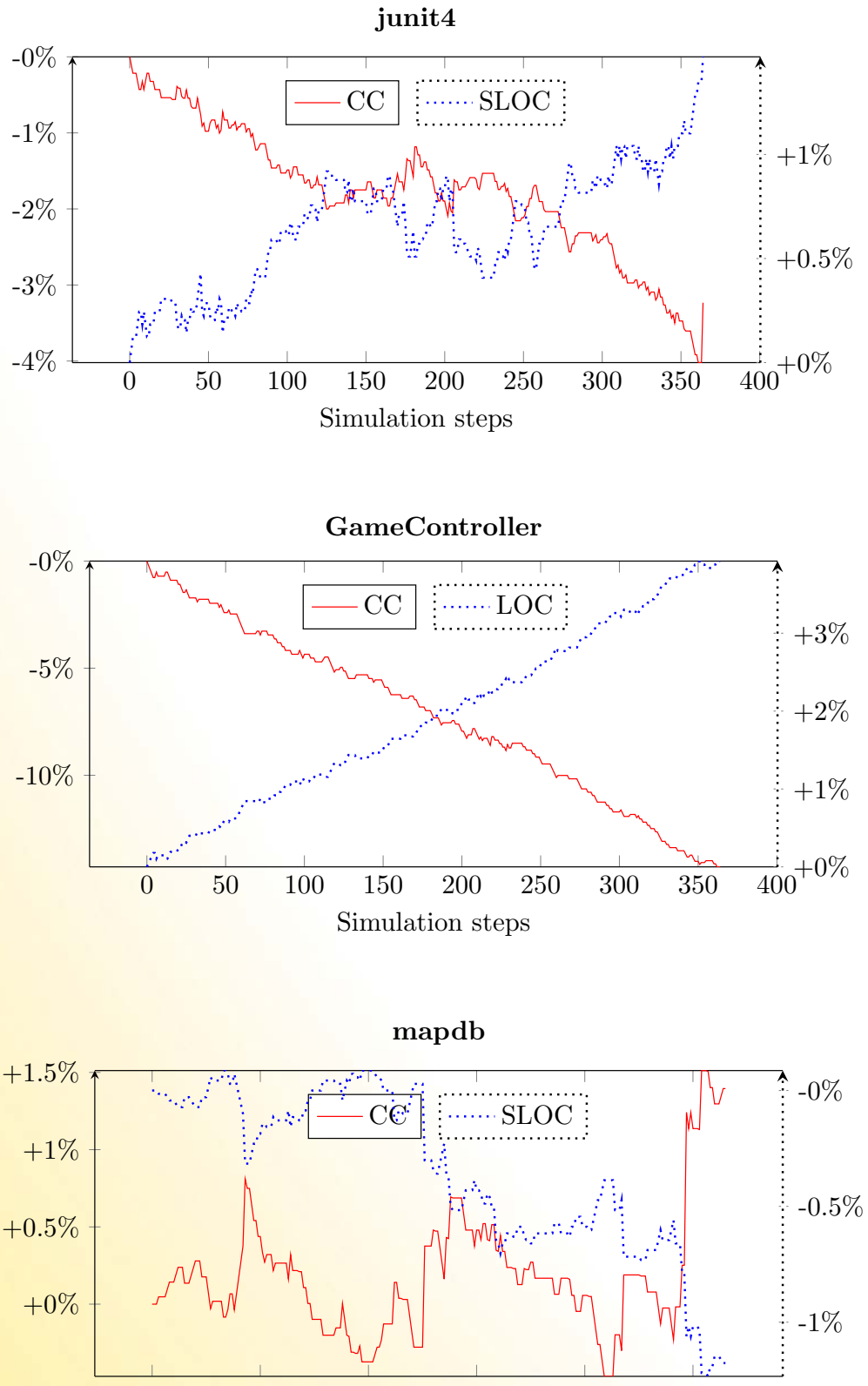

Figure 11: Average method complexity and size in simulation of software evolution. (see 3)

Case Study 3: Evolution of Change Coupling Graphs

The Change Coupling Graphs we use for assessment are an interesting abstraction: They can be easily created from version control histories, are independent of the programming language and reveal even implicit coupling between software components. On the other hand, we potentially lose out on information that static analysis could deliver (e.g., class inheritance graphs, call graphs).

To ensure that CCGs are a suitable tool, we built and analyzed CCGs of 150 open-source software repositories [23]. First, we look at superficial statistics/properties and verify that we can distinguish real-world CCGs from random graphs (Figure 12). This is obviously a basic requirement. In particular:

Average Clustering: the ratio of edges amongst a node and its neighbors to the maximum number of edges that would be possible, averaged over all nodes.

Degree Assortativity Coefficient: are nodes that are connected likely to have a similar degree, is this independent, or even the contrary?

Transitivity: for any triad of connected nodes, how many of them form a triangle?

Moreover, the graphs seem to have some deeper structure. We successfully trained a Convolutional Neural Network to distinguish real-world CCGs from random graphs generated ***with*** these properties [24].

We also looked at the evolution of individual CCGs over time.

The topmost point represents the first commit that was made in the repository. Then the properties of the graphs vary wildly. As expected early commits have a big impact on the structure. Once the structure has stabilized, we typically see zig-zag patterns (Figure 13). We find that these are related to alternating development phases that focus on consolidating existing files and phases that focus on adding new features.

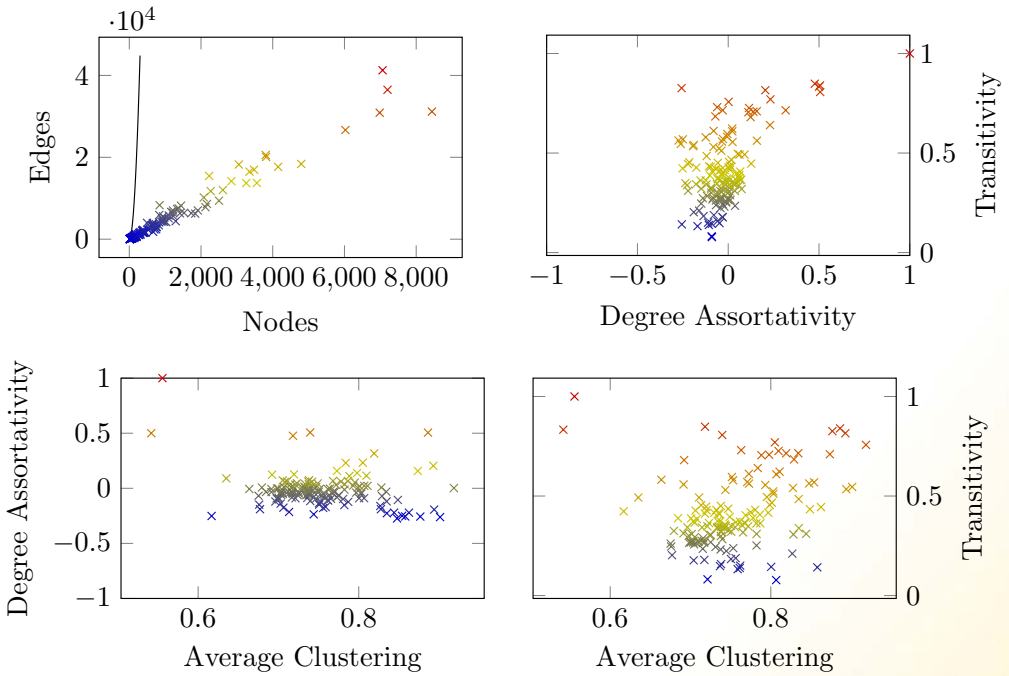

Figure 12: CCGs of 150 popular Java projects on GitHub.

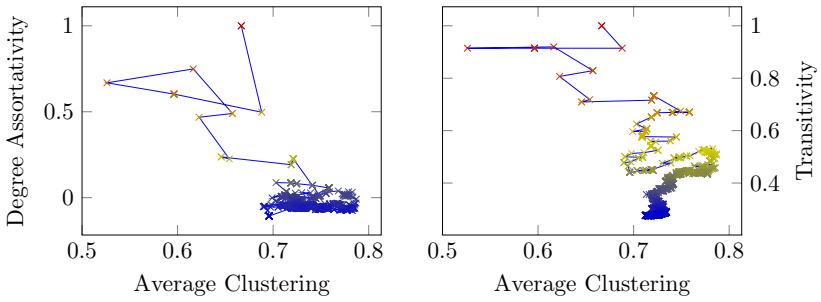

Figure 13: CCG of junit4 over time with typical zig-zag lines.

We plan to use these insights to assess the "realisticness" of our simulated Change Coupling Graphs.

Conclusion

We described our approach in software quality assurance and prediction as a decision help for project managers in charge of a software project. For this, we explained the overall process, which consist of parameter mining, agent-based modeling and simulation, and automatic assessment. In summary, we can conclude the following points: The applicability of HMMs for developer contribution behavior was demonstrated. Moreover, we were able to calculate a general model describing the dynamics developers perform in OSS projects. Interestingly, the emission distribution describing the workload of developers in the different states is more difficult to model generally, but it can be reflected using a general model. A major benefit of the general model is that it is able to calculate the states for every developer.

The usage of the general models embedded into our simulation was exemplified by experiments. The dynamics introduced by changing involvement states of developers and, thus, changing workload of developers, results in a more realistic growth curve.

We introduced a more fine-grained change behavior of developer where actions like refactorings can be described as graph transformations on the software graphs.

We analyzed pattern of change coupling evolution which are related to alternating software development phases.

From former studies, we learned that while taking the average over a set of software projects different in size and workload, the resulting simulation model performs best for midsize project. To take this into account, we currently work on a framework that instantiate project-specific simulation models, i.e., mine and process simulation parameters directly from the repository.

References

[1] G. Gousios, E. Kalliamvakou, and D. Spinellis. Measuring developer contribution from software repository data, in Proceedings of the International Working Conference on Mining Software Repositories (MSR), 2008.

[2] S. Kim, E. J. Whitehead, and Y. Zhang. Classifying Software Changes: Clean or Buggy?, IEEE Transactions on Software Engineering, 2008.

[3] S. Fortunato, Community detection in graphs, Physics Reports, vol. 486, no. 3-5, pp. 75-174, 2010.

[4] Verena Honsel, Daniel Honsel, Steffen Herbold, Jens Grabowski, Stephan Waack. Mining Software Dependency Networks for Agent-Based Simulation of Software Evolution, The 4th International Workshop on Software Mining (SoftMine), 2015

[5] Daniel Honsel, Verena Honsel, Marlon Welter, Stephan Waack, Jens Grabowski, Monitoring Software Quality by Means of Simulation Methods, ESEM '16 Proceedings of the 10th ACM/IEEE International Symposium on Empirical Software Engineering and Measurement, 2016

[6] Gerhard Weiss, Multiagent Systems, The MIT Press, 2013

[7] Rafael H. Bordini, Jomi Fred Hübner, and Michael Wooldridge, Programming Multi-Agent Systems in Agentspeak Using Jason (Wiley Series in Agent Technology), John Wiley & Sons, Inc., USA.

[8] Tobias Ahlbrecht, Jürgen Dix, Niklas Fiekas, Philipp Kraus, and Jörg P. Müller. An architecture for scalable simulation of systems of cognitive agents, International Journal of Agent-Oriented Software Engineering, 2016

[9] Ernst Ising. Beitrag zur Theorie des Ferromagnetismus. In: Z. Phys. 31.1 (1925), pp. 253-258.

[10] John Lafferty, Andrew McCallum, and Fernando Pereira. Conditional Random Fields: Probabilistic Models for Segmenting and Labeling Sequence Data, Proc. Of the 18th International Conf. on Machine Learning, 2001

[11] Ming-Hui Li, Lei Lin, Xiao-Long Wang, and Tao Liu. Protein-protein interaction site prediction based on conditional random fields, Bioinformatics 23.5, 2007

[12] Fei Sha and Fernando Pereira. 2003. Shallow parsing with conditional random fields, Proceedings of the 2003 Conference of the North American Chapter of the Association for Computational Linguistics on Human Language Technology - Volume 1 (NAACL '03), Vol. 1. Association for Computational Linguistics, Stroudsburg, PA, USA, 134-141. 2003

[13] Xuming He, R. S. Zemel and M. A. Carreira-Perpinan, Multiscale conditional random fields for image labeling. Proceedings of the 2004 IEEE Computer Society Conference on Computer Vision and Pattern Recognition, 2004.

[14] Andrew McCallum and Wei Li, Early results for named entity recognition with conditional random fields, feature induction and web-enhanced lexicons. Proceedings of the seventh conference on Natural language learning at HLT-NAACL 2003 - (CONLL '03), Vol. 4. Association for Computational Linguistics, Stroudsburg, 2003

[15] Marlon Welter, Daniel Honsel, Verena Herbold, Andre Staedtler, Jens Grabowski, Stephan Waack. *Assessing Simulated Software Graphs Using Conditional Random Fields*. Simulation Science, 2017

[16] Verena Herbold, Steffen Herbold, Jens Grabowski, *Hidden Markov Models for the Prediction of Developer Involvement Dynamics and Workload*, Proceedings of the The 12th International Conference on Predictive Models and Data Analytics in Software Engineering, 2016

[17] Daniel Honsel, Niklas Fiekas, Verena Herbold, Marlon Welter, Tobias Ahlbrecht, Stephan Waack, Jürgen Dix, Jens Grabowski, *Simulating Software Refactorings Based on Graph Transformations*. Simulation Science, 2017

[18] Martin Fowler. https://refactoring.com (last visited 07.03.2019)

[19] Hartmut Ehrig, Gregor Engels, Hans-Jörg Kreowski, and Grzegorz Rozenberg. *Handbook of Graph Grammars and Computing by Graph Transformation*. Volume 2: Applications, Languages and Tools. world Scientific, 1999

[20] Tom Mens, Niels Van Eetvelde, Serge Demeyer, and Dirk Janssens. Formalizing refactorings with graph transformations. Journal of Software Maintenance and Evolution: Research and Practice, 17(4):247-276, 2005.

[21] Fabian Trautsch, Steffen Herbold, Philip Makedonski, and Jens Grabowski. *Adressing problems with external validity of repository mining studies through a smart data platform*. In Mining Software Repositories (MSR), 2016 IEEE/ACM 13th Working Conference on, pages 97-108. IEEE, 2016.

[22] Tobias Ahlbrecht, Jürgen Dix, and Niklas Fiekas. *Scalable multi-agent simulation based on MapReduce*. In Proceedings of the 14th European Conference on Multi- Agent Systems, EUMAS 2016. Springer, December 2016.

[23] Tobias Ahlbrecht, Jürgen Dix, Niklas Fiekas, Jens Grabowski, Verena Herbold, Daniel Honsel, and Stephan Waak. Evolution of Change Coupling Graphs. Clausthal-Göttingen International Workshop on Simulation Science, May 2019. To appear.

[24] Phillip Czerner. Estimating 'Realisticness' of Change-coupling Graphs using Convolutional Neural Networks. Bachelorarbeit (TU Clausthal, 2018).

Project data

The project is funded from SWZ with 1.5 TV-L E13 staff position since April 2016 at the sites Clausthal and Göttingen. Involved scientists are:

Prof. Dr. Jens Grabowski
Research group for Software Engineering for Distributed Systems
Institute of Computer Science
University of Göttingen

Prof. Dr. Jürgen Dix
Research Group Computational Intelligence
Department of Informatics
Clausthal University of Technology

Prof. Dr. Stephan Waack
Theoretical Computer Science and Algorithmic Methods
Institute of Computer Science
University of Göttingen

Ringvorlesung „Simulationswissenschaften“

Im Rahmen der SWZ Ringvorlesung „Simulationswissenschaften“ berichten externe Gäste über aktuelle Ergebnisse aus ihrem jeweiligen Gebiet. Die Themen erstrecken sich dabei von dem Einsatz von Simulationsmethoden im Flugzeugbau über High-Performance-Computing bis hin zu Verkehrsplanung in Straßen- und Bahnnetzen sowie der Fabrikplanung.

Die Ringvorlesung findet im monatlichen Wechsel in Clausthal und in Göttingen statt. Wann immer möglich werden die Vorträge aufgezeichnet und unter folgende Adresse zum späteren Abruf angeboten:

www.simzentrum.de/lehre/ringvorlesung

Lecture series „Simulation Sciences“

In the SWZ lecture series “Simulation Sciences” external guests are reporting about their latest results in their field of research. The topics extend from the use of simulation methods in the design of aircrafts over high-performance computing to transport planning in road and rail networks and factory planning.

The lectures are hold in Clausthal and in Göttingen. Whenever possible, the lectures are recorded as videos and available for streaming at the following address:

www.simzentrum.de/en/teaching/lecture-series

Übersicht über die bisherigen Vorträge

Simulationsbasierte Produktionsplanung in der Halbleiterfertigung: Lösungsansätze und Herausforderungen

Prof. Dr. Lars Mönch
Fakultät für Mathematik und Informatik
FernUniversität in Hagen

Die Produktion von integrierten Schaltkreisen ist einer der komplexesten Produktionsprozesse. Eine einzelne Waferfab umfasst mehrere hundert, zum Teil sehr teure, Maschinen. Bis zu 1000 Jobs werden auf diesen Maschinen bearbeitet. Lange Durchlaufzeiten von bis zu zehn Wochen sind charakteristisch. Reihenfolgeabhängige Umrüstzeiten, schleifenförmige Durchläufe der Jobs, Batchmaschinen, automatisierte Transportsysteme sowie häufige Maschinenausfälle und Nachfrageschwankungen sind typisch. Die diskrete Simulation stellt eine etablierte Methode zur Unterstützung der Produktionssteuerung in Halbleiterfabriken dar. Durch die Bedürfnisse der komplexen Lieferketten in der Halbleiterindustrie motiviert, sind in den letzten Jahren aber Produktionsplanungsansätze stärker in den Mittelpunkt des wissenschaftlichen und praktischen Interesses gerückt. Von besonderem Interesse ist dabei die geeignete Modellierung der lastabhängigen Durchlaufzeiten in linearen Optimierungsformulierungen durch Clearingfunktionen, während konventionelle Formulierungen lediglich feste Durchlaufzeiten als exogene Parameter berücksichtigen. Im Vortrag wird die Leistungsfähigkeit moderner Produktionsplanungsansätze, die Clearingfunktionen verwenden, mit der Leistungsfähigkeit konventioneller Produktionsplanungsansätze verglichen. Der Einsatz von diskreter Simulation zur Bestimmung von Clearingfunktionen sowie zur Bewertung von Produktionsplänen wird diskutiert. Außerdem werden Fragen der simulationsbasierten Leistungsbewertung von Produktionsplanungsansätzen im Rahmen eines rollierenden Ansatzes besprochen. Herausforderungen für den Einsatz von Simulation, die sich insbesondere aufgrund der Größe der Lieferketten in der Halbleiterindustrie für die simulationsbasierten Produktionsplanungsansätze ergeben, werden am Ende des Vortrags dargestellt.

(Der Vortrag fand am 5. März 2014 an der Universität Göttingen statt.)

Von der Mikrostruktur zur Nanostruktur – Werkstoff- und Prozesstechnik für neue Stähle

Prof. Dr.-Ing. Wolfgang Bleck
Institut für Eisenhüttenkunde
RWTH Aachen

Angesichts von mehr als 2200 Stählen in der Werkstoffliste des Stahlinstituts VDEh lässt sich die Frage stellen, welche zukünftigen Anforderungen aus neuen Anwendungsgebieten hervorgehen und welche Optionen für neue Werkstoffentwicklungen bestehen.

Am Beispiel von Anwendungen im Automobilbau und im Bauwesen wird gezeigt, dass vor allem das Engineering von Gefügen auf einer Größenskala unterhalb der Mikroskala attraktive Eigenschaftskombinationen ermöglicht. Neue Untersuchungsmethoden wie die Atom Probe Tomography, High Resolution Transmission Electron Microscopy und die Electron Backscatter Diffraction Methoden resultieren in quantitativen Gefügeinformationen auf der nm-Skala. Die Modellierung, beispielsweise mit ab initio Methoden oder Repräsentativen Volumenelementen, führt zu einem erweiterten Werkstoff- und Prozessverständnis, und daraus abgeleitet zu neuen Produkten. Als Beispiele für neue Werkstoff-Konzepte werden hochfeste kalt umformbare Stähle mit außergewöhnlichem Verfestigungsverhalten, Stähle mit intrinsischer Fehlertoleranz und Stähle mit verbesserter Festigkeits-Zähigkeits-Bilanz besprochen. Die Beispiele für Prozesse betreffen das Warmwalzen mit Auste-

nitkonditionierung und robuster Gefügeeinstellung sowie die Justierung von Phasenumwandlungen bei der Wärmebehandlung.

(Der Vortrag fand am 7. Mai 2014 an der Technischen Universität Clausthal statt.)

Wie kommt Verkehr in den Computer? – Modellierung und Simulation von Verkehrssystemen

Prof. Dr.-Ing. Peter Vortisch
Institut für Verkehrswesen
Karlsruher Institut für Technologie

Bevor eine neue Straße gebaut oder eine neue Ampel in Betrieb geht, wird heutzutage der Verkehr vorher und nachher im Computer simuliert. Diese Simulationsmodelle können im Kleinen abbilden, wie Fahrzeuge über die Kreuzung fahren und aufeinander reagieren, aber auch im Großen, wie viele Pendler sich morgens in eine Stadt bewegen. Wie baut man solche Modelle? Welche Eingangsdaten braucht man dafür und wie bekommt man sie?

Im Vortrag wird zuerst erklärt, wie Verkehr überhaupt entsteht, und wie man erfassen kann, wer sich wann, wo und warum in den Verkehrssystemen bewegt. Anschließend wird die eher mikroskopische Sicht eingenommen: Wie bewegt sich ein Fußgänger? Wie fährt ein Auto dem anderen hinterher? Welche Wege wählen Autofahrer im Straßennetz? Für alle diese Aspekte des Verkehrs werden die gängigen Modellierungsansätze vorgestellt und dargestellt, wo sich die Forschung im Moment bewegt. Begleitend werden einige typische Anwendungen der Simulationsmodelle gezeigt.

(Der Vortrag fand am 4. Juni 2014 an der Universität Göttingen statt.)

Numerische Simulation in der Flugzeugentwicklung – Aktuelle Entwicklungen im DLR

Prof. Dr. Norbert Kroll
Institut für Aerodynamik und Strömungstechnik
DLR Braunschweig

In der Luftfahrtindustrie hat sich die numerische Strömungssimulation (CFD) in den letzten Jahren neben Windkanal- und Flugversuch als unverzichtbarer Bestandteil des aerodynamischen Entwurfsprozesses etabliert. Die kontinuierliche Weiterentwicklung der physikalischen Modelle und numerischen Verfahren sowie die Verfügbarkeit immer leistungsstärkerer Rechner legen nahe, die numerische Simulation wesentlich weitgehender als bisher einzusetzen und den Flugzeugentwicklungsprozess völlig umzugestalten. Daher orientieren sich die aktuellen und zukünftigen Aktivitäten des DLR im Bereich der Verfahrensentwicklung an der Vision eines „Erstflugs im Rechner" (Digitales Flugzeug).

Primäres Ziel ist die Entwicklung und Bereitstellung einer flexiblen, parallelen Softwareplattform zur multidisziplinären Analyse und Optimierung von Flugzeugen und Hubschraubern unter enger Einbindung von hochgenauen Verfahren aller relevanten Fachdisziplinen. Zum einen soll diese Plattform einen robusten, integrierten Entwurfsprozess von Aerodynamik und Struktur ermöglichen. Das derzeitige noch weitgehend sequentielle Vorgehen im Detailentwurf soll aufgebrochen und das volle Potenzial des multidisziplinären Entwurfs verfügbar gemacht werden. Zum anderen soll mit der Softwareplattform die Möglichkeit geschaffen werden, effiziente und verlässliche Simulationen von Flugmanövern im gesamten Flugbereich einschließlich der Flugbereichsgrenzen durchzuführen und somit die Ermittlung von aerodynamischen und aeroelastischen Datensätzen auf Basis höherwertiger Verfahren zur Bewertung der Flugeigenschaften zu erlauben.

Die sehr aufwendigen, disziplinübergreifenden Simulationen und die Herausforderungen hinsichtlich der physikalischen Modellierung im Bereich der Flugenveloppe erfordern Weiterentwicklungen und Verbesserungen des hybriden DLR-Strömungslösers TAU. Aktuelle Arbeiten zielen darauf ab, die Effizienz, Robustheit und Verlässlichkeit sowie den Automatisierungsgrad des TAU-Codes signifikant zu verbessern und dessen Einsatzspektrum zu erweitern. Vor dem Hintergrund der technologischen Entwicklung der Hochleistungsrechner ist die heute in den meisten Strömungslösern realisierte Parallelisierungsstrategie an die Grenzen der Skalierbarkeit gekommen. Daher sind der

Entwurf und die Implementierung eines Strömungslösers der nächsten Generation ein weiteres wesentliches Ziel zukünftiger Aktivitäten.

Im Vortrag werden einige der zukünftigen Zielanwendungen im Bereich der virtuellen Analyse und Erprobung im Flugzeugentwurf vorgestellt. Basierend auf dem aktuellen Status der CFD-Verfahren werden die wesentlichen Herausforderungen und Anforderungen in der numerischen Simulation abgeleitet und Lösungsansätze für fortschrittliche Simulationsstrategien vorgestellt.

(Der Vortrag fand am 2. Juli 2014 an der Technischen Universität Clausthal statt.)

HPC im Umbruch – Trends und Entwicklungen

Prof. Dr.-Ing. Dr. h.c. Dr. h.c. Michael M. Resch
High Performance Computing Center Stuttgart (HLRS)
Universität Stuttgart

Die theoretische Rechenleistung steigt weiter. Was lange Zeit als Moore's law bezeichnet wurde gilt zwar seit 2004 nicht mehr für einzelne Prozessoren. Trotzdem steigt die Geschwindigkeit von Systemen weiterhin etwa um einen Faktor 2 alle 18 Monate. Daraus ergeben sich neue Möglichkeiten und neue Probleme. In diesem Vortrag sollen diese aufgezeigt und diskutiert werden. Möglichkeiten ergeben sich vor allem durch eine erhebliche höhere Rechenleistung auch für kleinere Systeme. Verbunden damit sind Risiken die uns nicht bewusst sind. Gleichzeitig stellt sich die Frage, ob die Leistungsentwicklung fortgesetzt werden kann. Prognosen, die für das Jahr 2020 ein Exaflop vorhersagen, aber gleichzeitig einen Strombedarf von 50 MW erwarten sind wenig ermutigend. Spezifische Konzepte wie Beschleunigerkarten wirken zunächst wie ein Ausweg, stoßen aber ebenfalls an ihre Grenzen. Alle diese Themen werden angesprochen und in einen Kontext gesetzt. Das HLRS dient dabei als Beispiel für ein Zentrum und die Auswirkungen all dieser Trends auf nationaler Ebene.

(Der Vortrag fand am 2. Juli 2014 an der Technischen Universität Clausthal statt.)

HLRN-III: Hochleistungsrechner für Norddeutschland

PD Dr. Steffen Schulze-Kremer
HLRN und wissenschaftliche Anwendungsbetreuung
Leibniz Universität Hannover

Ende dieses Jahres wird der HLRN-III in der zweiten Ausbaustufe mit 2,5 PetaFlop/s, 85.000 Rechenkernen, 220 TeraByte Hauptspeicher und 8 PetaByte Festplattenspeicher die größte Ressource für wissenschaftliches Rechnen in Norddeutschland sein. Die Länder Berlin, Brandenburg, Bremen, Hamburg, Mecklenburg-Vorpommern, Niedersachsen und Schleswig-Holstein betreiben gemeinsam nun mittlerweile die dritte Generation ihres Hochleistungsrechners, die erfolgreich begutachteten Spitzenforschungsprojekten aus öffentlich-rechtlichen Institutionen ihrer Mitgliedsländer kostenfrei Rechenzeit in großem Umfang zur Verfügung stellt. Der Vortrag stellt die technischen und organisatorischen Besonderheiten des HLRN-III im Kontext des internationalen Supercomputing vor und gibt einen Einblick in seine Nutzung.

(Der Vortrag fand am 16. Juli 2014 an der Technischen Universität Clausthal statt.)

Towards Exascale Simulation Technology

Prof. Dr. Ulrich Rüde
Lehrstuhl für Informatik 10 (Systemsimulation)

Friedrich-Alexander-Universität Erlangen-Nürnberg

Exploiting heterogeneous and hierachically structured extreme scale computer systems to their full capability requires innovation on many levels: New algorithmic paradigms must address unprecedented levels of concurrency and must support asynchronous execution. A new performance-oriented software design technology must be developed to support efficiency, scalability, portability, and flexibility. I will report on our recent work in the waLBerla and HHG frameworks for simulating complex particulate flows based on the lattice Boltzmann method (LBM) and for solving Finite Element Systems using Multigrid Methods. Scalability and performance results for up to a

trillion degrees of freedom as well as experiments on accelerator based systems will be presented.

(Der Vortrag fand am 1. Oktober 2014 an der Universität Göttingen statt.)

Modelle und Methoden zur Lösung strategischer Fahrplanprobleme bei DB Netze

Prof. Dr. Karl Nachtigall
Professur für Verkehrsströmungslehre
Technische Universität Dresden

Seit etwa 10 Jahren entwickelt die Professur für Verkehrsströmungslehre im Auftrag von DB Netze prototypische Software zur automatischen Erzeugung und Optimierung von Fahrplänen. Die Programme werden in der Langfristplanung zur Bewertung und Analyse von Infrastrukturmaßnahmen eingesetzt. Als Basis der Modellierung wird ein streng getakteter 2h Fahrplan genutzt. Der Vortrag gibt einen Überblick über die Planungsstufen der strategischen Fahrplanung:

a) streng getaktete 2h-Taktfahrlagen
b) die Integration von Gütersystemtrassen in den Personenverkehr als 24 h Fahrplan
c) Belegungsverfahren, bei denen die als Platzhalter konstruierten Gütersystemtrassen zu konkreten Zugfahrten für Güterverkehrsnachfragen verknüpft werden

Wir stellen die grundlegenden mathematischen Modelle und Lösungsverfahren für diese Anwendungen vor. Streng getaktete Fahrplankonstruktion wird als periodische Ereignisplanung modelliert und dann sehr effizient als Erfüllbarkeitsproblem der Aussagenlogik gelöst. Gütersystemtrassen werden mit linearen Programmen erzeugt. Belegungsverfahren werden durch eine Kombination von linearer Programmierung (Spaltengenerierung) und Heuristiken gelöst.

(Der Vortrag fand am 3. Dezember 2014 an der Universität Göttingen statt.)

Quantitative Morphology-Transport Relationships for Disordered Porous Media by Morphological Reconstruction and High-Performance Computing of Flow and Transport

Prof. Dr. Ulrich Tallarek
Department of Chemistry
Philipps-Universität Marburg

The discovery of the morphology-transport relationships for disordered porous media used in chemical engineering and separation science (packings, monoliths) is a major challenge, because it requires the 3D physical reconstruction and/or computer-generation of the materials followed by 3D mass transport simulations to collect meaningful data for a detailed analysis of morphological and transport properties. This approach is the only direct as well as the most realistic way to understand and optimize materials with applications in chromatography or catalysis. Our latest progress regarding the following issues will be reported: (1) Systematic study of how individual parameters, such as the packing density and packing protocol, affect the morphology of computer-generated packings. (2) Physical reconstruction of packed and monolithic beds to collect information on how experimental parameters of the packing and preparation process influence morphology. (3) 3D mass transport simulations performed on a high-performance computing platform to analyze in detail the hydrodynamics and resulting dispersion. (4) Analysis of computer-generated and physically reconstructed packed and monolithic beds with statistical methods to derive structural descriptors for mass transport (diffusion, dispersion), which have potential for refining the existing theoretical framework.

(Der Vortrag fand am 4. März 2015 an der Technischen Universität Clausthal statt.)

How to order a waiting list?

Dr. Sebastian Stiller
Institut für Mathematik
Technische Universität Berlin

How to order the waiting list for an overbooked flight? This amounts to the problem of packing a knapsack without knowing its capacity. Whenever we attempt to pack an item that does not fit, the item is discarded; if the item fits, we have to include it in the packing. We show that there is always a policy that packs a value within factor 2

of the optimum packing, irrespective of the actual capacity. If all items have unit density, we achieve a factor equal to the golden ratio R = 1.618. Both factors are shown to be best possible. In fact, we obtain the above factors using packing policies that are universal in the sense that they fix a particular order of the items and try to pack the items in this order, independent of the observations made while packing. We give efficient algorithms computing these policies. On the other hand, we show that, for any R > 1, the problem of deciding whether a given universal policy achieves a factor of R is coNP-complete. If R is part of the input, the same problem is shown to be coNP-complete for items with unit densities. Finally, we show that it is coNP-hard to decide, for given R, whether a set of items admits a universal policy with factor R, even if all items have unit densities. This is joint work with Yann Disser, Max Klimm, and Nicole Megow.

(Der Vortrag fand am 6. Mai 2015 an der Universität Göttingen statt.)

Flüssiger Stahl in silico – numerische Simulation von Prozessen der Stahlherstellung

Prof. Dr.-Ing. Rüdiger Schwarze
Institut für Mechanik und Fluiddynamik
Technische Universität Bergakademie Freiberg

Die Prozesse der Eisen- und Stahlherstellung unterliegen einem permanenten Optimierungsdruck, der aktuell durch ökonomische (möglichst geringe Kosten) und ökologische (möglichst geringer CO2-Ausstoß) Vorgaben definiert wird. Entsprechende Innovationen in der Stahltechnologie erfordern ein vertieftes Verständnis aller beteiligten Prozessstufen, um beispielsweise die Ursachen für eine Qualitätsminderung gezielt bekämpfen zu können. Die Erforschung der Vorgänge in den Prozessstufen der flüssigen Phase ist allerdings aufgrund der physikalischen und chemischen Eigenschaften der Eisen- bzw. Stahlschmelzen sehr schwierig. In der Vergangenheit wurden deswegen vor allem Modellexperimente mit Wasser als Modellschmelze genutzt, um die Strömungen in diesen Prozessstufen zu erforschen. Da die Modellähnlichkeit mit diesem Ansatz nur sehr eingeschränkt erreicht wird, nutzt die moderne Forschung zunehmend die numerische Strömungssimulation (CFD). Mit CFD-Modellen lassen sich auch komplexere physikalische Vorgänge, etwa die elektromagnetische Beeinflussung einer strömenden Stahlschmelze, beschreiben. Im Vortrag wird das anhand verschiedener Beispiele aus den Prozessstufen der Eisen- und Stahlherstellung erläutert. Der aktuelle Forschungsstand und zukünftige Möglichkeiten werden diskutiert.

(Der Vortrag fand am 3. Juni 2015 an der Technischen Universität Clausthal statt.)

Effiziente Lokalisierung für drahtlose Sensornetzwerke

Salke Hartung, M. Sc.
Institut für Informatik
Georg-August-Universität Göttingen

Lokalisierung in Sensornetzwerken bezeichnet die Bestimmung der Position jedes Netzwerkknotens und ist eine grundlegende Notwendigkeit, da gesammelte Daten nur in Verbindung mit ihrer räumlichen Position sinnvoll genutzt werden können. Positionierungssysteme, wie GPS, stellen in der Regel keine Alternative in Sensornetzwerken dar, da die Kapazitäten der einzelnen Knoten nicht ausreichen, um den Betrieb des Netzes langfristig aufrecht zu erhalten. Als Alternative obliegt es den Netzwerkknoten mit Hilfe von Referenzknoten und eines Lokalisierungsalgorithmus ihre Position selbst zu bestimmen. Im Rahmen dieses Forschungsprojektes wurden unter anderem 2 verschiedene Möglichkeiten entwickelt, einen vorhandenen Algorithmus, „Monte Carlo Localization (MCL)“, zu verbessern. In diesem Vortrag werden beide Arbeiten vorgestellt, sowie die laufenden Projekte erläutert.

(Der Vortrag fand am 1. Juli 2015 an der Universität Göttingen statt.)

Simulation der Schallausbreitung in unbegrenzten Räumen

Prof. Dr.-Ing. Stefanie Retka
Juniorprofessur für Computational Dynamics
Institut für Technische Mechanik
Technische Universität Clausthal

Der Vortrag führt in die Anwendung der numerischen Akustik auf komplexe Außenraumprobleme ein. Nach einem kurzen Überblick über die numerischen Grundlagen werden verschiedene Beispiele genutzt, um den Einfluss der Geometrie und deren Modifikation auf die Schallausbreitung und Schallabstrahlung zu verdeutlichen.

Eine Besonderheit unbegrenzter Strukturen liegt in der ersten Eigenfrequenz. Der zugehörige Eigenvektor bildet lediglich ein Viertel einer Wellenlänge ab. Dieser Effekt ist auch als lambda/4 -Effekt bekannt und tritt bei geschlossenen Räumen nicht auf. Weiterhin wird der Einfluss von Änderungen der Raumgeometrie auf die Eigenfrequenzen des Mediums im und um diesen Raum untersucht. Für die oben genannten Effekte werden eine Flasche mit veränderlicher Flaschenhalslänge und -öffnung sowie ein Zimmer mit geöffnetem Fenster, dessen Größe und Position variabel ist, betrachtet.

Abschließend wird der Einfluss der Strömung auf die akustischen Eigenschaften am Beispiel des Klanges einer Blockflöte betrachtet. Die Berücksichtigung eines charakteristischen Strömungsprofils in den numerischen Berechnungen im Frequenzbereich ist eine wesentliche Neuerung und für alle Berechnungen von Bedeutung, bei denen Mechanismen durchströmt bzw. umströmt werden. Exemplarische seien hier Auspuffanlagen oder auch Flugzeugflügel genannt.

(Der Vortrag fand am 7. Oktober 2015 an der Technischen Universität Clausthal statt.)

Große mikroskopische verhaltensorientierte Verkehrssimulationen

Prof. Dr. Kai Nagel
Institut für Land- und Seeverkehr
Technische Universität Berlin

Durch die Fortschritte in der Computertechnik ist es inzwischen recht problemlos möglich, Systeme mit 108 Teilchen mikroskopisch zu simulieren. Dies ist aber bereits mehr, als man für die Simulation einer jeden Person und eines jeden Fahrzeugs in einem urbanen oder regionalen Verkehrssystem braucht. Es bleibt also die Aufgabe, die derart definierten synthetischen Personen mit entsprechender Verhaltenslogik auszustatten. Software-technisch ist das mit modernen objektorientierten Sprachen recht gut machbar; schwieriger ist es, die Modelle menschlichen Verhaltens zu formulieren. Ein typischer Kunstgriff ist die Annahme eines Nash-Gleichgewichtes, bei dem sich keine reisende Person durch einen unilateralen Wechsel - z.B. auf eine andere Route oder ein anderes Verkehrsmittel - verbessern kann. Dies reduziert die Anforderungen an das Verhaltensmodell, aber um den Preis einer rechentechnisch aufwändigeren Lösungsmethode mit vielen Iterationen, die man als simuliertes menschliches Lernen interpretieren kann, aber nicht muss. Bei anderen Fragestellungen, z.B. bzgl. Betrieb von Taxen oder autonomen Fahrzeugen, ist dieser Kunstgriff ohnehin nicht möglich, und man muss die Reaktionen bestimmter Teilnehmer in simulierter Echtzeit berechnen.

Der Vortrag wird beleuchten, was in diesem Rahmen derzeit machbar ist, einschließlich Fragestellungen wie: Was bewirkt eine Autobahnverlängerung in Berlin? Was bewirkt eine Autobahnschließung in Seattle? Welche Emissionen erzeugt das Verkehrssystem in München, und was kann man dagegen tun? Was bewirkt eine Maut im Großraum Johannesburg in Südafrika? Wie simuliert man südafrikanische Minibus-Taxis, wenn man nicht sehr viel über sie weiß? Wie würde man Systeme mit autonomen Fahrzeugen betreiben?

(Der Vortrag fand am 25. November 2015 an der Universität Göttingen statt.)

Dekomposition von Warteschlangennetzen mit Batch-Processing

Dipl.-Wirt.-Inf. Wiebke Klünder
Institut für Angewandte Stochastik
und Operation Research
Technische Universität Clausthal

Die Bedeutung von Simulationsmethoden zur Produktionsplanung und -steuerung hat in der industriellen Fertigung in den letzten Jahren ständig zugenommen. Zurückzuführen ist die Zunahme zum einen auf komplexer werdende Fertigungen und zum anderen auf immer kürzer werdende

Fertigungszyklen. Es besteht die Notwendigkeit, dass Unternehmen Fertigungsprozesse von Anfang an optimieren, da nachträgliche Korrekturen am Produktionsprozess in technischer und logistischer Hinsicht schwer umsetzbar sind. Das Entstehen von Warteschlangen ist aus betriebswirtschaftlicher Sicht ein Effekt, der möglichst vermieden bzw. minimiert werden sollte. Eine Warteschlange in einer Produktion bedeutet, dass sich der Produktionsvorgang durch Wartezeiten verlängert, was zu steigenden Lagerhaltungskosten bzw. gebundenem Material führt.

Die analytisch orientierte Methode der Warteschlangentheorie als Produktionsplanungswerkzeug bietet einen Ansatz der Optimierung und besitzt Vorteile gegenüber den etablierten Simulationsmethoden. Die jeweilige Fragestellung, z. B. wieviel Puffer an einer Bedienstation veranschlagt werden sollte, wird mathematisch modelliert und mit Hilfe von analytischen Formeln, die zuvor durch Simulation evaluiert wurden, approximativ gelöst. In diesem Vortrag wird ein Netz aus Produktions- bzw. Bedienstationen betrachtet, in dem Produkttyp-spezifische Aufträge in Stapeln von Bedienern verarbeitet werden. Der Einsatz der Dekompositionsmethode ermöglicht eine isolierte Betrachtung der einzelnen Bedienstationen im Netz, deren Leistungsgrößen anschließend mit Hilfe analytischer Formeln approximativ bestimmt werden können.

(Der Vortrag fand am 2. Dezember 2015 an der Technischen Universität Clausthal statt.)

Agent-Based Modeling and Simulation of Software Processes for Quality Assurance

Dipl.-Inf. Daniel Honsel, Dipl.-Math. Verena Honsel, Marlon Welter, M.Sc.
Institut für Informatik
Georg-August-Universität Göttingen

Project managers have to make decisions concerning the architecture, development strategy or team constellation and they have to estimate the consequences of the decisions. To have tool support for testing the interplay of different parameter constellations would be of great help. We created a simulation tool that can predict possible future scenarios and that makes the project manager aware of risky development trends. For the creation of this tool, understanding software evolution and its drivers is indispensable. To get a model with parameters close to the reality we examined Open Source Software (OSS) projects by repository mining and estimated the simulation's parameters from the gained insights. With the parameters we instantiate an Agent-based simulation of the software project which can be evaluated by project managers using Conditional Random Fields (CRFs) to gain the desired information about development trends.

(Der Vortrag fand am 13. Januar 2016 an der Universität Göttingen statt.)

Optimization problems in DSB long-term and strategic planning

Dr. Natalia Rezanova
Dänische Staatsbahnen (DSB)

Danish State Railways (DSB) is the largest passenger operator in Denmark. DSB Longterm Planning Department is responsible for the long-term traffic planning, including line planning, timetabling and rolling stock (2 years before the day of operations), as well as the strategic traffic planning (10+ years before the day of operations). Many optimization problems arise within the different strategic planning areas. Some of them are solved using commercial optimization software uniquely developed for DSB. Other optimization problems are addressed in-house. The talk will focus on two different optimization projects, where Mixed Integer Programming models formulated, implemented and solved. The line planning optimization model determines an optimal set of train lines, patterns and frequencies, and is used in the strategic planning on DSB S-train network. The facility location optimization model is developed to determine the size and location of maintenance, preparation, cleaning and stabling facilities required to service the fleet of electrical trains, which DSB is planning to acquire in the near future. Both projects, even though quite different in purpose and impact, exploit the advantages of Operations Research and help to address the real-life challenges of a railway operator.

(Der Vortrag fand am 13. Januar 2016 an der Universität Göttingen statt.)

Verspätungen in Verkehrsnetzen

Prof. Dr. Anita Schöbel
Institut für Numerische und Angewandte Mathematik
Universität Göttingen

Prof. Dr. Michael Kolonko
Institut für Angewandte Stochastik und Operation Research
Technische Universität Clausthal

Jonas Harbering, M.Sc.
Institut für Numerische und Angewandte Mathematik
Universität Göttingen

Die alltäglichen Verspätungen in öffentlichen Verkehrsnetzen können vielfältige Ursachen haben: von klemmenden Türen über unerwarteten Passagierandrang bis zu Baumaßnahmen auf den Gleisen.

Diese kleinen ‚Quellverspätungen' lassen sich im Alltag nicht ganz vermeiden. Ziel einer robusten Fahrplanung ist es daher, durch geschickte Platzierung von Zeitpuffern zu verhindern, dass sich diese Verspätung aufsummieren und über das Netz verbreiten und so zu ernsthaften Verspätungen führen können. Die dazu erforderliche genaue Untersuchung und Simulation des Verkehrsgeschehens unter zufälligen Verspätungen ist aber eine relativ komplexe Aufgabe.

In dem SWZ Projekt „Strukturuntersuchungen zur Entstehung und Fortpflanzung von Verspätungen in Verkehrsnetzen - Modellierung, Simulation und Optimierung eines stochastischen Netzwerkes" wurden von Arbeitsgruppen an der Universität Göttingen und der TU Clausthal verschiedene Ansätze untersucht, mit denen die Auswirkung von Fahrplanpuffern auf die resultierenden Verspätungen der Fahrgäste dargestellt und optimale Pufferallokationen gesucht werden können. Insbesondere konnte in diesem Projekt gezeigt werden, dass die für unterschiedliche Zwecke entwickelten szenario-basierten und stochastischen Modelle zu denselben Ergebnissen führen.

(Der Vortrag fand am 3. Februar 2016 an der Technischen Universität Clausthal statt.)

Modeling, deployment and scaling of simulation applications for and in the cloud

Fabian Glaser, M.Sc.
Institut für Informatik
Universität Göttingen

Often scientific simulations require more computational resources than locally available. While grid computing already offered on-demand access to large-scale distributed computing resources in the past, cloud computing is much more flexible since it offers the possibility to deploy the full hard- and software stack as desired. However, this increased flexibility also places an additional burden on scientists, who are willing to migrate their simulation applications to the cloud, since it requires a deep understanding of the cloud infrastructure and the related technologies. Therefore, our focus in scope of the project "A cloud-based software infrastructure for distributed simulation applications" was to identify the obstacles scientists face when moving their simulation applications to the cloud and develop a framework to simplify this process. The developed solution is based on the Topology and Orchestration Specification for Cloud Applications (TOSCA) and leverages domain-model knowledge of the scientist to scale the deployed simulation infrastructure.

(Der Vortrag fand am 9. März 2016 an der Universität Göttingen statt.)

Simulation-based impact assessment and strategy development in the automotive sector

Prof. Dr. Thomas S. Spengler
Institut für Automobilwirtschaft und Industrielle Produktion
Technische Universität Braunschweig

Electric vehicles are often seen as a promising way for rationalizing the use of fossil energy and cutting down greenhouse gas emissions in the

automotive sector. So far, however, the market success of electric vehicles and thus their impact on reducing fossil fuel consumption and greenhouse gas emissions are rather limited. In this talk, the automotive market simulator (AMaSi) is introduced, which combines system dynamics and agent-based simulation to analyze the leverage of manufacturers and policy to support the market diffusion of electric vehicles. Based on real-world data the model is applied to the German car market and different manufacturer and policy measures are simulated, including the currently discussed purchase premium for battery and plug-in hybrid electric vehicles. Additionally, validation issues are discussed when modeling the structure of complex socioeconomic/-technic systems and simulating their behavior.

(Der Vortrag fand am 22. Juni 2016 an der Universität Göttingen statt.)

HPC und Data Science in Göttingen

Prof. Dr. Ramin Yahyapour
Gesellschaft für wissenschaftliche Datenverarbeitung mbH Göttingen

Forschung gestaltet sich zunehmend rechen- und daten-intensiv, wofür eine geeignete Infrastruktur relevante Voraussetzung ist. Neben der Verfügbarkeit von solchen Infrastrukturen stellt auch das Wissen um den effektiven und effizienten Umgang eine Herausforderung dar. Am Göttingen Campus wird unter dem Begriff eResearch an einer institutionellen Strategie für Computational and Data Science gearbeitet. In dem Vortrag wird Einblick zu den aktuellen Entwicklungen gegeben und Beispiele zu Forschungsfragen geliefert.

(Der Vortrag fand am 26. Oktober 2016 an der Universität Göttingen statt.)

Kostenminimale Flüsse mit beschränktem Budget

Jun.-Prof. Dr. Clemens Thielen
Fachbereich Mathematik
Technische Universität Kaiserslautern

Das Minimalkostenflussproblem ist eines der bekanntesten Probleme der Graphentheorie und besitzt zahlreiche Anwendungen. Für gegebenen Kapazitäten und Kosten pro Flusseinheit auf den Pfeilen eines Netzwerks besteht die Aufgabe in der Bestimmung der kostengünstigsten Möglichkeit, eine vorgegebene Menge eines Gutes von einer gegebenen Quelle zu einer gegebenen Senke durch das Netzwerk zu transportieren. Das Minimalkostenflussproblem stellt somit einen allgemeinen mathematischen Rahmen für viele Distributions- und Transportprobleme dar. Zusätzlich lässt sich auch das Problem der Bestimmung eines maximalen dynamischen Flusses durch ein Netzwerk mit Reisezeiten auf den Pfeilen als Minimalkostenflussproblem formulieren. Daher lassen sich beispielsweise auch Probleme aus dem Bereich der Kapazitätsbestimmung von Abwassernetzen als Minimalkostenflussprobleme lösen.

In vielen Anwendungen des Minimalkostenflussproblems ist jedoch das zu benutzende Netzwerk noch nicht vollständig vorhanden, sondern muss erst (aus-) gebaut werden, bevor es zum Gütertransport verwendet werden kann. Dies motiviert die Erweiterung des Minimalkostenflussproblems um einen zweiten Kostenwert für jeden Pfeil, der die (Aus-) Baukosten des Pfeils pro Kapazitätseinheit beschreibt. Steht nur ein vorgegebenes Budget zum (Aus-) Bau des Netzwerks zur Verfügung, so ergibt sich das Problem, einen Fluss mit minimalen Kosten zu berechnen, der sich in einem Netzwerk mit durch das Budget beschränkten (Aus-) Baukosten realisieren lässt. Das resultierende Netzwerkflussproblem wird als Minimalkostenflussproblem mit Budgetbeschränkung bezeichnet.

Dieser Vortrag beschäftigt sich mit effizienten Algorithmen zur Lösung des Minimalkostenflussproblems mit Budgetbeschränkung. Wir werden zeigen, wie sich kombinatorische Algorithmen für das klassische Minimalkostenflussproblem in Kombination mit binärer oder parametrischer Suche benutzen lassen, um auch das Problem mit Budgetbeschränkung selbst auf großen Netzwerken effizient lösen zu können.

(Der Vortrag fand am 2. November 2016 an der Technischen Universität Clausthal statt.)

Integration based profile likelihood calculation for PDE constrained parameter estimation problems

Prof. Dr. Barbara Kaltenbacher
Institut für Mathematik
Alpen-Adria-Universtät Klagenfurt

Partial diferential equation (PDE) models are widely used in engineering and natural sciences to describe spatio-temporal processes. The parameters of the considered processes are often unknown and have to be estimated from experimental data. Due to partial observations and measurement noise, these parameter estimates are subject to uncertainty. This uncertainty can be assessed using profile likelihoods, a reliable but computationally intensive approach. In this talk, we present the integration based approach for the profile likelihood calculation developed by Chen and Jennrich, 2002, and adapt it to inverse problems with PDE constraints. While exiting methods for profile likelihood calculation in parameter estimation problems with PDE constraints rely on repeated optimization, the proposed approach exploits a dynamical system evolving along the likelihood profile. We derive the dynamical system for the unreduced estimation problem, prove convergence and study the properties of the integration based approach for the PDE case. To evaluate the proposed method, we compare it with state-of-the-art algorithms for a simple reaction-diffusion model for a cellular patterning process. We observe a good accuracy of the method as well as a significant speed up as compared to established methods. While our computational experiments have been done for an application example in systems biology, we emphasize that due to generality of this methodology, integration based profile calculation appears to facilitate rigorous uncertainty analysis for parameter estimation problems with PDE constraints also in many other fields.

(Der Vortrag fand am 7. Dezember 2016 an der Technischen Universität Clausthal statt.)

Pellet-aufgelöste Modellierung von katalytischen Festbettreaktoren

Prof. Dr.-Ing. Gregor D. Wehinger
Institut für Chemische und Elektrochemische Verfahrenstechnik
Technische Universität Clausthal

Festbettreaktoren sind ein häufig eingesetzter Reaktortyp in der chemischen Industrie. Festbettreaktoren mit kleinem Rohr-zu-Pelletdurchmesser-Verhältnis (D/dp =N) finden vor allem bei stark exo- oder endothermen Reaktionen Anwendung. Unter diesen Umständen bestimmt die lokale Bettstruktur maßgeblich die Transportgrößen. Signifikante Randgängigkeit, lokale Tot-zonen und Rückströmungen sind die Folge. Gängige Beschreibungen von katalytischen Fest-bettreaktoren beruhen jedoch auf Annahmen, die die örtliche Bettstruktur nicht berücksichtigen, etwa Pfropfenströmung (plug flow) oder pseudohomogene Kinetiken. Fehlerhafte Vorhersagen können die Folge sein, die zu Produktionsausfällen, etwa durch Überhitzung der Reaktorrohre, führen können. Eine genauere Beschreibung liefert hingegen die numerische Strömungsmechanik (CFD) gekoppelt mit detaillierten Reaktionsmechanismen.

Dabei wird jedes einzelne Pellet im Reaktor örtlich abgebildet.

In diesem Beitrag wird diese rigorose pellet-aufgelöste Modellierung von katalytischen Fest-bettreaktoren vorgestellt. Aspekte der Modellierung werden diskutiert und anhand experimenteller Daten kritisch bewertet. Diese Aspekte umfassen die Algorithmus-basierte Erzeugung von regellosen Schüttungen mit Hilfe der Diskreten-Elemente-Methode (DEM), mit CFD berechnete Geschwindigkeitsprofile in den Pellet-Zwischenräumen, Wärmetransport in der Gas- und Feststoffphase, heterogene Katalyse am Beispiel der Trockenreformierung von Methan, Strahlung zwischen festen Oberflächen, sowie die Modellierung von Porenprozessen in den porösen Pellets.

(Der Vortrag fand am 7. Juni 2017 an der Technischen Universität Clausthal statt.)

Molekulardynamik-Simulationen von heterogenen Materialien unter hoher mechanischer Belastung

Jun.-Prof. Dr. Nina Gunkelmann
Simulationswissenschaftliches
Zentrum Clausthal-Göttingen
Technische Universität Clausthal

Mit Hilfe von Molekulardynamik-Simulationen wird das Verhalten von heterogenen Materialien unter hoher mechanischer Belastung analysiert. Aufgrund der Komplexität der betrachteten Materialien existieren keine vollständigen analytischen Vorhersagen der Werkstoffantwort, sodass Computersimulationen ein nützliches Werkzeug sind, um die Materialeigenschaften bei mechanischer Beanspruchung zu analysieren. Als prototypisches Material wird polykristallines Eisen studiert, das eine druckinduzierte Phasenumwandlung von der kubisch-basiszentrierten zur hexagonal dichtest gepackten Struktur bei etwa 13 GPa zeigt. Es wird ein interatomares Wechselwirkungspotential verwendet, welches den Phasenübergang beim experimentell zu erwartenden Übergangsdruck modelliert. Die Simulationen zeigen, dass der Phasentransformation plastische Aktivität in der Form von Versetzungsbildung an den Korngrenzen vorausgeht, was als 3-Wellen-Struktur bezeichnet wird: Es wird eine elastische Kompressionswelle beobachtet, an die eine plastische Welle anschließt, die zuletzt zu einer Phasentransformationsfront führt.

Trotz großer Unterschiede in den Materialeigenschaften weisen Aluminium-Nanoschäume ebenfalls eine 3-Wellen-Struktur auf, die drei verschiedene Regimes kennzeichnet: Einem elastischen Vorläufer folgt plastische Aktivität in den Filamenten, bevor die Schaumstruktur letztendlich eingedrückt wird und ein kompaktifiziertes Material entsteht. Die Versetzungsbildung in den Filamenten kann veranschaulicht und mit dem Geschwindigkeitsprofil korreliert werden.

Dabei können Versetzungsstrukturen mit der Methode D2C charakterisiert werden, indem diskrete Versetzungslinien durch kontinuierliche Feldvariablen ausgedrückt werden. Am Beispiel von Molekulardynamik-Simulationen von Nanoritzen in Eisen wird in diesem Vortrag gezeigt, dass mittels D2C Eigenschaften der Versetzungsmikrostruktur ermittelt werden können, die nicht direkt aus den atomistischen Daten bestimmt werden können. So kann die Nukleationsrate von Versetzungsschleifen unter dem Indenter bestimmt werden, was als Input für Methoden auf der Mesoskala verwendet werden kann.

(Der Vortrag fand am 8. November 2017 an der Technischen Universität Clausthal statt.)

Continuum dislocation dynamics (CDD): a mesoscale crystal plasticity framework

Dr.-Ing. Mehran Monavari
Institute of Materials Simulation

Friedrich-Alexander-University Erlangen-Nürnberg
Since the discovery of dislocations as carriers of plastic deformation, developing a continuum theory for motion and interaction of dislocations has been a challenging task. Such a theory should address two interrelated problems: how to represent in a continuum setting the motion of dislocations, hence the kinematics of curved and connected lines, and how to capture dislocation interactions.

In this regard, we introduce the Continuum dislocation dynamics (CDD) as a framework for representing the evolution of systems of curved and connected dislocation lines. In CDD, the microstructure is described in terms of a series of density-like tensorial variables where the accuracy can be prescribed by the resolution of the computational domain or by the order at which the tensorial series is truncated. CDD can operate on a wider spatial and temporal range than microscale models such as Discrete Dislocation Dynamics (DDD) and with a higher physical accuracy than phenomenological crystal plasticity. Therefore it is able to bridge the gap between these models. We present a mesoscale FEM crystal plasticity framework based on CDD and demonstrate its potential though few examples.

(Der Vortrag fand am 7. Februar 2018 an der Technischen Universität Clausthal statt.)

Modeling and simulation based approaches in aeronautical Informatics

PD Dr. Umut Durak
German Aerospace Center (DLR)
Institute of Flight Systems, Braunschweig

Aeronautical informatics is advancing rapidly through the synergy between Information and Communication Technologies (ICT) and aeronautics. The history of aeronautics starts with the pioneer era. The introduction of mechanically powered controls is called the second era. The third era is characterized by the utilization of computers and automation in aircraft. Now, we are moving towards the Flight 4.0: the fourth era which emphasize "smart" and "connected" flight. Flight 4.0 promotes extensively exploiting the emerging ICT, such as Cloud/Fog/Edge Computing, Internet of Things, Cyber Physical Systems or Big Data. Along with that, the rise of unmanned aerial systems, new urban aviation concepts and future air traffic management systems are asking for innovative solutions. For democratization of engineering and stimulating the innovation potential of Small and Medium Size Enterprises (SMEs) and startups, we need new affordable and accessible tools, methods and techniques for designing, developing and assuring automation and autonomy across system boundaries. This talk elaborates modeling and simulation based approaches and promotes standardization and open-source for model based design, and simulation based analysis, training, validation and verification for achieving the future "smart" and "connected" flight. It further introduces the related research efforts of German Aerospace Center (DLR) - Clausthal University of Technology collaborative research group on aeronautical informatics.

(Der Vortrag fand am 13. April 2018 an der Technischen Universität Clausthal statt.)

A pilgrim scheduling approach to increase public safety during the great pilgrimage to Makkah, Saudi Arabia

Prof. Dr. Sven Müller
Hochschule Karlsruhe

The Hajj - the great pilgrimage to Makkah, Saudi Arabia - is one of the five pillars of the Islamic religion. With more than three million pilgrims performing Hajj rituals, it is also one of the largest pedestrian problems in the world. Until 2006, severe crowd disasters have repeatedly overshadowed the pilgrimage. Ramy al Jamarat – the stoning of the devil ritual – is known to be particularly crowded. In the aftermath of the Hajj in 2006, several measures were implemented to improve safety and to avoid crowd disasters. One particular measure is the development of a time schedule for the pilgrims to perform the stoning ritual. In this paper, we present a model and a solution approach to the Pilgrim Scheduling Problem. The model minimizes the deviation of the scheduled stoning time from the preferred stoning time, while considering infrastructure capacities to avoid critical densities of pilgrims. At the same time pilgrims are assigned to routes leading to the ritual site and back to the camp site. The routes enforce a rigor one-way ow in the surrounding area of the ritual site. We solve the Pilgrim Scheduling Problem by an intelligible fix-and-optimize heuristic. The schedule is evaluated using a mesoscopic pedestrian simulation and discussed with local authorities. Critical feedback is then incorporated into the final schedules. Our approach was an integral part of the planning process for Hajj in the years 2007–2014 and 2016, and no crowd disaster happened during this time. We illustrate our work with computational results and validation data for the Hajj in 2016. In 2015, a severe crowd crush happened close to the ritual site. In that year the authors were not in charge of the scheduling and routing for the stoning ritual. We provide a short discussion of the crowd accident and the approach used in 2015.

(Der Vortrag fand am 21. November 2018 an der Universität Göttingen statt.)

Multiscale Materials Modeling - New Developments with Special Emphasis on MD-Simulations

Prof. Dr. Dr. h. c. Siegfried Schmauder
Institut für Materialprüfung Werkstoffkunde und Festigkeitslehre, Universität Stuttgart

In this overview it will be shown how the first successful example of real multiscaling for metals was achieved. Multiscale simulation in the present context comprises the involvement of all length scales from atomistics via micromechanical con-

tributions to macroscopic materials behavior and further up to applications for components.

The main focus of the presentation will be put on new developments with special emphasis on MD-simulations and other methods involved and how they interact within the present approach. It will be shown that each method is superior on the respective length scale. Furthermore, the parameters which transport the relevant information from one length scale to the next one are decisive for the success of physically based multiscale simulations. While in the past different methods were tried to be combined into one simulation it is nowadays obvious in many fields of research that the only way to succeed in under-standing the mechanical behavior of materials is to do sequential multiscale simulations in order to achieve physically based practical material solutions without adjustment to any experiment. This has opened the door to real virtual material design strategies.

In a final step it will be shown that the approach is not limited to metals but can be extended to other material classes and can be also applied for composites as well as to many aspects of material problems in modern technical applications where all disciplines meet, from physics to materials science and further on to engineering applications.

(Der Vortrag fand am 28. November 2018 an der Technischen Universität Clausthal statt.)

Das Virtuelle Mikroskop - Visualisierung und Inspektion der Geometrie von Partikelschüttungen

Feng Gu, M.Sc.
Institut für Informatik, Abteilung Graphische Datenverarbeitung und Multimedia
Technische Universität Clausthal

Viele Materialien und Stoffe sind aus Partikeln aufgebaut, vom Beton bis zur Tablette. Manche Eigenschaften der fertigen Stoffe sind bereits stark durch die geometrischen Eigenschaften der Partikelmischungen bestimmt. Bei Beton ist z.B. die Raumausfüllung der trockenen Mischung, also das Verhältnis von Behältergröße zum Volumen der enthaltenen Partikel, ausschlaggebend für die Festigkeit des Betons nach der Aushärtung. In anderen Anwendungen, etwa bei der Herstellung von Schäumen, spielen Verteilung und Gestalt der Zwischenräume zwischen den ‚Partikeln', die in diesem Falle Hohlräume sind, eine entscheidende Rolle für die Eigenschaften des Materials.

Im Projekt „RaSim" wurde für solche Materialien eine parallele Collective-Rearrangement Simulation auf der GPU entwickelt, die mehrere Millionen unterschiedlich großer, kugelförmiger Partikel mit interaktiver Geschwindigkeit bewegen kann. Dabei werden die Kugeln an zufällige Startpositionen in einem Container gesetzt und stoßen sich danach bei Überlappung solange gegenseitig ab, bis ein konvergierter Zustand erreicht ist.

Um die Qualität dieser iterativen Simulation einschätzen zu können wurden im Projekt „Virtuelles Mikroskop" spezielle, dreidimensionale Visualisierungen entwickelt, die neben der einfachen Darstellung der Kugeln auch die aktuellen Überlappungsbereiche der Kugeln sowie die noch existierenden Freiräume im Container zeigen. Im Vortrag wird gezeigt wie solche Visualisierungen durch parallele Programmierung auf aktueller Grafikhardware mit einer Geschwindigkeit von 20 - 60 Bildern pro Sekunde für eine Million Kugeln umgesetzt werden können. Weiterhin werden auch erste Ergebnisse für die Simulation und Visualisierung von nicht-kugelförmigen Partikeln gezeigt.

Automatic Processing of Complex Geometries with the Lattice Boltzmann Method

Alexander Bufe, M.Sc.
Institut für Technische Mechanik
Technische Universität Clausthal

In order to determine correlations between fluid dynamic coefficients and geometrical properties a large number of data points, usually obtained in experiments and measurements, have to be examined. Applications may be found in aerodynamics, process engineering or other disciplines. For example, in porous media correlations between pressure loss or dispersion have to be parametrized depending on details of the geometrical structure. In biomedical applications, the flow though a large number of complex structures

has to be analyzed in a reliable and accurate way. In this context, computational approaches may offer an alternative route to provide such data. However, in classical fluid dynamics the mesh generation often requires manual processing, limiting the number of analyzable geometries. In contrast the lattice Boltzmann method, which usually operates on Cartesian grids, allows for easy and fully automatic mesh generation. Accuracy may be enhanced by using hierarchical refined meshes. Using a fully automated simulation setup the number of generated data is only limited by computational power and available input data. This talk gives a short introduction to the idea and basic concepts of LBM and illustrates the fully automatic approach drawing on examples from process engineering and medicine.

(Der Vortrag fand am 5. Dezember 2018 an der Technischen Universität Clausthal statt.)

Lehrangebote an den beiden Partneruniversitäten zum Thema Simulation

Jun.-Prof. Dr.-Ing. Marcus Baum
- Sensor Data Fusion (Universität Göttingen, 501933, Wintersemester 2016/2017)
- Hot Topics in Data Fusion and Analytics (Universität Göttingen, 501934, Wintersemester 2016/2017)
- Simulation-based Data Fusion and Analysis (Universität Göttingen, 502033, Sommersemester 2016 und Sommersemester 2017)
- Practical Course: Data Fusion (Universität Göttingen, 502082, Sommersemester 2016 und Sommersemester 2017)

Prof. Dr.-Ing. Gunther Brenner
- Computational Simulation (TU Clausthal, W 8036, Wintersemester 2015/2016, Wintersemester 2016/2017 und Wintersemester 2018/2019)
- Simulationsmethoden in den Ingenieurwissenschaften (TU Clausthal, W 8037, Wintersemester 2015/2016, Wintersemester 2016/2017 und Wintersemester 2018/2019)

Prof. Dr.-Ing. Uwe Bracht
- Seminar und Fachpraktikum „Digitale Fabrik“ (TU Clausthal, W 8351 und W 8352, Wintersemester 2017/2018 und Wintersemester 2018/2019)
- Fachpraktikum Materialflusssimulation (TU Clausthal, S 8353 und W 8353, Sommersemester 2017, Wintersemester 2017/2018 und Sommersemester 2018)

PD Dr.-Ing. habil. Umut Durak
- Simulation Engineering (TU Clausthal, W 1269, Wintersemester 2017/2018 und Wintersemester 2018/2019)
- Seminar: Graph Models and Simulation (TU Clausthal, S 1269, Sommersemester 2017 und Sommersemester 2018)

Jun.-Prof. Dr. Anja Fischer
- Kolloquium über Angewandte Mathematik (Universität Göttingen, 500166, Wintersemester 2016/2017)
- Theory of integer programming (Universität Göttingen, 502123, Wintersemester 2016/2017)
- Combinatorial optimization (Universität Göttingen, 501958, Sommersemester 2016)

Prof. Dr. Xiaoming Fu
- Computer Networks (previously Telematik) (Universität Göttingen, 990066, Wintersemester 2016/2017, Wintersemester 2017/2018 und Wintersemester 2018/2019)
- Advanced Computer Networks (Universität Göttingen, 501062, Sommersemester 2016, Sommersemester 2017 und Sommersemester 2018)
- Advanced Topics in Mobile Communications (Universität Göttingen, 501928, Sommersemester 2016, Sommersemester 2017, Sommersemester 2018 und Wintersemester 2018/2019)
- Seminar on Internet Technologies (Universität Göttingen, 990039, Sommersemester 2016 und Wintersemester 2016/2017)
- Practical Course Networking Lab

(Universität Göttingen, 990086 Sommersemester 2016)
- Practical Course Advanced Networking (Universität Göttingen, 990144, Sommersemester 2016)

Prof. Dr. Leonhard Ganzer
- Numerical Reservoir Simulation (TU Clausthal, S 6102, Sommersemester 2015, Sommersemester 2016, Sommersemester 2017 und Sommersemester 2018)

Prof. Dr. Jens Grabowski
- Practical Course on Software Testing (Universität Göttingen, 501882, Wintersemester 2016/2017, Wintersemester 2017/2018 und Wintersemester 2018/2019)
- Softwaretechnik (Universität Göttingen, 990045, Wintersemester 2016/2017)
- Software Testing (Universität Göttingen, 990052, Wintersemester 2016/2017 und Wintersemester 2018/2019)
- Advanced Topics in Software-Engineering (Universität Göttingen, 501216, Sommersemester 2016, Wintersemester 2016/2017, Sommersemester 2017, Wintersemester 2017/2018, Sommersemester 2018 und Wintersemester 2018/2019)
- Requirements Engineering (Universität Göttingen, 501217, Sommersemester 2016 und Sommersemester 2017)
- Software Evolution (Universität Göttingen, 501562, Sommersemester 2016 und Sommersemester 2017)
- Practical Course on Parallel Computing (Universität Göttingen, 990179, Sommersemester 2016 und Sommersemester 2018)
- Data Science and Big Data Analytics (Universität Göttingen, 501425, Wintersemester 2016/2017)
- Praktikum Simulationsmethoden in den Ingenieurwissenschaften (Universität Göttingen, gemeinsam mit TU Clausthal, 502637, Wintersemester 2018/2019)

Prof. Dr. Thorsten Grosch
- GPU Programming (TU Clausthal, W 1252, Wintersemester 2017/2018 und Wintersemester 2018/2019)

Jun.-Prof. Dr. Nina Gunkelmann
- Basic principles of molecular dynamics (TU Clausthal, Wintersemester 2017/2018 und Sommersemester 2018)
- Numerische Strömungsmechanik (TU Clausthal, Wintersemester 2018/2019)

Prof. Dr.-Ing. Stefan Hartmann
- Methode der finiten Elemente (TU Clausthal, Wintersemester 2015/2016, Wintersemester 2016/2017, Wintersemester 2017/2018, Wintersemester 2018/2019)

Prof. Dr. Dieter Hogrefe
- Mobile Communications (Universität Göttingen, 990092, Sommersemester 2016, Sommersemester 2017 und Sommersemester 2018)
- Security of Self-organizing Networks (Universität Göttingen, 990125, Sommersemester 2016, Sommersemester 2017 und Wintersemester 2017/2018)
- Security and Cooperation in Wireless Networks (Universität Göttingen, 501273, Wintersemester 2017/2018 und Wintersemester 2018/2019)
- Self-Organized Networks (Universität Göttingen, 990125, Sommersemester 2018 und Wintersemester 2018/2019)

Prof. Dr. Olaf Ippisch
- Wissenschaftliches Höchstleistungsrechnen (Paralleles Rechnen) (TU Clausthal, W 0628, Wintersemester 2017/2018 und Wintersemester 2018/2019)
- Wissenschaftliches Rechnen mit C++ (TU Clausthal, S 0630, Sommersemester 2018)

Prof. Dr. Michael Kolonko
- Stochastische Modellbildung und Simulation (TU Clausthal, W 0140, Wintersemester 2015/2016 und Wintersemester 2016/2017)
- Mathematische Methoden des OR: Optimierung und Simulation (TU Clausthal, S 0515, Sommersemester 2016)
- Stochastische Simulation und Statistik

(TU Clausthal, S 0260, Sommersemester 2016 und Sommersemester 2017)

Prof. Dr.-Ing. Dieter Meiners
- Simulation und Modellierung in der Kunststofftechnik (TU Clausthal, S 7920, Sommersemester 2015, Sommersemester 2016, Sommersemester 2017 und Sommersemester 2018)

Prof. Dr.-Ing. Dietmar P.F. Möller
- Computational Modeling and Simulation (TU Clausthal, W 0506, Wintersemester 2015/2016 und Wintersemester 2016/2017)
- Computational Modeling and Simulation I: Discrete Systems, Transatlantic Course (TU Clausthal, S 0503, Sommersemester 2015, Sommersemester 2016 und Sommersemester 2017)
- Grundlagen der Simulationstechnik 1 (TU Clausthal, S 0514, Sommersemester 2016)
- Computational Modeling and Simulation II: Continuous Systems, Transatlantic Course (TU Clausthal, W 0507, Wintersemester 2015/2016, Wintersemester 2016/2017 und Wintersemester 2017/2018)
- Introduction into Stochastic Systems Modeling and Simulation (TU Clausthal, W 0509, Wintersemester 2015/2016)
- Cyber-Physical Systems and Cybersecurity and its Application in Industry 4.0 (TU Clausthal, W 0505, Wintersemester 2018/2019)
- Simulationsmethoden und -technologien im Flughafenmanagement und in der Luftfahrt (TU Clausthal, W 0513, Wintersemester 2018/2019)

Prof. Dr. Jörg Müller
- Multiagentensysteme (TU Clausthal, S 1254, Sommersemester 2018)

Prof. Dr. Anita Schöbel
- Seminar on algorithms for (robust) integer programming (Universität Göttingen, 501926, Wintersemester 2016/2017)

Prof. Dr. Stephan Waack
- Algorithmisches Lernen und Probabilistische Datenmodelle (Universität Göttingen, 990002, Wintersemester 2016/2017, Wintersemester 2017/2018 und Wintersemester 2018/2019)
- Conditional Random Fields als Datenstruktur in Bioinformatik und Softwaretechnik (Universität Göttingen, 502106, Sommersemester 2016, Sommersemester 2017 und Sommersemester 2018)
- Grundlagen der Informationstheorie für Informatiker (Universität Göttingen, 990182, Sommersemester 2016, Sommersemester 2017 und Sommersemester 2018)

Prof. Dr. Ramin Yahyapour
- Parallel Computing (Universität Göttingen, 50096, Wintersemester 2016/2017, Wintersemester 2017/2018 und Wintersemester 2018/2019)
- Distributed Storage and Information Management (Universität Göttingen, 50049, Sommersemester 2016)
- Practical Course on Parallel Computing (Universität Göttingen, 990179, Sommersemester 2016)
- Service Computing (Universität Göttingen, 500948, Sommersemester 2017 und Sommersemester 2018)

International Simulation Science Semester

Jeweils im Wintersemester bietet die TU Clausthal das International Simulation Science Semester (IS3) an. Die Veranstaltung wird vom Simulationswissenschaftlichen Zentrum Clausthal-Göttingen (SWZ) und dem Internationalen Zentrum Clausthal (IZC, www.izc.tu-clausthal.de) organisiert. Das englischsprachige Vorlesungsangebot bietet einen sehr guten Einblick in verschiedene Aspekte der Simulationswissenschaften.

Every winter term TU Clausthal (TUC) offers an International Simulation Science Semester (IS3). It is organized jointly by the Simulation Science Center Clausthal / Göttingen (SWZ) and the International Center Clausthal (IZC, www.izc.tu-clausthal.de). This course offer is a great opportunity for students to gain experience and orientation in international study programs required in a globalized world.

Content

Module 1: Introduction into Computational Modeling and Simulation

3 ECTS Credits
Lecturer: Prof. Dr. Dietmar P. F. Moeller (TUC/UHH)

The power of simulation lies in the three R´s of science and engineering, namely: reductionism, repeatability, and refutation. That is why this course is organized as follows: The introductory part focuses on modeling and the essential mathematical methods executed in continuous-time, discrete-time and distributed systems following the fundamental laws in science and engineering. The subsequent training part focuses on the utilization of an industry standard simulation framework and the validation and verification of results of computer-based simulation. To this end, students develop, evaluate and present the simulation results in a plenary workshop at the end of the course.

Module 2: Introduction into Stochastic Systems Modeling and Simulation

3 ECTS Credits (Block Course)
Lecturer: Prof. Dr. Thomas Hanschke (TUC), Dr. Horst Zisgen (IBM)

Stochastic systems modeling and simulation explore stochastic systems which could be defi ned as anything random that changes in time. Stochastic systems are at the core of a number of disciplines in science and engineering, for example communication systems, machine learning, and more. The course will introduce students into the basics of the probability theory: probability spaces, conditional probability time and limits in probability, common probability distributions (binominal, exponential, Poisson, Gaussian), queuing systems models, Markov chains, random processes.

Module 3: Introduction into Computational Modeling and Simulation in Mechanical Engineering

3 ECTS Credits
Lecturer: Prof. Dr. Gunther Brenner (TUC)

In the 21st century decision making increasingly relies on computer simulations. Prominent examples are weather forecasts or predictions of fi nancial or environmental scenarios. Computational methods have become indispensable tools in the context of designing and optimization of processes and products. Therefore, students of engineering sciences have to be made familiar with the ideas of simulation and the use of modern software tools. The goal of the present course is to familiarize students with the basic concepts of computational methods and to provide com-

petences that allow them to utilize these tools in a targeted manner and to assess results critically. Further in-depth knowledge of physical and mathematical details may be imparted subsequently in further lectures.

Module 4: Agent-based Modeling and Simulation
1 ECTS Credit (Block course 2 days)
Lecturer: Prof. Dr. Jörg Müller (TUC)

We are witnesses to growing complexity of today's systems for managing/controlling critical networked infrastructure systems for traffic, logistics, energy, or industry automation. These systems are systems of systems (SoS), i.e., large-scale concurrent and distributed systems that are themselves comprised of complex autonomous systems and that are characterized by operational and managerial independence, geographic distribution, emergent behavior, and evolutionary development. Decentralization and the often stochastic nature of the environment are further properties of such systems. Modeling and simulation of systems of systems require suitable abstractions to express autonomy of systems and often loosely-coupled interaction between these systems. In this lecture, we shall introduce concepts of the multiagent-based modeling and simulation paradigm, which provides these types of abstractions. Starting from the notion of autonomous intelligent agents and multiagent systems, we shall review models for interaction, coordination, and cooperation. Benefi ts but also challenges of agentbased modeling and simulation will be discussed by means of selected application scenarios. In a practical part, attendants of the lecture will have the opportunity to model small examples of multiagent systems using the AgentSpeak modeling language.

Module 5: Transportation Analysis, Modeling and Simulation
3 ECTS Credits
Lecturer: Prof. Dr. Dietmar P. F. Moeller (TUC/UHH)

The transportation systems sector – comprising modes of transportation, each with different operational structures and approaches to security – is a vast, open, interdependent network, moving millions of tons of freight and millions of passengers. Every day, the transportation systems network connects cities, manufacturers, and retailers by moving large volumes of freight and passengers through a complex network of roads and highways, railways and train stations, sea ports and dry ports, and airports and hubs. Thus, the transportation systems sector is the most important component of any modern economy's infrastructure in the globalized world. It is also a core component of daily human life with all of its essential interdependencies, such as demands for travel within a given area and freight transportation in metropolitan areas, which require a comprehensive framework in which to integrate all aspects of the target system. Therefore, transportation systems models enable transportation managers to run their daily businesses safely and more effectively through a smarter use of transportation networks. But the transportation systems sector in today's open, interdependent network encompassing urban and metropolitan areas requires optimization of all operating conditions. This can be successfully achieved if the interactions between transportation modes, the economy, land use, and the impact on natural resources are included in transportation systems planning strategies. But the proposed future of multimodal transportation systems cannot be measured through planning alone. Mathematical models of transportation systems and mobility management, incorporating both realworld and hypothetical scenarios, should be embedded in transportation systems analysis, including the evaluation and/or design the of traffic flows, determining the most reliable mode of operation of physical (e.g., a new road) and organizational (e.g., a new destination) objects, and the interaction between the objects and their impact on the environment. These mathematical models are fundamental to the analysis, planning, and evaluation of small-, medium-, and large-scale multimodal transportation systems. The success of model-based scenario analysis can be evaluated by the resulting forecast or prediction of the transportation system response. An ideal design or operational methodology for a transportation system can be achieved using model-based analysis in conjunction with backcasting or backtracking. Thus, modeling and simulation play a central role in planning, developing, and evaluating multimodal transportation systems, improving transportation efficiency and

keeping pace with the rising demands for optimizing multimodal transportation systems.

Module 6: Student Team Project in Computational Modeling and Simulation
6 ECTS Credits

Student team project, supervisor depends on chosen topic Within the student team project, groups of students which work on a specifi c topic offered by the lecturers of the International Simulation Science Semester are formed. The student team project groups will analyze, present, discuss, and publish (conference or journal) one specifi c topic, such as:

- Dry port development in the maritime domain
- Turnaround optimization at airports
- Mobile autonomous robots in unstructured environments
- Urban mobility concepts for metropolitan areas

Module 7: Intercultural competence seminar
3 ECTS Credits
Various Lecturers

Interacting with people from different cultural backgrounds has become an important part of our daily lives. To benefit from cultural diversity, this course is designed to develop your intercultural competence in two areas: understanding culture and its impact on behavior in an international working environment, and developing communication strategies and skills to work successfully in international teams.

Module 8: Language Training – German A 1.1 Beginners
6 ECTS Credits
Various Lecturers

German language course for beginners or learners with little knowledge of German. This course focuses on developing listening and reading comprehension, active use of German, as well as on acquiring learning techniques and communicative competence needed to study successfully at a German university. Please note that German courses on all levels are available and can be exchanged for this course.

Module 9: Language Training – European and Non-European languages
2–6 ECTS Credits

Apart from German language courses, the course range comprises: Arabic, Brazilian Portuguese, Chinese, English, French, Greek, Italian, Norwegian, Polish, Russian and Spanish. This includes courses for beginners as well as for advanced learners.

Clausthal-Göttingen International Workshop on Simulation Science 2017

The first "Clausthal-Göttingen International Workshop on Simulation Science" brought together researchers and practitioners from both industry and academia to report on the latest advances in simulation science. The workshop took place in the "Convention Centre by the Observatory" in Göttingen, which is an outbuilding of the Historical Observatory – the former residence and place of work of Göttingen's famous academic Carl Friedrich Gauss. The welcome address of the workshop was given by Prof. Dr. Norbert Lossau (Vice-President of the University of Göttingen) and Prof. Dr. Thomas Hanschke (President of the TU Clausthal in 2017). In nearly 40 presentations, the workshop considered the broad area of modeling & simulation with a focus on

- simulation and optimization in networks,
- simulation of materials, and
- distributed simulations.

The state of the art in simulation science and an outlook to potential future developments was discussed in three plenary talks given by

- Achim Streit (Karlsruhe Institute of Technology),
- Samuel Forest (MINES Paristech), and
- Kai Nagel (TU Berlin).

The social program consisted of a guided city tour through Göttingen's historical old town and a workshop dinner that was held in the Bullerjahn – the "Ratskeller" of Göttingen.
The workshop was co-sponsored by the Gesellschaft für Operations Research e.V (GOR) and the Arbeitsgemeinschaft Simulation (ASIM).

Organization

General Co-Chairs

Marcus Baum, University of Göttingen
Gunther Brenner, TU Clausthal
Jens Grabowski, University of Göttingen
Thomas Hanschke, TU Clausthal
Stefan Hartmann, TU Clausthal
Anita Schöbel, University of Göttingen

Program Committee

Valentina Cacchiani, University of Bologna
Stefan Diebels, Saarland University
Jürgen Dix, TU Clausthal
Umut Durak, DLR Braunschweig
Felix Fritzen, University of Stuttgart
Igor Gilitschenski, ETH Zürich
Marc Goerigk, Lancester University
Marco Huber, USU AG, Karlsruhe
Tobias Kretz, PTV Group
Allan Larsen, Technical University of Denmark
Ming Li, Nanjing University
Laura De Lorenzis, TU Braunschweig
Kai Nagel, TU Berlin
Helmut Neukirchen, University of Iceland
Bernhard Neumair, Karlsruhe Institute of Technology
Natalia Rezanova, Danske Statsbaner (Danish State Railways)
Ulrich Rieder, Ulm University
Rüdiger Schwarze, TU Freiberg
Marie Schmidt, Erasmus University Rotterdam
Thomas Spengler, TU Braunschweig
Ulrich Tallarek, Philipps-Universität Marburg
Pieter Vansteenwegen, KU Leuven
Sigrid Wenzel, University of Kassel
Peter Wriggers, University of Hanover
Ramin Yahyapour, GWDG
Martin Zsifkovits, UniBw München

Finance Chair

Alexander Herzog, TU Clausthal

Local Arrangements Co-Chairs

Annette Kadziora, University of Göttingen
Fabian Sigges, University of Göttingen

Plenary Talks

Samuel Forest, Mines ParisTech CNRS, France

Crystal plasticity of polycrystalline aggregates under cyclic loading: 3D experiments and computations, size effects and fatigue cracking

BIO: Samuel Forest, 48 year old, is CNRS Research Director at Centre des Materiaux Mines ParisTech and continuum mechanics professor at Mines ParisTech. He is working on mechanics of materials focusing on crystal plasticity modelling and mechanics of generalized continua. He has beforesten the PhD advisor of 35 PhD students on these scientific topics, each of them corresponding to a contract with industrial partners (SAFRAN, RENAULT, EDF, Arcelor-Mittal, Michelin, CEA, EDF, etc.) or with the state and EU. He got the Bronze and Siver medals of CNRS INSIS and the Plumey prize of the Academie des Sciences. He published more than 120 papers in peer-reviewed international journals. He is associate editor of 5 international journals including Int. J. Solids Structures and Phil. Mag. He is leading the CNRS Federation of Mechanics labs in the Paris Region, promoting cooperation between 14 mechanics labs in the Paris region.

ABSTRACT: The mustiscale approach to the plasticity and fracture of crystalline metals and alloys is based nowadays on large scale simulations of representative volume elements of polycrystalline aggregates. The deformation modes inside the individual grains are described by continuum crystal plasticity models involving dislocation densities and suitable interface conditions at grain boundaries. Recent 3D experiments performed under synchrotron radiation at ESRF reveal the plastic events in the grains like slip banding and development of crystal lattice curvature. These results are compared to finite element simulations involving millions of degrees of freedom for a detailed description of intragranular mechanical fields. The cyclic loading of such samples leads to the initiation and propagation of fatigue cracks going through the grains and stopping at or overcoming grain boundaries. This damage process can also be observed by 3D images and simulated by corresponding finite element simulations.

The constitutive laws for crystal plasticity and damage incorporate gradient plasticity and gradient damage contributions in order to account for size effects in the material behaviour. These effects include the size-dependent piling-up of dislocations during cyclic loading and the description of finite width localization bands and cracks. The provided examples deal with cubic aluminum, titanium and nickel-based alloys.

Achim Streit, Karlsruhe Institute of Technology (KIT), Germany

Enabling Data-Intensive Science in the Helmholtz Association

BIO: Prof. Dr. Achim Streit is the director of the Steinbuch Centre for Computing (SCC) and professor for computer science at Karlsruhe Institute of Technology (KIT) since mid-2010. He is responsible for the HPC and Big Data activities at SCC – both systems as well as R&D activities. He is topic speaker "Data-Intensive Science and Federated Computing" in the Helmholtz Programme "Supercomputing & Big Data" (of which he is also the deputy speaker). He is the coordinator of the Large Scale Data Management and Analysis (LSDMA) initiative in Helmholtz, which is about fostering data-intensive science in Germany through Data Life Cycle Labs and generic methods research. He is the coordinator of the Helmholtz Data Federation (HDF), a 5-year multi-million Euro investment project to establish an open federated research data infrastructure in Germany. He and his institute are involved in major European e-Infrastructure projects such as EUDAT2020, EOSCpilot, INDIGO-Datacloud,

AARC as well as the FET flagship Human Brain project. Prior to KIT, he was at the Jülich Supercomputing Centre (JSC) of Forschungszentrum Jülich, Germany, where he was responsible for the Grid activities and active in several EU e-infrastructure projects such as DEISA, PRACE, OMII-Europe, EGI-InSPIRE and helped to initiate the EMI and EUDAT projects.

ABSTRACT: The Helmholtz Association of German research centres pursues long-term research with large-scale scientific projects and research facilities ranging from life sciences, climate and environment up to matter and the universe. One of its long-term programs is dedicated to research on "Supercomputing & Big Data" (SBD) which is of major importance and provides enabling technologies to all Helmholtz research fields.
In data-intensive science collaboration is a key factor. On the national level we lead the multidisciplinary initiative LSDMA across the Helmholtz research fields to foster the exchange of knowledge, expertise and technologies. Data experts from the program collaborate closely with domain researchers from other Helmholtz programs and German universities within so-called "Data Life Cycle Labs" (DLCL). These aim at optimizing data life cycles and developing community-specific tools and services in joint R&D with the scientific communities. In addition, new generic data methods and technologies for data life cycle management are designed and developed, large scale data facilities and federated data infrastructures are enhanced and operated, and national/international collaborations such as HDF, EUDAT, INDIGO-DataCloud, EU-T0 and WLCG are advanced.

Kai Nagel, TU Berlin, Germany

Addressing negative effects of transport systems with large scale behavioral transportation simulations

BIO: Kai Nagel is full professor for "Transport systems planning and transport telematics" at the Berlin Institute of Technology (TU Berlin), Germany. He was trained in physics and climate research, and holds a Ph.D. in informatics from University of Cologne, Germany. He worked at Los Alamos National Laboratory, USA, from 1995 to 1999, at ETH Zürich from 1999 to 2004, and holds his current post since 2004. His research interests include large-scale transportation simulations, modeling and simulation of socio-economic systems, and large-scale computing. He leads a group of eight Ph.D. students, six of them funded from competetive sources including the German National Science Foundation and the EU. He has authored more than 100 publications. He is area editor of the journal "Networks and Spatial Economics", member of TRB committee ADB10 "travel behavior and values", and a frequent reviewer for a large number of scientific journals, scientific conferences, research proposals, and scholarships. Also see www.vsp.tu-berlin.de/menue/ueber_uns/team/prof_dr_kai_nagel/

ABSTRACT: The presentation will have three parts. In the first part, I will explain how our own MATSim software (= Multi Agent Transport Simulation, see www.matsim.org) for transport systems simulation works. It is, in short, a system that tracks its entities, in particular persons and vehicles, individuall, and lets them learn from one synthetic day to the next. In the second part, I will show use cases of what one can do with such a system. The use cases will center around externalities, i.e. congestion, noise, and particulate emissions, and what can be done to reduce them. The third part of my presentation will deal with computational methods, i.e. methods and tools from computer science & engineering that we have put to good use vs. methods that have not worked so well.

List of Abstracts

Simulation and optimization in networks I

Solving Robust Optimization Problems by an Iterative Simulation-Based Approach
Julius Pätzold and Anita Schöbel

Heuristics and Simulation for Water Tank Optimization
Corinna Hallmann, Sascha Burmeister, Michaela Beckschaefer, and Leena Suhl

Simulation and Optimization with a Bayesian Selection of Alternatives
Björn Görder and Michael Kolonko

LP Decoding: When Channel Coding meets Optimization
Florian Gensheimer, Stefan Ruzika, Norbert Wehn, and Kira Kraft

Simulation and optimization in networks II

Modelling Vehicle Sharing with Driverless Cars
Markus Friedrich, Maximilian Hartl and Christoph Magg

Detecting Structures in Network Models of Integrated Traffic Planning
Marco Lübbecke, Christian Puchert, Philine Schiewe, and Anita Schöbel

A Complementary Optimization-Simulation Framework for the Evacuation of Large Urban Areas
Stefan Ruzika and David Willems

Agent-based Simulation of Passengers in Rail Networks
Sebastian Albert, Philipp Kraus, Jörg Müller, and Anita Schöbel

Simulation and optimization in networks III

Combining Simulation and Optimization for Extended Double Row Facility Layout Problems in Factory Planning
Uwe Bracht, Mirko Dahlbeck, Anja Fischer, and Thomas Krüger

Solving multiobjective optimization problems with parameter uncertainty: an interactive approach
Yue Zhou-Kangas, Anita Schöbel, Kaisa Miettinen, and Karthik Sindhya

Decomposition of multi class open queueing networks with batch service
Wiebke Klünder

Confidence Intervals for Coagulation-Advection Simulations
Robert I. A. Patterson

Simulation of materials I

Numerical investigation of mass transfer in bulk, random packings of core-shell particles
Dzmitry Hlushkou, Anton Daneyko, Vasili Baranau, Ulrich Tallarek

Multiscale simulation of anisotropic surface stress and bulk stresses
in transition metal oxide nanoparticles
Peter Stein, Ashkan Moradabadi, Manuel Diehm, Bai-Xiang Xu, and Karsten Albe

Validation of a synthetic 3D mesoscale model of hot mix asphalt
Johannes Neumann, Jaan-Willem Simon, and Stefanie Reese

Mechanical Simulation of 3D-Microstructures in Dual-Phase Steel
Frederik Scherff, Sebastian Scholl, and Stefan Diebels

Simulation of materials II

Sensitivity Analysis of VOF Simulations regarding Free Falling Metal Melt Jets
Sebastian Neumann, Rüdiger Schwarze

Quantification of relationships between structural characteristics and
mechanical properties of agglomerates
M. Weber, A. Spettl, M. Dosta, S. Heinrich and V. Schmidt

Modelling and simulation of polycrystalline microstructures by tessellations
Ondřej Šedivý, Daniel Westhoff, Carl E. Krill III, and Volker Schmidt

Time-adaptive finite element computations in Solid Mechanics of inelastic materials
Stefan Hartmann and Matthias Grafenhorst

Simulation of materials III

Numerical Investigation of Inclusions Filtration in an Induction Crucible Furnace
Amjad Asad, Rüdiger Schwarze

Quantification of the microstructure influence on effective conductivity by virtual materials testing
Matthias Neumann, Lorenz Holzer, and Volker Schmidt

Parallel hybrid Molecular Statics / Monte Carlo for Segregation of Interstitials in Solids
Godehard Sutmann, Hariprasath Ganesan, and Christoph Begau

3D microstructure modelling und simulation of materials in lithium-ion battery cells
J. Feinauer, D. Westhoff and V. Schmidt

Distributed simulations I

Transparent Model-Driven Provisioning of Computing Resources
for Numerically Intensive Simulations
*Fabian Glaser, Alexander Bufe, Christian Köhler, Gunther Brenner,
Jens Grabowski and Philipp Wieder*

Performance of Big Data versus High-Performance Computing: Some Observations
Helmut Neukirchen

Assessing Simulated Software Graphs using Conditional Random Fields
*Marlon Welter, Daniel Honsel Verena Herbold, Andre Staedtler,
Jens Grabowski and Stephan Waack*

Parallel Radio Channel Emulation and Protocol Simulation
for Wireless Sensor Networks with Hardware-in-the-Loop
Sebastian Boehm and Michael Kirsche

Distributed simulations II

Simulation-based Technician Field Service Management
Michael Voessing, Clemens Wolff and Jannis Walk

Simulation-based Multi-Object Tracking using the Ensemble Kalman Filter
Fabian Sigges and Marcus Baum

Using Monte Carlo Simulation for Reliability Assessment of Cloud Applications
Xiaowei Wang, Fabian Glaser, Steffen Herbold and Jens Grabowski

High-Performance Computing and Simulation in Clouds
Pavle Ivanovic and Harald Richter

Distributed simulations III

The Virtual Microscope – Simulation and Visualization of Particle Mixtures on Parallel Hardware
Feng Gu, Zhixing Yang, Thorsten Grosch, and Michael Kolonko

Two-layered Cyber-Physical System Simulation
Tobias Koch, Dietmar P. F. Möller, and Andreas Deutschmann

A simulation-based genetic algorithm approach for competitive analysis of online scheduling problems
Martin Dahmen

Simulating Software Refactorings based on Graph Transformations
Daniel Honsel, Niklas Fiekas, Verena Herbold, Marlon Welter, Tobias Ahlbrecht, Stephan Waack, Jürgen Dix, and Jens Grabowski

Poster Session

Tailoring CMMI Engineering Process Areas for Simulation Systems Engineering
Somaye Mahmoodi, Umut Durak, Torsten Gerlach, Sven Hartmann and Andrea D'Ambrogio

Numerical Simulation of Gas-Well Casing Shoe
Jithin Mohan, Stefan Hartmann, Leonhard Ganzer and Birger Hagemann

Learning State Mappings in Mulit-Level-Simulation
Stefan H. A. Wittek





Outlook: Clausthal-Göttingen International Workshop on Simulation Science 2019

The next Clausthal-Göttingen International Workshop on Simulation Science will start on

May 8th 2019 at Clausthal-Zellerfeld.

The conference location will be Aula Academica of TU Clausthal. Plenary speakers are:
– Benoît Appolaire, University of Lorraine, Nancy (France)
– Thomas Drescher, Volkswagen AG, Wolfsburg (Germany)
– Peter Vortisch, Karlsruhe Institute of Technology (Germany)

Due to an increased number of submissions the conference will be extended to three days. In addition, we will have a panel discussion where we discuss the requirements and challenges arising from simulation and modeling in the era of digitalization. Registration is possible up to conference start via the homepage:

www.simscience2019.tu-clausthal.de

Weitere Erfolge // More Achievements

Simulationswissenschaftliches Zentrum Clausthal-Göttingen: Erste internationale Konferenz ausgerichtet

International Workshop on Simulation Science 2017, Foto: Herzog

08.05.2017
Göttingen. Das Simulationswissenschaftliche Zentrum Clausthal-Göttingen (SWZ), eine gemeinsame interdisziplinäre Einrichtung der Technischen Universität (TU) Clausthal und der Universität Göttingen, entwickelt sich zu einem Erfolgsmodell: Die erstmals ausgerichtete Konferenz „International Workshop on Simulation Science“ stieß auf großes Interesse. Und der externe Beirat des SWZ stellte diesem auf seiner jüngsten Sitzung ein sehr gutes Zeugnis aus.

Nahezu 70 Wissenschaftlerinnen und Wissenschaftler aus dem In- und Ausland hatten sich auf der zweitägigen Konferenz über neueste Entwicklungen auf dem Gebiet der Simulationswissenschaften ausgetauscht und vernetzt. „Simulation birgt ein hohes Potenzial für die zukünftige wissenschaftliche und wirtschaftliche Entwicklung, für die wir in Göttingen und Clausthal durch unser Zentrum hervorragend aufgestellt sind“, sagte Professorin Anita Schöbel. Die Mathematikerin an der Universität Göttingen und Vorstandsvor-

sitzende des SWZ freute sich besonders über die hohe Beteiligung von jungen Wissenschaftlern. Veranstaltungsort war das Tagungszentrum an der historischen Sternwarte in Göttingen, einst Wohn- und Arbeitsstätte des großen Gelehrten Carl Friedrich Gauß.

Thematisch ging es um drei Bereiche hoher wissenschaftlicher Aktualität: Simulation und Optimierung von Netzen, Simulation von Materialien und verteilte Simulation. Plenarredner waren Professor Achim Streit, der am Karlsruher Institut für Technologie das Steinbuch Centre for Computing leitet, Professor Samuel Forest von der französischen Elitehochschule Mines Paristech sowie Professor Kai Nagel vom Institut für Land- und Seeverkehr der TU Berlin. Insgesamt standen an beiden Tagen annähernd 40 Fachvorträge auf dem Programm. Die Organisation lag federführend in den Händen von Marcus Baum, Professor am Institut für Informatik in Göttingen.

„Das Feedback der Teilnehmenden fiel rundum positiv aus. Aufgrund der großen Resonanz soll in 2019 der ‚2nd Clausthal-Göttingen International Workshop on Simulation Science' stattfinden - dann in Clausthal", sagte Professor Gunther Brenner. Der Strömungsmechaniker der TU Clausthal ist auf der SWZ-Versammlung am 27. April als Nachfolger von Professorin Anita Schöbel zum neuen Vorstandsvorsitzenden gewählt worden.

Die SWZ-Verantwortlichen nutzten den Rahmen der wissenschaftlichen Konferenz, um das neue Jahrbuch des Forschungszentrums zu präsentieren. Die 230-seitige Broschüre, in deutscher und englischer Sprache, ist im Internet verfügbar unter: www.simzentrum.de/de/ueber-uns/informationsmaterialien. Informiert wird über die Forschungsaktivitäten am SWZ. Themen sind beispielsweise das Internet der Dinge, die Simulation von Gasbohrungen, die Simulation von Verspätungen im Zugverkehr oder die simulationsbasierte Qualitätssicherung von Softwaresystemen.

Best Paper Award für SWZ-Wissenschaftler

Herr Christos Zaroliagis (Mitte), Vorsitzender des Steering Committees des 2017er ATMOS-Workshops, überreicht die „Best Paper Award"-Urkunde an Herrn Schiewe (links) und Herr Pätzold (rechts).

22.08.2017
Auf dem diesjährigen ATMOS-Workshop (Workshop on Algorithmic Approaches for Transportation Modeling, Optimization and Systems) in Wien wurde das Paper „Look-Ahead Approaches for Integrated Planning in Public Transportation" von Julius Pätzold, Alexander Schiewe, Philine Schiewe und Anita Schöbel mit dem „Best Paper Award" ausgezeichnet. In der Arbeit, die im Rahmen des SWZ-Projekts „ASimOV: Agentenbasierte Simulation des Passagierverhaltens zur Optimierung des Verspätungsmanagements im Bahnverkehr" und „Simulation unsicherer Optimierungsprobleme mit Anwendung in der Fahrplangestaltung" entstanden ist, werden Konzepte zur Verknüpfung der bisher meist getrennt durchgeführten Schritte zur Linienplanung, Fahrplanerstellung und Fahrzeugzuordnung vorgestellt. Durch die Berücksichtigung des jeweils nächsten Planungsschritts bereits in dem jeweils vorausgehenden Schritt können die Gesamtkosten für den öffentlichen Personenverkehr signifikant verringert werden.

Dr. Nina Gunkelmann zur SWZ-Juniorprofessorin ernannt

Neue Juniorprofessorin am SWZ: Nina Gunkelmann. Foto: Lena Hoffmann

22.08.2017

Dr. Nina Gunkelmann ist an der Technischen Universität Clausthal mit Wirkung vom 1. September zur SWZ-Juniorprofessorin ernannt worden. Sie wird auf dem Gebiet „Computational Material Sciences" am Simulationswissenschaftlichen Zentrum Clausthal-Göttingen forschen und lehren. Nina Gunkelmann hat an der Technischen Universität ihrer Geburtsstadt Kaiserslautern sowie an der Universität im französischen Grenoble Physik und im Nebenfach Informatik studiert. Nach ihrem Abschluss 2012 arbeitete sie zunächst für zwei Jahre als wissenschaftliche Mitarbeiterin am Lehrstuhl für Multiscale Simulation der Universität Erlangen-Nürnberg. Ab 2014 trieb sie ihre Promotion an der Universität Kaiserslautern voran, die sie 2016 abschloss. Es folgte ein Jahr als „Post-Doc" am Lehrstuhl für Materials Simulation der Universität Erlangen-Nürnberg, bevor sie im Frühjahr 2017 an das Institut für Mechanik und Fluiddynamik der TU Bergakademie Freiberg wechselte. Von der sächsischen Universität kommend, tritt die 30-Jährige nun ihre Juniorprofessur an der TU Clausthal an.

In der Forschung beschäftigt sich die junge Wissenschaftlerin insbesondere mit der atomistischen Simulation und der Diskrete-Elemente-Simulation von heterogenen Materialien (bisher: polykristallines Eisen, Eisen-Legierungen, metallische Schäume und granulare Materialien) zur Bestimmung der Materialeigenschaften unter Belastung, wie zum Beispiel Riss- und Bruchverhalten, plastische Verformung, Kompaktifizierung und vieles mehr.

Know-how der Clausthaler Simulationsexperten im Saarland gefragt

18.09.2018

Dillingen. Die Expertise der Clausthaler Simulationswissenschaftler wird bei der AG der Dillinger Hüttenwerke, größter Hersteller für Grobblech in Europa und einer der größten Arbeitgeber im Saarland, hoch geschätzt. In einem dreijährigen, noch bis 2020 laufenden Projekt unterstützen die Forscher der Harzer Universität das Unternehmen dabei, die Produktionslogistik in ihrem Walzwerk zu optimieren.

Bei dem Traditionsunternehmen mit über 5000 Beschäftigten stehen Neuerungen hoch im Kurs: Wie lassen sich Innovationen gezielt vorantreiben? Wie spielen Innovationen und Digitalisierung zusammen? Um Antworten auf solche Zukunftsfragen zu erhalten, organisierte der Industriebetrieb im September zum zweiten Mal die Dillinger Innovationstage.

Inspirieren ließ sich der Konzern dabei nicht nur vom saarländischen Ministerpräsidenten Tobias Hans, sondern unter anderem auch von Professor Thomas Hanschke. Der Clausthaler Universitätspräsident und Simulationswissenschaftler hielt zusammen mit seiner ehemaligen Doktorandin, Dr. Heike Busch, vor rund 600 Gästen einen der drei Hauptvorträge. Anschließend brachte er sich, unter anderem mit Ministerpräsident Hans und dem Dillinger Technikvorstand Dr. Bernd Münnich, in eine Podiumsdiskussion zum Thema „Digitalisierte Primärindustrie: Ein Zukunftsmodell!" ein. Das eigene Unternehmen hat der Stahlhersteller in verschiedene Bereiche unterteilt, beispielsweise in Rohstoffe, Logistik, Materialforschung, Verfahrens- oder Produktionstechnik. All diese Themen sind auch an der TU Clausthal verankert. Das Drittmittelprojekt zwischen beiden

Podiumsdiskussion: der saarländische Ministerpräsident Tobias Hans (2.v.l.) im Austausch mit TU-Präsident Professor Thomas Hanschke. Foto: Dillinger

Seiten im Umfang von mehreren hunderttausend Euro zielt darauf ab, die zunehmend komplexer werdende Logistik im Walzwerk zu verbessern. Dafür modellieren die Forschenden um Doktorandin Wiebke Klünder die Abläufe in der Produktion in Form eines virtuellen Logistikzwillings und entwickeln einen Simulator, in dem Experimente mit diesem Modell durchgeführt werden können. „Die Dillinger Hütte ist ein mehr als 300 Jahre alter Industriebetrieb, aber heutzutage steckt in der Stahlbranche schon jede Menge High-Tech", unterstreicht Professor Hanschke, dass die Digitalisierung in der Primärindustrie längst in vollem Gange ist.

Start des Leitprojektes Heterogene Mensch-Maschine-Teams

Auftakt-Meeting der ambitionierten Clausthaler Graduiertenschule HerMes. Foto: Lena Hoffmann

20.09.2018
Digitalisierung bedeutet in vielen Fällen, dass physische Systeme in Produktion, Logistik und Verkehr mit IT-Prozessen gekoppelt werden. Diesen Themen widmet sich die TU Clausthal im Kontext des Forschungsschwerpunktes Offene Cyberphysische Systeme und Simulation (OCSS). Auch mehrere SWZ-geförderte Projekte hatten und haben die Untersuchung solcher Systeme zum Ziel. In den betrachteten vernetzten Systemen kommt insbesondere dem reibungslosen Zusammenspiel von Menschen und Maschinen – seien es Mitarbeiter und Fertigungsroboter oder Fußgänger und autonome Fahrzeuge – eine stetig größer werdende Rolle zu.

Durch den Startschuss für das Leitprojekt „Heterogene Mensch-Maschine-Teams" (HerMes) am 18.9.2018 wurde ein wichtiger Schritt in Richtung auf eine mittelfristige Etablierung von Spitzenforschung in diesem Bereich unternommen. Das HerMes-Projekt wird anteilig durch das SWZ und die TU Clausthal finanziert. Die in diesem Promotionsprogramm beschäftigten, aus verschiedenen Fachbereichen stammenden Doktoranden haben ihre gemeinsame Heimat im SWZ, so dass hier eine gelebte Interdisziplinarität entsteht und ganzheitliche Ansätze verfolgt werden können. Über das Anwendungsfeld „Intelligente Demontagefabrik" besteht außerdem eine enge Zusammenarbeit zum Forschungszentrum CUTEC, insbesondere mit dem Forschungsfeld Rohstoffsicherung und Ressourceneffizienz.

SWZ-Juniorprofessorin Nina Gunkelmann richtet Symposium auf dem Kongress „Materials Science and Engineering“ aus

Materials Science and Engineering Kongress (26. bis 28. September 2018 in Darmstadt).

26.9.2018
SWZ-Juniorprofessorin Dr. Nina Gunkelmann hat zusammen mit Kooperationspartnern aus Deutschland (Daniel Schneider, KIT), der Schweiz (Markus Stricker, EPFL Lausanne) und Frankreich (Benoit Appolaire, Yann Le Bouar, University of Lorraine) ein Symposium auf dem Materials Science and Engineering Kongress - vom 26. bis 28. September 2018 in Darmstadt organisiert. Die Konferenz ist mit über 1500 Teilnehmern eine der größten internationalen Konferenzen im Bereich Materialwissenschaften und Werkstofftechnik. Das Symposium mit dem Titel Plasticity Across the Scales - From Microstructure Changes to Bulk Mechanical Behavior setzte einen Fokus auf Multiskalensimulationen der plastischen Verformung, von der atomistischen bis zur Makroskala. Das makroskopische mechanische Verhalten von Metallen wird hauptsächlich durch die Erzeugung und Bewegung von Versetzungen bestimmt. Eine atomistische Beschreibung der Versetzungsdynamik ist sehr präzise, aber in Längen- und Zeitskalen begrenzt, weshalb mesoskopische Ansätze verwendet werden. Diese benötigen jedoch Informationen aus der Atomistik, weshalb nur ein Zusammenspiel aller Methoden, wie sie im Symposium gefordert war, erfolgreich ist.

Als Keynote-Sprecher für das Symposium konnten Größen des Fachs wie Alexander Stukowski und Alphonse Finel gewonnen werden. Mit fast 20 Vorträgen und 3 Sessions wurde eine große Teilnehmerzahl angezogen. Aus der Gruppe Computational Material Science/Engineering wurde ein Vortrag zum Thema Atomistic and mesoscale simulations of nanoindentation and nanoscratching of metals – A statistical approach to characterize discrete dislocation microstructures von Nina Gunkelmann sowie ein Poster von Hoang-Thien Luu mit dem Titel Low carbon iron under high pressure: Understanding the role of plasticity during phase transition beigesteuert.

Wissenschaftsnacht: Optische Highlights und Themen wie Virtual Reality und Simulation ziehen die Gäste an

Schön anzuschauen: das illuminierte Hauptgebäude. Für die Lichttechnik zuständig war C-Laze Media & Event. Foto: Christian Kreutzmann

16.11.2018
Clausthal-Zellerfeld. Die „Lange Nacht der Wissenschaften“ an der Technischen Universität Clausthal war ein echter Hingucker und eine Fundgrube für interessantes Wissen. Mehr als tausend Besucher erfreuten sich am 15. November ebenso an funkensprühenden Vorführungen in der Metallurgie, Lasershows und illuminierten Gebäuden wie an Science Slams, Institutsbesichtigungen und Workshops.

Zum dritten Mal hatte der Verein „Science on the Rocks“ an der TU Clausthal eine Wissenschaftsnacht ausgerichtet. Anliegen war es, das Thema Wissenschaft der Öffentlichkeit unterhaltsam zu präsentieren. Institute, Forschungszentren, Kooperationspartner der Uni und Studierende brachten sich in die Wissenschaftsnacht ein und stellten mehr als 60 Veranstaltungen auf die Beine. Publikumsmagnete waren ein Science Slam, Experimentalvorlesungen und Lasershows. Auch Workshops avancierten zum Anlaufpunkt. So reichten beim Workshop „Die andere Schlange ist immer schneller! – Wie man Warteschlangen effizient anlegt“ die 32 Sitzplätze nicht aus. Mehr als ein Dutzend Gäste verfolgte die Ausführungen zu dem Thema von Dr. Alexander Herzog vom Simulationswissenschaftlichen Zentrum Clausthal-Göttingen (SWZ) im Stehen. Andrang herrschte auch bei der Führung „Fabrikplanung in virtuellen Welten“. „Mich interessieren insbesondere Themen wie Virtual Reality, Digitalisierung und Simulation“, sagte einer der Besucher und spiegelte damit den Zeitgeist wider.

Das große Finale der „Langen Nacht der Wissenschaften“ fand am Hauptgebäude der Technischen Universität statt. Hunderte Teilnehmende wohnten einem Clausthaler Brauch bei, dem Mitternachtsschrei mit gesungenem Steigerlied.

Frau Prof. Dr. Anita Schöbel übernimmt Leitung des Fraunhofer-ITMW

8.12.2018
Das Fraunhofer-Institut für Techno- und Wirtschaftsmathematik (ITWM) in Kaiserslautern bekommt eine neue Institutsleitung: Anita Schöbel übernimmt zum 1. April 2019 die Amtsgeschäfte von Dieter Prätzel-Wolters, der in den Ruhestand geht. Neben der Leitung des ITWM wird Prof. Schöbel am Fachbereich Mathematik der Technischen Universität (TU) Kaiserslautern als Professorin wirken.

Anita Schöbel, die derzeit noch in Göttingen an der Universität lehrt, kehrt damit an ihre ehemalige Wirkungsstätte zurück: Sie hat in Kaiserslautern Mathematik studiert, promoviert und sich habilitiert. Zudem war sie in den Jahren 1998 und 1999 am Fraunhofer-ITWM als wissenschaftliche Mitarbeiterin tätig, danach wechselte sie in den Fachbereich Mathematik der Universität.

Seit Juli 2004 war sie Professorin an der Georg-August-Universität Göttingen, hatte den Lehrstuhl für Optimierung am Institut für Numerische und Angewandte Mathematik inne und war Gründungsmitglied des Simulationswissenschaftlichen Zentrums Clausthal-Göttingen, in dem sie auch Mitglied des Vorstands war.

„Ich bin überzeugt davon, dass wir mit Anita Schöbel eine exzellente Institutsleiterin gewonnen haben, die das ITWM auf der Erfolgsspur halten wird“, sagt Prätzel-Wolters, der das Institut seit der Übernahme in der Fraunhofer-Gesellschaft 2001 führt. Prof. Schöbel arbeitet unter anderem auf dem Gebiet der Diskreten Optimierung, insbesondere in der Planung des öffentlichen Verkehrs: Dazu zählen die Planungen von Linien, Fahrplänen und Tarifen sowie Anschlusssicherung.

DFG verlängert Forschungsgruppe „Integrierte Planung im öffentlichen Verkehr“ unter der Leitung der Universität Göttingen

11.12.2018

Für einen reibungslosen Ablauf in den Verkehrsbetrieben müssen diverse Pläne abgestimmt werden. Wissenschaftler sehen hier erheblichen Optimierungsbedarf. Die Deutsche Forschungsgemeinschaft (DFG) hat die Förderung für eine Forschergruppe unter Leitung von Prof. Dr. Antia Schöbel zum Thema verlängert. Die Forschungsgruppe (FOR 2083) „Integrierte Planung im öffentlichen Verkehr“ an der Universität Göttingen beschäftigt sich mit der Optimierung der Planungspraxis im öffentlichen Verkehr. Neben der Universität Göttingen sind die Universitäten Halle-Wittenberg und Stuttgart sowie das Karlsruher Institut für Technologie beteiligt.

Verschiedene Teilaspekte des Projektes wurden im Rahmen der vom Simulationswissenschaftlichen Zentrum Clausthal-Göttingen geförderten Projekte „Strukturuntersuchungen zur Entstehung und Fortpflanzung von Verspätungen in Verkehrsnetzen - Modellierung, Simulation und Optimierung eines stochastischen Netzwerks“ und „ASimOV: Agentenbasierte Simulation des Passagierverhaltens zur Optimierung des Verspätungsmanagements im Bahnverkehr“ untersucht. Die DFG fördert das Vorhaben in den kommenden drei Jahren mit insgesamt 1,5 Millionen Euro.

W3-Professur für SWZ-Juniorprofessor Marcus Baum

Der SWZ-Juniorprofessur Dr.-Ing. Marcus Baum vom Institut für Informatik der Universität Göttingen hat einen Ruf an die Universität Rostock auf die W2-Professur für Multi-Sensor-Systeme sowie einen weiteren Ruf an die Universität Passau auf die W3-Professur für Sensor-Based Systems abgelehnt. Der Vorstand des Simulationswissenschaftlichen Zentrums Clausthal-Göttingen freut sich sehr, dass Herr Baum als W3-Professur an der Universität Göttingen verbleibt und weiterhin im SWZ mitwirkt. Prof. Dr.-Ing. Marcus Baum leitet die Arbeitsgruppe Data Fusion am Institut für Informatik. Untersuchungsgebiete sind stochastische Methoden zur Zusammenführung von (Sensor-)Daten und Informationen aus verschiedenen Quellen, Methoden zur nichtlinearen Schätzung sowie zur Datenanalyse. Ein besonderer Schwerpunkt der Gruppe sind Tracking-Probleme, d.h. die sukzessive Lokalisierung eines oder mehrerer mobiler Objekte wie sie z.B. bei der Objektverfolgung in der Verkehrsüberwachung auftreten.

Mitglieder // Members

Vorstand des SWZ // Board of Directors

Prof. Dr.-Ing. Gunther Brenner
(Vorstandsvorsitzender)
Arbeitsgruppe Strömungsmechanik
Institut für Technische Mechanik
Technische Universität Clausthal

Prof. Dr. Jens Grabowski
Arbeitsgruppe Softwaretechnik für
Verteilte Systeme
Institut für Informatik
Georg-August-Universität Göttingen

Dipl.-Wirt.-Inf. Wiebke Klünder
Arbeitsgruppe Stochastische Modelle
in den Ingenieurwissenschaften
Institut für Angewandte Stochastik und
Operations Research
Technische Universität Clausthal

Fabian Korte, M.Sc.
Arbeitsgruppe Softwaretechnik für
Verteilte Systeme
Institut für Informatik
Georg-August-Universität Göttingen

Prof. Dr. Jörg Müller
Arbeitsgruppe Wirtschaftsinformatik
Institut für Informatik
Technische Universität Clausthal

Prof. Dr. Anita Schöbel
(Stellvertretende Vorstandsvorsitzende)
Arbeitsgruppe Optimierung
Institut für Numerische und
Angewandte Mathematik
Georg-August-Universität Göttingen

Beirat des SWZ // Advisors

Prof. Dr. Bernhard Neumair
Steinbuch Centre for Computing
Karlsruher Institut für Technologie

Prof. Dr. Ulrich Rieder
Institut für Optimierung und Operations Research
Universität Ulm

Prof. Dr. rer. nat. Dr. h. c. Kurt Rothermel
Institut für Parallele und Verteilte Systeme
Universität Stuttgart

Univ.-Prof. Dr.-Ing. Sigrid Wenzel
Arbeitsgruppe Produktionsorganisation
und Fabrikplanung
Institut für Produktionstechnik und Logistik
Universität Kassel

**Prof. Dr.-Ing. habil. Dr. h.c. mult.
Peter Wriggers**
Institut für Kontinuumsmechanik
Leibniz Universität Hannover

Mitglieder und Angehörige des SWZ // Members

Professoren

Jun.-Prof. Dr.-Ing. Marcus Baum
Arbeitsgruppe Datenfusion
Institut für Informatik
Georg-August-Universität Göttingen

Prof. Dr.-Ing. Uwe Bracht
Arbeitsgruppe Anlagenprojektierung
und Materialflusslogistik
Institut für Maschinelle Anlagentechnik
und Betriebsfestigkeit
Technische Universität Clausthal

Prof. Dr.-Ing. Gunther Brenner
Arbeitsgruppe Strömungsmechanik
Institut für Technische Mechanik
Technische Universität Clausthal

Prof. Dr. Jürgen Dix
Arbeitsgruppe Computational Intelligence
Institut für Informatik
Technische Universität Clausthal

Priv.-Doz. Dr. Umut Durak
Arbeitsgruppe Aeronautical Informatics
Institut für Informatik
Technische Universität Clausthal

Jun.-Prof. Dr. Anja Fischer
Arbeitsgruppe Optimierung
Institut für Numerische und
Angewandte Mathematik
Georg-August-Universität Göttingen

Prof. Dr. Xiaoming Fu
Arbeitsgruppe Computer Networks Group
Institut für Informatik
Georg-August-Universität Göttingen

Prof. Dr. Leonhard Ganzer
Arbeitsgruppe Lagerstättentechnik
Institut für Erdöl- und Erdgastechnik
Technische Universität Clausthal

Prof. Dr. Jens Grabowski
Arbeitsgruppe Softwaretechnik für
Verteilte Systeme
Institut für Informatik
Georg-August-Universität Göttingen

Prof. Dr. Thorsten Grosch
Arbeitsgruppe Graphische
Datenverarbeitung und Multimedia
Institut für Informatik
Technische Universität Clausthal

Jun.-Prof. Dr. Nina Gunkelmann
Arbeitsgruppe Computational Material Sciences
Institut für Technische Mechanik
Technische Universität Clausthal

Prof. Dr. Thomas Hanschke
Arbeitsgruppe Stochastische Modelle
in den Ingenieurwissenschaften
Institut für Angewandte Stochastik
und Operations Research
Technische Universität Clausthal

Prof. Dr.-Ing. Stefan Hartmann
Arbeitsgruppe Festkörpermechanik
Institut für Technische Mechanik
Technische Universität Clausthal

Prof. Dr. Dieter Hogrefe
Arbeitsgruppe Telematik
Institut für Informatik
Georg-August-Universität Göttingen

Prof. Dr. Olaf Ippisch
Arbeitsgruppe Wissenschaftliches Rechnen
Institut für Mathematik
Technische Universität Clausthal

Prof. Dr. Michael Kolonko
Arbeitsgruppe Stochastische Optimierung
Institut für Angewandte Stochastik
und Operations Research
Technische Universität Clausthal

Prof. Dr.-Ing. Dieter Meiners
Institut für Polymerwerkstoffe und Kunststofftechnik
Technische Universität Clausthal

Prof. Dr. Dietmar P.F. Möller
Arbeitsgruppe Stochastische Modelle
in den Ingenieurwissenschaften
Institut für Angewandte Stochastik
und Operations Research
Technische Universität Clausthal

Prof. Dr. Jörg Müller
Arbeitsgruppe Wirtschaftsinformatik
Institut für Informatik
Technische Universität Clausthal

Prof. Dr. Gerlind Plonka-Hoch
Arbeitsgruppe Mathematische Signal-
und Bildverarbeitung
Institut für Numerische und
Angewandte Mathematik
Georg-August-Universität Göttingen

Prof. Dr. Andreas Rausch
Software Systems Engineering
Institut für Informatik
Technische Universität Clausthal

Dr.-Ing. Andreas Reinhardt
Arbeitsgruppe Energieinformatik
Institut für Informatik
Technische Universität Clausthal

**Prof. Dr.-Ing. Dr. rer. nat. habil.
Harald Richter**
Arbeitsgruppe Technische Informatik
und Rechnersysteme
Institut für Informatik
Technische Universität Clausthal

Prof. Dr. Anita Schöbel
Arbeitsgruppe Optimierung
Institut für Numerische und
Angewandte Mathematik
Georg-August-Universität Göttingen

Prof. Dr. Stephan Waack
Arbeitsgruppe Theoretische
Informatik und Algorithmische Methoden
Institut für Informatik
Georg-August-Universität Göttingen

Prof. Dr. Stephan Westphal
Arbeitsgruppe Diskrete Optimierung
Institut für Angewandte Stochastik
und Operations Research
Technische Universität Clausthal

Prof. Dr. Ramin Yahyapour
Arbeitsgruppe Praktische Informatik
Institut für Informatik
Georg-August-Universität Göttingen

Prof. Dr. Horst Zisgen
Fachbereich Mathematik und
Naturwissenschaften
Hochschule Darmstadt

Wissenschaftliche Mitarbeiter

Tobias Ahlbrecht, B.Sc.
Arbeitsgruppe Computational Intelligence
Institut für Informatik
Technische Universität Clausthal

Sebastian Albert
Arbeitsgruppe Optimierung
Institut für Numerische und
Angewandte Mathematik
Georg-August-Universität Göttingen

Alexander Bufe, M.Sc.
Arbeitsgruppe Strömungsmechanik
Institut für Technische Mechanik
Technische Universität Clausthal

Mirko Dahlbeck, M.Sc.
Arbeitsgruppe Optimierung
Institut für Numerische und
Angewandte Mathematik
Georg-August-Universität Göttingen

Martin Dahmen, M.Sc.
Arbeitsgruppe Diskrete Optimierung
Institut für Angewandte Stochastik
und Operations Research
Technische Universität Clausthal

Niklas Fiekas, B.Sc.
Arbeitsgruppe Computational Intelligence
Institut für Informatik
Technische Universität Clausthal

Michael Göttsche, M.Sc.
Arbeitsgruppe Software Engineering
for Distributed Systems
Institut für Informatik
Georg-August-Universität Göttingen

Dr. Salke Hartung
Arbeitsgruppe Telematik
Institut für Informatik
Georg-August-Universität Göttingen

Dr. Alexander Herzog
Geschäftsführer des
Simulationswissenschaftlichen Zentrums
Arbeitsgruppe Stochastische Modelle
in den Ingenieurwissenschaften
Institut für Angewandte Stochastik
und Operations Research
Technische Universität Clausthal

Dipl.-Math. Verena Herbold
Arbeitsgruppe Softwaretechnik für
Verteilte Systeme
Institut für Informatik
Georg-August-Universität Göttingen

Dipl.-Inf. Daniel Honsel
Arbeitsgruppe Theoretische Informatik
und Algorithmische Methoden
Institut für Informatik
Georg-August-Universität Göttingen

Dr. Wiebke Klünder
Arbeitsgruppe Stochastische Modelle
in den Ingenieurwissenschaften
Institut für Angewandte Stochastik
und Operations Research
Technische Universität Clausthal

Fabian Korte, M.Sc.
Arbeitsgruppe Softwaretechnik für
Verteilte Systeme
Institut für Informatik
Georg-August-Universität Göttingen

Dipl.-Inf. Philipp Kraus
Arbeitsgruppe Wirtschaftsinformatik
Institut für Informatik
Technische Universität Clausthal

Dipl.-Wirtschaftsing. Thomas Krüger
Arbeitsgruppe Anlagenprojektierung
und Materialflusslogistik
Institut für Maschinelle Anlagentechnik
und Betriebsfestigkeit
Technische Universität Clausthal

Dr. Robert Mettin
Arbeitsgruppe für Molekulare und Zelluläre Biophysik
Drittes Physikalisches Institut
Georg-August-Universität Göttingen

Julius Pätzold, M.Sc.
Arbeitsgruppe Optimierung
Institut für Numerische und
Angewandte Mathematik
Georg-August-Universität Göttingen

Alexander Schiewe, M.Sc.
Arbeitsgruppe Optimierung
Institut für Numerische und
Angewandte Mathematik
Georg-August-Universität Göttingen

Dr. Jochen Schulz
Arbeitsgruppe Optimierung
Institut für Numerische und
Angewandte Mathematik
Georg-August-Universität Göttingen

Fabian Sigges, M.Sc.
Arbeitsgruppe Datenfusion
Institut für Informatik
Georg-August-Universität Göttingen

Marlon Welter, M.Sc.
Arbeitsgruppe Theoretische
Informatik und Algorithmische Methoden
Institut für Informatik
Georg-August-Universität Göttingen

Johannes Wölck, M.Sc.
Arbeitsgruppe Strömungsmechanik
Institut für Technische Mechanik
Technische Universität Clausthal

Veröffentlichungen // Publications

Strukturuntersuchungen zur Entstehung und Fortpflanzung von Verspätungen in Verkehrsnetzen – Modellierung, Simulation und Optimierung eines stochastischen Netzwerks

2014

R. Bauer and A. Schöbel. Rules of thumb - practical online strategies for delay management. Public Transport, 6(1):85-105, 2014.

M. Goerigk, M. Knoth, M. Müller-Hannemann, M. Schmidt, and A. Schöbel. The Price of Strict and Light Robustness in Timetable Information. Transportation Science, 48:225-242, 2014.

M. Goerigk and A. Schöbel. Recovery-to-optimality: A new two-stage approach to robustness with an application to aperiodic timetabling. Computers and Operations Research, 2014. to appear.

B. Görder and M. Kolonko. Ranking and selection: A new sequential Bayesian procedure for use with common random numbers. 2014. submitted, http://arxiv.org/abs/1410.6782.

J. Harbering. A Line Planning Model for Delay Resistance. Technical report, Preprint-Reihe, Institut für Numerische und Angewandte Mathematik, Georg-August Universität Göttingen, 2014.

J. Harbering, F. Kirchhoff, M. Kolonko, and A. Schöbel. Delay propagation in public transport - stochastic modeling meets scenario approach. Technical report, 2014. zur Veröffentlichung vorgesehen.

F. Kirchhoff and M. Kolonko. Modeling delay propagation in railway networks with closed families of distributions. submitted, 2014.

J. Manitz, J. Harbering, M. Schmidt, T. Kneib, and A. Schöbel. Network-based source detection for train delays on railway systems. Technical Report 2014-01, Preprint-Reihe, Institut für Numerische und Angewandte Mathematik, Georg-August Universität Göttingen, 2014.

J. Manitz, J. Harbering, M. Schmidt, T. Kneib, and A. Schöbel. Network-based source detection: From infectious disease spreading to train delay propagation. In Proceedings of the 29th International Workshop on Statistical Modelling, 2014.

F. Kirchhoff. Modelling delay propagation in railway networks. In Operations Research Proceedings 2013, pages 237 - 242, 2014.

M. Schmidt and A. Schöbel. Timetabling with passenger routing. OR Spectrum, pages 1-23, 2014.

Z. Wu and M. Kolonko. Asymptotic properties of a generalized cross entropy optimization algorithm. IEEE Transactions on Evolutionary Computation, 18:1-16, 2014.

Z. Wu and M. Kolonko. Absorption in model-based search algorithms for combinatorial optimization. In Evolutionary Computation (CEC), 2014 IEEE Congress on, pages 1744-1751. IEEE, 2014.

2013

P. Bouman, M. Schmidt, L. Kroon, and A. Schöbel. Passenger route choice in case of disruptions. In Proceedings of the 16th International IEEE Conference on Intelligent Transport Systems (IEEE-ITSC), 2013. http://www.computr.eu/wp-content/uploads/2013/10/IEEE-ITS2013-PassengerChoice.pdf.

E. Carrizosa, J. Harbering, and A. Schöbel. The Stop Location Problem with Realistic Traveling Time. In Daniele Frigioni and Sebastian Stiller, editors, 13th Workshop on Algorithmic Approaches for Transportation Modelling, Optimization, and Systems, volume 33 of OpenAccess Series in Informatics (OASIcs), pages 80-93, Dagstuhl, Germany, 2013. Schloss Dagstuhl-Leibniz-Zentrum fuer Informatik.

T. Dollevoet, D. Huisman, L. Kroon, M. Schmidt, and A. Schöbel. Delay management including capacities of stations. Transportation Science, 2013. Available online before print, http://

dx.doi.org/10.1287/trsc.2013.0506.
M. Goerigk, S. Heße, M. Müller-Hannemann, M. Schmidt, and A. Schöbel. Recoverable Robust Timetable Information. In Daniele Frigioni and Sebastian Stiller, editors, 13th Workshop on Algorithmic Approaches for Transportation Modelling, Optimization, and Systems, volume 33 of OpenAccess Series in Informatics (OASIcs), pages 1-14, Dagstuhl, Germany, 2013. Schloss Dagstuhl-Leibniz-Zentrum fuer Informatik.
M. Goerigk and A. Schöbel. Algorithm engineering in robust optimization. Technical report, Preprint-Reihe, Institut für Numerische und Angewandte Mathematik, Universität Göttingen, 2013.
M. Hintermayer. Column Generation in der Linienplanung. Bachelor Thesis, 2013.
T. Jung. Algorithmischer Ausbau von Schienennetzen - Optimierung im Delay Management. Bachelor Thesis, 2013.
S. Schäfer. A new model for line planning including improvement of infrastructure. Master's thesis, Fakultät für Mathematik und Informatik, Georg August Universität Göttingen, 2013.
A. Schöbel and S. Schwarze. Finding delay-resistant line concepts using a game-theoretic approach. Netnomics, 14(3):95-117, 2013.
R. Wichmann. Online delay management - Heuristiken und Experimente. Bachelor Thesis, 2013.

2012

Z. Yang. Modellierung und Simulation von Verspätungsdaten mit PH-Verteilungen. Masterarbeit, TU Clausthal, 2012.

Sichere Kommunikation in Internet of Things (IoT) Umgebungen

2014

D. Koll, J. Li, and X. Fu, "SOUP: An Online Social Network By The People, For The People," in Proc. of 15th Annual ACM/IFIP/USENIX Middleware Conference (Middleware 2014), Bordeaux, France. (acceptance rate: 18.75%), December 2014.
Q. Li, X. Zhang, Q. Zheng, R. Sandhu, and X. Fu, "LIVE: Lightweight Integrity Verification and Content Access Control for Named Data Networking," IEEE Transactions on Information Forensics and Security, IEEE, to appear., October 2014.
L. Jiao, J. Li, T. Xu,W. Du, and X. Fu, "Optimizing Cost for Online Social Networks on Geo-Distributed Clouds," IEEE/ACM Transactions on Networking (accepted), September 2014.
M. Arumaithurai, J. Chen, E. Monticelli, X. Fu, and K. K. Ramakrishnan, "Exploiting ICN for Flexible Management of Software-Defined Networks," in Proc. of 1st ACM Conference on Information-Centric Networking (ICN 2014), Paris, France (Won the Best Paper Award, acceptance rate: 17%), September 2014.
W. Du, Y. Liao, N. Tao, P. Geurts, X. Fu, and G. Leduc, "Rating Network Paths for Locality-Aware Overlay Construction and Routing," IEEE/ACM Transactions on Networking, July 2014.
S. Hartung, S. Taheri, and D. Hogrefe, "Sensor-Assisted Monte Carlo Localization for Wireless Sensor Networks," in 6th IEEE International Conference on Cyber Technology (CYBER), Hong Kong, HK, June 2014.
S. Hartung, A. Kellner, A. Bochem, and D. Hogrefe, "Sensor-Assisted Monte Carlo Localization for Wireless Sensor Networks," in 6th IFIP International Conference on New Technologies, Mobility and Security (NTMS) - Poster + Demo Session, Dubai, UAE, April 2014.

2013

S. Hartung, H. Brosenne, and D. Hogrefe, "Practical RSSI Long Distance Measurement Evaluation in Wireless Sensor Networks," in The 2013 IEEE Conference on Wireless Sensors (ICWiSe 2013), Kuching, Malaysia, December 2013.
S. Taheri and D. Hogrefe, "Robust and Scalable Secure Neighbor Discovery for Wireless Ad Hoc Networks," in The 2013 IEEE International Conference on Communications (ICC 2013), Budapest, Hungary, June 2013.

Dekomposition von Mehrprodukt-Warteschlangennetzen mit „Batch-Processing"

2018

Wiebke Klünder. Dekomposition von Mehrprodukt-Warteschlangennetzwerken mit Batch-

Processing. Dissertation, 2018. TU Clausthal. 978-3-86948-667-3.

2016

Wiebke Klünder, Horst Zisgen, Thomas Hanschke. Decomposition of open queueing networks with batch service. Jahrbuch 2015/16 des Simulationswissenschaftlichen Zentrums Clausthal-Göttingen, 66-69, 978-3-946340-79-9

Simulation unsicherer Optimierungsprobleme mit Anwendung in der Fahrplangestaltung und der Maschinenbelegung

2017

E. Carrizosa, M. Goerigk, and A. Schöbel. A biobjective approach to recovery robustness based on location planning. European Journal of Operational Research, 261:421-435, 2017.

2016

M. Goerigk and A. Schöbel. Algorithm engineering in robust optimization. In L. Kliemann and P. Sanders, editors, Algorithm Engineering: Selected Results and Surveys, volume 9220 of LNCS State of the Art, pages 245-279. 2016.

2014

M. Goerigk and A. Schöbel. Recoveryto-optimality: A new two-stage approach to robustness with an application to aperiodic timetabling. Computers and Operations Research, 52:1-15, 2014.

A. Schöbel. Generalized light robustness and the trade-o between robustness and nominal quality. MMOR, 80(2):161-191, 2014.

ASimOV: Agentenbasierte Simulation des Passagierverhaltens zur Optimierung des Verspätungsmanagements im Bahnverkehr

2017

A. Schöbel.: An Eigenmodel for Iterative Line Planning, Timetabling and Vehicle Scheduling in Public Transportation, Transportation Research C 74, 348-365, 2017.

M.C. Lopez-de-los-Mozos and J. A. Mesa and A. Schöbel: A general approach for the location of transfer points on a network with a trip covering criterion and mixed distances, European Journal of Operational Research 260-1, 108-121, 2017.

E. Carrizosa, M. Goerigk, A. Schöbel: A biobjective approach to recoverable robustness based on location planning, European Journal of Operational Research 261, 421-435, 2017.

J. Manitz, J. Harbering, M. Schmidt, T. Kneib, A. Schöbel: Source Estimation for Propagation Processes on Complex Networks with an Application to Delays in Public Transportation Systems, Journal of the Royal Statistical Society: Series C 66, 521-536, 2017.

M. Schmidt, L. Kroon, A. Schöbel, P. Bouman: The Traveler's Route Choice Problem under Uncertainty: Dominance Relations between Strategies, Operations Research 65-1, 184-199, 2017.

P. Gattermann, J. Harbering, A. Schöbel: Line Pool Generation, Public Transport 9-1, 7-32, 2017.

M. Friedrich, M. Hartl, A. Schiewe, A. Schöbel: Integrating Passengers' Assignment in Cost-Optimal Line Planning, OASIcs 59, 1-16, 2017.

J. Pätzold, A. Schiewe, P. Schiewe, A. Schöbel: Look-Ahead Approaches for Integrated Planning in Public Transportation, OASIcs 59, 1-16, 2017.

M. Friedrich, M. Müller-Hannemann, R. Rückert, A. Schiewe, A. Schöbel: Robustness Tests for Public Transport Planning, OASIcs 59, 1-16, 2017.

2018

T. Dollevoet, D. Huisman, M. Schmidt, A. Schöbel: Delay propagation and delay management in transportation networks, Handbook of Optimization in the Railway Industry, C. Manino et al. (Editor), Springer, 2018.

M. Friedrich, M. {Müller-Hannemann}, R. Rückert, A. Schiewe, A. Schöbel: Robustness as a Third Dimension for Evaluating Public Transport Plans. OASIcs 65, 4:1-4:17, 2018.

J. Pätzold, A. Schiewe, A. Schöbel: Cost-Minimal Public Transport Planning, OASIcs 65, 8:1-8:22, 2018.

S. Albert, P. Kraus, J.P. Müller, A. Schöbel: Passenger-induced delay propagation: Agent-based

simulation of passengers in rail networks, Communications in Computer and Information Science (CCIS) 889, 3-23, 2018.
J. Pätzold and A. Schöbel: Approximate Cutting Plane Approaches for Exact Solutions to Robust Optimization Problems, Submitted to European Journal of Operations Research, 2018.

Auszeichnung

„Best Paper Award" für das Paper „Look-Ahead Approaches for Integrated Planning in Public Transportation" von Julius Pätzold, Alexander Schiewe, Philine Schiewe und Anita Schöbel auf dem ATMOS-Workshop (Workshop on Algorithmic Approaches for Transportation Modeling, Optimization and Systems) 2017 in Wien.

Anforderungsrobuste Anordnung von Betriebseinheiten und Maschinen durch Kombination von Optimierung und Simulation

2018

Bracht, U.; Schlegel, M.: Ein neuer Ansatz zur Modellbildung und Simulation mit VR- und AR-Brillen am Beispiel der Fabrikplanung. ASIM 2018 - 24. Symposium Simulationsrechnik (2018), S. 143–147.
Bracht, U.; Dahlbeck, M.; Fischer, A.; Krüger, T.: Combining Simulation and Optimization for Extended Double Row Facility Layout Problems in Factory Planning. In: Baum, M; Brenner, G; Grabowski, J; Hanschke, T; Hartmann, S; Schöbel, A. (Hrsg.): Simulation science. First International Workshop, SimScience 2017, Göttingen, Germany, April 27-28, 2017, Revised selected papers. Springer, Cham, Switzerland 2018, S. 39–59.
Anjos, M.; Fischer, A.; Hungerländer, P.: Improved exact approaches for row layout problems with departments of equal length. European Journal of Operational Research 270 (2018) 2, S. 514–529.

2017

Bracht, U.; Fischer, A.; Krüger, T.: Mathematische Anordnungsoptimierung und Simulation. Ein kombinierter Ansatz zur Fabriklayoutplanung. wt - Werkstattstechnik online 107 (2017) 4, S. 200–206.

2015

Fischer, A.; Fischer, F.; Hungerländer, P.: New Exact Approaches to Row Layout Problems 2015. http://num.math.uni-goettingen.de/preprints/files/2015-11.pdf.

Kopplung multi-physikalischer Prozesse zur Simulation von Gasbohrungen

2018

Hartmann, S., Gilbert, R. R.: Identifiability of material parameters in solid mechanics, Archive of Applied Mechanics 88 (1), 3 - 26, 2018
Grafenhorst, M., Rang, J., Hartmann, S.: Time-adaptive finite element simulations of dynamical problems for temperature-dependent materials, Journal of Mechanics of Materials and Structures 12(1), 2017, 57 – 91
Rothe, S., Erbts, P., Düster, A., Hartmann, S.: Monolithic and partitioned coupling schemes for thermo-viscoplasticity, Computer Methods in Applied Mechanics and Engineering 293, 2015, 375-410

Das Virtuelle Mikroskop – Visualisierung und Inspektion der Geometrie von Partikelschüttungen

2017

Zhixing Yang, Feng Gu, Thorsten Grosch, and Michael Kolonko. Accelerated Simulation of Sphere Packings Using Parallel Hardware. Simulation Science(2017), Springer
Feng Gu, Zhixing Yang, Michael Kolonko and Thorsten Grosch. Interactive Visualization of Gaps and Overlaps for Large and Dynamic Sphere Packings. Vision, Modeling and Visualization (VMV), 2017

Druckinduzierte Festkörperphasenübergänge und plastische Verformung in Eisen-Kohlenstoff-Legierungen

2014

N. Gunkelmann, D. R. Tramontina, E. M. Bringa und H. M. Urbassek, Interplay of plasticity and phase transformation in shock wave propagation in nanocrystalline iron, New J. Phys. 16:093032, 2014.

N. Gunkelmann, E. M. Bringa, D. R. Tramontina, C. J. Ruestes, M. J. Suggit, A. Higginbotham, J. S. Wark und H. M. Urbassek, Shock waves in polycrystalline iron: Plasticity and phase transitions, Phys. Rev. B. 89:140102, 2014.

2015

N. Gunkelmann, E. M. Bringa und H. M. Urbassek. Influence of phase transition on shock-induced spallation in nanocrystalline iron. J. Appl. Phys. 118:185902, 2015.

N. Gunkelmann, D. R. Tramontina, E. M. Bringa und H. M. Urbassek, Morphological changes in polycrystalline Fe after compression and release, J. Appl. Phys. 117:085901, 2015.

2017

N. Gunkelmann, I. A. Alhafez, D. Steinberger, H. M. Urbassek und S. Sandfeld, Nanoscratching of iron: A novel approach to characterize dislocation microstructures, Comput. Mater. Sci., 135:181, 2017.

Highlighted Paper:

N. Gunkelmann, A. Kataoka, C. P. Dullemond und H. M. Urbassek. Low-velocity collisions of chondrules: How a thin dust cover helps enhance the sticking probability. Astron. Astrophys., 599:L4, 2017.

2018

N. Gunkelmann, E. M. Bringa und Y. Rosandi, Molecular Dynamics Simulations of Aluminium Foams under Tension: Influence of Oxidation, J. Phys. Chem. C 122, 26243, 2018.

Eine Cloud-basierte Software Infrastruktur für verteilte Simulation

2016

F. Glaser, Domain Model Optimized Deployment and Execution of Cloud Applications with TOSCA , Proceedings of the 9th System Analysis and Modelling Conference (SAM 2016), Saint-Malo, France, 2016.

2015

F. Glaser, J. N. Serrano, J. Grabowski, A. Quadt, ATLAS user analysis on private cloud resources at GoeGrid , Proceedings of the 21st Conference on Computing in High Energy Physics and Nuclear Physics (CHEP 2015), 13-17 April, Okinawa, Japan, available online: http://iopscience.iop.org/article/10.1088/1742-6596/664/2/022020, 2015

F. Glaser, Towards Domain-Model Optimized Deployment and Execution of Scientific Applications in Cloud Environments , Proceedings of the Doctoral Symposium at the 5th Conference on Cloud Computing and Services Sciences (DCCLOSER 2015), Lisbon, Portugal, 2015.

M. Göttsche, F. Glaser, S. Herbold, J. Grabowski, Automated Deployment and Parallel Execution of Legacy Applications in Cloud Environments, Proceedings of the 8th IEEE International Conference on Service Oriented Computing & Applications (SOCA 2015), Rom, Italy, 2015.

H. Richter, About the Suitability of Clouds in High-Performance Computing, to be published in Proc. ISC Cloud&Big Data, Sept. 28–30, Frankfurt, Germany, 2015.

H. Richter and A. Keidel and R. Ledyayev, Über die Eignung von Clouds für das Hochleistungsrechnen (HPC), in Ifl Technical Report Series ISSN 1860-8477, Ifl-15-03, editor: Department of Computer Science, Clausthal University of Technology, Germany, 2015.

2014

R. Ledyayev, H. Richter, High Performance Computing in a Cloud Using OpenStack, The Fifth International Conference on Cloud Computing, GRIDs, and Virtualization, CLOUD COMPUTING 2014, http://www.iaria.org/conferences2014/CLOUDCOMPUTING14.html, Venice, Italy, 6 pages, May 25 - 29, 2014.

H. Richter, A. Keidel, Hochleistungsrechnen und Echtzeit in virtualisierten Maschinen und Clouds

- Die Intel Virtualisierungshilfen, in Ifl Technical Report Series ISSN 1860-8477, Ifl-14-03, http://www.in.tu-clausthal.de/forschung/technical-reports/, editor: Department of Computer Science, Clausthal University of Technology, Germany, 44 pages, 2014.
H. Richter, A. Keidel, Analyses and Methods of High-Performance Computing with Cloud Technology, in Ifl Technical Report Series ISSN 1860-8477, http://www.in.tu-clausthal.de/forschung/technical-reports/, editor: Department of Computer Science, Clausthal University of Technology, Germany, 2014.

2013

F. Glaser, H. Neukirchen, T. Rings, J. Grabowski, Using MapReduce for High Energy Physics Data Analysis , Proceedings of the 2013 International Symposium on MapReduce and Big Data Infrastructure (MR.BDI 2013), 03-05 December 2013, Sydney, Australia 2013, DOI: http://dx.doi.org/10.1109/CSE.2013.189 , 201

Simulationsbasierte Qualitätssicherung für Software Systeme

2016

V. Honsel, S. Herbold and J. Grabowski. Learning from Software Project Histories: Predictive Studies Based on Mining Software Repositories, European Conference on Machine Learning and Principles and Practice of Knowledge Discovery (ECML-PKDD) 2016 - NEKTAR Track.
D. Honsel, V. Honsel, M. Welter, S. Waack and J. Grabowski. Monitoring Software Quality by Means of Simulation Methods, 10th International Symposium on Empirical Software Engineering and Measurement (ESEM), 2016.
V. Honsel, S. Herbold and J. Grabowski. Hidden Markov Models for the Prediction of Developer Involvement Dynamics and Workload, 12th International Conference on Predictive Models and Data Analytics in Software Engineering (PROMISE 2016).

2015

V. Honsel, D. Honsel, J. Grabowski and S. Waack. Developer Oriented and Quality Assurance Based Simulation of Software Processes, Proceedings of the Seminar Series on Advanced Techniques & Tools for Software Evolution (SATToSE) 2015.
V. Honsel, Statistical Learning and Software Mining for Agent Based Simulation of Software Evolution, Doctoral Symposium at the 37th International Conference on Software Engineering (ICSE 2015), Florence, Italy.
V. Honsel, D. Honsel, S. Herbold, J. Grabowski and S. Waack; Mining Software Dependency Networks for Agent-Based Simulation of Software Evolution, The 4th International Workshop on Software Mining, 2015.

2014

V. Honsel, D. Honsel, J. Grabowski. Software Process Simulation Based on Mining Software Repositories; Proceedings of the Third International Workshop on Software Mining (accepted), 2014
Z. Dong, K. Wang L. Dang, M. Gültas, M. Welter, T. Wierschin, M. Stanke, S. Waack. CRF-based models of protein surfaces improve protein-protein interaction site predictions; BMC Bioinformatics 15, 277, 2014.

2013

P. Makedonski, F. Sudau, and J. Grabowski. Towards a model-based software mining infrastructure, Second International Workshop on Software Mining (SoftMine'13), 2013

DeSim: Dezentrale Architekturen und Konzepte für die Simulation von Systems of Systems

2016

Tobias Ahlbrecht, Jürgen Dix, Niklas Fiekas, Michael Köster, Philipp Kraus, Jörg P. Müller: An architecture for scalable simulation of systems of cognitive agents. IJAOSE 5(2/3): 232-265 (2016)
- Malte Aschermann, Philipp Kraus, Jörg P. Müller LightJason: A BDI Framework Inspired by Jason Technical Report Ifl-16-04, Clausthal University of Technology, November 2016.

2015

Ahlbrecht T; Dix J; Schlesinger F. From Testing Agent Systems to a Scalable Simulation Platform. In T. Eiter et al. (Eds.): Brewka Festschrift, LNAI 9060, pp. 47-62. Springer International Publishing Switzerland, 2015.

2014

Ahlbrecht T; Dix J; Köster M; Kraus P; Müller JP. A scalable runtime platform for multiagent-based simulation. In F. Dalpiaz et al., editors, Engineering Multiagent Systems II, volume 8758 of Lecture Notes in Artificial Intelligence (LNAI), pages 81-102, Switzerland, 2014. Springer International Publishing.

Bulling N; Popovici M. A game-theoretic approach to compute stable topologies in mobile ad hoc networks. Journal of Logic and Computation (2014).

Bulling N; A survey of multi-agent decision-making. KI 28, 3 (2014), 147–158.

Dalpiaz F; Dix J; van Riemsdijk B, Eds. Engineering Multi-Agent Systems - Second International Workshop, EMAS 2014, Paris, France, May 5–7, 2014, Revised Selected Papers (2014), vol. 8758 of Lecture Notes in Computer Science, Springer.

Gernert B; Schildt S; Wolf L; Zeise B; Fritsche P; Wagner B; Fiosins M; Manesh R; Müller JP (2014). An interdisciplinary approach to autonomous team-based exploration in disaster scenarios. In Proceedings of 12th IEEE International Symposium on Safety, Security, and Rescue Robotics (SSRR 2014). IEEE Press.

2013

Bulling N; Dastani M; Knobbout M. Monitoring norm violations in multi-agent systems. In International conference on Autonomous Agents and Multi-Agent Systems, AAMAS '13, Saint Paul, MN, USA, May 6-10, 2013 (2013), M. L. Gini, O. Shehory, T. Ito, and C. M. Jonker, Eds., IFAAMAS, pp. 491–498.

Fiosina J; Fiosins M; Müller JP (2013). Decentralised cooperative agent-based clustering in intelligent traffic clouds. In M. Klusch, M. Paprzycki, and M. Thimm, editors, Multiagent System Technologies: Proceedings of the 11th German Conference on Multiagent System Technologies, volume 8076 of Lecture Notes in Artificial Intelligence (LNAI), pages 59-72. Springer Berlin Heidelberg, 2013.

Fiosina J; Fiosins M; Müller JP (2013). Mining the traffic cloud: Data analysis and optimization strategies for cloud-based cooperative mobility management. In J. Casillas et al., editors, Management Intelligent Systems, volume 220 of Advances in Intelligent Systems and Computing, pages 25-32. Springer Berlin Heidelberg.

Fiosins M; Müller JP; Huhn M (2013). A norm-based probabilistic decision-making model for autonomic traffic networks. In J. M. Corchado et al., editors, Highlights on Practical Applications of Agents and Multi-Agent Systems, volume 365 of Communications in Computer and Information Science, pages 49-60. Springer Berlin Heidelberg.

2012

Mechs S; Müller JP; Lamparter S; Peschke J (2012). Networked priced timed automata for energy-efficient factory automation. In Proceedings of the 2012 American Control Conference (ACC 2012), pages 5310-5317. IEEE Press.

Multi-Level Simulation

2016

S. Wittek, M. Göttsche, A. Rausch, J. Grabowski. Towards Multi-Level-Simulation using Dynamic Cloud Environments, SIMULTECH 2016 - 6th International Conference on Simulation and Modeling Methodologies, Technologies and Applications, 2016 (S. 297-303, DOI: 10.5220/0005997502970303).

2018

Wittek, S., Rausch, A., 2018. Learning state mappings in Multi-Level-Simulation. Communications in Computer and Information Science (Vol. 889). Springer, Cham. https://doi.org/10.1007/978-3-319-96271-9_13145

Erbel, J., Korte, F., Grabowski J. 2018. Comparison and Runtime Adaptation of Cloud Application Topologies based on OCCI, Proceedings of the 8th International Conference on Cloud

Computing and Services Science (CLOSER 2018)

J. Erbel, F. Korte, J. Grabowski. Scheduling Architectures for Scientific Workflows in the Cloud, Proceedings of the 10th System Analysis and Modelling Conference (SAM 2018), 2018

2017

Erbel, J., 2017. Declarative Cloud Resource Provisioning Using OCCI Models, INFORMATIK 2017, 2017

2016

Wittek, S., Göttsche, M., Rausch, A., Grabowski, J., 2016. Towards Multi-Level-Simulation using Dynamic Cloud Environments, Proceedings of the 6th International Conference on Simulation and Modeling Methodologies, Technologies and Applications (SIMULTECH 2016), Lisbon, Portugal, July 29-31, 2016. Sci-TePress 2016, ISBN 978-989-758-199-1.

Auszeichnung

„Best Poster Award" für die Präsentation des Papers „Towards Multi-Level-Simulation using Dynamic Cloud Environments" auf der 6th International Conference on Simulation and Modeling Methodologies, Technologies and Applications (SIMULTECH 2016)

Cloud-Efficient Modelling and Simulation of Magnetic Nano Materials

2018

P. Ivanovic, H. Richter, OpenStack Cloud Tuning for High Performance Computing, Proc. 3rd IEEE International Conference on Cloud Computing and Big Data Analysis (ICCCBDA 2018), http://www.icccbd.com/, Chengdu, China, April 20-22, 2018.

2017

P. Ivanovic, H. Richter, Performance Analysis of ivshmem for High-Performance Computing in Virtual Machines, Proc. 2nd International Conference on Virtualization Application and Technology (ICVAT 2017), Shenzhen, China, Nov. 17-19, 2017.

Numerisch intensive Simulationen auf einer integrierten Recheninfrastruktur

2017

F. Korte, A. Bufe, C. Köhler, G. Brenner, J. Grabowski, P. Wieder: „Transparent Model-Driven Provisioning of Computing Resources for Numerically Intensive Simulation"', in Proceedings of the Clausthal-Göttingen International Workshop on Simulation Science (SimScience 2017), 2017.

Überwachung von Softwarequalität mithilfe von Agenten-basierter Simulation

2019

Steffen Herbold, Fabian Trautsch, Patrick Harms, Verena Herbold, Jens Grabowski. Experiences With Replicable Experiments and Replication Kits for Software Engineering Research, Advances in Computers, Vol. 113, Elsevier, 2019

2018

Marlon Welter, Daniel Honsel, Verena Herbold, Andre Staedler, Jens Grabowski, Stephan Waack. Assessing Simulated Software Graphs using Conditional Random Fields, Post-Proceedings of the Clausthal-Göttingen International Workshop on Simulation Science 2017, Springer, 2018

Daniel Honsel, Niklas Fiekas, Verena Herbold, Marlon Welter, Tobias Ahlbrecht, Stephan Waack, Jürgen Dix, Jens Grabowski. Simulating Software Refactorings based on Graph Transformations, Post-Proceedings of the Clausthal-Göttingen International Workshop on Simulation Science 2017, Springer, 2018

2016

Philip Makedonski, Verena Herbold, Steffen Herbold, Daniel Honsel, Jens Grabowski, Stephan Waack. Mining Big Data for Analyzing and Simulating Collaboration Factors Influencing

Software Development Decisions , To appear in: Social Network Analysis: Interdisciplinary Approaches and Case Studies, CRC Press, 2016

Verena Herbold, Steffen Herbold, Jens Grabowski. Learning from Software Project Histories: Predictive Studies Based on Mining Software Repositories , European Conference on Machine Learning and Principles and Practice of Knowledge Discovery (ECML-PKDD) - NEKTAR Track, 2016

Daniel Honsel, Verena Herbold, Marlon Welter, Jens Grabowski, Stephan Waack. Monitoring Software Quality by Means of Simulation Methods, 10th International Symposium on Empirical Software Engineering and Measurement (ESEM) - Short Paper, 2016

Verena Herbold, Steffen Herbold, Jens Grabowski. Hidden Markov Models for the Prediction of Developer Involvement Dynamics and Workload, 12th International Conference on Predictive Models and Data Analytics in Software Engineering (PROMISE), 2016

Fabian Trautsch, Steffen Herbold, Philip Makedonski, Jens Grabowski. Addressing Problems with External Validity of Repository Mining Studies Through a Smart Data Platform, 13th International Conference on Mining Software Repositories (MSR), 2016

2015

Verena Herbold, Daniel Honsel, Jens Grabowski, Stephan Waack. Developer Oriented and Quality Assurance Based Simulation of Software Processes, Proceedings of the Seminar Series on Advanced Techniques & Tools for Software Evolution (SATToSE), 2015

Verena Herbold, Steffen Herbold, Jens Grabowski. Intuition vs. Truth: Evaluation of Common Myths about StackOverflow Posts, The 12th Working Conference on Mining Software Repositories (MSR) - Challenge Track, 2015

Verena Herbold, Daniel Honsel, Steffen Herbold, Jens Grabowski, Stephan Waack. Mining Software Dependency Networks for Agent-Based Simulation of Software Evolution, The 4th International Workshop on Software Mining (SoftMine), 2015

Verena Herbold. Statistical Learning and Software Mining for Agent Based Simulation of Software Evolution, Doctoral Symposium at the 37th International Conference on Software Engineering (ICSE), Florence, Italy , 2015

Verena Herbold, Daniel Honsel, Jens Grabowski. Software Process Simulation based on Mining Software Repositories, The Third International Workshop on Software Mining (SoftMine), 2014

Philip Makedonski, Fabian Sudau, Jens Grabowski. Towards a Model-based Software Mining Infrastructure, ACM SIGSOFT Software Engineering Notes 40(1), ACM, 2015

Philip Makedonski, Jens Grabowski. Weighted Multi-Factor Multi-Layer Identification of Potential Causes for Events of Interest in Software Repositories, Proceedings of the Seminar Series on Advanced Techniques & Tools for Software Evolution (SATToSE), 2015

Auszeichnung

ACM SIGSOFT Distinguished Paper Award auf der MSR 2016 für das Paper „Adressing Problems with External Validity of Repository Mining Studies Through a Smart Data Platform“

Postanschrift
Simulationswissenschaftliches Zentrum Clausthal-Göttingen
Geschäftsstelle
Dr. Alexander Herzog
Arnold-Sommerfeld-Straße 6
38678 Clausthal-Zellerfeld
E-Mail: simzentrum@tu-clausthal.de
Telefon: +49 5323 72-2966

Impressum
Herausgeber: Simulationswissenschaftliches Zentrum Clausthal-Göttingen
Redaktion: Dr. Alexander Herzog
Layout und Satz: Melanie Bruchmann, TU Clausthal
Bildnachweis: Titelbild – stock.adobe.com (© striZh)

Hier nicht erwähnte Bilder stammen von den Autoren.

DOI 10.21268/20190404-7